



University
of Glasgow

Tang, Haoran (2012) Scar/WAVE complex suppresses cell invasion and cancer cell transformation. PhD thesis

<http://theses.gla.ac.uk/3633/>

Copyright and moral rights for this thesis are retained by the author

A copy can be downloaded for personal non-commercial research or study, without prior permission or charge

This thesis cannot be reproduced or quoted extensively from without first obtaining permission in writing from the Author

The content must not be changed in any way or sold commercially in any format or medium without the formal permission of the Author

When referring to this work, full bibliographic details including the author, title, awarding institution and date of the thesis must be given.

**Scar/WAVE complex suppresses cell
invasion and cancer cell transformation**

Haoran Tang

**Submitted in fulfilment of the requirements
for the Degree of Doctor of Philosophy**

**Beatson Institute for Cancer Research
University of Glasgow**

Oct 2012

Abstract

The mechanisms by which cancer cells hijack the actin cytoskeleton to invade and disseminate to distant sites of metastasis remains one of the great frontiers in cancer research. Many actin-regulating proteins have been identified to be important in cancer cell invasion and metastasis. However the role of a major actin assembly promoting complex, Scar/WAVE regulatory complex (WRC) in cancer cell invasion is poorly understood.

WRC has a well-known motility-promoting role in 2D planar cell migration, but a recent study on human epithelial cancers suggests WRC may be anti-invasive in vivo. To investigate the controversy, human epithelial cancer cells with reduced WRC expression were tested in multiple 3D cell motility assays. Interestingly, WRC demonstrates a robust anti-invasive role in these exciting experiments.

To understand how loss of WRC promotes invasion, the molecular mechanism is investigated. N-WASP is the other major actin assembly promoting protein. Unlike WRC, N-WASP is interestingly not required for 2D planar cell migration, but is important for motility in 3D. The interplay of the two major actin assembly promoting proteins has not been explored in 3D cell motility. I report here that loss of WRC promotes hyper-activation of focal adhesion kinase that leads to N-WASP accumulation and activation at the invasive front. This chain of events results in enhanced invasion providing a molecular mechanism of WRC's anti-invasive function.

In addition to this FAK-N-WASP core mechanism, I also identified a novel pro-invasive role of HSPC300 independently of WRC. Loss of WRC possibly releases free HSPC300 that could subsequently interact with and regulate N-WASP activation during invasion providing a potential direct molecular link between the two proteins. Furthermore, WRC also suppresses focal adhesion kinase mediated cell transformation and tumour formation in vivo.

In this thesis I therefore demonstrate novel anti-invasion and anti-tumorigenesis functions of WRC. I also show how a novel WRC binding protein, NHS, could negatively regulate WRC function.

Declaration

I declare that all of the work in this thesis was performed personally. No part of this work has been submitted for consideration as part of any other degree or award.

Acknowledgments

I would love to thank my supervisor Prof. Laura Machesky for offering me the great opportunity to study for a PhD degree, and for her patient guidance and advice throughout my study. My research progress was only made possible with the support of my supervisor, and all the other lab members. I want to thank Prof. Robert Insall, all lab members in Insall's lab and my advisor Prof. Owen Sansom for their inspiring ideas and helpful discussions. I also want to express my appreciation to Prof. Kurt Anderson, Tom Gilbey and Margaret O'Prey for their expertise in imaging techniques, without them this thesis would be much less colorful.

I also want to express my gratitude to my parents who worked hard to support my study and my life. I must acknowledge my wife, Jing Bi, for her kind, patient and caring support during my study, and for her encouragement on my research.

I recognize that this research would not have been possible without the financial support from Cancer Research UK and the Beatson Institute for Cancer Research.

Publications arising from this work

Actin-based protrusions: promoters or inhibitors of cancer invasion?

Machesky LM, Tang HR

Cancer cell. 2009 Jul;16(1):5-7

The Nance-Horan syndrome protein encodes a functional WAVE homology domain (WHD) and is important for co-ordinating actin remodelling and maintaining cell morphology.

Brooks SP, Coccia M, Tang HR, Kanuga N, Machesky LM, Bailly M, Cheetham ME, Hardcastle AJ

Hum Mol Genet. 2010 Jun 15;19(12):2421-32

Scar/WAVE3 contributes to motility and plasticity of lamellipodial dynamics but not invasion in 3D.

Spence HJ, Timpson P, Tang HR, Insall RH, Machesky LM

Biochem J. 2012 Aug 21.

Loss of Scar/WAVE complex promotes N-WASP and FAK dependent invasion

Hao Ran Tang¹, Ang Li¹, Jing Bi², Douwe M. Veltman¹, Tobias Zech¹, Heather J. Spence¹, Xinzi Yu¹, Paul Timpson¹, Robert H. Insall¹, Margaret C. Frame², and Laura M. Machesky¹

¹The Beatson Institute for Cancer Research, Switchback Road, Glasgow, UK

²Edinburgh Cancer Research Center, Edinburgh University, Edinburgh, UK

Current Biology, under revision.

Abbreviations

Abi	Abl-kinase interactor
Akt	RAC-alpha serine/threonine-protein kinase
Arf1	ADP ribosylation factor 1
ARP	Actin related protein
Arp2/3	Actin related protein 2/3
ARPC	Actin-related protein 2/3 complex subunit
ATP	Adenosine Triphosphate
BSA	Bovine serum albumin
Cdc42	Cell division control protein 42 homolog
CO	Collagen
CREB	cAMP response element binding
Crk	CT10 Regulator of Kinase
CYFIP	Cytoplasmic fragile-X mental retardation interacting protein
DMEM	Dulbecco's Modified Eagle Medium
DOCK	Dedicator of cytokinesis
ECM	Extracellular matrix
eIF4E	eukaryotic translation initiation factor 4E
Erk	Extracellular signal-regulated kinase
FAK	Focal adhesion kinase
FAT	Focal adhesion targeting
FBS	Foetal Bovine Serum
FERM	4.1 protein, Ezrin, Radixin, Moesin
FMRP	Fragile-X mental retardation protein
FN	Fibronectin
GAP	GTPase activating protein

GAPDH	Glyceraldehyde 3-phosphate dehydrogenase
GDP	Guanosine diphosphate
GEF	Guanine nucleotide exchange factor
GFP	Green fluorescent protein
Grb2	Growth factor receptor-bound protein 2
GTP	Guanosine triphosphate
hDlg	human Discs large
hScrib	human Scribble
HSPC300	Haematopoietic stem/progenitor cell protein 300
hTERT	human telomerase reverse transcriptase
IF	Immunofluorescence
IHC	Immunohistochemistry
JMY	Junction mediating and regulatory protein, p53 cofactor
MAP	Mitogen-activated protein kinase
MEM	Modified Eagle Medium
MLCK	Myosin light chain kinase
MNK	MAPK interacting kinase
mRNA	Massager RNA
MT1-MMP	Membrane-type 1 matrix metalloproteinase
N-WASP	Neural Wiskott-Aldrich syndrome protein
Nap1	Nck-associated protein 1
Nck	Non-catalytic region of tyrosine kinase adaptor protein 1
NPF	Nucleation-promoting factor
p	Phosphor
p130Cas	Breast cancer anti-estrogen resistance protein 1
PBS	Phosphate buffered saline
PDK1	Phosphoinositide dependent kinase 1

PI3K	Phosphatidylinositol 3-kinases
PIP2	Phosphatidylinositol 4,5-bisphosphate
PR	Proline rich
QRT-PCR	Quantitative reverse transcriptase polymerase chain reaction
Rac	Ras-related C3 botulinum toxin substrate
Raf	Rapidly accelerated fibrosarcoma
Ras	Rat sarcoma
RFP	Red fluorescent protein
RPE	Retinal pigment epithelium
RSK	Ribosomal protein S6 kinase
Scar	Suppressor of mutations in a cAMP receptor
SH3	Src homology 3
shRNA	Small hairpin RNA
siRNA	Small interfering RNA
SOS	Son of Sevenless
Sra1	Specifically Rac-1-associated Protein
Src	Sarcoma
TBST	Tris-buffered saline and tween 20
Tyr or Y	Tyrosine
TIRF	Total internal reflection fluorescence microscopy
VCA	Verprolin central acidic domain
VSMC	Vascular smooth muscle cells
WASH	WASP and SCAR homologue
WASP	Wiskott-Aldrich syndrome protein
WAVE	WASP family verprolin homologous
WB	Western blotting
WH2	WASP-homology 2 motif

WHAMM WASP homolog NPF associated with actin, membranes and microtubules

WRC Scar/WAVE regulatory complex

Table of contains

ABSTRACT	2
DECLARATION	4
ACKNOWLEDGMENTS	5
PUBLICATIONS ARISING FROM THIS WORK	6
ABBREVIATIONS	8
TABLE OF CONTAINS	12
LIST OF FIGURES AND TABLES	16
CHAPTER 1: INTRODUCTION	19
1.1 CELL MIGRATION IN BIOLOGY	20
1.2 STRUCTURES AND MOLECULES OF CELL MIGRATION	21
1.2.1 <i>Membrane Protrusions</i>	21
1.2.1.1 Lamellipodia & Filopodia	21
1.2.1.2 Invadopodia & Podosomes	22
1.2.1.3 Pseudopods in 3D	23
1.2.1.4 Membrane Blebs	24
1.2.2 <i>Actin cytoskeleton</i>	25
1.2.2.1 Nucleation of actin polymerization --- Arp2/3 complex	28
1.2.2.2 Regulation of Arp2/3 complex	30
1.2.3 <i>Regulation and function of Nucleation-Promoting Factors</i>	32
1.2.3.1 Scar/WAVE regulatory complex	32
1.2.3.2 Biological functions of WRC subunits	35
1.2.3.2.1 Nap1	35
1.2.3.2.2 Sra1/PIR121	35
1.2.3.2.3 Abi proteins	36
1.2.3.2.4 HSPC300	37
1.2.3.2.5 Scar proteins	38
1.2.3.3 WASP & N-WASP	39
1.3 ADHESION AND CELL MIGRATION	43
1.3.1 <i>Adhesion Formation</i>	45
1.3.2 <i>Adhesion Signalling</i>	47
1.3.3 <i>Focal Adhesion Kinase Signalling</i>	47
1.3.3.1 Migration and Invasion	49
1.3.3.2 MAPK/Erk pathway	49
1.3.3.3 PI3K/Akt pathway	50
1.3.3.4 Adhesion Disassembly	51
1.4 ARP2/3 COMPLEX, NPFs, AND ADHESIONS	52
1.4.1 <i>Arp2/3 complex and adhesion</i>	52

1.4.2 <i>WRC and adhesion</i>	54
1.4.3 <i>N-WASP and adhesion</i>	55
1.5 AIM OF THESIS	56
CHAPTER 2: MATERIALS AND METHODS	57
2.1 MATERIALS	58
2.2 CELL CULTURE	58
2.2.1 <i>Cell lines</i>	58
2.2.2 <i>Tissue culture</i>	58
2.2.3 <i>Cell passaging and counting</i>	58
2.2.4 <i>Cryopreservation and cell recovery</i>	59
2.2.5 <i>Transfection</i>	59
2.2.6 <i>Stable cell line selection</i>	61
2.2.7 <i>Soft agarose growth assay</i>	61
2.2.8 <i>Cell growth assay</i>	62
2.3 PROTEIN ANALYSIS	62
2.3.1 <i>Protein extraction</i>	62
2.3.2 <i>Protein concentration</i>	63
2.3.3 <i>Protein separation</i>	63
2.3.4 <i>Western blotting</i>	63
2.3.5 <i>Native protein complex extraction and separation</i>	64
2.3.6 <i>Immunoprecipitation</i>	65
2.3.7 <i>Effector domain pulldown assay</i>	66
2.3.8 <i>Rac1 Activation Assay</i>	66
2.4 MOTILITY ASSAYS	67
2.4.1 <i>Wound healing assay</i>	67
2.4.2 <i>Wound healing induced Matrigel invasion assay</i>	67
2.4.3 <i>Cell spreading assay</i>	67
2.4.4 <i>Organotypic invasion assay</i>	68
2.4.5 <i>3D collagen gel invasion assay</i>	69
2.4.6 <i>Thick collagen gel invasion assay</i>	69
2.5 IMAGING	69
2.5.1 <i>Matrix-coated glass bottom dish</i>	69
2.5.2 <i>Cell derived matrix</i>	70
2.5.3 <i>Live cell imaging</i>	70
2.5.4 <i>Immunofluorescence</i>	71
2.5.5 <i>Fluorescent gelatin degradation assay</i>	73
2.6 XENOGRAFTS AND IMMUNOHISTOCHEMISTRY	73
2.6.1 <i>Xenograft</i>	73

2.6.2 Immunohistochemistry	74
2.7 RNA ANALYSIS.....	74
2.7.1 RNA extraction	74
2.7.2 Quantitative RT-PCR.....	75
2.8 PLASMID PURIFICATION	75
2.9 QUANTIFICATION AND STATISTICS.....	76
CHAPTER 3: LOCALIZATION OF WRC	77
3.1 INTRODUCTION.....	78
3.2 LOCALIZATION OF WRC IN LIVE CELLS	79
3.3 DISCUSSION.....	86
CHAPTER 4: ROLE OF WRC IN 3D CELL MIGRATION	87
4.1 INTRODUCTION.....	88
4.2 LOSS OF WRC PROMOTES INVASION OF EPITHELIAL CELLS.....	89
4.2.1 Generation and characterization of stable WRC knockdown cell lines	89
4.2.2 WRC suppresses epithelial cancer cell invasion.....	94
4.2.3 Arp2/3 complex is required for invasion	98
4.2.4 N-WASP activates Arp2/3 complex.....	101
4.2.5 Loss of WRC promotes invasion in normal epithelial cells.....	108
4.2.6 Rac1 and Cdc42 activation status in the absence of WRC.....	112
4.3 DISCUSSION.....	114
CHAPTER 5: FOCAL ADHESION KINASE IS REQUIRED FOR INVASION AND CELL TRANSFORMATION	117
5.1 INTRODUCTION.....	118
5.2 FOCAL ADHESION KINASE PROMOTES N-WASP DEPENDENT INVASION.....	120
5.2.1 Loss of WRC alters cell-substrate adhesion	120
5.2.2 Focal adhesion kinase is over activated without WRC.....	122
5.2.3 Focal adhesion kinase promotes N-WASP dependent cell invasion.....	123
5.2.4 Focal adhesion kinase promotes cell transformation	129
5.3 LOSS OF WRC PROMOTES FORMATION OF DEGRADATIVE FOCAL ADHESIONS	135
5.4 DISCUSSION.....	137
CHAPTER 6: HSPC300 IS UNIQUE	140
6.1 INTRODUCTION.....	141
6.2 HSPC300 IS REQUIRED FOR INVASION INDEPENDENTLY OF WRC.....	142
6.2.1 HSPC300 is required for invasion of WRC depleted cells.....	142
6.2.2 HSPC300 is required for N-WASP and Arp2/3 complex localization	144
6.2.3 HSPC300 interacts with N-WASP	147
6.3 DISCUSSION.....	148

CHAPTER 7: NHS, A NOVEL WRC BINDING PROTEIN	150
7.1 INTRODUCTION.....	151
7.2 NHS-1A IS A PUTATIVE NEGATIVE REGULATOR OF WRC.....	154
7.2.1 <i>NHS-1A interacts with WRC subunits</i>	154
7.2.2 <i>NHS-1A localizations</i>	156
7.2.3 <i>NHS-1A is not required for cell-cell junction</i>	159
7.2.4 <i>NHS-1A is a negative regulator of Rac1</i>	161
7.3 DISCUSSION.....	165
CHAPTER 8: SUMMARY AND FUTURE DIRECTIONS	167
8.1 SUMMARY	168
8.2 FUTURE DIRECTIONS	169
8.3 CONCLUSIONS	172
CHAPTER 9: REFERENCES	173

List of Figures and Tables

Figure 1.1 Morphology of a migrating cell.....	22
Figure 1.2 Invadopodia and Podosomes	23
Figure 1.3 Morphology of a moving cell in 3D collagen gel	24
Figure 1.4 Assembly of actin filaments	27
Figure 1.5 Structure of Arp2/3 complex.....	29
Figure 1.6 Branched actin network in lamellipodium	30
Figure 1.7 Wiskott-Aldrich Syndrome Protein (WASP) family proteins.....	31
Figure 1.8 Model of WRC activation	34
Figure 1.9 Differential localization of Scar proteins	38
Figure 1.10 Lamellipodia formation requires Scar2.....	39
Figure 1.11 Model of N-WASP activation	42
Figure 1.12 Integrin based adhesion	46
Figure 1.13 Focal adhesion kinase activation.....	48
Figure 1.14 FAK mediated signalling cascades.....	51
Figure 1.15 Arp2/3 complex localizes to new adhesions.....	53
Figure 1.16 <i>Drosophila</i> WRC localizes to integrin based adhesions.....	54
Table 2.1 List of fusion protein constructs	60
Table 2.2 List of siRNAs	60
Table 2.3 List of shRNAs	61
Table 2.4 List of primary antibodies used for western blotting.....	64
Table 2.5 List of antibodies and phalloidin used for IF.	72
Figure 3.1 Localization of Scar2 in B16F10 cells.....	79
Figure 3.2 Scar2-GFP represents WRC localization	81
Figure 3.3 WRC dynamics in live cells	83
Figure 3.4 Internalization of WRC.....	84
Figure 3.5 WRC localization on CDM	85
Figure 4.1 Characterizations of WRC shRNAs.....	90
Figure 4.2 WRC expression level revealed by Blue NativePAGE	91
Figure 4.3 Morphology of various WRC KD cells	92
Figure 4.4 Cell spreading defects of various WRC KD cells.....	93
Figure 4.5 WRC KD cells are invasive in organotypical assays	94
Figure 4.6 WRC KD cells are invasive in 3D collagen gel.....	95

Figure 4.7 Cell migration defects of WRC KD cells	96
Figure 4.8 Loss of WRC promotes invasion through matrigel	97
Figure 4.9 WRC KD cells produce blunt protrusions in collagen gel	98
Figure 4.10 Loss of WRC promotes Arp2/3 complex localization to cell front during invasion.	99
Figure 4.11 Arp2/3 complex is required for invasion	100
Figure 4.12 Without WRC, N-WASP activates Arp2/3 complex	102
Figure 4.13 N-WASP is required for Arp2/3 complex localization	104
Figure 4.14 N-WASP is required for invasion	105
Figure 4.15 N-WASP and Arp2/3 complex co-localization in Matrigel invasion...	106
Figure 4.16 N-WASP and Arp2/3 complex localization is invasion specific.....	107
Figure 4.17 Loss of WRC promotes invasion of a normal human epithelial cell line.	109
Figure 4.18 N-WASP promotes pseudopods formation in 3D	111
Figure 4.19 Rac1 and Cdc42 activation status in WRC KD cells	113
Figure 5.1 Loss of WRC enhances cell-substrate adhesion	120
Figure 5.2 Loss of WRC alters focal adhesion dynamics	121
Figure 5.3 Over activation of FAK in WRC KD cells	122
Figure 5.4 FAK is required for lamellipodia formation.....	123
Figure 5.5 FAK is required for invasion	124
Figure 5.6 FAK co-localizes with N-WASP	125
Figure 5.7 FAK is required for N-WASP and Arp2/3 complex localization	127
Figure 5.8 N-WASP is phosphorylated at the invasive pseudopods	128
Figure 5.9 Loss of WRC promotes FAK dependent cell transformation	130
Figure 5.10 Hela cells are transformed upon loss of WRC.....	131
Figure 5.11 Loss of WRC promotes tumour formation in vivo	132
Figure 5.12 Loss of WRC promotes Akt activation	134
Figure 5.13 Loss of WRC promotes matrix degradation through FAK dependent degradative focal adhesions.....	136
Figure 6.1 HSPC300 is stable without WRC	142
Figure 6.2 Free HSPC300 is required for invasion	143
Figure 6.3 HSPC300 is required for N-WASP and Arp2/3 complex localization .	145
Figure 6.4 HSPC300 promotes invasion and pseudopods formation.....	146
Figure 6.5 HSPC300 interacts with N-WASP	147
Figure 7.1 NHS contains WHD	152

Figure 7.2 NHS interacts with multiple proteins.....	155
Figure 7.3 NHS-1A localization at the leading edge in a mouse melanoma cell line	156
Figure 7.4 NHS-1A localization at the leading edge and cell-cell junction in a human epithelial cell line	157
Figure 7.5 Co-localization of WRC and NHS-1A at cell-cell junctions	158
Figure 7.6 NHS is not required for cell-cell junctions.....	160
Figure 7.7 Loss of NHS promotes spreading on collagen	162
Figure 7.8 Loss of NHS promotes WRC localization during spreading	163
Figure 7.9 Loss of NHS promotes Rac1 activation.....	164
Figure 8.1 HSPC300 is required for FAK activation	170
Figure 8.2 Loss of NHS reduces focal adhesions.....	171
Figure 8.3 Graphic summary	172

Chapter 1: Introduction

1.1 Cell migration in biology

Cell motility is a fundamental process in biology. It is required for embryo development, wound healing and immunity. At a very early stage of human embryo development, invasion and migration of trophoblasts into maternal uterus epithelium is critical for blastocyst implantation (Pijnenborg et al., 1983). As trophoblasts migrate deeper and across the uterus epithelium, they invade maternal spiral arteries and trigger vascular transformation to establish vital fetoplacental blood supply, hence the establishment of pregnancy (Pijnenborg et al., 2011).

During later stages of development, cell motility is also critical for morphogenesis during gastrulation and neurulation, as individual cells and sheets of cells need to move into their appropriate positions to form the proper body plan. In Sea Urchin embryo gastrulation, cells at the most vegetal mesoderm undergo a process called epithelial to mesenchymal transition to become motile. These primary mesenchyme cells migrate as single cells towards the blastocoel at the vegetal pole to secrete the calcified endoskeleton (Sharma and Ettensohn, 2011). In vertebrate embryos, during neurulation, just after the neural tube closure, neural crest cells also undergo an epithelial to mesenchymal transition (Duband, 2010) and migrate away from the neural tube to form neurons, glia, and melanocytes (Bronner-Fraser, 1994).

Healing and immunity is also critically dependent on cell motility. Fibroblasts and endothelial cells migrate to wound to secrete collagen and generate new blood vessels respectively to regenerate the damaged tissue. Meanwhile, keratinocytes migrate and proliferate over the newly produced collagen to generate new epithelium to cover the wound. Just shortly after injury, immune cells, namely neutrophils and macrophages, move to the site of injury to clean up pathogens and debris. While migration of immune cells is required, it is not restricted to wound healing. Infection of microbes also triggers inflammatory response. In response to the infection, leukocytes originated from bone marrow migrate to the site and kill the invading microbes. This innate immunity forms the first line of defence against pathogens. While innate immunity provides a quick defence mechanism, to establish long-term immunity, dendritic cells migrate from the site of infection to lymph nodes to present processed antigen to T cells and B cells.

Therefore, as a result of dendritic cell migration long-term adaptive immunity can be established.

Cell migration is clearly critical to physiology, however it also contributes to cancer malignancy. While solid primary tumours can often be surgically removed, motile cancer cells invade surrounding tissue stroma, and can invade to other distal organs to establish metastasis. Just like embryonic cells, epithelial cancer cells also undergo epithelial to mesenchymal transition to become motile. These motile cancer cells now can move through underlying basement membrane, and invade deep into surrounding tissues. In order to spread to distant organs, cancer cells trans-migrate into nearby blood vessels. Although blood circulation can bring cancer cells to distant organs, cancer cells have to migrate out blood vessels to establish metastasis. This ability of cancer cells to move to and occupy various vital organs, like lungs, liver and brain, contributes to cancer malignancy, as these invading cancer cells grow and form a new tumour.

1.2 Structures and Molecules of cell migration

1.2.1 Membrane Protrusions

1.2.1.1 Lamellipodia & Filopodia

Cells make various structures to migrate under different conditions. Cell motility is most extensively studied using cultured cells on rigid 2D surfaces. Under such conditions cells become polarized and generate distinct membrane protrusions to migrate. At the front of a migrating cell, a broad sheet-like membrane protrusion, lamellipodium, and spike-like membrane protrusions, filopodia, dominate the advancing front. The two kinds of membrane protrusions drive the cell forward by extending the membrane at the front. In contrast, stress fibres contract the rear of a migrating cell to pull the whole cell body forward resulting in a thin retracting tail (**Figure 1.1**).

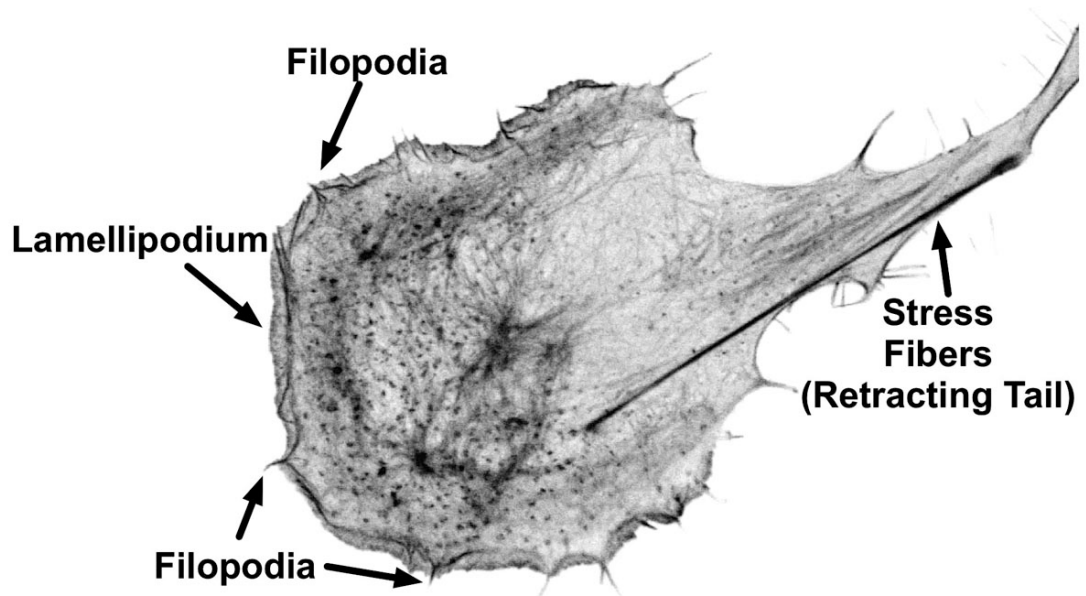


Figure 1.1 Morphology of a migrating cell

Confocal micrograph of a GFP-Lifeact (F-Actin) expressing B16F10 mouse melanoma cell.

1.2.1.2 Invadopodia & Podosomes

When cells are trying to invade a layer of soft extra cellular matrix (ECM, eg. Gelatin) or native basement membrane, finger like degradative membrane protrusions are formed at the ventral surface (**Figure 1.2**) (Murphy and Courtneidge, 2011). In non-cancer cells, including osteoclasts (Zamboni-Zallone et al., 1988), macrophages, megakaryocytes, dendritic cells, endothelial cells and vascular smooth muscle cells (VSMC) (Gimona et al., 2008), these ventral protrusions are known as podosomes, while in many cancer cells similar ventral protrusions are known as invadopodia. Although both membrane structures are sites of matrix degradation, invadopodia are longer membrane protrusions with longer lifetime, and therefore more degradative. ECM is remodelled by metalloproteinases at both invadopodia and podosomes to facilitate cell migration (Artym et al., 2006, Gawden-Bone et al., 2010, Buccione et al., 2004). For cancer cells, the ability to form invadopodia is thought to correlate with the invasive potential (Li et al., 2010). On the other hand, podosome formation in VSMC and megakaryocytes is required for cell migration in vivo (Quintavalle et al., 2010, Sabri et al., 2006).

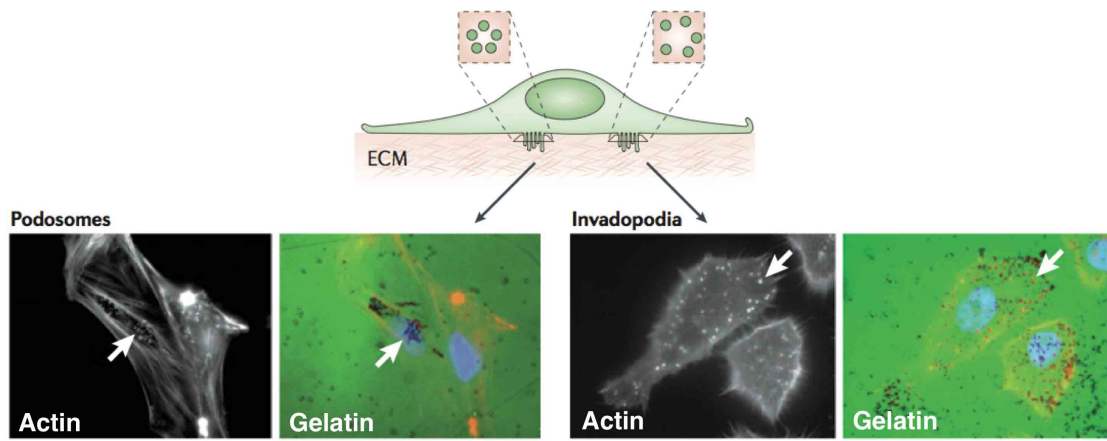


Figure 1.2 Invadopodia and Podosomes

Cells use specialized membrane protrusions to degrade ECM. When cells are cultured on top of fluorescent gelatin (green), depending on the cell type, invadopodia or podosomes are formed from the ventral surface (actin puncta). The protrusive membrane structures are specifically associated with matrix degradation leading to loss of fluorescent gelatin (black holes). These degradative protrusions are able to help cell motility by removing unnecessary ECM, which can be a physical barrier. Figure adapted from (Murphy and Courtneidge, 2011).

1.2.1.3 Pseudopods in 3D

Although in 3D cell culture and in vivo, invadopodia or podosomes are hard to define, polarized cells generate pseudopods at the cell front to migrate in a 3D matrix (Li et al., 2011, Caswell et al., 2007, Friedl and Wolf, 2003). These pseudopods are protruding membrane structures therefore can drive cell migration. Additionally, pseudopods in 3D also serve as an important platform of cell-matrix interaction permitting adhesion and remodelling of the matrix by metalloproteinases (Wolf and Friedl, 2009, Friedl and Gilmour, 2009). At the rear of a migrating cell in 3D, contraction also pulls the cell body forward, however in 3D the contraction often generates a rounded cell body at the rear of a migrating cell, rather than a thin tail (**Figure 1.3**).

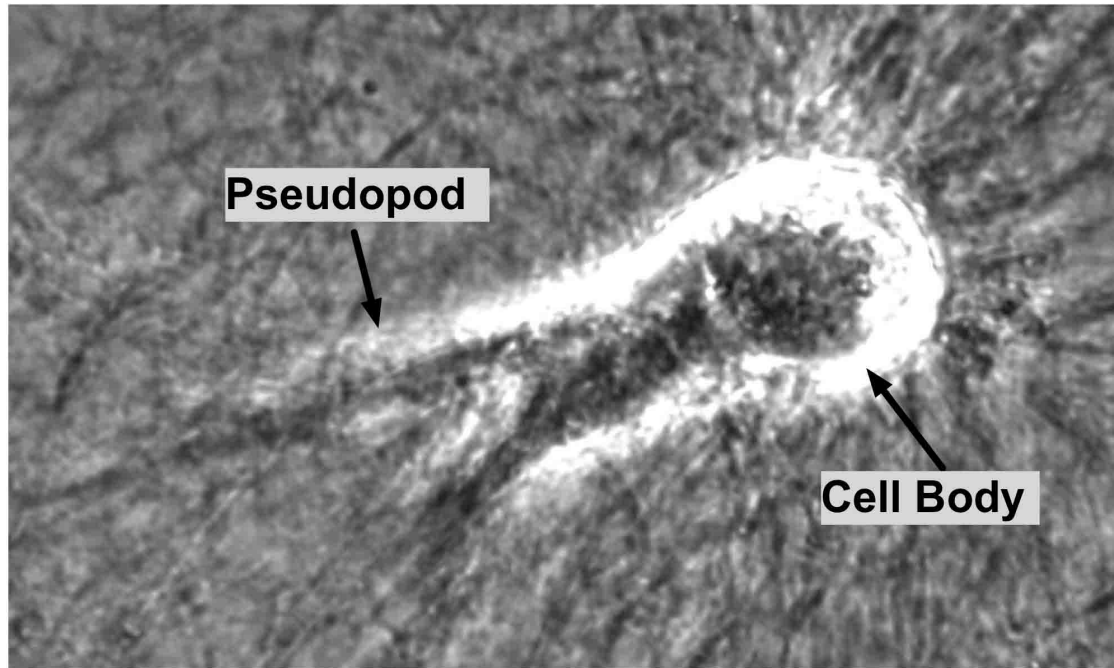


Figure 1.3 Morphology of a moving cell in 3D collagen gel

Bright field micrograph shows a human retinal pigment epithelial cell (hTERT-RPE1) in collagen gel.

1.2.1.4 Membrane Blebs

Membrane blebs are rounded and bulky plasma membrane extensions. Unlike other membrane protrusions mentioned above, membrane blebs are very dynamic structures with a lifetime usually around 1min (Fackler and Grosse, 2008). The expansion of membrane blebs is a relative passive process, and actin polymerization is not required (Cunningham, 1995). For a membrane bleb to expand, uneven hydrostatic pressure within a blebbing cell drives flow of the cytoplasmic fluid to inflate the plasma membrane that has detached from the underlying actin cytoskeleton (Charras et al., 2005). Although polymerised actin is not observed in expanding membrane blebs, the detachment of the plasma membrane requires acto-myosin contraction, which generates a hydrostatic pressure to tear a small part of the membrane free from the underlying actin cortex (Charras et al., 2005) allowing inflation by cytoplasmic fluid. While actin is not required for membrane bleb expansion, the retraction of membrane blebs requires actin and myosin II. Once the inflation of membrane blebs slows, actin starts to polymerise under the plasma membrane in the bleb with simultaneous

accumulation of myosin II. As a result, a new cortex is attached to the plasma membrane, and cortical contraction leads to membrane bleb retraction (Charras et al., 2005, Blaser et al., 2006).

Although membrane blebs are frequently observed during apoptosis (Mills et al., 1998), cell migration also involves membrane blebbing. Most noticeably, Zebrafish primordial germ cells predominantly use membrane blebs to migrate (Blaser et al., 2006). Although cancer cells can also form membrane blebs, the ability of membrane blebs to drive cancer cell migration is likely to be cell type dependent. For example, certain cancer cells isolated from human malignant melanomas generate membrane blebs yet they have impaired cell motility (Cunningham et al., 1992). In contrast, rat Walker 256 carcinosarcoma cells migrate using a combination of membrane blebbing and lamellipodia formation (Bergert et al., 2012).

1.2.2 Actin cytoskeleton

All membrane protrusions required for cell migration mentioned above are based on the actin cytoskeleton with the exception of membrane blebs. Actin monomers polymerise just under the plasma membrane to push the membrane forward. Actin monomer is a polarised globular molecule (G-Actin) that can bind to and hydrolyse ATP (Small et al., 1978, Korn et al., 1987) (**Figure 1.4A**). During actin polymerization one ATP bound G-actin is added to the plus or barbed end of another G-actin (**Figure 1.4B**) resulting in a polarised actin filament that consists of two twisted helices (**Figure 1.4C**) (Holmes et al., 1990, Bugyi and Carlier, 2010). When actin filaments extend at the plus end, ATP is hydrolysed to ADP at the minus or pointed end. As ADP bound actin has lower binding affinity to the filaments, ADP-bound actin disassociates from the filament. ADP on these G-actin monomers is later replaced by ATP in a process called nucleotide exchange to become ATP-bound again, and to be available for polymerization again (**Figure 1.4B**). As actin plus ends point to plasma membrane, this cycle of polymerization and depolymerization drives actin filament growth towards the membrane (Small et al., 1978). As a result, the growing actin filaments push the membrane forward to drive cell migration.

It is thought that actin polymerizes against the plasma membrane to drive protrusion, but if the actin plus end were constantly associated with the membrane, there would be little room for the addition of actin monomers. In fact because of Brownian motion, the relative position of actin plus end and the plasma membrane is believed to fluctuate. In this model, when the fluctuation of the membrane and actin plus end provides a large enough gap, one actin monomer is added to the plus end pushing the membrane forward. Meanwhile, a long enough actin filament can bend providing space for actin monomer insertion to the plus end. The lengthened actin filament can then apply an elastic force to push the membrane forward. (Peskin et al., 1993, Mogilner and Oster, 1996).

While actin polymerisation provides the force needed for membrane expansion, the geometry of polymerised actin filaments decides the morphology of the membrane protrusions. While highly branched actin filaments generate the sheet-like lamellipodia, bundled actin filaments generate spike-like filopodia (Pollard and Borisy, 2003, Nemethova et al., 2008, Korobova and Svitkina, 2008). One recent report demonstrates that side branching from existing actin filaments that are parallel to the membrane can initiate lamellipodia formation (Vinzenz et al., 2012). In contrast, one in vitro study suggests filopodia can be formed from the existing branched actin network by plus end elongation of actin filaments followed by cross-linking to form actin bundles (Vignjevic et al., 2003). Indeed when investigated with platinum replica transmission electron microscopy, filopodium with bundled actin filaments was found to rise from a branched actin network in a mouse melanoma cell (Svitkina et al., 2003). Additionally, filopodia can also form independently of the branching actin network, as loss of the branched actin network does not prevent filopodia formation (Wu et al., 2012).

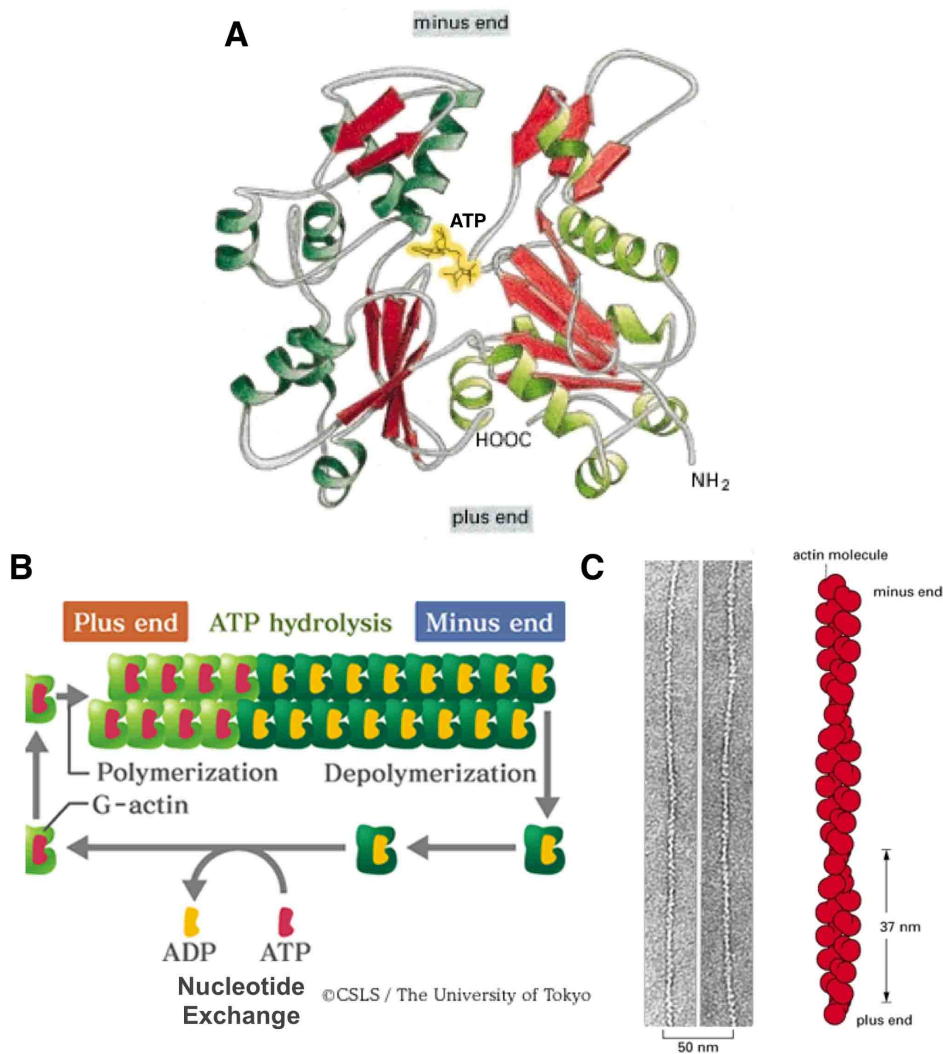


Figure 1.4 Assembly of actin filaments

(A) Crystal structure of an actin monomer. The presentation demonstrates actin monomer as a polarised globular molecule. A deep cleft split the molecule open at the minus end allowing binding of ATP at the center of actin monomer. (B) During the formation of actin filaments, ATP-bound actin monomer is added to the plus end of another monomer. Meanwhile ATP on the minus end is hydrolysed leading to filament disassembly. Growth of actin filaments depends on the balance of the two processes. (C) The resulting actin filaments consist of two twisted helices as shown by electron micrographs. A,C adapted from Alberts B, Johnson A, Lewis J, et al. *Molecular Biology of the Cell*. 4th edition. New York: Garland Science; 2002. B adapted from http://csls-text.c.u-tokyo.ac.jp/active/06_01.html

1.2.2.1 Nucleation of actin polymerization --- Arp2/3 complex

Nucleation is the first step towards building a polymer. Although filamentous actin (F-actin) is common in cells, spontaneous nucleation of actin monomers is slow. During nucleation, free G-actin monomers only slowly form unstable trimeric nuclei. However once formed these nuclei initiate fast actin polymerization (Pollard, 1984). During migration, cells generate highly dynamic actin structures, therefore the spontaneous slow formation of actin nuclei needs to be speeded up. Cells have to overcome this strong kinetic barrier to rapidly produce actin filaments. Cells express specialised proteins that act as actin nucleators to speed up actin nucleation hence actin polymerisation. While many actin nucleators have been identified, Arp2/3 complex is a major nucleator in lamellipodia (Suraneni et al., 2012, Lai et al., 2008), invadopodia (Yamaguchi et al., 2005), podosomes (Kaverina et al., 2003) and pseudopods (Li et al., 2011).

Arp2/3 complex consists of seven subunits and was first identified as a profilin binding complex in *Acanthamoeba castellanii* (Machesky et al., 1994). Although five subunits of Arp2/3 complex, ARPC1-5, are unique in structure, two subunits, namely Arp2 and Arp3, are structurally similar to actin monomer (Robinson et al., 2001) (**Figure 1.5A**). These two subunits sit side by side in the active Arp2/3 complex (Boczkowska et al., 2008, Rouiller et al., 2008) (**Figure 1.5B**) and can serve as a readily available actin nucleus for polymerisation to reduce the kinetic barrier of actin nucleation. A G-actin monomer binds to the plus end of Arp3 to complete a full trimeric nucleus hence promoting rapid actin polymerisation. Additionally, as Arp2/3 complex binds to the minus end of a polymerising actin filament, it prevents ADP-bound actin monomer dissociating from the growing filament (Mullins et al., 1998).

Although Arp2 and Arp3 are critical for actin polymerisation, the other five subunits form a platform that binds to the side of an existing actin filament (**Figure 1.5B**) (Rouiller et al., 2008). This association of Arp2/3 complex with a pre-existing actin filament (mother filament) is important for the formation of branched actin network necessary for lamellipodium formation (**Figure 1.6A, B**). As new actin filaments (daughter filaments) branch at a 70-degree angle from mother filaments (Mullins et al., 1998), growing actin network pushes plasma membrane forward and expands the membrane laterally to generate the broad lamellipodia.

Conservation of each ARP family modeled on the structure of human actin

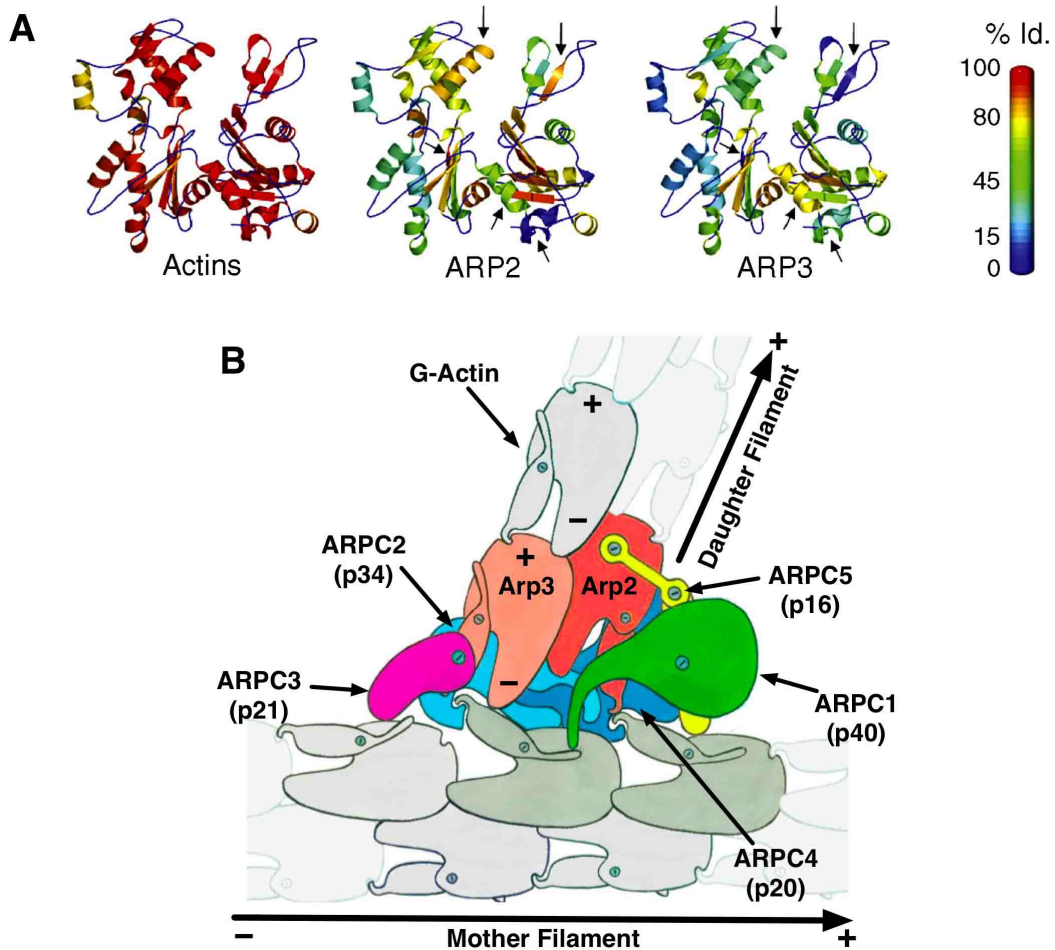


Figure 1.5 Structure of Arp2/3 complex

(A) Crystal structures show that Arp2 and Arp3 are structurally similar to actin monomer. (B) Cartoon shows an active Arp2/3 complex in association with a mother actin filament to initiate daughter filament formation. Due to the structure similarity, Arp2 & Arp3 are able to bind G-Actin leading to actin polymerisation, while ARPC1-5 prevents dissociation of actin from the minus end by forming a mother filament-binding platform. A adapted from (Dion et al., 2010). B adapted from (Rouiller et al., 2008)

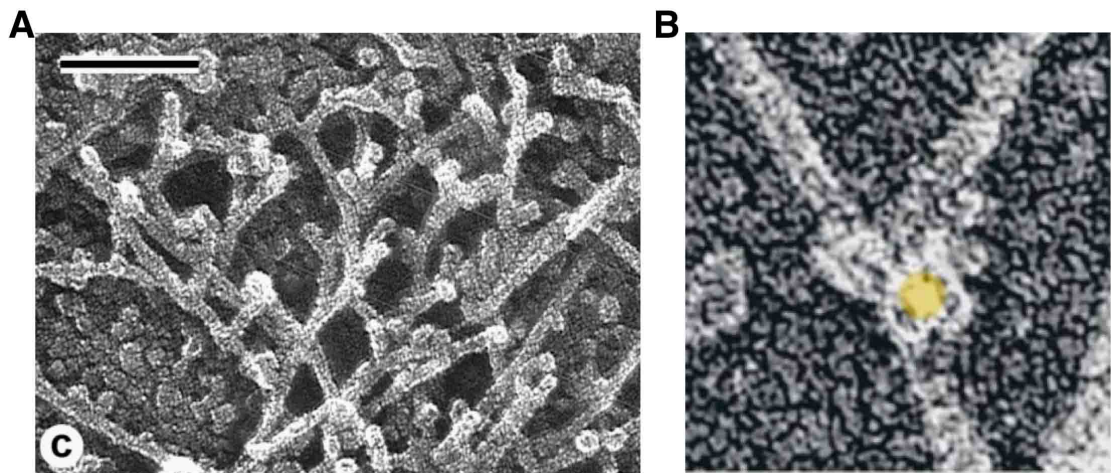


Figure 1.6 Branched actin network in lamellipodium

(A) Electron micrograph of branched actin network in lamellipodium of a mouse fibroblast. Scale bar, 0.1 μ m. (B) Localization of Arp2/3 complex at the actin branch (yellow dot). Figure adapted from (Svitkina and Borisy, 1999)

1.2.2.2 Regulation of Arp2/3 complex

Arp2/3 complex is a potent actin nucleator. Its activity must be tightly regulated to allow controlled actin polymerisation. The fact that purified Arp2/3 complex is inactive suggests additional activators are required (Machesky et al., 1999). Indeed, a number of nucleation-promoting factors (NPFs) are identified to activate Arp2/3 complex. The largest group of NPFs is Wiskott-Aldrich Syndrome Protein (WASP)-family proteins (Padrick and Rosen, 2010). Eight members of this protein family have been identified, namely, WASP, neural WASP (N-WASP) and Scar/WAVE 1,2,3, WASH, WHAMM, and JMY (**Figure 1.7A**) (Campellone and Welch, 2010). All WASP family members have an Arp2/3 complex activating verprolin central acidic domain (VCA or WCA) at the C-terminus (**Figure 1.7B**). Binding of VCA domain to Arp2/3 complex brings Arp2 and Arp3 into proximity to potentially activate the complex hence promoting actin polymerisation (Rodal et al., 2005). VCA domain contains three small motifs. WASP-homology 2 motif (V motif or WH2) binds to one actin monomer, and brings this actin monomer to Arp3 to initiate actin polymerisation. The central C motif and the acidic A motif also simultaneously interacts with other Arp2/3 complex subunits to stabilise the active complex (Boczkowska et al., 2008).

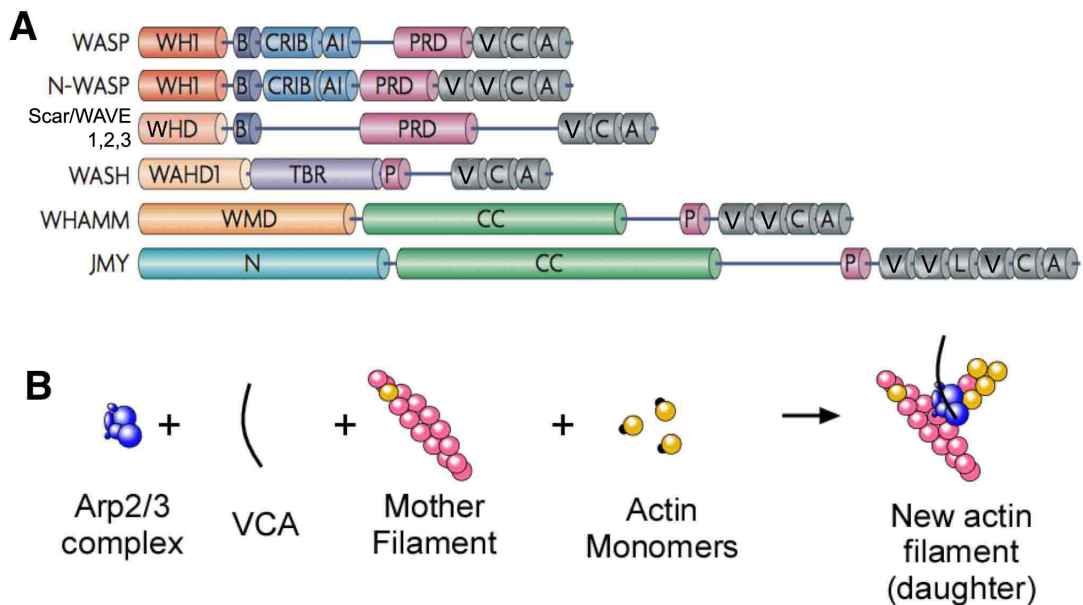


Figure 1.7 Wiskott-Aldrich Syndrome Protein (WASP) family proteins

(A) Domain structures of various WASP family proteins. (WH1, WASP homology 1; B, basic region; CRIB, Cdc42 and Rac interactive binding; AI, autoinhibitory domain; PRD, proline rich domain; VCA, verprolin central acidic domain; WHD, WAVE homology domain; WAHD1, WASH homology domain 1; TBR, tubulin binding region; WMD, WHAMM membrane interaction domain; CC, coiled-coil region; N, N terminus.) (B) VCA domain on WASP family proteins is used to activate Arp2/3 complex. A adapted from (Campellone and Welch, 2010). B adapted from <http://www.dayel.com/research/arp23-complex/>

In contrast, the N-terminus of WASP family proteins are not well conserved. Various regulatory domains are found on different WASP family proteins allowing different regulation of these proteins (**Figure 1.7A**). Regulatory domains on N-WASP and Scar/WAVE proteins are the most studied, while less is known about the function of N-terminal domains on other WASP family proteins. N-WASP can bind to the active small GTPase Cdc42 or Rac1 via N-terminal CRIB domain (Hemsath et al., 2005, Tomasevic et al., 2007). This direct interaction activates otherwise inactive N-WASP leading to Arp2/3 complex activation (Rohatgi et al., 1999). On the other hand, a regulatory protein complex associates with the N-terminus of Scar/WAVE proteins. Active small GTPase Rac binds to this complex removing the inhibitory effect to activate Arp2/3 complex (Eden et al., 2002). As small GTPases are important molecular switches in receptor activation, cell adhesion and other signalling events, Arp2/3 complex activation is tightly and specifically controlled by activation of small GTPases and corresponding WASP family proteins to generate unique actin structures.

1.2.3 Regulation and function of Nucleation-Promoting Factors

1.2.3.1 Scar/WAVE regulatory complex

Scar/WAVE (Scar) proteins are the major NPFs responsible for Arp2/3 complex activation in lamellipodium during cell migration on rigid surfaces. Human Scar1 protein was first identified in a yeast two-hybrid screening for Arp2/3 (ARPC3) interacting proteins (Machesky and Insall, 1998). Since then two human Scar proteins, namely Scar2,3, were also identified (Suetsugu et al., 1999). All Scar proteins share the same domain structure with Scar/WAVE Homology domain (WHD) at the N-terminus, followed by basic domain, and proline-rich domain (PRD), and VCA at the C-terminus (**Figure 1.7A**).

While purified Scar protein activates Arp2/3 complex in vitro (Machesky et al., 1999), Scar proteins exist in a pentameric complex consisting of four additional subunits, namely, Nap1, Sra1/PIR121, Abi1/2 and HSPC300. This Scar/WAVE regulatory complex (WRC) is inactive towards Arp2/3 complex, as Sra1 and the N-terminus of Scar protein sequester the Arp2/3 activating VCA domain on Scar proteins (Chen et al., 2010, Ismail et al., 2009).

A number of factors have been identified to activate WRC. The most noticeable ones are the small GTPase Rac1 (Chen et al., 2010, Eden et al., 2002) and negatively charged phospholipids (Lebensohn and Kirschner, 2009). Sra1 of WRC is believed to mediate the Rac1 binding. In fact, Sra1 was identified as the Specifically Rac-1-associated Protein in an attempt of finding novel Rac1 interacting proteins (Kobayashi et al., 1998). The latest crystal structure shows that Sra1 and Nap1 form a positively charged surface on one side of WRC. Current model of WRC activation suggests that this positively charged surface can interact with negatively charged phospholipids on the plasma membrane. As the Rac1 binding site is also located on this surface, simultaneous binding of Rac1 and negatively charged phospholipids is thought to trigger WRC conformational change to expose the VCA domain for Arp2/3 complex activation (**Figure 1.8**). As the opposite side of WRC is negatively charged, the exposed VCA domain faces away from the plasma membrane to interact with Arp2/3 complex (Chen et al., 2010).

Although Rac1 can bind to and activate WRC, the affinity of this binding is low (Chen et al., 2010). Therefore it is thought that additional factors might be required for sufficient WRC activation. In addition to Rac1, another small GTPase, Arf1, is also suggested to activate WRC. Using silica beads coated with a lipid bilayer (PIP3) to reconstitute actin polymerisation by WRC, Arf1 was identified to be required for Rac1 dependent activation of WRC. In this in vitro system Rac1 alone or Arf1 alone cannot sufficiently recruit recombinant WRC. However when both GTPases are present WRC is effectively recruited and activated. Interestingly, Arf1 also binds to the positively charged surface formed by Sra1 and Nap1 (Koronakis et al., 2011). Therefore, it is proposed that simultaneous binding of Rac1, Arf1 and negatively charged phospholipids activates WRC to the full potential. However, loss of Arf1 has no impact on lamellipodia formation (Boulay et al., 2008), and Arf1 localizes to trans-Golgi network (Anitei et al., 2010), WRC activation by Arf1 is possibly not essential in vivo.

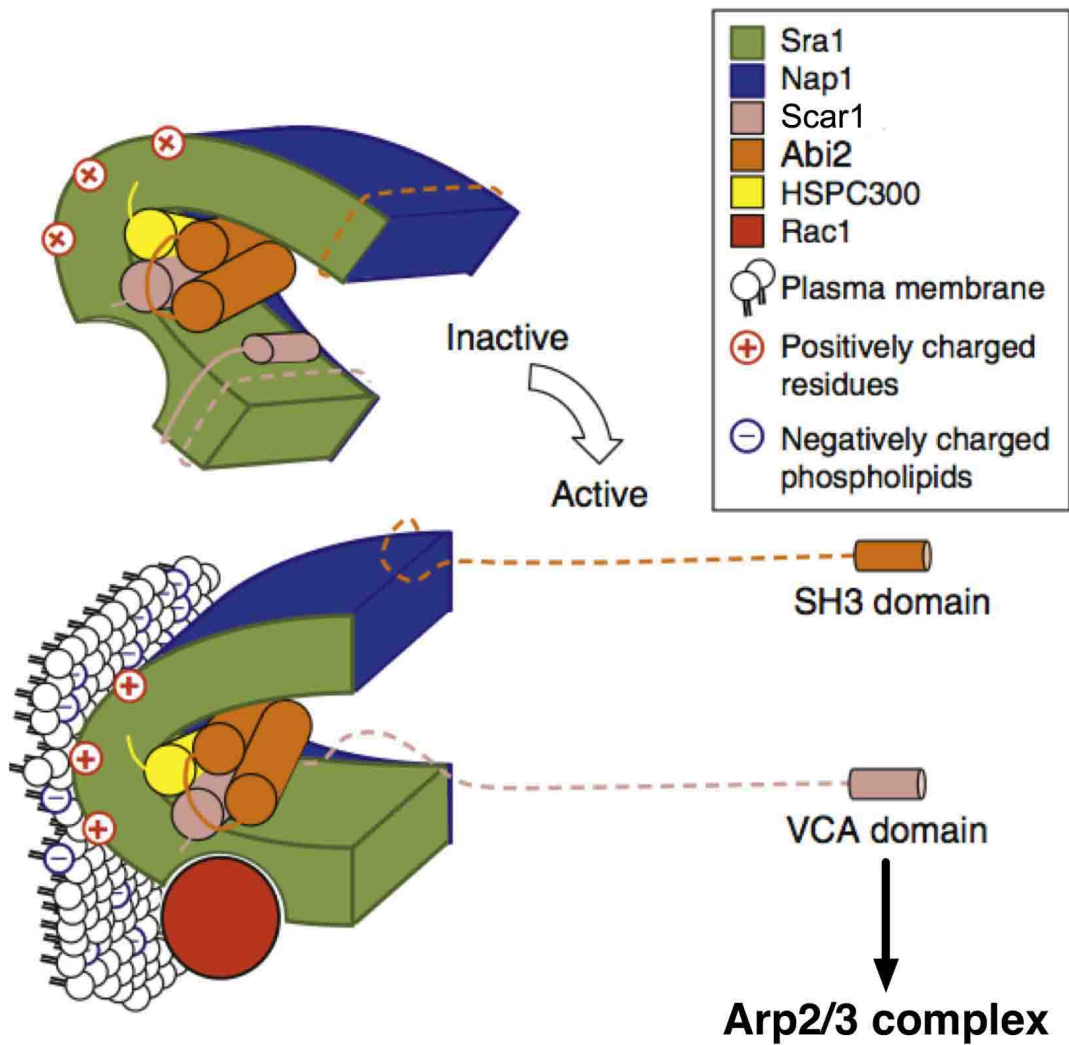


Figure 1.8 Model of WRC activation

Sra1 and Nap1 on WRC form a large positively charged surface. Together with Rac1 binding via Sra1, WRC interacts with the negatively charged plasma membrane. The interaction perhaps triggers WRC conformational change to expose Scar VCA to activate Arp2/3 complex. Figure adapted from (Davidson and Insall, 2011)

1.2.3.2 Biological functions of WRC subunits

All five subunits of WRC are required to make a stable complex. Deletion of any WRC components destabilises the whole complex leading to disruption of WRC function in many biological systems (Derivery et al., 2008, Silva et al., 2009, Kunda et al., 2003). It is therefore important to understand the biological function of each WRC subunit, so the function of whole WRC can be revealed.

1.2.3.2.1 Nap1

Nap1 (Nck associated protein 1) was first identified as a binding protein of Nck, which is an SH2 and SH3 domain containing adapter protein (Kitamura et al., 1996). This interaction between Nap1 and Nck is believed to help WRC activation by Rac1 (Eden et al., 2002, Kitamura et al., 1997). In vivo, loss of Nap1 prevents mouse anterior visceral endoderm cell migration that is important for specification of the anterior-posterior body axis in animals (Rakeman and Anderson, 2006). However, surprisingly, Nap1 is not expressed in actively migrating mouse neurons, and pre-mature expression of Nap1 suppresses cell migration in vivo (Yokota et al., 2007). In contrast, Nap1 is required for lamellipodia formation in cultured mammalian cells (Steffen et al., 2004) and for cell migration in *Dictyostelium* cells (Ibarra et al., 2006). Thus, apart from mouse neurons, Nap1 is required for lamellipodia formation and cell motility in multiple systems reflecting its role as part of WRC.

1.2.3.2.2 Sra1/PIR121

Sra1 is another important component of WRC required for complex activation (**Figure 1.8**) (Chen et al., 2010, Kobayashi et al., 1998). PIR121 is 88% identical to Sra1 and the Rac1 binding domain is conserved between the two proteins, so PIR121 may play a similar function as Sra1 in WRC. In cultured cells, Sra1 and Nap1 co-localizes to the leading edge to promote cell migration (Kunda et al., 2003, Steffen et al., 2004). However Sra1 is recently reported to act as an invasion suppressor in many human epithelial cancers (Silva et al., 2009). Therefore the impact of Sra1 on cell motility may be context dependent. In addition to cell migration, Sra1 and PIR121 are also involved in the biogenesis of clathrin-AP1

coated cargo transport at the trans-Golgi network presumably in the context of WRC, as Rac1, Arf1 and actin are involved in this process (Anitei et al., 2010).

Sra1/PIR121 are also known as CYFIP1/2 (cytoplasmic FMR1-interacting protein 1/2) respectively. They can interact directly with FMRP that is responsible for the fragile X mental retardation (Schenck et al., 2001). Sra1 (or CYFIP1) binds directly to both FMRP and the translation initiation factor eIF4E to inhibit translation initiation (Napoli et al., 2008). However in the crystal structure of WRC, eIF4E cannot fit to the putative binding site when Sra1 is in WRC suggesting Sra1 may regulate translation independently of WRC.

1.2.3.2.3 Abi proteins

Abi (Abelson interactor) proteins were first identified to interact with Abl tyrosine kinase (Dai and Pendergast, 1995, Shi et al., 1995). In Bcr-Abl induced leukemia, Abi1 is an important mediator of Bcr-Abl mediated cell transformation, as loss of Abi1 blocks Src kinase (Lyn) activation (Yu et al., 2008). However Abi1 is also an important component of WRC required for the formation and activation of WRC (Innocenti et al., 2004). Indeed, the latest crystal structure of WRC shows that the two helices at the N-terminus of Abi protein contribute to the core of WRC (Chen et al., 2010).

Interestingly, the SH3 domain at the C-terminus allows Abi1 to interact with N-WASP at a very high affinity as well (Innocenti et al., 2005). It is suggested that Abi1 modulates N-WASP activity during endocytosis and vesicle trafficking, as well as participates in WRC to regulate cell migration. As a result, despite being structurally important to WRC, Abi proteins are involved in distinct protein complexes to regulate different actin based processes. Nonetheless, loss of Abi1 in mouse embryos leads to migration and adhesion defects resulting in impaired vasculogenesis, angiogenesis and chorio-allantonic fusion (Dubielecka et al., 2011, Ring et al., 2011).

1.2.3.2.4 HSPC300

HSPC300 (haematopoietic stem cell protein 300) also known as Brick1 in plants was first identified to function with Scar protein and the Arp2/3 complex to regulate cell shape in *Arabidopsis* (Djakovic et al., 2006, Le et al., 2006). HSPC300 is the smallest subunit (9KD) of WRC consisting of only a short helix. However HSPC300 is crucial for the assembly of the whole WRC. Recent biochemical studies and crystal structures show that HSPC300 exists as homotrimers (a bundle of three HSPC300 helices) independently of the WRC. The structure of HSPC300 homotrimers resembles the core triple helices (one helix from HSPC300, one from Scar protein, and one from Abi protein) found in fully assembled WRC. HSPC300 homotrimers serve as a platform for WRC assembly where two of the HSPC300 helices are gradually replaced by one helix from Abi and one helix from Scar. The assembly is completed when Sra1 and Nap1 are recruited to the core through their direct interactions with Scar and Abi (Derivery et al., 2008, Linkner et al., 2011, Chen et al., 2010).

As part of the WRC, HSPC300 is required for generation of membrane protrusions (Derivery et al., 2008, Escobar et al., 2010). HSPC300, together with other WRC subunits, controls axonal and neuromuscular junction growth in *Drosophila* neuron system (Qurashi et al., 2007). Loss of HSPC300 in *Dictyostelium* cells leads to loss of Scar protein and migration defects suggesting a biological role of HSPC300 within WRC (Pollitt and Insall, 2009). However in mouse embryos loss of HSPC300 also triggers apoptosis in addition to migration defect implying HSPC300 also regulates cell survival (Escobar et al., 2010).

1.2.3.2.5 Scar proteins

Scar proteins are the subunit of WRC responsible for Arp2/3 complex dependent actin nucleation (Chen et al., 2010). There are three Scar proteins in mammalian cells. Interestingly, Scar1, Scar2 and Scar3 are found to localize differently in growth cones of cultured neural cells. In these cells, Scar1 localizes exclusively to the leading edge of lamellipodia, while Scar2/3 can also localise to tips of filopodia suggesting differential regulation or activation of WRC varieties (**Figure 1.9**) (Nozumi et al., 2003).

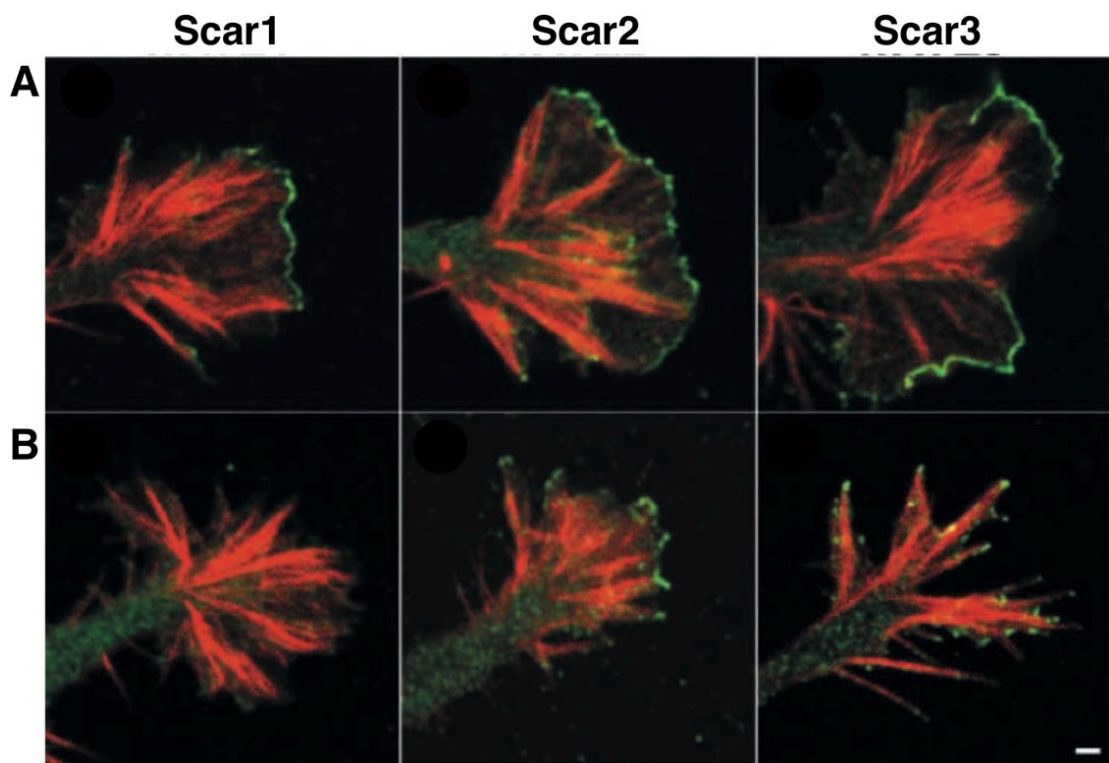


Figure 1.9 Differential localization of Scar proteins

(A) All three Scar proteins localizes to lamellipodia of neuronal growth cones. (B) Unlike Scar2&3, Scar1 does not localize to tip of filopodia tips. Scar proteins are GFP labelled (green). Actin is shown as rhodamine phalloidin staining (red). Figure adapted from (Nozumi et al., 2003). Scale bar 1 μ m.

In vivo, Scar2 is widely expressed in all tissues, low Scar3 expression is detected in many tissues and the expression is highest in brain (Sossey-Alaoui et al., 2002). Scar1 expression is however limited to adult human and mouse central nervous system (CNS) (Dahl et al., 2003). Although Scar1 is expressed in the entire mouse embryo at the early stage of development (all human fetal tissues too), as the embryo matures, Scar1 expression is restricted to CNS. Scar1 knockout mice do

not have anatomical abnormalities but the cerebral cortex is reduced suggesting Scar1 is only required for early CNS development. However neurons without Scar1 have normal morphology with polarized apical dendrites (Dahl et al., 2003). Similarly, Scar1 knockout mouse embryonic fibroblasts are also able to generate normal membrane protrusions and migrate normally, but Scar2 is required for membrane protrusion formation and migration in the same cells (**Figure 1.10**) (Suetsugu et al., 2003). Scar2 knockout in mouse is embryonic lethal despite Scar1 expression suggesting a non-redundant role of Scar2 during development. Although Scar3 localizes to lamellipodia (Stovold et al., 2005, Nozumi et al., 2003), it is the least studied Scar protein and the exact function of Scar3 remains to be explored.

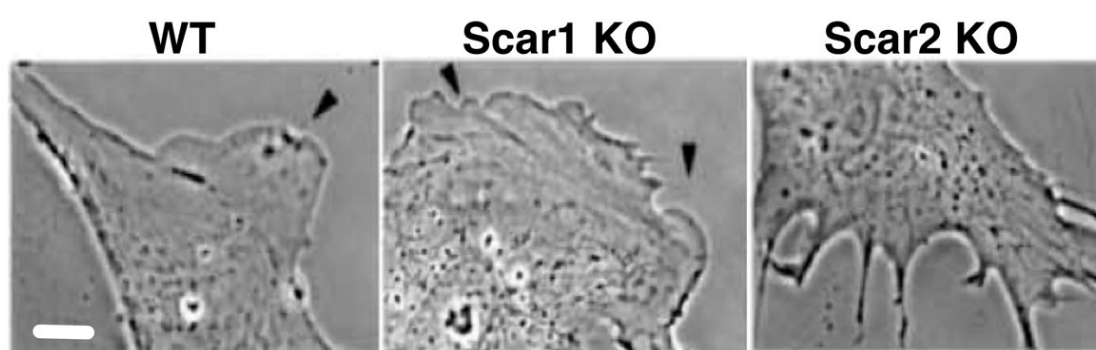


Figure 1.10 Lamellipodia formation requires Scar2

Scar2, not Scar1, is required for lamellipodia formation in mouse embryonic fibroblasts. Figure adapted from (Suetsugu et al., 2003). Scale bar 10µm.

1.2.3.3 WASP & N-WASP

WASP was first identified as a novel gene mutated in immunodeficiency disorder Wiskott-Aldrich Syndrome (WAS) (Derry et al., 1994). WASP expression is hematopoietic specific. WASP was found to be important for podosome formation in human macrophages (Linder et al., 1999), and in megakaryocytes (Sabri et al., 2006). Macrophages isolated from most WAS patients have no functional WASP, and cannot form podosomes (Linder et al., 1999). In contrast, WASP homolog N-WASP (Neural WASP) was first identified in a screening for Ash/Grb2 binding proteins (Miki et al., 1996). Despite being highly enriched in brain (hence the name), N-WASP is ubiquitously expressed. Similar to WASP, N-WASP also localises to podosomes in macrophages, however N-WASP does not contribute to

podosome formation. Instead, loss of N-WASP renders podosomes non-degradative, as one major metalloprotease, MT1-MMP, is no longer recruited (Nusblat et al., 2011). N-WASP is also involved in intra-cellular motility of many microbes (Suzuki et al., 1998, Dodding and Way, 2009), and clathrin mediated endocytosis (Benesch et al., 2005). Although N-WASP was reported to be required for filopodia formation (Miki et al., 1998), recent studies suggest otherwise. As Arp2/3 complex is not required for filopodia formation (Suraneni et al., 2012, Steffen et al., 2006), the role of N-WASP mediated Arp2/3 complex activation in filopodia formation remains controversial.

WASP and N-WASP share the same domain structure (**Figure 1.7A**). Both proteins are auto-inhibited. The intramolecular interaction between VCA domain and CRIB domain leads to auto-inhibition of the proteins (**Figure 1.11**). The surface of CRIB domain interacts with the C motif of VCA, hence reducing WASP/N-WASP VCA's affinity towards Arp2/3 complex. The N-terminal basic region on N-WASP also interacts with the acidic VCA domain contributing to the auto-inhibition of N-WASP. The X-ray crystal structure of inactive N-WASP shows that the inactive molecule is folded on itself preventing the VCA from interacting with Arp2/3 complex. (Kim et al., 2000, Miki et al., 1998).

This intramolecular auto-inhibition can be relieved by interaction with active Cdc42 (**Figure 1.11**) (Kolluri et al., 1996). Binding of Cdc42 to the CRIB domain activates WASP and N-WASP by causing a dramatic conformational change hence the release of VCA domain (Kim et al., 2000). Additionally, the basic region can also interact with negatively charged phospholipid, PIP₂, on the plasma membrane (**Figure 1.11**). This interaction with PIP₂ greatly enhances Cdc42 dependent activation of N-WASP (Higgs and Pollard, 2000). Interestingly, using purified autoinhibited human WASP and N-WASP, Rac1 was identified to exclusively activate N-WASP. This N-WASP activation by Rac1 is more potent than Cdc42 activation of N-WASP. It is therefore suggested that Cdc42 is the major activator of WASP, while Rac1 activates N-WASP (Tomasevic et al., 2007).

N-WASP is phosphorylated at multiple residues to sustain its activation. Src family kinases (Fyn) bind to and phosphorylate N-WASP at Tyr256 (Tyr291 on WASP), which lies just after the CRIB domain (Banin et al., 1996). However the

phosphorylation can only happen after N-WASP activation by Cdc42, i.e. when the folded molecule is open. In this open (active) confirmation, the tyrosine residue is exposed to Src family kinases leading to phosphorylation (Cory et al., 2002). Interestingly, once phosphorylated, even when Cdc42 activation is terminated, pTyr291 WASP remains activated towards Arp2/3 complex, as this phosphorylation introduces negative charge to CRIB domain region blocking auto-inhibition of N-WASP (Suetsugu et al., 2002, Banin et al., 1996). As a result N-WASP phosphorylation by Src family kinases sustains the activation status by preventing auto-inhibition (Torres and Rosen, 2003). Similarly, focal adhesion kinase (FAK) also binds to N-WASP directly leading to N-WASP phosphorylation at Tyr256 to enhance N-WASP activities and N-WASP membrane localisation (Wu et al., 2004).

In addition to Cdc42 activation of N-WASP, the Nck adapter protein is reported to activate N-WASP independently of Cdc42 (**Figure 1.11**). Nck SH3 domains bind directly to the proline rich motif of WASP/N-WASP (Rivero-Lezcano et al., 1995, Rohatgi et al., 2001). In the presence of PIP₂, Nck activates N-WASP to promote Arp2/3 dependent actin polymerisation. All three SH3 domains of Nck are required for maximum activation of N-WASP (Rohatgi et al., 2001). This multivalent interaction has recently been shown to promote N-WASP-Nck polymer formation, which triggers Arp2/3 complex activation in vitro. In cells with the help of a transmembrane protein nephrin, N-WASP-Nck complex is organised into a platform that resembles N-WASP-Nck polymer under the plasma membrane to activate Arp2/3 complex (Li et al., 2012).

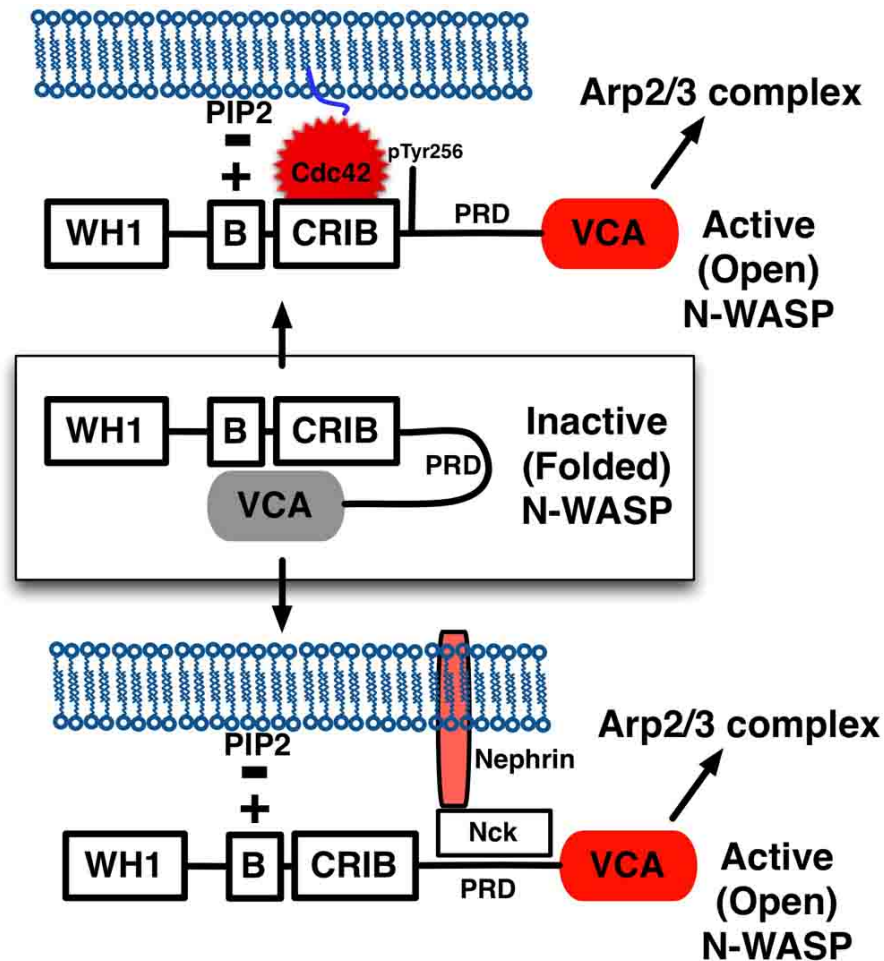


Figure 1.11 Model of N-WASP activation

Before activation CRIB (Cdc42 and Rac interactive binding) domain and the basic region (B) bind to N-WASP or WASP VCA preventing Arp2/3 complex binding. The protein is now autoinhibited in a folded conformation. Interaction with Cdc42 or Rac1 to CRIB domain relieves the inhibitory effects through conformational change that opens up the protein allowing VCA binding to Arp2/3 complex. This process is greatly enhanced by PIP2 binding via the basic region. Alternatively, together with PIP2 multiple Nck adaptor proteins bind to N-WASP proline rich region (PRD) to promote N-WASP activation. Finally, N-WASP activation is also sustained by phosphorylation that prevents CRIB domain binding to VCA. WH1, WASP homology 1; VCA, verprolin central acidic domain.

1.3 Adhesion and cell migration

When actin polymerisation pushes the plasma membrane forward to drive cell migration, small cell-ECM adhesions are formed at the leading edge. They are the first adhesions to anchor the advancing membrane to the substrate. Otherwise, without adhesion, the protruding membrane folds back to the dorsal surface of the cell resulting in membrane ruffles without productive forward cell movement (Borm et al., 2005). As the cell moves, these adhesions mature into bigger adhesions and are now located towards the rear of a moving cell. Large, mature adhesions are usually associated with strong contracting actin stress fibres. As a result, mature adhesions can serve as traction points for cell translocation. However effective cell migration requires proper coordination of adhesion formation and disassembly. Old strong adhesions must be disassembled when cell body contracts to release the moving cell from the substrate. Collectively, when new adhesions are formed at the front, old mature adhesions are disassembled at the rear of a migrating cell releasing the contracting tail, and allowing the translocation of the cell body.

Depending on the size, stability and location, various cell-ECM adhesions are found in motile cells, including nascent adhesions, focal complexes and focal adhesions (Parsons et al., 2010). Nascent adhesions are small short-lived adhesions formed just behind the lamellipodium leading edge (Choi et al., 2008). As the leading edge moves forward, nascent adhesions mature into slightly bigger focal complexes, which now localise at the lamellum of the advancing lamellipodium. Both nascent adhesions and focal complexes serve to anchor the advancing lamellipodium to ECM. As a result, expanding membrane is stabilised at the front of a migrating cell.

Cell-ECM adhesions also conduct forces required for cell migration. In migrating Goldfish fin fibroblasts, small nascent adhesions near the leading edge apply strong traction force to drive cell migration. Focal complexes can further mature into bigger, and more stable focal adhesions, which are associated with large stress fibres (Rottner et al., 1999). Although the propelling force increases briefly at the initiation of focal adhesion maturation, the force eventually decreases to a basal level in migrating cells (Beningo et al., 2001). In contrast, in stationary cells,

the strength of traction force is correlated with the size of focal adhesions. The strong force associated focal adhesions in this case can deform an elastomeric substrate (Balaban et al., 2001, Fraley et al., 2010).

At least in fish keratinocytes, migrating cells generate about 40nN force (Prass et al., 2006, Oliver et al., 1995). It is thought that this force is far greater than the actual force required for cell migration. Cells may therefore use the extra force for other functions. When cells migrate on a 2D elastic surface, the excessive force causes deformation of the soft substrate suggesting the force could be used for ECM remodelling. This is particularly important for cells migrating in 3D matrices where active remodelling of the ECM matrix is required to achieve effective motility (Ehrbar et al., 2011, Friedl and Wolf, 2009, Fraley et al., 2010). Fibroblasts deform surrounding matrix when embedded in polyethylene glycol hydrogel. Interestingly, in this 3D environment, strong traction force is associated with long membrane extensions, while the cell body exert less force (Legant et al., 2010). It is therefore suggested that cells could probe and remodel surrounding matrix through strong traction forces near the tip of long membrane extensions (Legant et al., 2010). In cancer cells, depending on cell types, high traction forces could contribute to better invasion in collagen gels (Koch et al., 2012). In tissue, traction forces exerted by fibroblasts are required for collagen remodelling during wound healing leading to increased tissue stiffness and wound contraction (Tomasek et al., 2002). Finally, focal adhesions are recently observed in cells cultured in 3D collagen gel (Kubow and Horwitz, 2011). It is likely that focal adhesions could conduct the traction force in 3D.

1.3.1 Adhesion Formation

All cell-ECM adhesions are integrin based. Integrin family proteins are a group of heterodimeric (α and β subunit) trans-membrane proteins. Structural studies reveal that inactive integrin heterodimers exist in a 'bent' or close conformation. In this conformation, the extracellular ligand binding domains face toward the plasma membrane making ligand binding unfavourable. In this close conformation cytoplasmic tails of α and β integrins interact between membrane proximal regions to stabilize the heterodimer in an inactive low affinity state (Beglova et al., 2002, Takagi et al., 2002, Takagi et al., 2001). Mutations that disrupt the cytoplasmic tail interaction at membrane proximal regions activate integrins (O'Toole et al., 1994). Talin is believed to play an important role in integrin activation, as it binds to the membrane proximal regions of integrin cytoplasmic tails leading to cytoplasmic tail separation. Consequently, transmembrane domains of the heterodimer are unclasped leading to extension of the extracellular ligand binding domains in a switchblade-like fashion. In this extended conformation, integrin heterodimers have high ligand binding affinity. Subsequent ligand binding leads to full activation of integrins. (Tadokoro et al., 2003, Banno and Ginsberg, 2008, Carman and Springer, 2003). Once activated, the exposed cytoplasmic tail interacts directly with many adhesion proteins (typically vinculin and α -actinin, in addition to talin) that link integrin to actin cytoskeleton hence the formation of actin based cell-ECM adhesions (**Figure 1.12**) (Vicente-Manzanares et al., 2009).

During expansion of lamellipodium, integrins are first engaged with ECM at the leading edge. Short-lived nascent adhesions form just under the expanding lamellipodium. These early adhesions are not associated with contractile actin stress fibres and their formation is independent of myosin II, hence little contraction can occur. However Arp2/3 complex mediated actin polymerisation is required for nascent adhesion formation (Choi et al., 2008).

As the lamellipodium expands, nascent adhesions either disassemble when actin depolymerises or mature into focal adhesions at the back of the lamellipodium. Maturation of nascent adhesions depends on actin cross-linking activity of α -actinin and myosin II, and is associated with formation of actin stress fibres. Although the mechanism of nascent adhesion maturation is not completely known, it is thought that myosin II bundles actin causing accumulation of α -actinin and

other adhesion molecules (e.g., talin, vinculin) that link integrin to actin fibres. The clustering of adhesion proteins therefore leads to elongation and growth of nascent adhesions into focal adhesions (Choi et al., 2008). These mature focal adhesions can now serve as traction points as associated actin stress fibres contract under the control of myosin II. As a result of the contraction, the cell body is pulled forward.

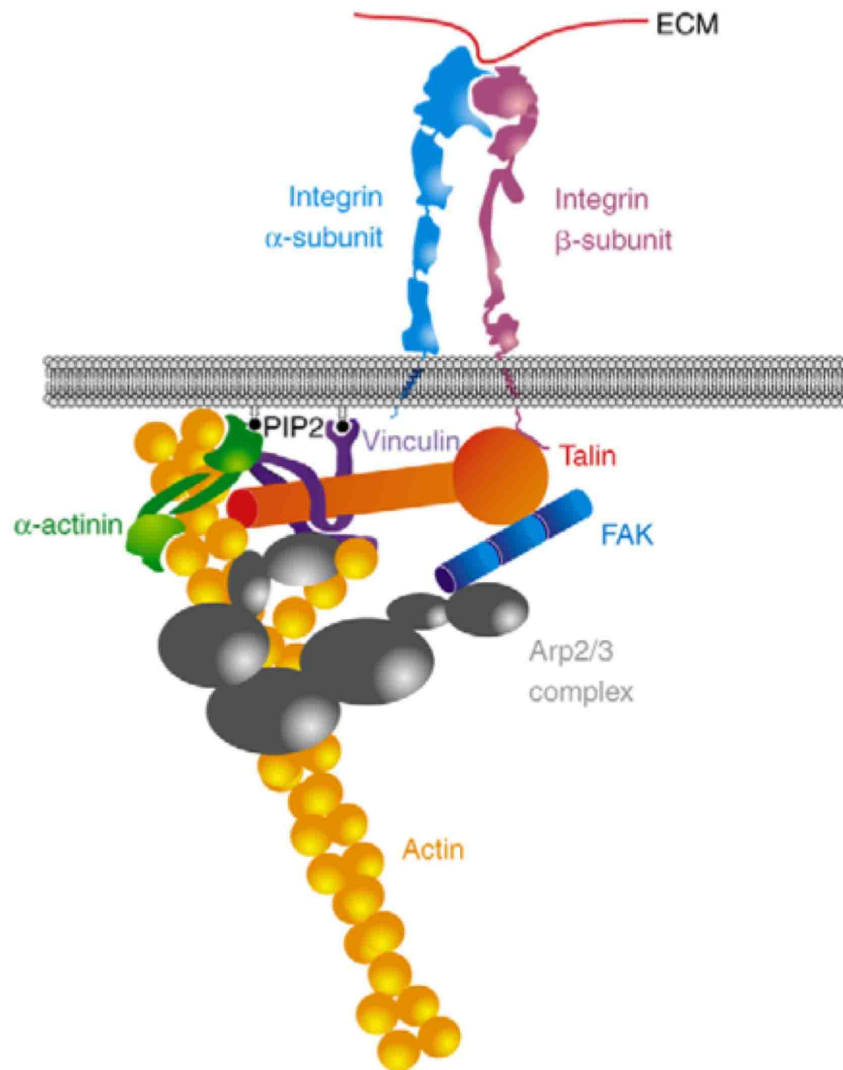


Figure 1.12 Integrin based adhesion

Integrin links ECM to Arp2/3 complex polymerised actin filaments at adhesion sites via actin binding adaptor proteins, talin, vinculin and α -actinin. Adhesion regulatory protein, focal adhesion kinase (FAK) is also recruited through multiple interactions with the adhesion assembly. Figure adapted from (Vicente-Manzanares et al., 2009)

1.3.2 Adhesion Signalling

Cell-ECM adhesions physically anchor cells to the substrate and provide part of the mechanical force for cell migration. These adhesions are also important sites of active signalling where external signals are conducted into cell to regulate cell proliferation, survival, growth and motility. Meanwhile, internal signals are also transmitted to integrins to regulate adhesion affinity and dynamics (Ginsberg et al., 2005). Upon clustering and activation of integrin dimers, talin and α -actinin binds directly to β -integrin tails and actin filaments to establish the structural core of focal adhesions (Liu et al., 2000). Adaptor proteins, vinculin and paxillin, and signalling proteins, focal adhesion kinase and Src kinases are then recruited to early adhesions. This process of adhesion formation triggers conformational changes in many adaptor proteins leading to exposure of protein binding sites, which then lead to extensive protein-protein interactions (Wozniak et al., 2004, Petit and Thiery, 2000). At the same time, focal adhesion kinase and other kinases are also recruited and activated upon adhesion formation resulting in phosphorylation of multiple proteins (Parsons et al., 2000). Collectively, adaptor proteins and adhesion-associated kinases initiate important signalling events upon integrin activation and adhesion formation to control various aspects of cell biology, including cell proliferation, cell survival, and cell migration. (Zaidel-Bar et al., 2007, Schwartz and Assoian, 2001, Stupack and Cheresch, 2002, Vicente-Manzanares et al., 2009).

1.3.3 Focal Adhesion Kinase Signalling

While many adaptor proteins and signalling proteins are important to adhesion signalling, focal adhesion kinase (FAK) is one of the major mediators of integrin signalling in the regulation of cell migration, invasion, proliferation and survival (Schlaepfer et al., 1999, Wozniak et al., 2004). FAK consists of five major domains, namely, FERM domain, kinase domain, two proline rich domains (PR2&3), and focal adhesion targeting (FAT) domain (**Figure 1.13**). As a cytoplasmic tyrosine kinase, the kinase domain is critical to the kinase activity of FAK, while FERM domain and FAT domain are important sites for protein-protein interactions (Mitra et al., 2005).

FAK is auto-inhibited. Clustering of FAK at adhesion sites triggers auto-phosphorylation of FAK at Tyr397, which activates the otherwise auto-inhibited FAK (Toutant et al., 2002). This auto-phosphorylation of FAK at Tyr397 (pY397FAK) creates a high-affinity binding site for Src family kinases. Binding of Src kinases to pY397FAK also promotes and enhances Src kinase activation. Within the transient FAK-Src kinase complex, active Src kinase can further phosphorylate FAK at the activation loop of kinase domain (Tyr576 and Tyr577), and at the FAT domain (Tyr861 and Tyr925). These Src dependent phosphorylations enhance FAK kinase activity to the maximum and promote signalling transductions via various protein-protein interactions (**Figure 1.13**) (Mitra et al., 2005).

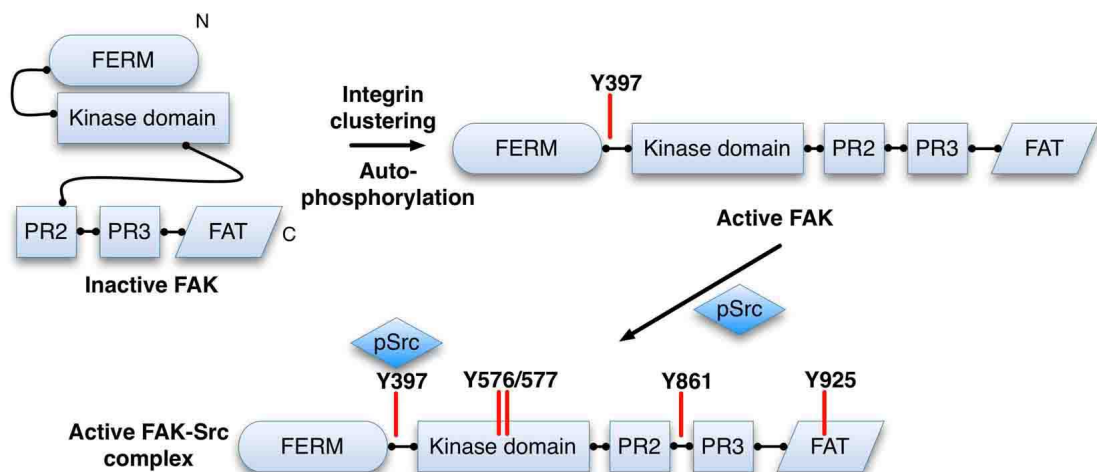


Figure 1.13 Focal adhesion kinase activation

FAK is activated by auto-phosphorylation that is thought to happen upon integrin clustering. Phosphorylation of FAK Tyr397 relieves the inhibitory effects of FAK FERM domain on the kinase domain, and creates a binding site for Src kinase, which can further phosphorylate FAK at multiple sites. Collectively, these phosphorylated tyrosines on FAK provide multiple docking sites for additional protein interactions. FERM, 4.1 protein, Ezrin, Radixin, Moesin; PR, proline rich; FAT, focal adhesion targeting.

While it is well known that phosphorylation on Tyr397 and Tyr576/577 activates FAK, the precise mechanism of FAK auto-inhibition and activation has only been recently explored (Lietha et al., 2007). In auto-inhibited FAK, the FERM domain interacts with the kinase domain directly preventing auto-phosphorylation of Tyr397. Binding of an activator protein can trigger a conformational change in the FERM domain leading to the exposure of Tyr397. However the activator has yet to

be investigated. It is speculated that the direct interaction of FERM domain with the cytoplasmic tail of β integrins (Guan and Shalloway, 1992, Schaller et al., 1992) or growth factors (Sieg et al., 2000) could mediate the conformational change. Nonetheless, once the FAK FERM domain is released from the kinase domain, FAK Tyr397 is exposed and rapidly auto-phosphorylated. Src mediated phosphorylation of Tyr576/577 on the activation loop of the kinase domain then leads to further exposure of the catalytic centre resulting in full activation of FAK. Phosphorylation of Tyr576/577 also prevents the FERM domain from binding to the kinase domain, thereby blocking autoinhibition (Lietha et al., 2007).

1.3.3.1 Migration and Invasion

The now fully phosphorylated FAK controls a number of signalling pathways. Src phosphorylation of FAK at Tyr861 (Calalb et al., 1996) increases the SH3 domain mediated binding of p130Cas docking protein to the FAK proline rich domains (PR2&3) (Lim et al., 2004), allowing tyrosine phosphorylation of p130Cas by Src kinase (Sharma and Mayer, 2008) (**Figure 1.14**). To regulate cell migration, phosphorylated p130Cas triggers Rac activation by forming a complex with adapter protein Crk and Rac guanine nucleotide exchange factor (GEF) DOCK180 at the adhesion sites (Sakai et al., 1994, Cote and Vuori, 2007). This localised activation of Rac promotes lamellipodial extension and cell migration presumably through activation of WRC. In addition to cell migration, FAK-p130Cas has also been recently shown to promote formation of degradative focal adhesions, where metalloprotease MT1-MMP is recruited to adhesion sites by FAK-p130Cas (Wang and McNiven, 2012). The finding of degradative focal adhesions therefore provides a mechanistic explanation for the pro-invasive role of FAK and p130Cas (Cunningham-Edmondson and Hanks, 2009).

1.3.3.2 MAPK/Erk pathway

Src phosphorylation of FAK at Tyr925 also leads to binding of SH2-domain containing adaptor protein Grb2 (Schlaepfer et al., 1994, Schlaepfer and Hunter, 1996) (**Figure 1.14**). While the Grb2 SH2 domain interacts with the phospho-tyrosine on FAK, the two SH3 domains bind to SOS, which is a Ras GEF.

Activated SOS now removes GDP from Ras small GTPase allowing Ras binding to GTP and subsequent Ras activation. The protein kinase activity of Raf kinase is then activated by active Ras leading to initiation of the mitogen activated protein (MAP) kinase cascade (Howe et al., 1992, Pearson et al., 2001).

At the end of the cascade, a member of the conserved family of MAP kinases (MAPK), Erk1/2, is phosphorylated and activated. Erk1/2 can then interact with and activate ribosomal protein S6 kinases (RSKs). Activation of RSKs subsequently leads to cell proliferation, cell survival, cell migration and invasion either by subsequent interactions with eukaryotic translation initiation factors in the cytosol, or through interactions with transcriptional factors in the nucleus (Hauge and Frodin, 2006, Doehn et al., 2009). Alternatively, active Erk1/2 can enter the nucleus to regulate more transcription factors, for example, Myc is stabilized by phosphorylation, and resulting in change of gene expression (Sears et al., 1999, Sears et al., 2000). Erk1/2 can also regulate translation by phosphorylating and activating MAPK interacting kinase (MNK)1/2 which regulates the eukaryotic translation initiation factor 4E (eIF4E) (Fukunaga and Hunter, 1997, Walsh and Mohr, 2004). Consequently, adhesion induced activation of Erk1/2 through FAK and MAP kinase cascade is important for cell proliferation, survival and motility.

1.3.3.3 PI3K/Akt pathway

Integrin dependent FAK activation also controls cell viability pathways and cell migration through PI3K/Akt (**Figure 1.14**). Auto-phosphorylation of FAK on Tyrosine 397 upon integrin clustering leads to direct interaction with the p85 subunit of PI3K. This direct interaction then leads to increased tyrosine phosphorylation of the p85 subunit (Chen and Guan, 1994, Xia et al., 2004). Phosphorylation of the p85 subunit activates the p110 catalytic subunit of PI3K leading to production of PI(3,4,5)P3 and PI(3,4)P2 on the plasma membrane (Klippel et al., 1994, Yu et al., 1998, Cuevas et al., 2001). Phosphoinositide dependent kinase 1 (PDK1) is then activated by these inositol phospholipids. PDK1 later activates Akt by direct phosphorylation leading to the activation of PI3K/Akt pathway (Cantley, 2002). Similar to MAPK/Erk pathway, PI3K/Akt pathway is also well known to regulate cell proliferation, survival (Franke et al., 2003) and cell migration (Kim et al., 2001, Enomoto et al., 2005). Collectively, fully

activated FAK plays an important role on regulating various aspects of cell biology by the activation of MAPK and PI3K/Akt pathways.

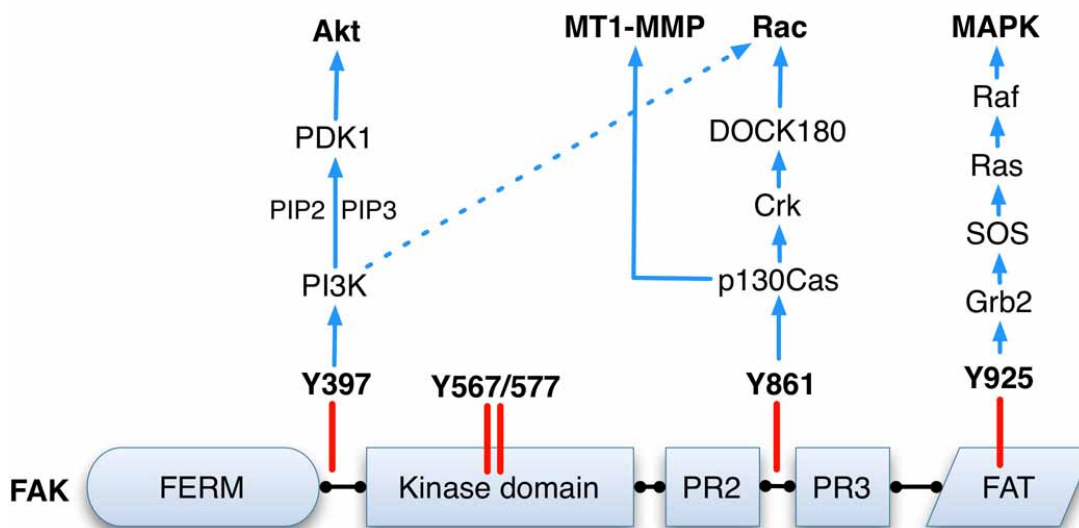


Figure 1.14 FAK mediated signalling cascades

Active FAK serves as a scaffold to interact with many signalling proteins to regulate various aspects of cell biology. Docking of PI3K on phospho-Y397 leads to subsequent activation of Akt and Rac. Similarly, phospho-Y861 mediated interaction with p130Cas leads to MT1-MMP recruitment to focal adhesions and Rac activation. MAPK signalling cascade is otherwise initiated by phosphorylation on FAK Y925. Together all the FAK mediated signalling events regulate cell proliferation, cell survival, migration and invasion. FERM, 4.1 protein, Ezrin, Radixin, Moesin; PR, proline rich; FAT, focal adhesion targeting.

1.3.3.4 Adhesion Disassembly

FAK also regulates the disassembly of focal adhesions through FAK dependent signalling pathways. Active FAK is believed to regulate focal adhesion turnover, as FAK knockout cells have large stable peripheral adhesions (Webb et al., 2004). It is also known that microtubule targeting to focal adhesions is required for adhesions disassembly (Kaverina et al., 1999, Kaverina et al., 1998). A microtubule associated large GTPase, dynamin, is required in this process to remove integrins from adhesions by endocytosis (Obar et al., 1991, Maeda et al., 1992, Ezratty et al., 2005). Interestingly, active FAK is involved in this microtubule

dependent process by recruiting dynamin to focal adhesions. However the interaction between FAK and dynamin is not direct, adaptor protein Grb2 binds to phosphorylated Try925 on FAK and to dynamin, therefore bridging active FAK to dynamin (Ezratty et al., 2005).

1.4 Arp2/3 complex, NPFs, and Adhesions

1.4.1 Arp2/3 complex and adhesion

Although it is known that lamellipodia are important for the formation of new adhesions, the coupling of molecular mechanisms that control membrane expansion and adhesion formation is not well studied. The major driving force of membrane expansion at the leading edge is Arp2/3 complex mediated actin polymerisation. While Arp2/3 complex mostly localises to the leading edge, it also transiently localises to new adhesions (**Figure 1.15**) (DeMali et al., 2002). It is known that active Rac induces formation of nascent adhesions at the leading edge (Nobes and Hall, 1995). As Rac leads to Arp2/3 complex activation through WRC, it is possible that Arp2/3 complex dependent actin polymerisation is required for proper adhesion assembly. Indeed, loss of Arp2/3 complex leads to altered adhesion assembly and disrupted global adhesion alignment. Importantly, in cells without Arp2/3 complex the haptotaxis response to various ECM concentrations is abolished, as these cells are now unable to sense ECM gradient through their adhesions. These findings suggest that Arp2/3 complex mediated actin polymerisation is required for proper adhesion assembly and proper integrin signalling during cell migration (Wu et al., 2012).

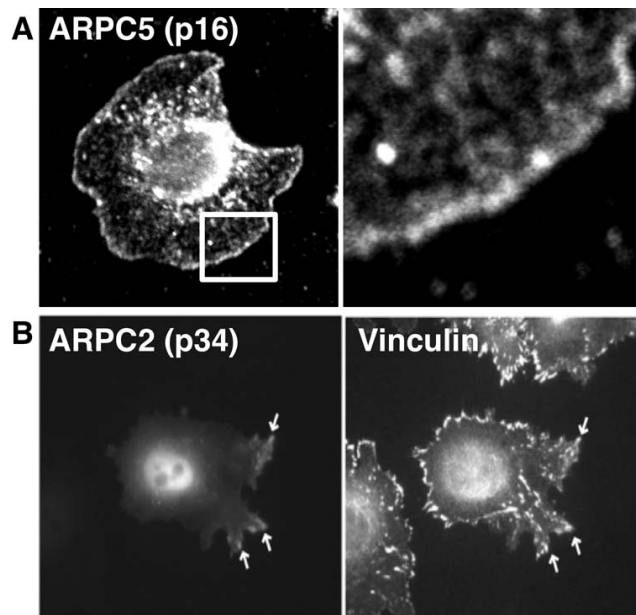


Figure 1.15 Arp2/3 complex localizes to new adhesions

(A) Arp2/3 complex as labelled by ARPC5 localizes mostly to the leading edge of lamellipodia. (B) However Arp2/3 complex also transiently localizes to vinculin labelled adhesions. B adapted from (DeMali et al., 2002)

On the other hand, adhesions can also actively regulate Arp2/3 complex. Rac is locally activated at adhesions in response to integrin activation by FAK/p130Cas/Crk/DOCK180, and alternatively by FAK/PI3K (**Figure 1.14**). This active Rac could locally activate Arp2/3 complex. In fact, Rac activated Arp2/3 complex is reported to interact with vinculin (a focal adhesion protein that interacts with talin, α -actinin and actin) directly (DeMali et al., 2002). This recruitment of active Arp2/3 complex to early adhesions can perhaps promote local actin assembly leading to maturation of nascent adhesions.

Additionally, FAK interacts with Arp2/3 complex directly via its FERM domain (Serrels et al., 2007). This interaction is necessary for normal cell spreading and actin polymerisation, as disruption of FAK/Arp2/3 complex leads to lack of membrane protrusions. FAK also moderately promotes Arp2/3 complex activation directly through its FERM domain. Notably, FAK only interacts directly with Arp2/3 complex in an auto-inhibited status, as FAK auto-phosphorylation at Tyr397 disrupts Arp2/3 complex binding to FAK FERM domain (Serrels et al., 2007). Therefore there are two possible ways that FAK can regulate Arp2/3 activation.

Firstly, auto-inhibited FAK directly promotes Arp2/3 complex activation prior to FAK auto-phosphorylation that can subsequently lead to the release of active Arp2/3 complex. Secondly, fully activated FAK regulates Arp2/3 complex indirectly through Rac activation. Collectively, both mechanisms can lead to Arp2/3 complex dependent membrane protrusion formation, or subsequent active Arp2/3 complex binding to vinculin to promote adhesion formation. FAK therefore couples membrane protrusions to adhesion dynamics.

1.4.2 WRC and adhesion

While Arp2/3 complex interacts with adhesion molecules, surprisingly little research has been done on the nucleation promoting factors that could activate these adhesion associated Arp2/3 complexes. As adhesions signal to Rac to promote Arp2/3 complex activation, WRC is believed to be involved. Recent research on *Drosophila* WRC in vivo shows the complex colocalizes with integrin and talin in the wing epithelium (**Figure 1.16**). Loss of WRC and Arp2/3 complex leads to mild adhesion defects of the wing epithelium. It is therefore concluded that WRC is involved in the maintenance of stable cell-ECM adhesion (Gohl et al., 2010).

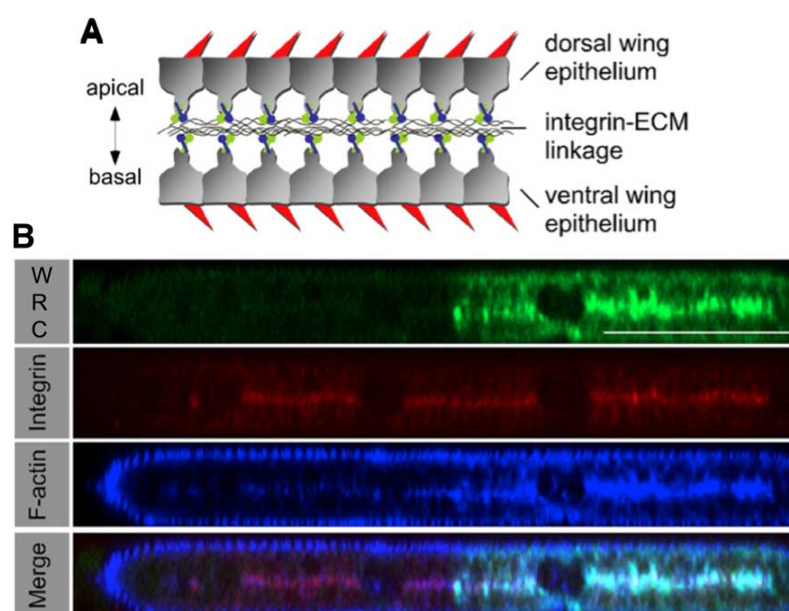


Figure 1.16 *Drosophila* WRC localizes to integrin based adhesions

(A) Cartoon shows the cross-section of a *Drosophila* pupal wing. (B) WRC (green) co-localizes with integrin (red) and actin (blue) in the *Drosophila* pupal wing. Figure adapted from (Gohl et al., 2010)

In cultured mammalian cells, similar colocalization of WRC and adhesion molecules is controversial. However, loss of WRC in many cell types leads to altered focal adhesion structure that phenocopies FAK knockout and β 1-integrin knockout cells. In both cultured human mammary epithelial cells and human keratinocytes, loss of WRC results in large focal adhesions at the cell periphery (Silva et al., 2009). The same enlarged focal adhesion phenotype has also been reported in cancer cells with reduced WRC expression (Escobar et al., 2010). Although cells without WRC eventually form large focal adhesions, early adhesion to various substrates is delayed (Silva et al., 2009). Many reports therefore suggest WRC is required for normal regulation of cell-ECM adhesions.

1.4.3 N-WASP and adhesion

N-WASP interacts with FAK, and FAK can regulate N-WASP activities, therefore it is thought that N-WASP is the ideal candidate to regulate Arp2/3 complex at adhesions. However N-WASP null keratinocytes have normal focal adhesions and can adhere normally to ECM (Lefever et al., 2010). This is in direct contrast to WRC deficient keratinocytes where focal adhesions are enlarged (Silva et al., 2009). In addition, mice lacking N-WASP expression in skin keratinocytes have normal epidermis, where keratinocytes established normal integrin based adhesions with basement membrane in vivo (Lefever et al., 2010). Hence at least in keratinocytes, N-WASP has no obvious function in cell-ECM adhesion.

1.5 Aim of thesis

Cancer cell invasion and metastatic development involves cell migration/invasion in complicated 3D environments making standard 2D migration assays less representative. Therefore it is necessary to reinvestigate the role of major motility regulators in a 3D environment. WRC drives lamellipodia assembly via Arp2/3 complex and cell migration across 2D substrates, WRC function in 3D cell motility is however not clear. The major aim of this thesis is to investigate the role of WRC and regulated proteins in 3D cell migration.

HSPC300 is the least studied subunit of WRC. Recent biochemical studies demonstrate HSPC300 can exist independently of WRC, however the biological function of this free pool of HSPC300 is not known. The other aim of this thesis is to explore possible roles of HSPC300 in 3D cell motility.

The mechanism of WRC activation is extensively studied. How WRC activation is negatively regulated is not known. A putative negative regulator of WRC, NHS, was recently identified. The mechanism by which NHS negatively regulates WRC is also investigated in this thesis.

Chapter 2: Materials and methods

2.1 Materials

Materials are listed by technique. All chemicals are from Sigma-Aldrich unless otherwise stated. All laboratory plastics are from Nunclon, Thermo Scientific, unless otherwise stated. Pre-designed primers are all ordered from Qiagen.

2.2 Cell culture

2.2.1 Cell lines

A431 cells and B16F10 cells were kindly provided by Dr. Kurt Anderson (Beatson Institute for Cancer Research, Glasgow, UK). MCF7 cells and hTERT-RPE1 cells were kindly provided by Dr. Jing Bi and Dr. Nick Gilbert (Edinburgh Cancer Research Centre, Edinburgh, UK).

2.2.2 Tissue culture

A431, MCF7 and B16F10 cells were cultured in DMEM (Dulbecco's modified eagle medium, Gibco, Invitrogen) supplemented with 10% foetal bovine serum (FBS, Autogen Bioclear), 2mM Glutamine and 1% penicillin and streptomycin (Gibco, Invitrogen). For hTERT-RPE1 cells, DMEM/F-12 medium (1:1) (Gibco, Invitrogen) supplemented with 10% FBS, 2mM Glutamine and 1% penicillin and streptomycin. All cell lines were maintained in a humidified atmosphere at 37°C and 5% CO₂.

2.2.3 Cell passaging and counting

For all cell types, subconfluent cells were first washed in phosphate buffer saline (PBS, 3.3mM KCl, 170mM NaCl, 1.8mM Na₂HPO₄ and 10.6mM H₂PO₄). Cells were then detached using an appropriate volume of 1X Trypsin (Invitrogen) and incubated at 37°C for up to 15min. Cell detachment was checked, before adding full growth media to inactivate Trypsin. The suspended cells were then carefully mixed by gentle pipetting. 400µl of well suspended cells were then diluted in 20ml PBS before counting with a CASY cell counter (Roche). Once counted, 1x10⁶ cells were seeded to make a fresh culture. Otherwise, a desired number of cells was used for subsequent experiments.

2.2.4 Cryopreservation and cell recovery

For all cell types, subconfluent cells were detached using trypsin and re-suspended as described above. Cell suspension was then centrifuged at 1,000rpm for 5min. Cell culture media was then discarded. Cell pellet was then re-suspended in 4ml freezing mix (10% DMSO (dimethyl sulphoxide) in FBS). The mixture was then aliquoted to cryovial tubes (Nuncleon, Fisher Scientific) at 1ml each. Aliquots were frozen immediately at -80°C before being transferred to liquid nitrogen storage.

To recover cells from liquid nitrogen storage, cells were quickly defrosted in a 37°C waterbath. Cells were then pelleted by centrifugation at 1,000rpm for 5min. After centrifugation, the upper freezing mix was removed and cells were re-suspended in warm fresh cell culture medium. Re-suspended cells were then plated and allowed to recover for at least 2 days before use.

2.2.5 Transfection

All cells were transfected by nucleofection using Amaxa Nucleofection Kit (Lonza). For A431 cells Kit T was used. For B16F10 and MCF7 cells Kit V was used. Cells were transfected according to manufactures' instructions. Briefly, 1×10^6 A431 cells, 2×10^6 B16F10 or MCF7 cells were pelleted by centrifugation and re-suspended in 100µl room temperature appropriate Nucleofector solution. Appropriate amount of DNA or RNA was then added to the mixture. For transfection of all GFP constructs, 2ug plasmid DNA was used. For siRNA transfections 10ul of the 20µM siRNA stock was used. The mixture was then transferred to a cuvette and transfected on a Nucleofector device using an appropriate programme for each cell type. Cells were subsequently re-plated and allowed to recover for at least 24 hours before next experiments. For transient knock down experiments with siRNAs, cells were transfected again 48 hours after the initial transfection to achieve the best effects of RNAi. Fusion protein constructs and siRNAs used are listed below (**Table 2.1&2.2**).

Constructs	Source
Scar2-GFP	Laura Machesky
PIR121-GFP	
Abi1-RFP	
Paxillin-GFP	
p21-Arc-GFP	
GFP-N-WASP	Douwe Veltman
Lifect-RFP	Kurt Anderson
GFP-Lifect	Roland Wedlich-Soldner
RFP-Actin	Maddy Parsons
GFP-NHS-1A	Alison Hardcastle
Myc-NHS-1A	
pEGFP-N1	Clontech

Table 2.1 List of fusion protein constructs

Target	No.	siRNA Sequence	Source
N-WASP	1	AACCTTAATGTAATTTACT	Qiagen
	2	CAGATACGACAGGGTATCCAA	
Nap1		CAGGCATATACTAGTGTCTCA	
Sra1		ATCGAGAGTCATTCTTCTACA	
p34-Arc		AAGGATTCCATTGTGCATCAA	
HSPC300	SMARTPool	CGAUAUGUCUUGUCGUUCA	Dharmacon
		GAACGGAGAAUAGAGUACA	
		ACACUAAACGAGAAAUUGA	
		GGGCUAACCGGGAGUACAU	
FAK		GAAGUUGGGUUGUCUAGAAU	

Table 2.2 List of siRNAs

All siRNAs are human specific.

2.2.6 Stable cell line selection

To establish cell lines stably expressing shRNA, all shRNA plasmids were first transfected into cells. Transfected cells were first cultured in normal cell culture media for two days before being selected with puromycin (InvivoGen) containing cell culture media. For selection of A431 stable cell lines, 3 μ g/ml puromycin was added to the cell culture media. For MCF7 stable cell line selection, 1 μ g/ml puromycin was used in the cell culture media. Once stabilized, cells were maintained in the same selection culture media. shRNAs used are listed below (Table 2.3).

Target	No.	shRNA Sequence	Source
Nap1	A	CAATGAATGTGTATGAGTT	Open Biosystems
	B	GCAATCATTGGATTATACA	
	C	CATCCTATCTTATCGACAA	
Sra1	GCAAAGATGAGATTATTAA		
Scar2		GTCGACCGACTACAGGTTAAA	
PIR121	B	ACTGTCAAATGTACCATATTT	Sigma
	C	TGCTGTCCTGGATGAGCTAAA	
	D	TCATGTACCAGGCTAACTTTG	
	E	CAGCTGTTGGGTAGATCAATT	
NHS	a	CCAGGTTCTTAAACTAACAAA	
	b	CCGAGTGATGACTCCATCATT	
	c	CCAAATGATTTGGATGGTAAA	
	d	CCTCAGTTAGATGCTTCGGAT	

Table 2.3 List of shRNAs

All shRNAs are human specific.

2.2.7 Soft agarose growth assay

To set up soft agarose growth assay or anchorage independent growth assay, 2ml 1% hot agarose in water was first added to each well of a 6-well plate. Agarose was then allowed to set at room temperature for 30min. Meanwhile, 0.3% hot soft agarose was prepared and maintained in 37°C water bath. Then 10000 cells were suspended in 1.5ml 0.3% soft agarose and added to each well of the plate with set agarose. The agarose-cell mixture was allowed to set at room temperature for

30min. Cells were then cultured in 2ml cell culture medium for indicated times to form colonies in a humidified atmosphere at 37°C and 5% CO₂. 1μM FAK inhibitor (PF-562271) from Symansis in DMSO was added to both agarose and cell culture medium in this assay to suppress FAK activation.

2.2.8 Cell growth assay

On day 0, 5x10⁵ A431 cells were plated in each well of 6-well plate. The number of cells was counted every day for 5 days with a CASY cell counter (Roche).

2.3 Protein analysis

2.3.1 Protein extraction

To extract protein of cells cultured on tissue culture dish, cells were placed on top of ice and washed briefly with PBS before being lysed with ice-cold TNE buffer (150 mM NaCl, 50mM Tris-HCl pH7.5, 1% Triton X-100 and 1mM EDTA) supplemented with fresh Halt protease inhibitor cocktail and Halt phosphatase inhibitor cocktail (Pierce). Cells were scraped from tissue culture dishes using cell scrapers and lysate was collected into eppendorf tubes. Lysate was incubated on ice for about 5min before centrifugation at 13,000rpm for 10min at 4°C. Clear cell lysate was then collected for further analysis.

To extract protein of cells cultured in collagen gel, whole gel was first emerged in 300μl ice-cold TNE buffer with proteases and phosphatase inhibitors in a Precellys 24 Lysing tube. The sample was then homogenized with an electronic homogenizer (Precellys 24, Stretton Scientific Ltd). The Lysate was incubated on ice for 5min before centrifugation at 13,000rpm for 10min at 4°C. Clear cell lysate was then collected for further analysis.

2.3.2 Protein concentration

All protein cell lysates were tested for protein concentration before protein separation using Precision red advanced protein assay (Cytoskeleton. Inc.). Briefly, 10µl cell lysate was mixed with 1ml Precision red reagent and protein concentration (the absorbance at 600nm X10) was read using a spectrometer. All cell lysates were then diluted to equal concentration with appropriate ice-cold lyse buffer before protein separation.

2.3.3 Protein separation

For protein separation by polyacrylamide gel electrophoresis (SDS-PAGE), NuPAGE LDS Sample Buffer and NuPAGE Reducing Agent (Invitrogen) were added to cell lysate to make a 1X solution and boiled at 90°C for 10min. Samples were then resolved using precast Novex Bis-Tris Mini Gels (10% or 4%-12%, Invitrogen) with NuPAGE MOPS SDS Running Buffer (Invitrogen) at 180V for up to 80min in a mini gel tank. 10µl Novex Sharp Pre-stained Protein Standard (Invitrogen) was used to mark protein sizes.

2.3.4 Western blotting

For subsequent antibody probing, separated proteins were first transferred from the min gel to a methanol activated Hybond-P PVDF membrane (GE Healthcare) with NuPAGE Transfer Buffer (Invitrogen) at 250mA for 180 min. The membrane was blocked using 5% BSA in TBST (150 mM NaCl, 10mM Tris-HCl, pH 7.4, 2.7mM KCl, 0.1%Tween 20) for 10min at room temperature. Primary antibodies were diluted to a suitable concentration in 5%BSA/TBST (**Table 2.4**). Blocked membrane was then incubated with diluted primary antibody at 4°C overnight. To remove excessive primary antibody, the membrane was washed 3 times in TBST with gentle agitation at room temperature. The membrane was then incubated with anti-Rabbit or Mouse IgG HRP (horseradish peroxidase) linked secondary antibody (Cell Signaling Technology) at a 1:5,000 dilution in 5%BSA/TBST for 1 hour at room temperature. To remove excessive secondary antibody, the membrane was washed 3 times in TBST again. Finally, the membrane was blotted

using SuperSignal[®] West Pico Chemiluminescent Substrate (ECL) (Thermo Scientific), and was exposed to X-Ray film (Fuji Film) and developed.

Antibodies	Dilution Factor	Source	
Mouse anti-GFP	1:1,000	Abcam	
Mouse anti-HSPC300	1:2,000	Alexis Gautreau	
Mouse anti-Dlg	1:2,000	BD Biosciences	
Rabbit anti-Abi1	1:2,000	Bethyl Laboratories	
Rabbit anti-Scar2	1:2,000	Cell Signalling Technology	
Mouse anti-Myc (9B11)	1:2,000		
Rabbit anti-GAPDH	1:5,000		
Rabbit anti-FAK	1:2,000		
Rabbit anti-Erk1/2	1:2,000		
Rabbit anti-phospho-Erk1/2	1:2,000		
Rabbit anti-Akt	1:2,000		
Rabbit anti-pAkt	1:2,000		
Mouse anti-Rac1	1:2,000		Cytoskeleton Inc.
Mouse anti-ZO1	1:2,000		Invitrogen
Rabbit anti-pY397FAK	1:3,000		
Rabbit anti-Nap1	1:2,000	Millipore	
Rabbit anti-Sra1	1:2,000		
Rabbit anti-p34-Arc	1:2,000		
Mouse anti-Scribble (7C6.D10)	1:2,000		
Rabbit anti-pY256N-WASP	1:5,000		
Rabbit anti-Scribble	1:2,000		
Goat anti-Scar1 (L-19)	1:2,000	Santa Cruz Biotechnology	
Rabbit anti-Abi2	1:5,00		
Mouse anti-Cdc42	1:5,00		
Rabbit anti-PIR121	1:5,00	Sigma	
Mouse anti-Tubulin	1:5,000		
Rabbit anti-a-actinin	1:2,000		
Mouse anti-Paxillin	1:2,000		
Mouse anti-Vinculin	1:2,000		
Rabbit anti-N-WASP (WASL)	1:4,000	Sigma Atlas	

Table 2.4 List of primary antibodies used for western blotting

2.3.5 Native protein complex extraction and separation

All reagents used for native protein complex extraction and separation were from Invitrogen unless stated otherwise.

To extract native protein complex from cells cultured on tissue culture dish, cells were placed on top of ice and washed briefly with ice-cold PBS before being lysed with ice-cold NativePAGE Sample Buffer supplemented with 10% DDM (n-Dodecyl β -D-Maltoside) and proteases and phosphatase inhibitors. Cells were then scraped and lysate was collected as usual. Native cell lysate was incubated on ice

for 5 min then centrifuged at 13,000rpm for 10min at 4°C. Clear cell lysate was then collected for immediate protein separation using Blue NativePAGE. Prior to separation at room temperature, the protein concentration of native cell lysate was tested and equalized as described above. 1µl NativePAGE 5% G-250 Sample Additive was added to every 20µl native cell lysate just before protein separation. Samples were then resolved using precast NativePAGE Novex 3%-12% Bis-Tis Gel. Samples were first allowed to electrophoresis for 10min at 150V with NativePAGE Running Buffer at the anode and NativePAGE Running Buffer with 5% NativePAGE Cathode Additive at the cathode of the mini gel tank. The electrophoresis was then paused to change the cathode buffer to NativePAGE Running Buffer with 0.5% NativePAGE Cathode Additive. Finally the electrophoresis was continued for at least 2 hour to resolve native protein complexes. Subsequent transfer of separated protein complexes and western blotting were performed as usual.

2.3.6 Immunoprecipitation

For immunoprecipitation (IP), at least 3×10^6 cells cultured on 10cm tissue culture dish were lysed as described above. Cell lysates were used immediately for IP. Appropriate amount of primary antibody and corresponding control anti serum was added to cell lysates. The mixture was then incubated at 4°C rotating wheel at 15rpm for 3 hours. Meanwhile, protein A or G-Sepharose beads were prepared by washing twice in 1% BSA/PBS, and three times with TNE buffer with centrifugation at 2000rpm at 4°C after each wash. Beads were then suspended in TNE buffer and an appropriate amount of beads were added to cell lysate after the initial 3-hour incubation. The mixture was incubated at 4°C rotating at 15rpm overnight. To recover the bound protein, beads were collected by centrifugation at 2000rpm at 4°C. The supernatant was removed and discarded. The beads were washed three times with ice-cold TNE buffer with centrifugation at 2000rpm at 4°C after each wash. To release bound protein from beads, suitable amount of TNE buffer supplemented with NuPAGE LDS Sample Buffer and NuPAGE Reducing Agent was added to beads. The whole mixture was then boiled at 90°C for 10min. The resulting solution was subjected to usual SDS-PAGE and western blotting. 1µg Mouse anti-HSPC300 antibody (Alexis Gautreau) and 2µg GFP-trap (Chromotek) was used for IP.

2.3.7 Effector domain pulldown assay

For effector domain pulldown assay, cell lysate was prepared in the same way as for IP. 10µl Glutathione-agarose immobilized GST-PAK1-PBD beads were added to the cell lysate. The mixture was incubated at 4°C rotating at 15rpm for 1 hour. Bound active Rac1 and Cdc42 were released from the beads as described above, and analysed using SDS-PAGE and western blotting.

2.3.8 Rac1 Activation Assay

G-LISA Rac1 activation assay biochem kit (luminescence format, Cytoskeleton, Inc) was used for quantitative Rac1 activation measurement. The assay was performed following manufacture's protocol. Briefly, spreading cells on collagen-coated 6-well plates were washed with ice cold PBS and lysed using ice cold lysis buffer at indicated time points. Cell lysates were collected with a cell scraper and transferred to 1.5ml tubes on ice. The lysate was clarified by centrifugation at 14,000rpm at 4°C for 2min. Concentrations of lysates were measured immediately using Precision red advanced protein assay (Cytoskeleton, Inc.). The concentrations of cell lysates were then equalized. The Rac1 affinity plate was prepared by dissolving the powders in the wells with 100µl ice cold water. Meanwhile 30µl ice cold binding buffer was added to 30µl cell lysate. The water was then removed from the Rac1 affinity plate before adding 50µl cell lysate mix to respective wells. 25µl lysis buffer + 25µl binding buffer mix was used as a blank control, and 2ng purified active Rac1 was used as a positive control. The plate was then placed on a microplate shaker at 400rpm, 4°C for 30min. The solution was then removed from the plate and washed twice with wash buffer at room temperature. 200µl antigen presenting buffer was then added to each well and incubated at room temperature for 2min. Wells were then washed three times with wash buffer before adding 50µl anti-Rac1 primary antibody (1:250) to each well. The plate was then incubated on an orbital microplate shaker 400rpm at room temperature for 45min. The primary antibody was removed and wells were washed three times with wash buffer at room temperature. 50µl diluted secondary HRP-linked antibody (1:200) was added to each well before shaking the plate on a microplate shaker 400rpm at room temperature for 45min. The plate was then washed three times with room temperature wash buffer before adding 50µl HRP

detection reagent to each well. The luminescence signal was detected using a microplate luminescence reader.

2.4 Motility Assays

2.4.1 Wound healing assay

To set up wound healing assays, a large wound was first created on a monolayer of cells cultured on glass bottom dish (MatTek) with a cell scraper. The wounded monolayer was then washed twice with fresh cell culture media to remove debris. Cells were then subjected to time lapse imaging for 24 hours after wounding using a Nikon TE2000 microscope with a Nikon Plan Fluor 10X/0.30 NA objective in a 37°C chamber with 5% CO₂.

2.4.2 Wound healing induced Matrigel invasion assay

A monolayer of cells cultured on glass bottom dish was wounded with a cell scraper. Debris was removed by washing with fresh cell culture medium. After the last wash, remaining media was carefully removed using an aspirator. 500µl ice-cold Matrigel (BD Biosciences) mixed with ice-cold PBS (1:1) was immediately added atop the wounded monolayer. Matrigel was then allowed to polymerize for 1 hour at 37°C before adding 2ml warm cell culture medium. The setup was then subjected to time lapse imaging for 24 hours using a Nikon TE2000 microscope with a Nikon Plan Fluor 10X/0.30 NA objective in a 37°C chamber with 5% CO₂.

2.4.3 Cell spreading assay

Before the spreading assay, glass bottom dishes were first coated with collagen Type 1 (BD Biosciences). Collagen was diluted in 0.02M acetic acid at a concentration of 3µg/ml. Glass bottom dishes were then coated with diluted collagen for 1 hour at 37°C before washing with PBS to remove excessive acetic acid. 1×10^4 cells suspended in 3 ml warm cell culture medium were then added to

the collagen-coated dish. Cell spreading was imaged immediately using a Nikon TE2000 microscope with a Nikon Plan Fluor 10X/0.30 NA objective in a 37°C chamber with 5% CO₂.

2.4.4 Organotypic invasion assay

Organotypic invasion assay was set up as described (Timpson et al., 2011). Briefly, collagen type 1 from rat tail tendons was extracted with 0.5M acetic acid at 4°C for 48 hour with stirring. Debris were removed by centrifugation at 7,500xg for 30min. Collagen was precipitated by equal volume of 10% (W/V)NaCl, and collected by centrifugation at 10,000xg for 30min. Collagen was re-dissolved in 0.25M acetic acid at 1:1 with stirring at 4°C for 24 hours. Collagen solution was dialyzed against 17.5mM acetic acid with 6-8 changes at 4°C. The concentration of the rat-tail collagen was adjusted to 2mg/ml and stored at 4°C. All subsequent collagen-mixing procedures were carried out on ice. 25ml rat-tail collagen was mixed with 3ml 10X MEM (Invitrogen) and 3ml 0.22M NaOH to adjust pH of the collagen, before mixing with 1X10⁶ primary fibroblasts (Paul Timpson). 2.5ml of the fibroblasts containing collagen was added to 35mm plastic tissue culture dish, and allowed to set at 37°C for 30min in a humidified atmosphere with 5% CO₂ before adding 1ml fibroblast growth media (DMEM+10%FBS). To permit gel contraction by fibroblasts, collagen gel was detached from the sides of tissue culture dish with pipette. The collagen gel was allowed to contract for 8 days. The media was changed every other day. Once the gel had contracted to the well size of a 24-well plate, the gel was transferred to the 24-well plate. 4x10⁴ cells of interest in 1ml cell culture medium were added on top of the collagen gel. The cells were then allowed to grow to confluence. Once confluent the gel was moved atop a stainless steel grid standing in a 6cm tissue culture dish. Normal cell culture medium of the cell of interest was then added to the 6cm tissue culture dish to just contact the bottom of the collagen gel creating a liquid/air interface. The interface creates a gradient promoting cell invasion. The medium was replaced every two days. For A431 cells, cells were allowed to invade for 3 weeks.

2.4.5 3D collagen gel invasion assay

Acid extracted rat-tail collagen 2mg/ml (the same as organotypical assay) was mixed with ice-cold 10X MEM and ice-cold 0.22M NaOH at 8:1:1 . 5×10^5 cells were then mixed with the ice-cold collagen mixture in the well of a 96-well tissue culture plate. The collagen-cell mix was allowed to set at 37°C for 1 hour in a humidified atmosphere with 5% CO₂. The polymerized gel (cell plug) was then carefully removed and transferred to a well of a 24-well tissue culture plate with 1ml ice-cold collagen. The cell plug was placed at the center of the well in suspension, so it was not touching the bottom or the sides. Collagen was allowed to set at 37°C for 1 hour in a humidified atmosphere with 5% CO₂ before adding 1ml cell culture media. A431 cells were allowed to invade in this assay for 5 days. hTRET-RPE1 cells were allowed to invade for 2 days.

2.4.6 Thick collagen gel invasion assay

Acid extracted rat-tail collagen or concentrated rat-tail collagen type 1 (BD Biosciences) (diluted to 2.2mg/ml with ice-cold PBS before use) was mixed with 10X MEM and 0.22M NaOH as described above. For visualization of polymerized collagen, FITC conjugated Collagen Type 1 was added to the mixture at 1:1000 when needed. 500µl collagen was added to a well of a 24-well tissue culture plate and allowed to set at 37°C for 1 hour in a humidified atmosphere with 5% CO₂ before adding 2×10^4 cells in 1ml cell culture media. Cells were then cultured for 3 days allowing invasion to the top of the thick collagen gel.

2.5 Imaging

2.5.1 Matrix-coated glass bottom dish

For all imaging samples, when required, 14.5µg/ml human fibronectin (BD Biosciences) in PBS was used to coat the glass bottom dishes at 37°C for 1hour. Fibronectin-coated dishes were washed once in PBS before use. Alternatively, Collagen Type 1 (BD Biosciences) was diluted in 0.02M acetic acid at a

concentration of 3µg/ml. Glass bottom dishes were then coated with the diluted collagen for 1 hour at 37°C before washing with PBS to remove excessive acetic acid. Collagen coated dishes were washed once in PBS before use.

2.5.2 Cell derived matrix

Cell derived matrix (CDM) was prepared by the Beatson Institute Central Services as previously described (Cukierman et al., 2001, Bass et al., 2007). Briefly, glass bottom dishes were coated with 0.2% gelatin at 37°C for 1 hour followed by cross-linking with 1% glutaraldehyde in PBS for 30min at room temperature. After three washes with PBS, the cross linker was quenched with 1M glycine in PBS for 20min at room temperature. After three additional PBS washes, cell culture media was added to the dish and incubated 37°C for 30 min. 5×10^5 NIH 3T3 fibroblasts were then seeded and cultured in DMEM +10% FBS+ 50µg/ml ascorbic acid for 8 days. The media was change daily. Once the matrix was mature, fibroblasts were removed using 1.5ml lysis buffer (20mM NH₄OH, 0.5% Triton X-100 in PBS). The lysate was removed and dishes were washed carefully with PBS. Residual DNA was digested with 10µg/ml DNase I (Roche) at 37°C for 30min in a humidified atmosphere with 5% CO₂ before washing with Dulbecco's PBS containing calcium and magnesium. Dishes were washed with PBS before adding 5×10^4 B16F10 cells in 2ml cell culture medium to each dish.

2.5.3 Live cell imaging

Live cells expressing fluorescently labelled proteins were imaged with an Olympus FV1000 confocal microscope with an Olympus UPanSApo 60x/1.35 NA oil immersion objective. TIRF (Total internal reflection fluorescence microscopy) imaging of live cells were performed on a Nikon Eclipse TE 2000-U microscope equipped with 60X and 100X 1.45 NA Nikon TIRF oil-immersion objectives (Nikon Eclipse TE 2000-U TIRF microscope). Glass bottom dishes with live cells were kept in a stage heater at 37°C and supplied with 5% CO₂ during imaging. For B16F10 cells, 5×10^4 cells in 2ml cell culture medium were added to fibronectin- or collagen- coated 35mm glass bottom dishes one day before live cell imaging.

2.5.4 Immunofluorescence

For immunofluorescence (IF), cells cultured in all assays were fixed with 4% formaldehyde for 15min at room temperature. Excessive formaldehyde was removed and samples were washed three times with PBS before permeablizing with 0.1% Triton X-100 in PBS for 15min at room temperature. After washing with PBS for three times, primary antibodies diluted in PBS were added to samples and incubated at room temperature for 1hour (**Table 2.5**). Excessive primary antibodies were then removed and samples were washed three times with PBS. Fluorescently labelled secondary antibodies or rhodamine phalloidin diluted in PBS were then added to samples and incubated at room temperature for 1hour (**Table 2.5**). Samples were then washed three times with PBS.

For samples in glass bottom dishes, 1ml PBS was preserved in the dish for subsequent imaging with a Nikon Eclipse TE 2000-U TIRF microscope with a Nikon Plan Apo TIRF 100x/1.45 NA oil immersion objective or an Olympus FV1000 confocal microscope with an Olympus UPanSApo 60x/1.35 NA oil immersion objective. For cells invading atop the thick collagen gel assay, prior to imaging, the gel was removed from the 24-well cell culture plate, inverted and placed gently on a glass bottom dish, so cells were close to the glass. The inverted gel was then imaged with an Olympus FV1000 confocal microscope.

	Antibodies	Dilution Factor	Source
Primary	Mouse anti-Myc (9B11)	1:1,00	Cell Signalling Technology
	Rabbit anti-Scar2		
	Mouse anti-Abi1		MBL International
	Rabbit anti-N-WASP (WASL)		Sigma Atlas
	Mouse anti-p16-Arc		Synaptic Systems
	Rabbit anti-pY397FAK		Invitrogen
	Mouse anti-Dlg		BD Biosciences
	Rabbit anti-pY256N-WASP		Millipore
	Rabbit anti-Scribble		
Secondary	Alexa Fluor 488 Donkey anti-Rabbit	1:5,00	Invitrogen
	Alexa Fluor 488 Donkey anti-Mouse		
	Alexa Fluor 594 Donkey anti-Rabbit		
	Alexa Fluor 594 Donkey anti-Mouse		
	Alexa Fluor 647 Donkey anti-Rabbit		
	Alexa Fluor 647 Donkey anti-Mouse		
	Phalloidin	Dilution Factor	Source
	Rhodamine Phalloidin	1:1,000	Invitrogen

Table 2.5 List of antibodies and phalloidin used for IF.

2.5.5 Fluorescent gelatin degradation assay

Glass bottom dishes were acid washed in 1M HNO₃ for 5min. The acid was removed with extensive wash by PBS followed by one wash with ethanol. The dish was coated with 50µg/ml poly-L-lysine for 15min at room temperature. The dish was then washed three times with PBS, and cross-linked with 0.5% glutaraldehyde for 15min. Dishes were then coated with Alexa Fluor 488 conjugated gelatin (Invitrogen) at 37°C for 10min. Excessive gelatin was removed and dishes were washed three times with PBS. 5mg/ml sodium borohydride was then added to quench residue glutaraldehyde for 3min before washing three times with PBS. The dish was sterilized in 70% ethanol for 5min followed by incubation in cell culture medium for 1hour at 37°C in a humidified atmosphere with 5% CO₂ before use.

For RPE1 cells, 5x10⁴ cells were seeded on the fluorescent gelatin coated dish in 2ml cell culture medium containing 5µM GM6001 metalloprotease inhibitor. The cells were then cultured overnight. GM6001-containing medium was then removed and cells were washed carefully in PBS for three times. Fresh normal cell culture medium was then added to the dish and cells were allowed to degrade the gelatin for 1.5hour before being fixed and processed for imaging.

2.6 Xenografts and Immunohistochemistry

2.6.1 Xenograft

All experiments were performed according to UK Home Office regulations. The Beatson Institute Animal House Services kindly performed injection of A431 stable cell lines into nude mice. 1x10⁶ cells suspended in PBS 100µl PBS were subcutaneously injected into the flanks of 5 nude mice per cohort. Tumour diameters were measured daily from when tumours first appeared and mice were humanely killed when tumour diameter reached 1.5cm. Tumours were then excised and processed for histology.

2.6.2 Immunohistochemistry

For immunohistochemistry (IHC), formalin fixed paraffin-embedded tumour sections were first de-waxed in xylene for 10min, and re-hydrated by washing in decreasing concentration of ethanol (100%, 95% and 70%). Antigen was then retrieved by cooking the tumour section in 800ml pre-heated citrate buffer pH6.4 (Dako) in a pressure cooker for 12min in a microwave oven. Samples were left to cool at room temperature for 30 min, and rinsed in water. Samples were subsequently blocked in 0.03% hydrogen peroxide (Dako) for 10min followed by washing in TBST twice. 5% goat serum in TBST was then used to block the sample again for 30min. Samples were then incubated with primary antibody diluted with 5% goat serum in TBST at 4°C overnight. The primary antibody was removed by washing in TBST twice. Peroxidase-labelled polymer (EnVision Detection Systems Peroxidase/DAB, Rabbit/Mouse, Dako) was then incubated with the sample for 30min at room temperature. Following three washes in TBST, the staining was visualized with liquid DAB + substrate-chromogen solution (Dako) according to manufacture's introduction. Stained samples were counterstained in Meyers Heamatoxylin for about 30 seconds, before being washed in Scott's tap water and dehydrated in increasing concentration of ethanol (70%, 95% and 100%). Finally samples were washed in xylene for 10min and subjected to mount with histomount (National Diagnostics).

2.7 RNA analysis

2.7.1 RNA extraction

Total RNA was extracted from A431 cells using absolutely RNA Miniprep Kit (Stratagene) following the manufacturer's protocol. Briefly, 350µl of lysis buffer containing 2.5µl of fresh β-Mercaptoethanol was used to lyse cells cultured in 6-well plate. Centrifuging through an RNA binding spin cup isolated RNA in the lysate. Residue DNA was removed by on-column-digest with DNase I (Roche) at 37°C for 15min. RNA was then eluted in 30µl of elution buffer and collected in a 1.5ml tube. RNA concentration was measured using a Nanodrop spectrophotometer (GE Healthcare).

2.7.2 Quantitative RT-PCR

Purified RNA samples were subjected to One-step RT-PCR (Qiagen) following the manufacturer's protocol to test and quantify mRNA expression level. 100ng of RNA, 7.5µl of SYBR green Master Mix, 0.375µl of a 20µM predesigned QuantiTect primer mix (Qiagen), 0.15µl QuantiTect RT-mix, and appropriate amount of RNase-free water were mixed in a total reaction volume of 15µl. All RNA samples were run in triplicate on a Rotor-Gene RG-3000 (Corbett Research) real time cyclers using following protocol, 50°C/20min (reverse transcription), 95°C/15min (polymerase activation), then 50 cycles of 94°C/15s, 55~60°C/30s (using specific annealing temperatures for different primer sets), 72°C/30s and finish at 72°C for 5min. A standard curve was generated for each primer set using serial dilutions of cDNA. Relative expression values were normalized to mRNA level of GAPDH. Predesigned QuantiTect primers (Qiagen) were used for NHS detection, and GAPDH control.

2.8 Plasmid Purification

Bacteria glycerol stocks (*E.coli*, DH5a) of various over expression constructs and shRNA constructs were recovered in 200ml Luria Broth (LB) with appropriate antibiotics (100µg/ml Ampicillin or 50µg/ml Kanamycin). The culture was inoculated for 8 hours at 37°C with vigorous shaking. Bacteria were collected by centrifugation at 5,000rpm at 4°C for 20min. The bacteria pellet was then subjected to plasmid purification with GenElute HP Plasmid DNA Midiprep Kit according to manufactures' protocol. Briefly, the bacteria pellet was re-suspended in re-suspension solution and lysed with lysis solution. After neutralization, debris in cell lysate was removed by passing the lysate through a filter syringe. Clear cell lysate was collected in a DNA binding column that was connected to a vacuum scaffold. As the cell lysate aspirated by the vacuum, plasmid DNA bound the DNA binding column. The column was then washed twice with the two wash solutions. The column was left to dry on the vacuum scaffold for 10min. Purified plasmid DNA was then dissolved in 500µl elution solution and collected in a 1.5ml tube by

centrifugation at 3,000xg for 5min. The plasmid DNA concentration was measured using a Nanodrop spectrophotometer (GE Healthcare).

2.9 Quantification and Statistics

Scanned images of western blots were inverted and quantified using histogram mean function in Adobe Photoshop CS5.1. A constant area of selection was applied to the bands of interest during quantification.

Cell invasion distance and invasion area, area of wound closure, cell area during spreading, colony diameter and number in soft agarose assay, focal adhesion size and number were measured using ImageJ.

The fluorescence intensities of protein enrichment at pseudopods were measured using ImageJ. Pseudopods of invading cells were selected randomly based on actin structures. The same area of selection was applied to different channels of a multi-channel image. The relative fluorescence intensity was the of mean pseudopod fluorescence intensity to mean cytosolic background.

For fluorescent gelatin degradation assay, the area of degradation was quantified using a purpose built Image J plug-in (Manuel Forero-Vargas, unpublished data).

For all quantifications, differences were considered significant when $p < 0.01$ using unpaired Students t-test.

Chapter 3: Localization of WRC

3.1 Introduction

At the leading edge of a migrating cell, WRC promotes Arp2/3 complex activation to generate lamellipodia. The localization of WRC at the advancing membrane protrusions has been studied in multiple systems. In cultured *Drosophila* cells, endogenous Scar protein localizes to the leading edge of the lamellipodia, and at the tips of filopodia. Identical localization of Kette, which is the *Drosophila* ortholog of Nap1, has also been found in cultured *Drosophila* cells (Kunda et al., 2003). In mammalian cells, WRC also localizes to tips of membrane protrusions, as Sra1 and Nap1 localize to the leading edge of lamellipodia (Steffen et al., 2004). However little information is available about the dynamics of WRC in live cells, as most studies report endogenous protein localizations in fixed cells. As cell migration is a dynamic process, it is important to know the dynamics of WRC in motile cells. Additionally, the localization of WRC in cells migrating in a 3D environment has not been explored.

3.2 Localization of WRC in live cells

To study the localization of WRC in live cells, GFP labeled WRC components, were expressed in a highly motile mouse melanoma cell line, B16F10. I first tested if a GFP WRC probe could be used to accurately represent the complex localization. As Scar2 is the major Scar protein expressed in mammalian cells, GFP tagged Scar2 construct was used. The localization of the GFP fusion protein was tested in B16F10 cells co-expressing RFP-Actin. On fibronectin (FN) coated glass bottom dishes, these B16F10 cells generated large lamellipodia at the cell front. Scar2-GFP localized nicely to the leading edge of lamellipodia and the tips of filopodia consistent with the reported localization of WRC (**Figure 3.1A**). Similarly, when the same cells were plated on collagen (CO) coated glass bottom dish, Scar2-GFP localized to the leading edge of lamellipodia and the tips of filopodia too (**Figure 3.1B**).

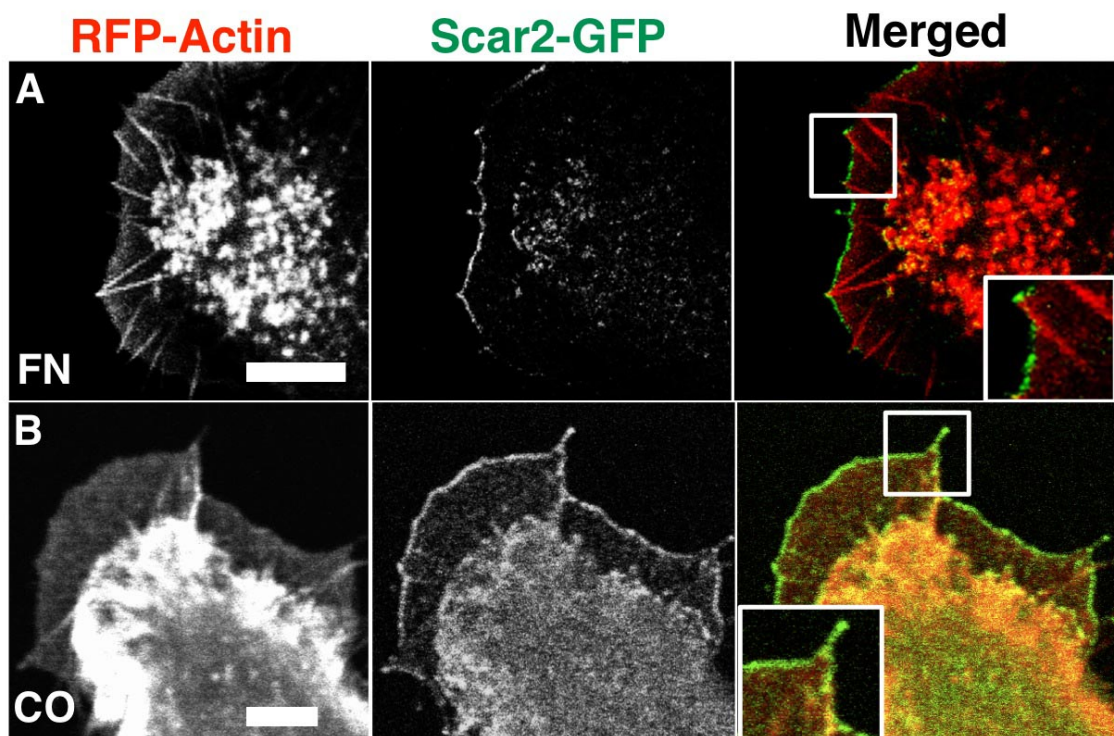


Figure 3.1 Localization of Scar2 in B16F10 cells

All panels show B16F10 cells. Confocal micrographs of Scar2-GFP (green) and RFP-actin (red) expressing cells migrating on (A) fibronectin (FN) or (B) collagen (CO) coated glass bottom dish. On both substrates Scar2-GFP localized to lamellipodia leading edge and filopodia tips. Scale bar A 10 μ m, B 5 μ m.

To verify the localization of Scar2-GFP, PIR121-GFP was expressed in B16F10 cells. When PIR121-GFP expressing B16F10 cells were allowed to migrate on FN coated glass bottom dish, PIR121-GFP demonstrated identical localization to the leading edge of lamellipodia and the tips of filopodia when compared with Scar2-GFP (**Figure 3.2A&B**). To confirm Scar2-GFP represented WRC, Abi1-RFP was co-expressed with Scar2-GFP in B16F10. When cells were allowed to migrate on fibronectin coated glass bottom dish, Abi1-RFP and Scar2-GFP demonstrated complete co-localization at the leading edge of lamellipodia (**Figure 3.2C**). Collectively, Scar2-GFP is believed to accurately represent WRC localization in live cells. As PIR121-GFP and Abi1-RFP had very low expression levels in B16F10 cells, Scar2-GFP was used in subsequent experiments to localize WRC.

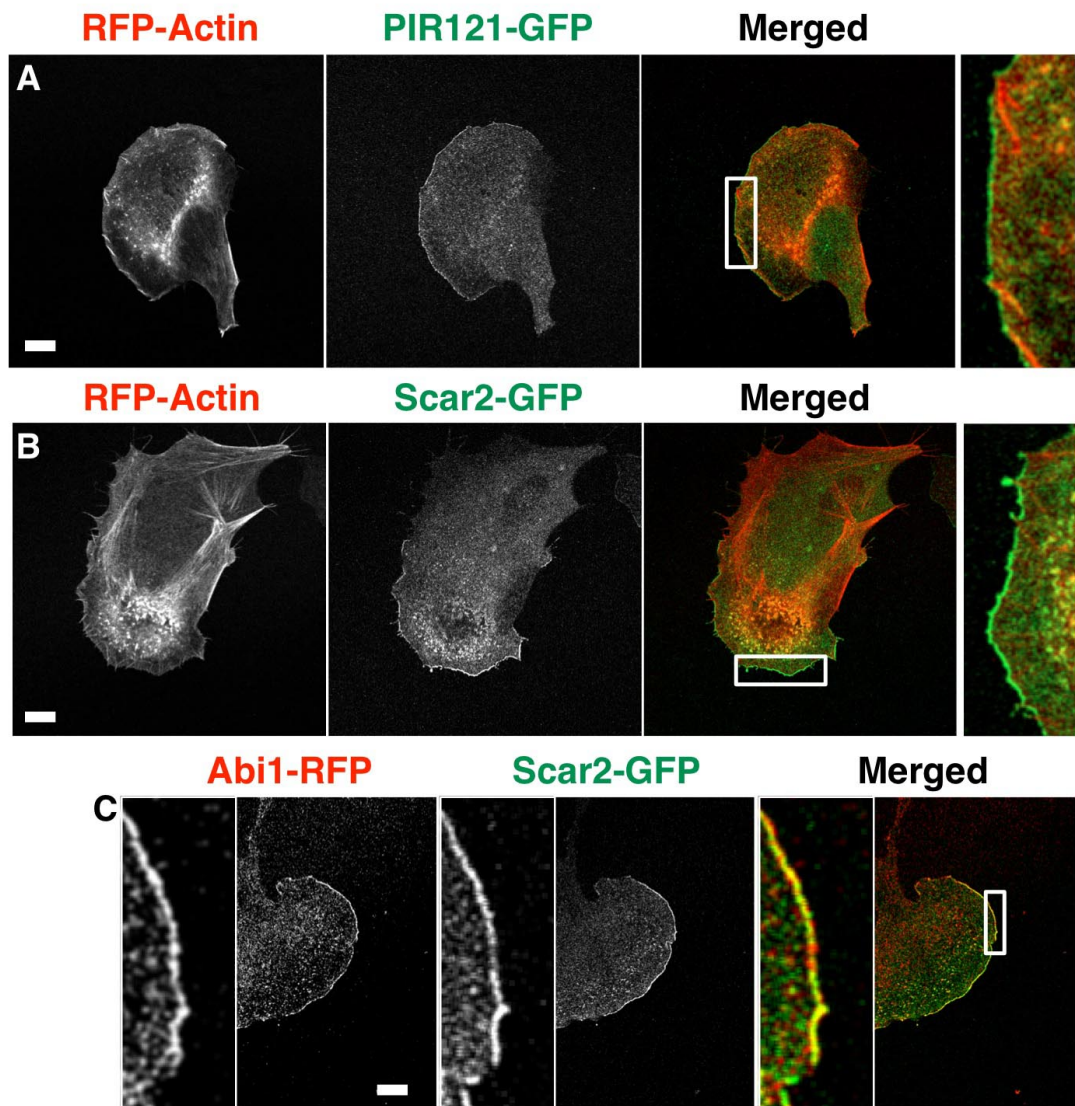


Figure 3.2 Scar2-GFP represents WRC localization

Confocal micrographs of cells expressing (A) PIR121-GFP (green) and actin-RFP (red), (B) Scar2-GFP (green) and actin-RFP (red), (C) Scar2-GFP (green) and Abi1-RFP (red). All fluorescent probes of WRC subunits had leading edge localization. All panels show B16F10 cells. Scale bar 10 μ m.

The dynamics of Scar2-GFP in B16F10 cells migrating on fibronectin coated glass bottom dish was studied using confocal microscopy. Interestingly, in addition to the leading edge, Scar2-GFP also localized to traveling waves at the back of the leading edge. While most waves at the back of the lamellipodium moved in a random fashion, waves closer to the leading edge moved towards the cell front (**Figure 3.3A**). Kymograph revealed that waves at the cell front traveled at the same speed ($1.96 \pm 0.199 \mu\text{m}/\text{min}$) as the protruding leading edge, however these waves never reached the leading edge. When the leading edge collapsed, the traveling wave also moved backwards and dispersed (**Figure 3.3B**). It is reported that, at least in human neutrophils, WRC forms propagating waves at the bottom of cells. These waves move towards cell periphery to promote lamellipodium formation (Weiner et al., 2007). To verify this behavior, the localization of WRC in live B16F10 cells was also studied using TIRF microscopy. While propagating waves of Scar2-GFP were observed at the cell-glass interface, these waves moved randomly beneath the nucleus (**Figure 3.3C**). Therefore, at least in B16F10 cells traveling Scar2-GFP waves do not contribute to the formation of lamellipodium. They are likely small membrane ruffles generated by WRC at the dorsal and ventral surface of migrating cells.

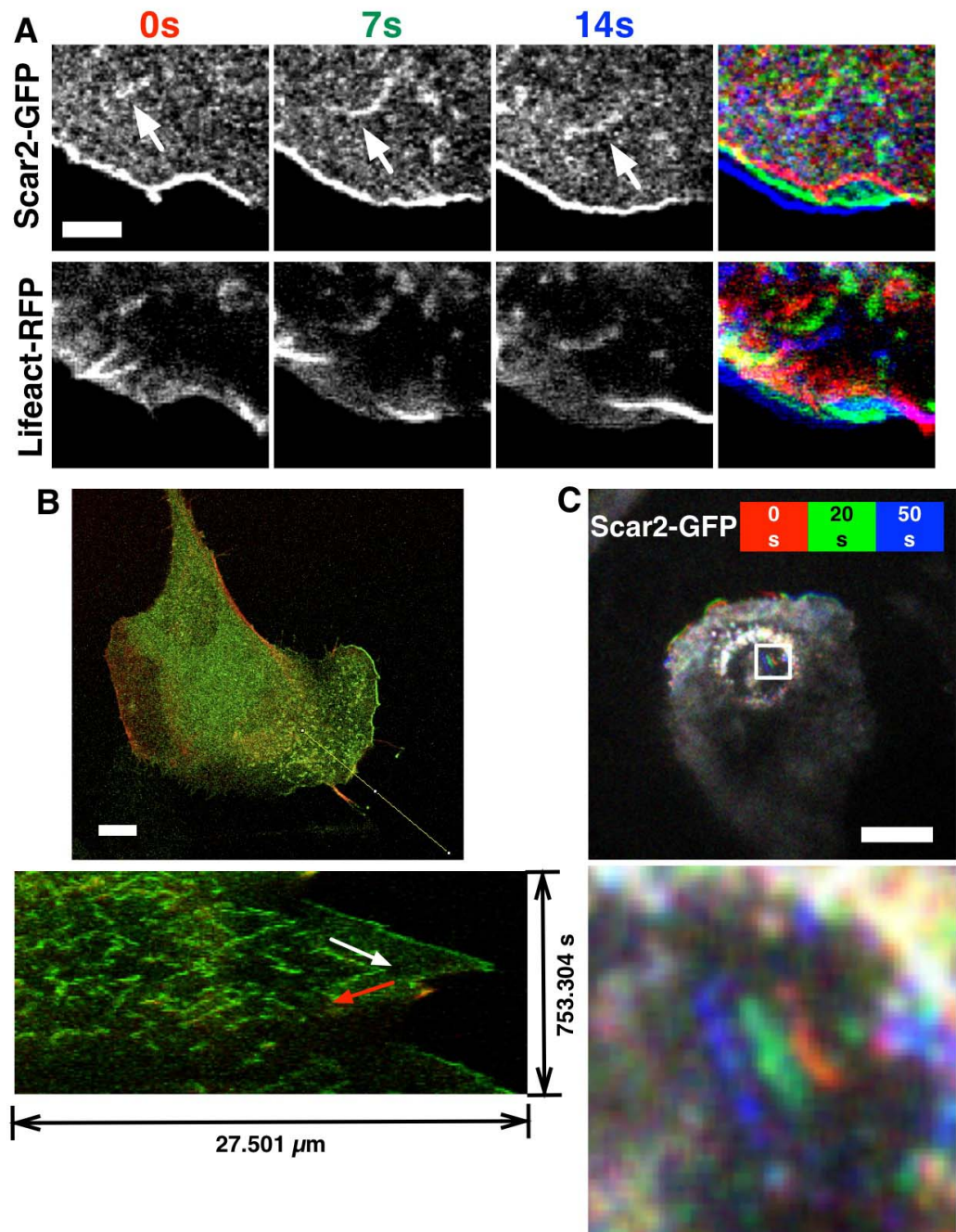


Figure 3.3 WRC dynamics in live cells

(A) Still micrographs of a confocal time lapses movie showing WRC dynamics at the leading edge and on the little traveling wave (arrow). Cells co-expressing Scar2-GFP as a marker for WRC, and Lifeact-RFP for F-actin were imaged. Still micrographs at indicated time points were pseudo-coloured accordingly and merged to form an image showing WRC dynamics. Scale bar 3 μm. (B) Kymograph of Scar2-GFP in a migrating cell. Scale bar 10 μm. (C) TIRF micrograph showing a travelling wave of Scar2-GFP just under the nucleus. Scale bar 10 μm. All panels show B16F10 cells.

Lipids and active Rac1 activates WRC on the plasma membrane. Interestingly, Scar2-GFP was observed to frequently fall off from the membrane, without causing the expanding membrane to retract. A small bud of Scar2-GFP was first formed on the membrane. At this point the bud was still tethered to the membrane. However in just a few seconds, the bud broke away from the membrane, and moved towards the cell body (**Figure 3.4**). Since this movement of Scar2-GFP was against the direction of expanding leading edge, it was likely an active process of transporting WRC back to the cytosol. In contrast, no active delivery of WRC to the leading edge was observed using the Scar2-GFP probe.

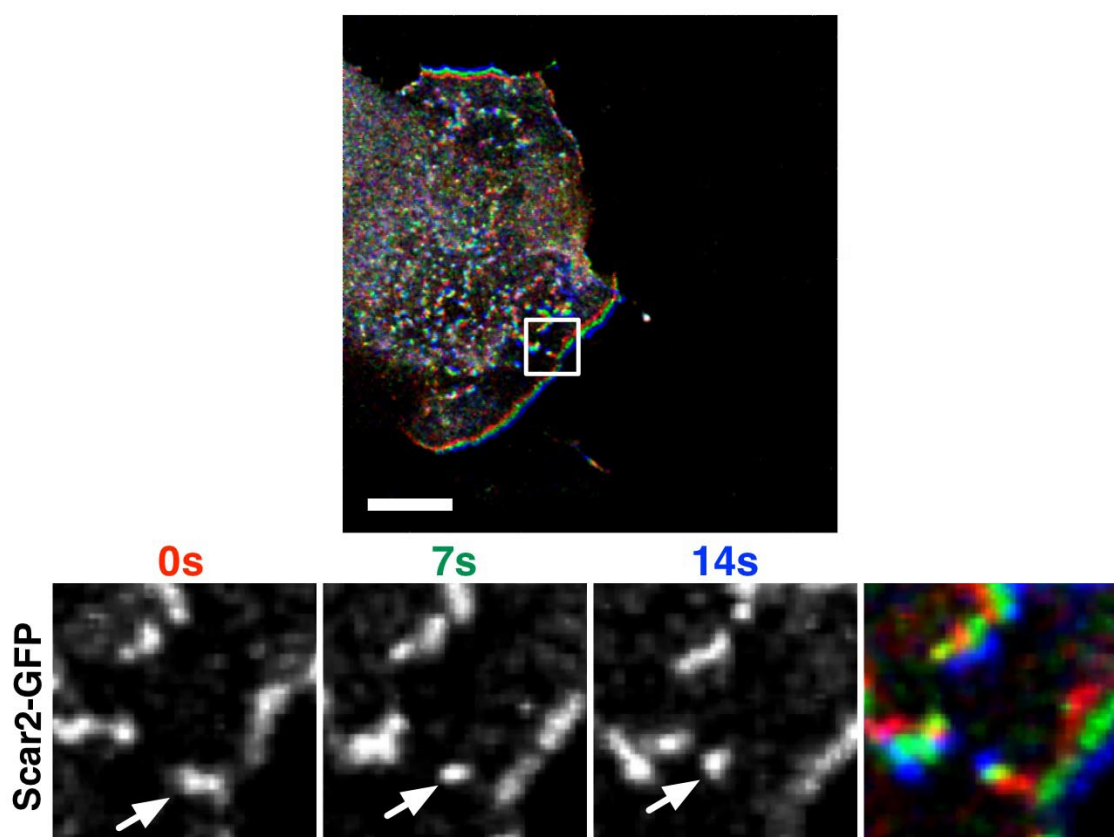


Figure 3.4 Internalization of WRC

Confocal micrograph showing Scar2-GFP labelled WRC (arrow) moving away from the leading edge of a B16F10 cell. Scale bar 10 μ m.

To exam WRC localization in live cells in 3D, B16F10 cells expressing Scar2-GFP were cultured on cell derived matrix (CDM). Cells generated long membrane protrusions on CDM. At the tips of these protrusions, multiple small ruffles were formed (**Figure 3.5A**). WRC localized to the edge of these small ruffles, as shown by strong Scar2-GFP localization (**Figure 3.5A**). Similar to the localization in 2D, little Scar2-GFP waves were also observed at the back of the membrane ruffles (**Figure 3.5B**). As the Scar2-GFP rich membrane ruffles moved forward, the whole cell migrated (**Figure 3.5A**). It is possible that WRC promotes extension of long protrusions by forming membrane ruffles at pseudopods tips in 3D.

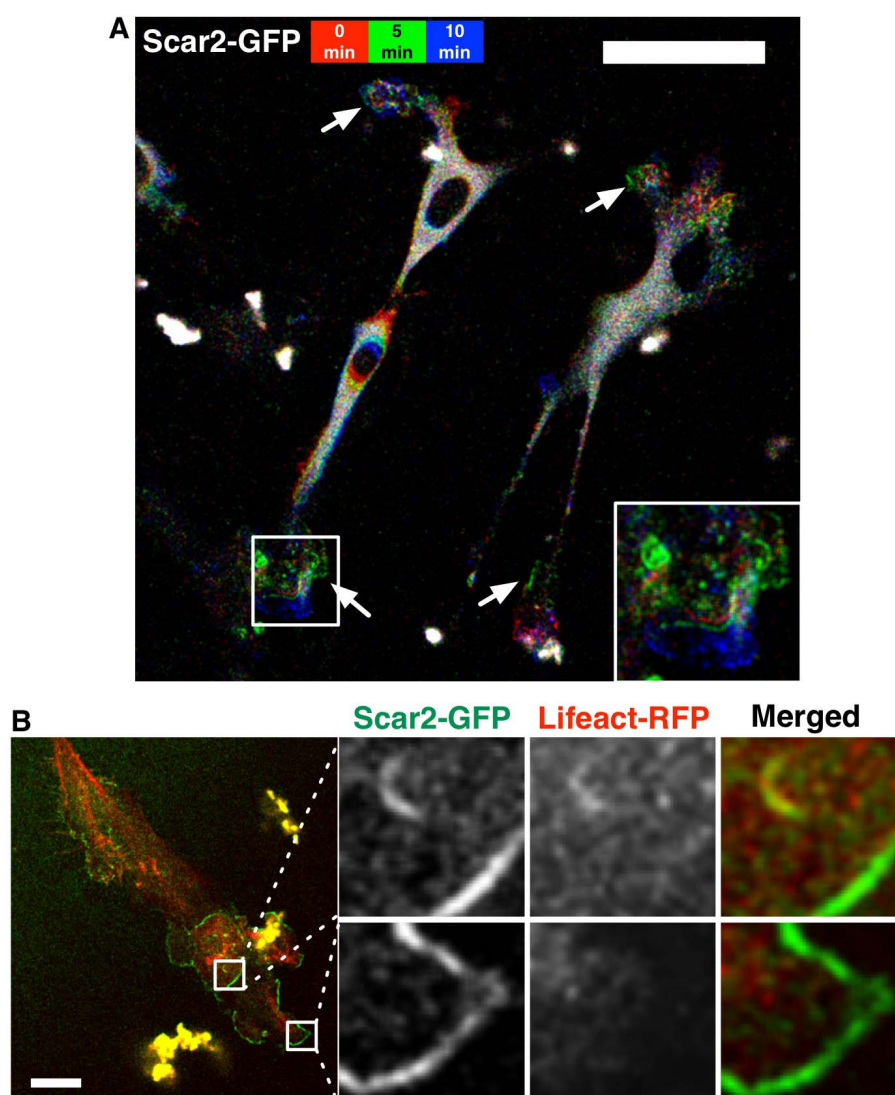


Figure 3.5 WRC localization on CDM

All panels show B16F10 cells. (A) Confocal micrograph showing WRC localization to membrane ruffle (arrow) at the tips of multiple protrusions when Scar2-GFP expressing cells were cultured on CDM. Scale bar 50 μ m. (B) Enlarged view of a thin protrusion in CDM. Scar2-GFP (green) and Lifeact-RFP (red) was co-expressed in cells to visualize WRC and F-actin respectively. Scale bar 10 μ m.

3.3 Discussion

In this study, WRC in live cells was visualized by using Scar2-GFP as a fluorescence probe. In live migrating mouse melanoma cells, WRC mostly localized to the leading edge of lamellipodia, and the tips filopodia. This observation is consistent with the reported localizations of WRC in fixed cells, and can be confirmed using other WRC fluorescence probes in live cells.

WRC can also form propagating waves at the dorsal and ventral surfaces of a migrating cell as observed with confocal microscopy and TIRF microscopy respectively. Similar waves are also observed in human neutrophils, where the propagating waves at the ventral surface contributed to the formation of leading edge (Weiner et al., 2007). Traveling actin waves also contribute to leading edge protrusion in *Dictyostelium* cells recovering from latrunculin A treatment (Gerisch et al., 2004). In contrast, mouse melanoma cells had small propagating waves oscillate at the back of advancing lamellipodia or just under the nucleus without contributing to the formation of leading edge. The little waves at the back of lamallipodium are most likely to be small membrane ruffles formed by WRC. Although the waves under nucleus could also be small membrane ruffles formed by WRC, the movement of these ruffles is perhaps restricted by focal adhesions at the bottom of cells. In contrast, neutrophils and *Dictyostelium* cells form relatively small/weak adhesions potentially allowing WRC generated ruffles to progress into propagating waves to form leading edge.

WRC was also observed to fall from the leading edge in migrating mouse melanoma cells. This observation is consistent with a recent report where WRC undergoes retrograde flow in a *Xenopus laevis* cell line (Millius et al., 2012). Therefore the retrograde movement of WRC is probably a general phenomenon. As Arp2/4 complex is frequently observed to undergo retrograde movement too, it is suggested that WRC associates with Arp2/3 complex on the membrane first to initiate actin nucleation. WRC/Arp2/3 complex is then removed form the membrane by actin retrograde flow (Millius et al., 2012).

Chapter 4: Role of WRC in 3D cell migration

4.1 Introduction

It is well known that 2D cell migration on rigid surfaces requires WRC. Recent researches using knockout animal models and cancer samples however reveal a more complex picture of WRC function in vivo. During embryonic development, depending on the specific tissue or cell type, subunits of WRC can be either pro-migratory or anti-migratory. For example, Nap1 is required for anterior visceral endoderm cell migration (Rakeman and Anderson, 2006) but pre-mature expression of Nap1 in cortical neurons prevents cell migration (Yokota et al., 2007). In epithelial cancers, Sra1 and Scar2 suppresses cancer cell invasion (Silva et al., 2009), while HSPC300 is required for cancer cells to invade and survive (Escobar et al., 2010). It is therefore important to understand the role of WRC in 3D cell motility. Although animal studies have high biological fidelity and in this case, can reveal physiologically relevant functions of WRC, it is technically more difficult to study molecular mechanisms in vivo. Instead, in vitro systems are used. However in this study, to mimic the in vivo three-dimensional environment, multiple types of collagen gel based 3D cell culture systems were used to study WRC function in 3D cell motility. Using these in vitro systems, loss of WRC was found to promote 3D cell motility through a novel N-WASP/Arp2/3 complex dependent mechanism.

4.2 Loss of WRC promotes invasion of epithelial cells

4.2.1 Generation and characterization of stable WRC knockdown cell lines

To investigate the role of WRC in epithelial cancer cell invasion, I generated stable WRC knockdowns in A431 squamous carcinoma cells, where epithelial properties, like cell-cell junctions, are still preserved. To effectively reduce the whole complex expression and to avoid off target effects, four components of WRC, namely, Nap1, Sra1, PIR121(PIR) and Scar2, were first targeted by various shRNAs. Among the resulting stable cell lines, I identified three cell lines with substantial Nap1 reduction (**Figure 4.1A**), two cell lines with substantial PIR121 reduction (**Figure 4.1B**), one cell line with substantial Sra1 reduction (**Figure 4.1C**), and one cell line with substantial Scar2 reduction (**Figure 4.1C**).

It is unknown how WRC subunits protein expression is regulated, but protein stability of many WRC components requires intact WRC. (Escobar et al., 2010, Innocenti et al., 2005, Silva et al., 2009, Kunda et al., 2003). In order to test the whole complex was indeed disrupted, four stable cell lines, namely shNap (Nap1 shRNA C), shSra1, shPIR (PIR121 shRNA E) and shScar2, were selected to test the protein level of all WRC subunits including various isoforms of some components (**Figure 4.1C**). As a result, shNap1 and shSra1 cells demonstrated strong reduction of Nap1, Sra1/PIR121, Scar1/2, but modest reduction of Abi1/2 and HSPC300. In contrast, shPIR cells only had slight reduction of Scar1/2 and Abi2. In Scar2 stable knockdown cells, PIR121 was also dramatically reduced, but there was only mild reduction for Nap1 and Abi2. There was also slight reduction of HSPC300 in Scar2 knockdown cells. Protein levels of Sra1 and Abi1 were not affected by Scar2 depletion. Interestingly, Scar1 protein level was increased in Scar2 stable knockdown cells. Collectively, these results suggest various subunits, and their isoforms contribute differently to WRC stability, Nap1 and Sra1 are among the most important ones required to form the complex.

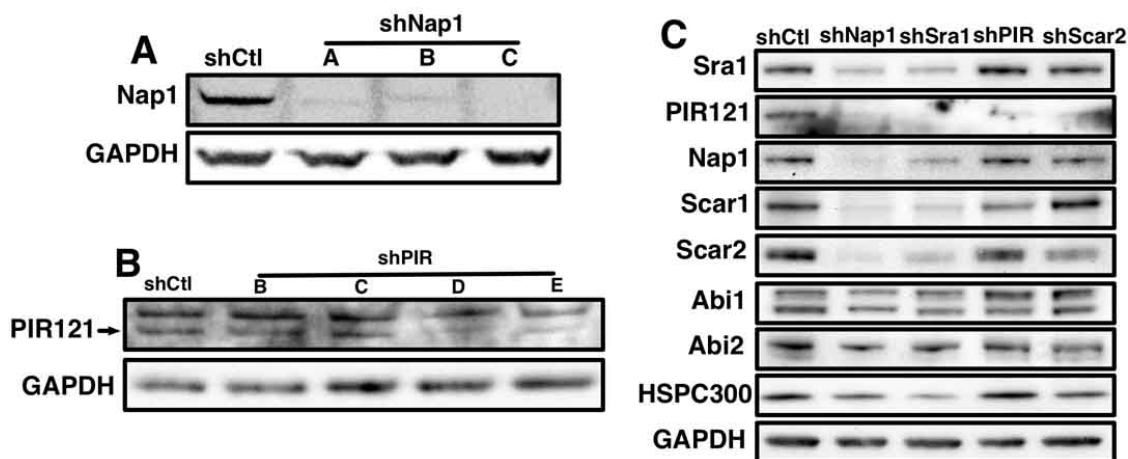


Figure 4.1 Characterizations of WRC shRNAs.

All panels show A431 cells. (A) Western blot shows three working shRNAs targeting Nap1, namely, A, B, C. (B) Western blot shows four shRNAs targeting PIR121. Only shRNA, D & E mediated sufficient reduction of PIR121. (C) Representative western blots for individual subunits of WRC in shCtl, shNap1 (shRNA C), shSra1, shPIR (shRNA E) and shScar2 stable knockdown cell lines. The blot is representative of at least 3 repeats. Antibody specificity to Sra1 or PIR121 was verified using GFP labelled proteins, not shown.

To further analyze the total WRC level in the stable knock down cell lines, I performed Blue NativePAGE (Schagger et al., 1994) to reveal the native complex. An anti-HSPC300 antibody (Derivery et al., 2008) was used for immunoblotting of the complex separated by Blue NativePAGE. As HSPC300 has no known isoforms in human cells and is an essential part of the complex, using HSPC300 as a probe should reveal the total WRC protein level. Consistently, the result confirmed strong reduction of total WRC level (approx. 400kDa) in Nap1 and Sra1 stable knockdown cells (**Figure 4.2A**). Because of Scar1 over-expression in Scar2 stable knockdown cells, there was only a small reduction of the total complex level in these cells. When ‘Scar1 complex’ was probed using Blue NativePAGE, loss of Scar2 in fact promoted formation of the ‘Scar1 complex’ suggesting compensation from Scar1 protein (**Figure 4.2B**). Loss of PIR121, however, had little impact on the stability of the complex, as there was only a slight reduction of the total complex level (**Figure 4.2A**).

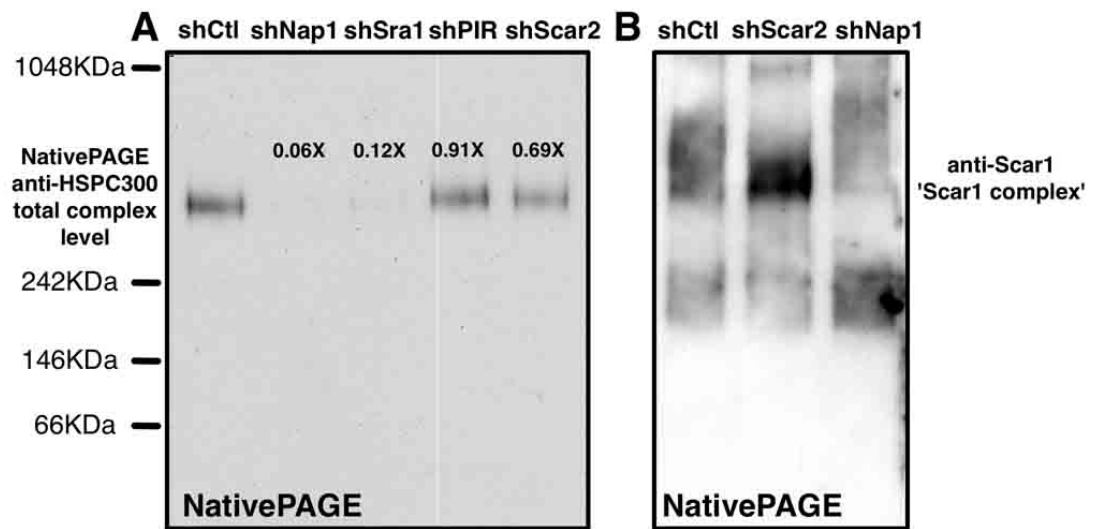


Figure 4.2 WRC expression level revealed by Blue NativePAGE

All panels show A431 cells. (A) Representative Blue NativePAGE probed with an anti-HSPC300 antibody showing levels of total WRC in various WRC KD cells. Numbers on top of the band show the relative level of the remaining complex. The blot is representative of at least 3 repeats. (B) Representative Blue NativePAGE probed with an anti-Scar1 antibody showing elevation of Scar1 WRC expression in cells depleted of Scar2. The blot is representative of at least 3 repeats.

Morphology of these knockdown cells correlated nicely with the complex level, as Nap1 and Sra1 knockdown cells demonstrated typical blebby membrane phenotype with no lamellipodia, while PIR121 and Scar2 knockdown cells maintained the ability to generate membrane protrusions and ruffles (**Figure 4.3**). Although PIR121 and Scar2 depleted cells appeared normal when fixed (**Figure 4.3**), time-lapse movies demonstrated that these cells were unable to generate stable lamellipodia during spreading and spread more slowly and to a lesser extent than non-targetting shCtl cells (**Figure 4.4A,B**). Nap1 and Sra1 stable knockdown cells also had severe spreading defects due to strong defects in membrane protrusion formation. Nap1 and Sra1 stable depleted cells (WRC KD cells) were therefore selected for subsequent experiments, as they gave the most robust loss of WRC subunits (Sra1, PIR121, Nap1, Scar1/2) and reduction of total complex levels.

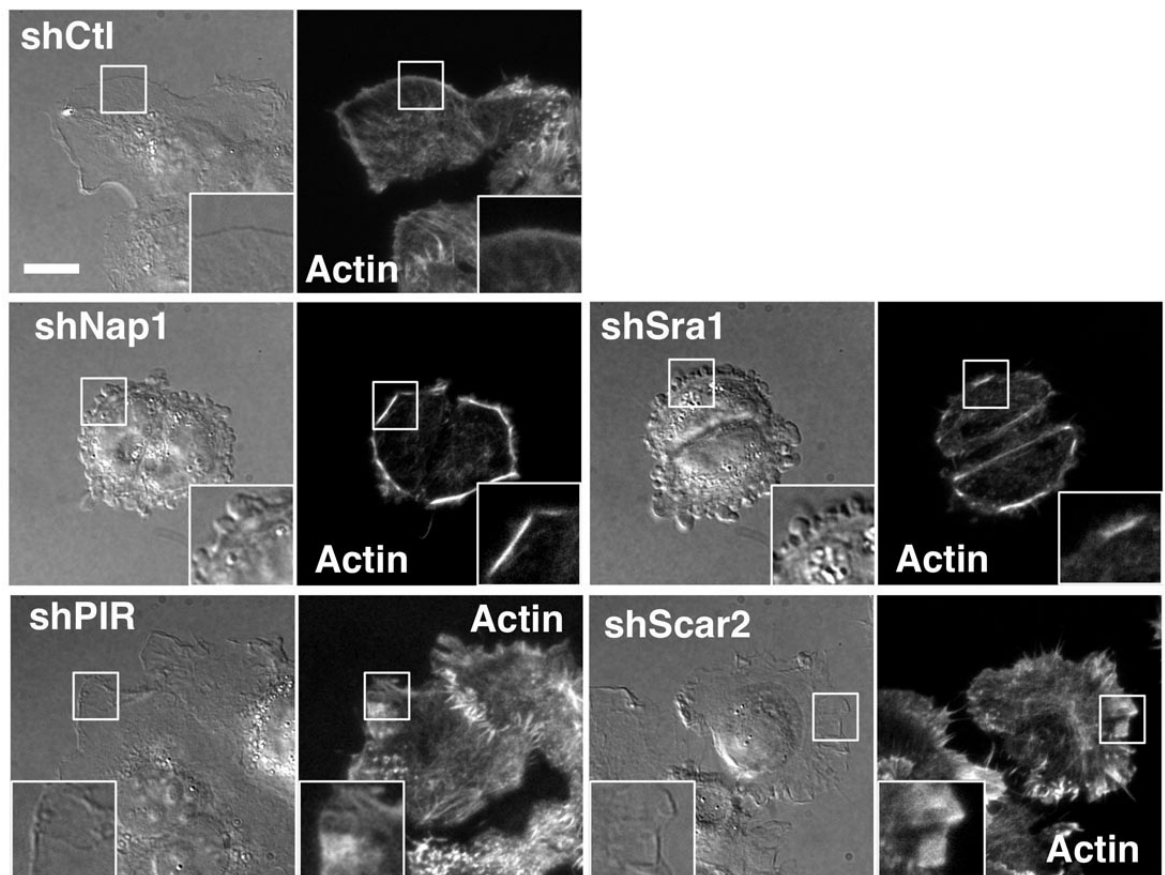


Figure 4.3 Morphology of various WRC KD cells

Stable WRC KD cells in DIC and accompanying TIRF micrograph showing rhodamine phalloidin labelled filamentous actin. Scale bar 30 μ m. All panels show A431 cells on collagen coated glass bottom dish.

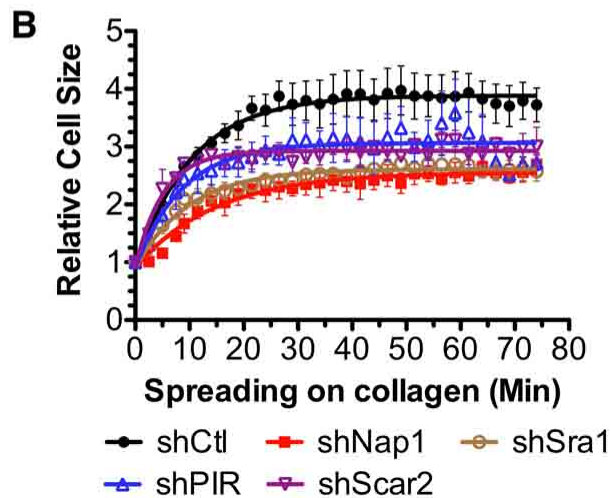
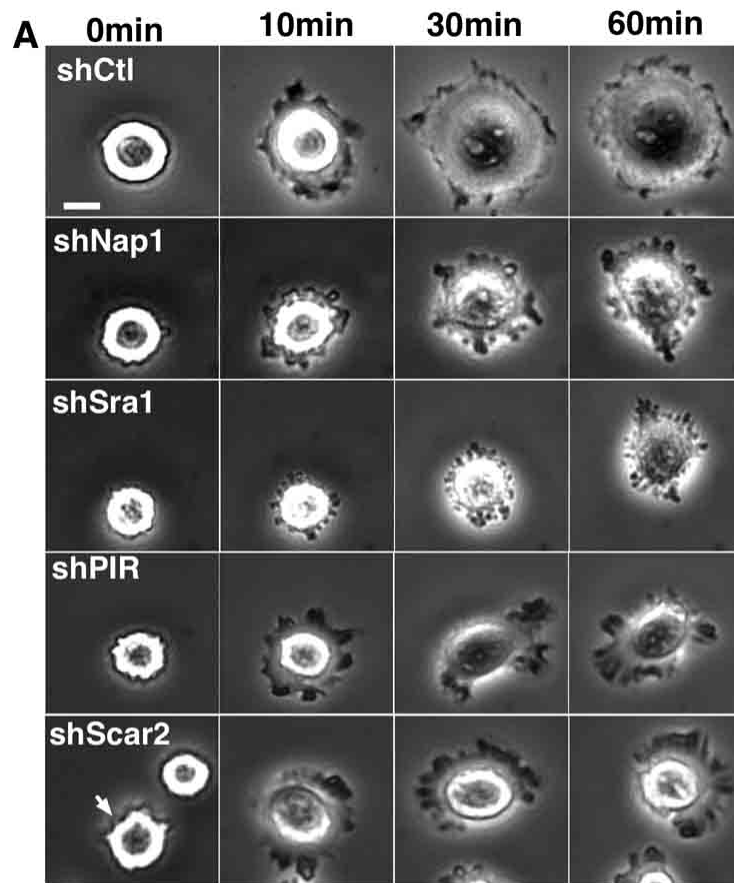


Figure 4.4 Cell spreading defects of various WRC KD cells

All panels show A431 cells. (A) Representative time points of various WRC KD cells spreading on collagen-coated glass dishes. Scale bar 10 μ m. (B) Cell area of WRC KD cells was measured at the start and at indicated time points. 4 cells were measured from 4 independent time-lapse movies for each cell line. The relative cell size reflects the size at indicated time divided by the size at t=0. (Data points are means \pm SEM, n=4. Curves are fitted with nonlinear regression).

4.2.2 WRC suppresses epithelial cancer cell invasion

Sra1 expression is reduced in some epithelial cancers and its loss can cooperate with Ras to promote invasive carcinomas (Silva et al., 2009). Collagen gel based invasion assays were used to test the invasiveness of WRC KD cells. Interestingly, WRC KD cells invaded at least 4x deeper into collagen gel organotypic assays than non-targeting (NT) control cells (shCtl) and showed much higher relative invasion area (**Figure 4.5**). This invasive phenotype of WRC KD cells was also confirmed in 3D collagen gel invasion assay where a cell plug was fully embedded in the collagen gel (**Figure 4.6A**) (Hotary et al., 2006). WRC KD cells invaded 5-fold more deeply into the collagen from the plug and showed 8 times higher relative invasion area (**Figure 4.6B,C**).

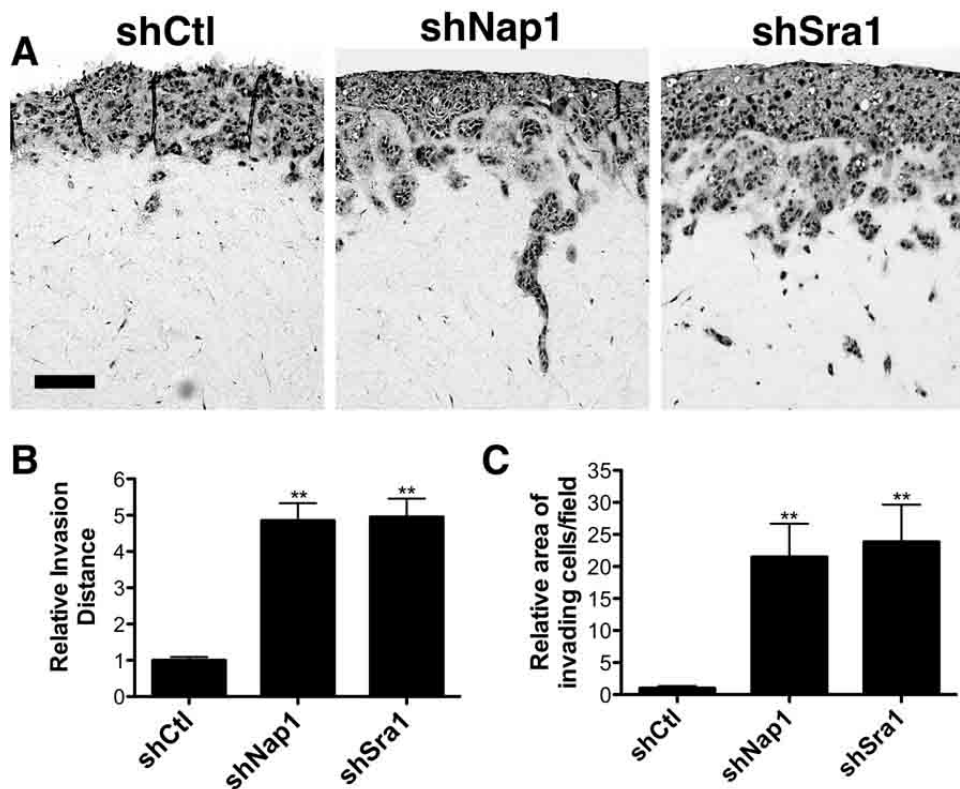


Figure 4.5 WRC KD cells are invasive in organotypic assays

All panels show A431 cells. (A) H&E-stained sections of shNap1 and shSra1 cells invading into collagen gel in a 3D organotypic assay. Scale bar 100 μ m. (B) Quantification of the relative invasion distance in the organotypic assay. (Data are means \pm SEM, n=24 images from 3 independent assays, **p<0.01). (C) Quantification of the relative area of invading cells per field in the organotypic assay. (Data are means \pm SEM, n=5 images from 3 independent assays, **p<0.01).

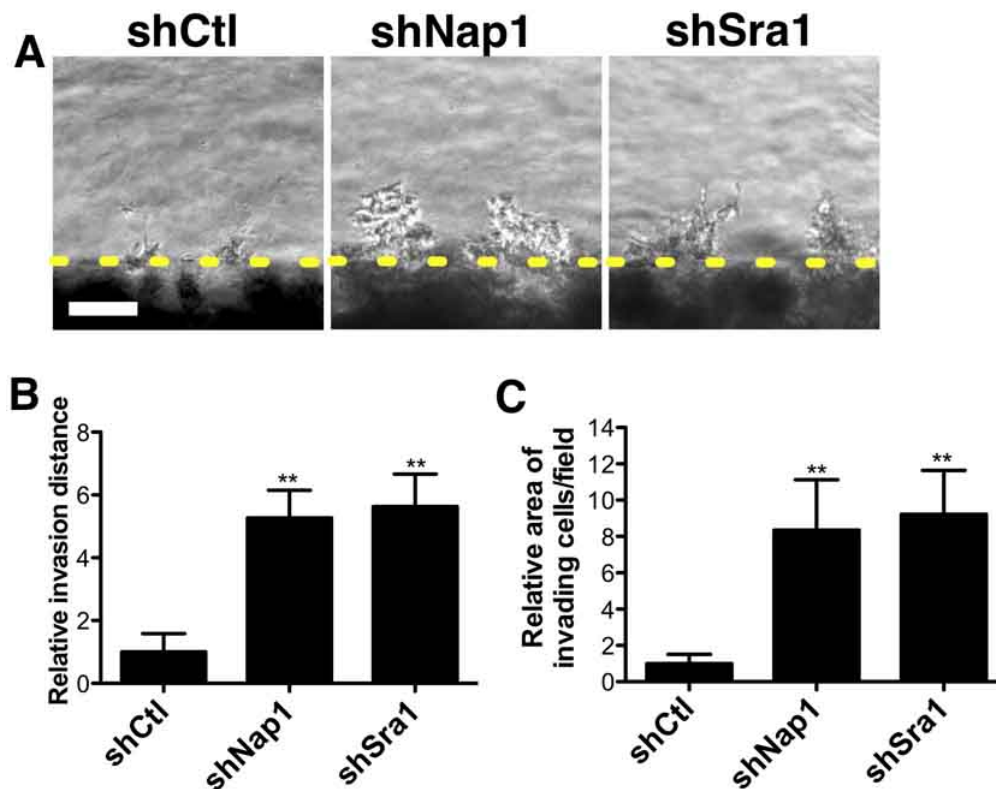


Figure 4.6 WRC KD cells are invasive in 3D collagen gel

All panels show A431 cells. (A) Phase contrast micrograph demonstrate invasion of shNap1 and shSra1 cells in a 3D collagen gel invasion assay. Scale bar 100 μ m. (B) Quantification of 3D collagen gel invasion assay shows the relative invasion distance and (C) the relative area of invading cells per field (Data are means \pm SEM, n=9 images from 3 independent assays, **p<0.01).

In contrast, the same cells migrated up to 70% slower in 2D planar wound healing assays (**Figure 4.7**). To confirm that increased 3D motility of WRC KD cells was a unique response to ECM, which can be a barrier for 3D cell migration, a thick layer of Matrigel was added on top of the wound healing assay. Cells were thus required to migrate through the Matrigel to close the wound (Yu and Machesky, 2012). Interestingly, WRC KD cells showed more rapid invasion in this assay as well (**Figure 4.8A,B**). As GM6001, a metalloprotease inhibitor, retarded WRC KD cell motility in this assay (**Figure 4.8C**), the result suggests that WRC is not limiting for invasive migration in this assay. Thus, I conclude that while WRC promotes motility in 2D, its depletion does not inhibit and can actually promote invasion in multiple types of 3D environment.

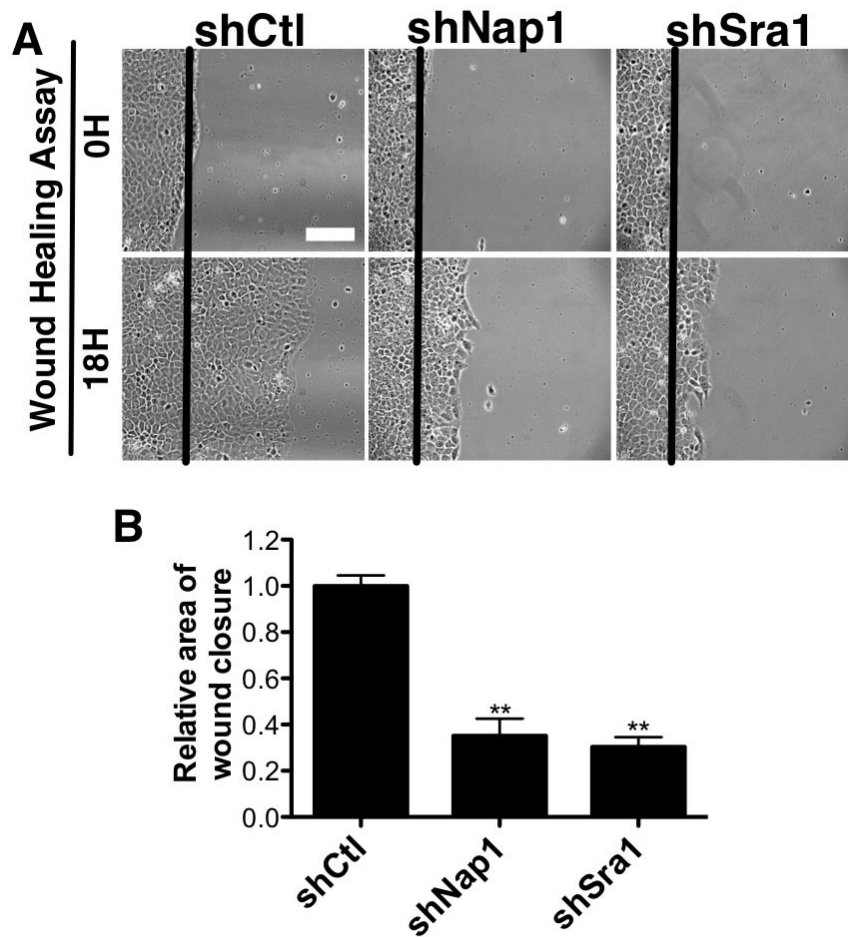


Figure 4.7 Cell migration defects of WRC KD cells

(A) Still photos from time-lapse of wound healing assay. Scale bar 200 μ m. (B) Relative area of wound closure of control and WRC (Nap1&Sra1) depleted cells. (All data are means \pm SEM, n=3 independent samples **p<0.01). All panels show A431 cells.

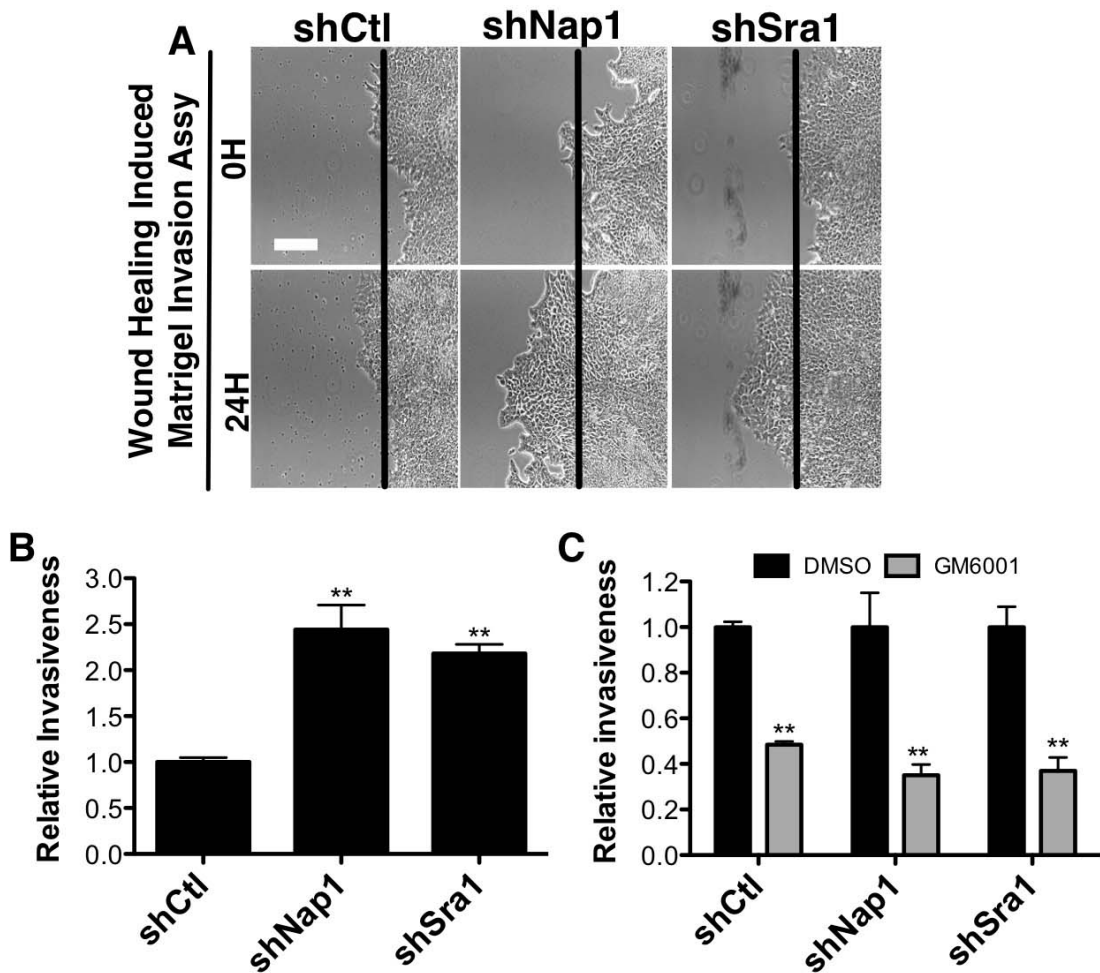


Figure 4.8 Loss of WRC promotes invasion through matrigel

(A) Still photos from time-lapse of wound healing induced Matrigel invasion assay. Scale bar 200 μ m. (B) Quantification of the matrigel invasion assay (Data are means \pm SEM, n=8 independent samples, **p<0.01). (C) Metalloproteinase inhibitor, GM6001, induces sharp reduction of cell invasion in wound healing induced matrigel invasion assay (Data are means \pm SEM, n=9 independent samples. **p<0.01). All panels show A431 cells.

4.2.3 Arp2/3 complex is required for invasion

Since WRC drives actin assembly via the Arp2/3 complex, I asked whether the mechanism of invasion in WRC depleted cells was Arp2/3 dependent. When cells were cultured atop of a thick collagen gel (thick collagen gel invasion assay), control cells invaded into thick collagen gel with leading edge cells nearly always showing long thin protrusions. In contrast, WRC KD cells generated short actin rich protrusions when invading into the collagen gel (**Figure 4.9**).

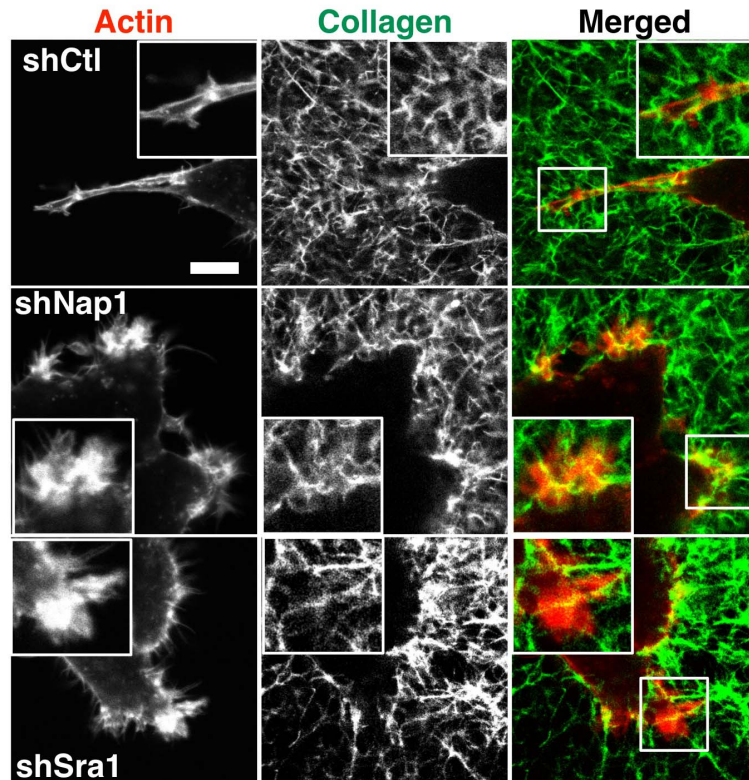


Figure 4.9 WRC KD cells produce blunt protrusions in collagen gel

Stable A431 WRC KD cells invading in FITC collagen gel. Confocal micrographs show rhodamine phalloidin labelled filamentous actin (red) and collagen (green). Scale bar 10 μ m.

The presence of Arp2/3 complex in the two types of protrusions was then analysed. When a GFP Arp2/3 complex probe, p21-Arc-GFP, was expressed in cells, the long thin protrusions produced by control cells in collagen gel contained only modest enrichment of Arp2/3 complex at their tips. In contrast, the less elongated protrusions (pseudopods) in WRC KD cells had a strong enrichment of Arp2/3 complex accumulating in a jagged front (**Figure 4.10**). It is likely that Arp2/3 complex rich short protrusions promote the invasion of WRC KD cells in collagen gel.

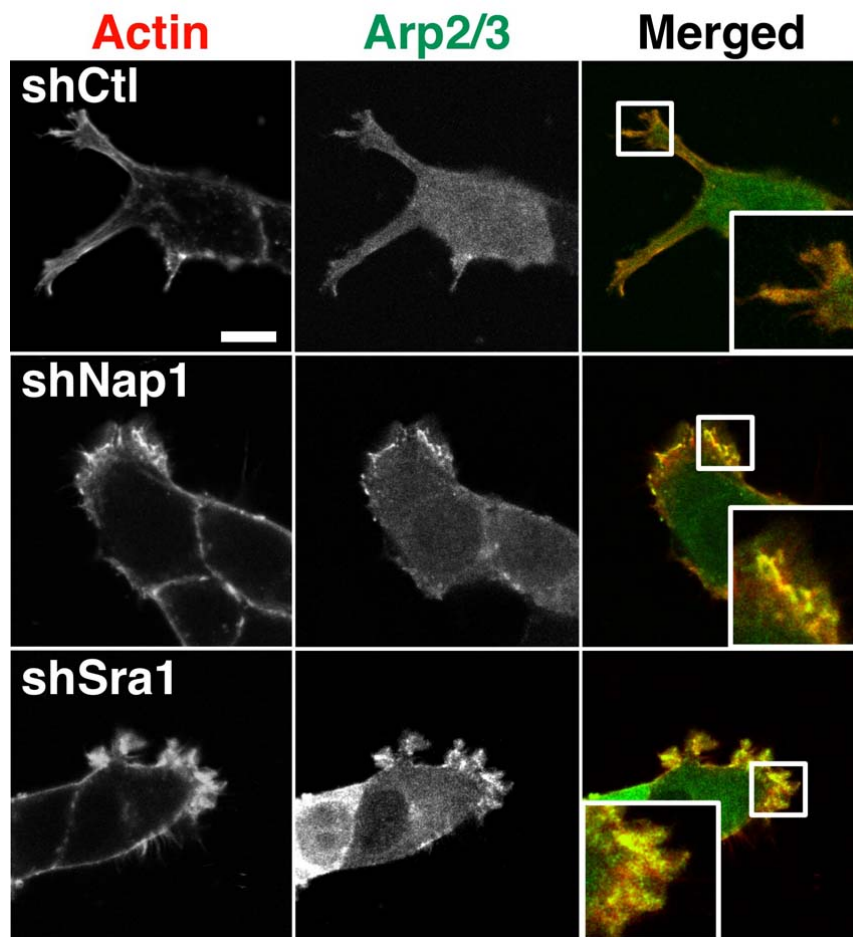


Figure 4.10 Loss of WRC promotes Arp2/3 complex localization to cell front during invasion.

Control and WRC depleted cells expressing p21-Arc-GFP (Arp2/3 complex marker, green) and stained with rhodamine phalloidin (filamentous actin, red) invading into thick collagen gels. Scale bar 10µm. All panels show A431 cells and confocal micrographs.

To study if Arp2/3 complex was required for the invasion of WRC KD cells, Arp2/3 complex expression was reduced using siRNAs targeting p34-Arc subunit (**Figure 4.11A**). When cells were allowed to invade in the 3D collagen gel invasion assay, loss of Arp2/3 complex did not promote the invasion of control cells, while the invasion of Nap1 and Sra1 stable KD cells was heavily reduced upon loss of Arp2/3 complex. Both the invasion distance and the relative invasion area were reduced when Arp2/3 complex was removed from these WRC KD cells (**Figure 4.11B,C,D**). Thus, depletion of WRC does not prevent accumulation of Arp2/3 complex at the front of invading pseudopods. Moreover, cells depleted of WRC can actually invade more efficiently than controls. Arp2/3 complex, in contrast, is required for invasion in both control and WRC-depleted cells.

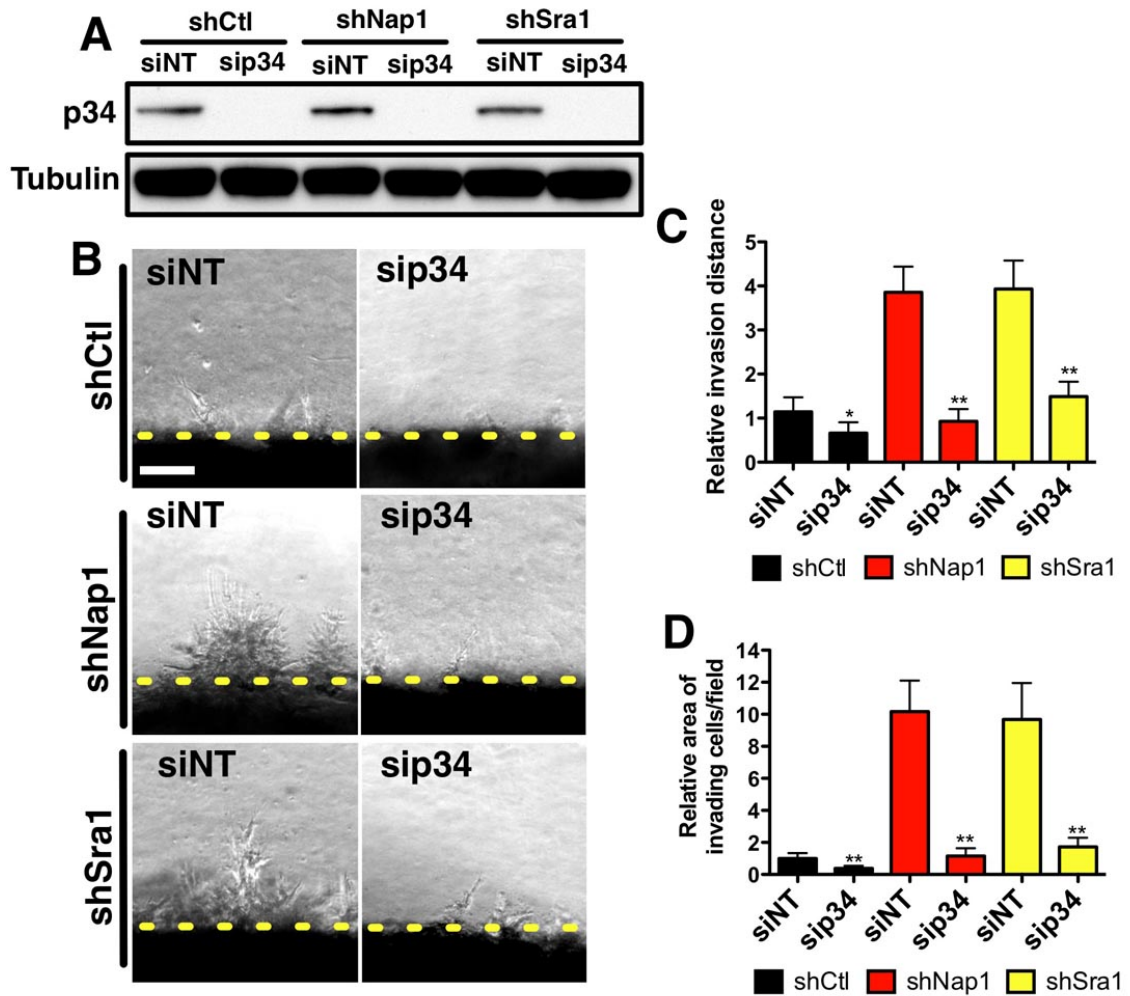


Figure 4.11 Arp2/3 complex is required for invasion

(A) Western blot showing p34-Arc (Arp2/3) level and tubulin control of cells treated with a p34 siRNA. (B) Phase contrast micrographs of Nap1 and Sra1 knockdown cells invading into collagen gels either with control transient siRNA (siNT) or knockdown of Arp2/3 complex (sip34, p34-Arc subunit). Scale bar 100 μ m. (C,D) Quantification of invasion into thick collagen gels (Data are shown as means \pm SEM, n=12 images from 3 independent assays, *p=not significant, **p<0.01). All panels show A431 cells.

4.2.4 N-WASP activates Arp2/3 complex

The strong presence and requirement for Arp2/3 complex in invasive pseudopods in WRC depleted cells raised the question of how Arp2/3 complex was being activated in the absence of WRC. In addition to WRC, N-WASP also activates Arp2/3 complex to promote actin polymerization at the plasma membrane (Kim et al., 2000). N-WASP localization was then studied in WRC KD cells using the thick collagen gel invasion assay. N-WASP accumulated with Arp2/3 complex to pseudopod tips of WRC depleted cells where both N-WASP and Arp2/3 complex relative fluorescence intensity was increased by two fold (**Figure 4.12A,B**). This accumulation of N-WASP and Arp2/3 complex was not simply a reflection of increased thickness at the invasive front, as GFP labeled Arp2/3 complex localized specifically to actin rich structures, while GFP alone did not (**Figure 4.12C**).

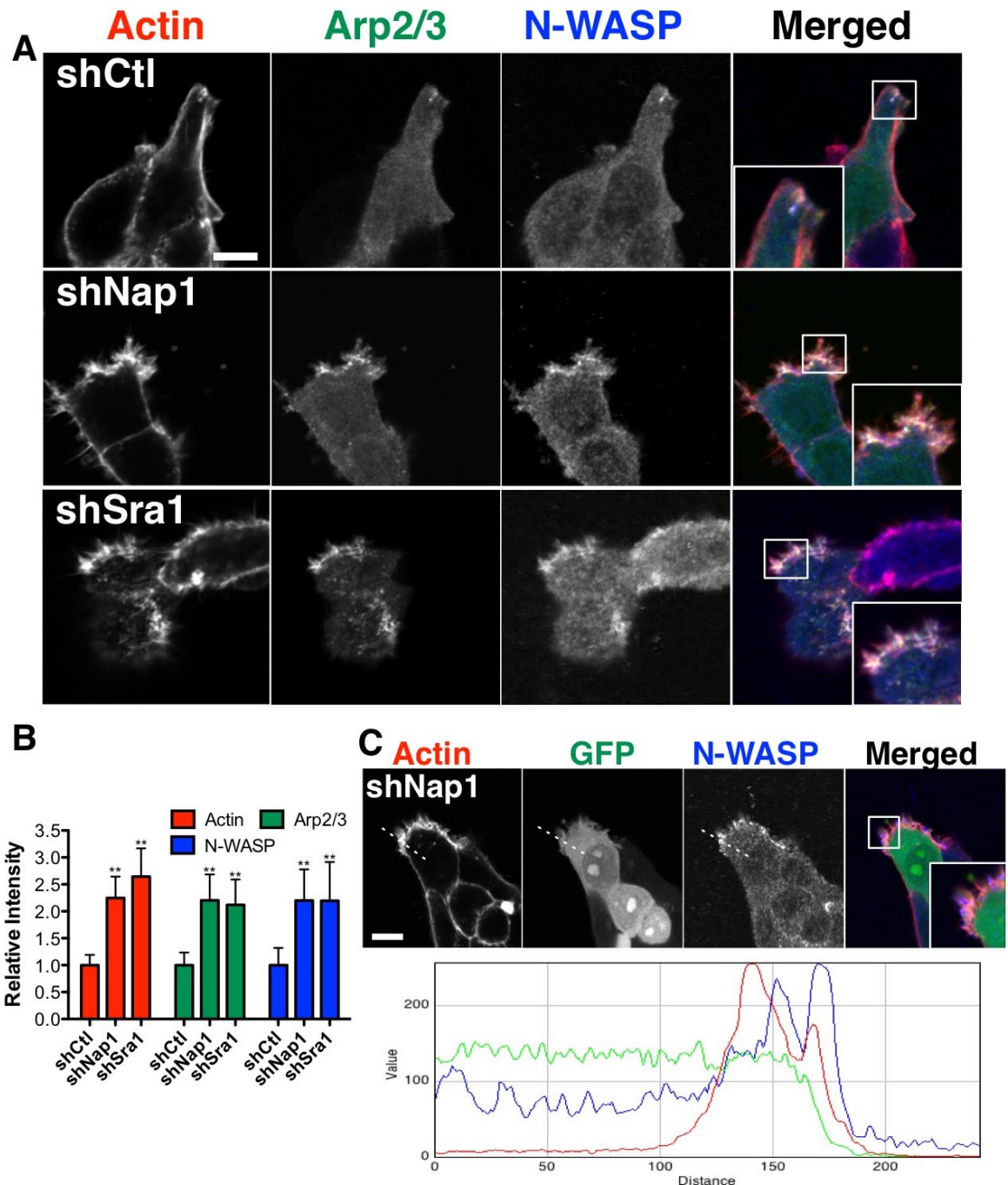


Figure 4.12 Without WRC, N-WASP activates Arp2/3 complex

(A) Confocal micrographs demonstrate co-localization of endogenous N-WASP (anti-N-WASP, blue) and Arp2/3 complex (p21-Arc-GFP, green) and filamentous actin (rhodamine phalloidin, red) in WRC depleted or control cells during invasion into thick collagen gels. Scale bar 10 μ m. (B) Nap1 and Sra1 depleted cells had increased Actin, Arp2/3 (p21-Arc-GFP) and endogenous N-WASP fluorescence intensity in pseudopods relative to shCtl cells. (Data are shown as means \pm SD, n=10 for relative intensity, **p<0.01). (C) Confocal micrographs demonstrate cytoplasmic GFP (green), endogenous N-WASP (anti-N-WASP, blue) and filamentous actin (rhodamine phalloidin, red) in WRC depleted cells. Scale bar 10 μ m. Plot of fluorescent intensity along the dotted line shows no cytoplasmic GFP accumulation at the actin/N-WASP rich protrusion. All panels show A431 cells.

Co-localization and enrichment of N-WASP with Arp2/3 complex and actin at the tip of invasive pseudopods suggests N-WASP dependent activation of Arp2/3. Indeed, when N-WASP expression was reduced using siRNAs in Nap1 and Sra1 stable KD cells (**Figure 4.13A**), depletion of N-WASP triggered loss of Arp2/3 localization and reduction of actin enrichment (a 60% reduction in relative fluorescence intensity for both) at the cell front of WRC depleted cells suggesting loss of Arp2/3 complex function (**Figure 4.13B,C,D**). When cells were tested in 3D collagen gel invasion assay, loss of N-WASP prevented invasion of Nap1 and Sra1 stable KD cell, and did not promote invasion of control cells (**Figure 4.14**). Collectively, the data demonstrate that N-WASP accumulation at leading edges of cells in 3D matrix drives Arp2/3 complex dependent invasion and that this increases in WRC knockdown cells.

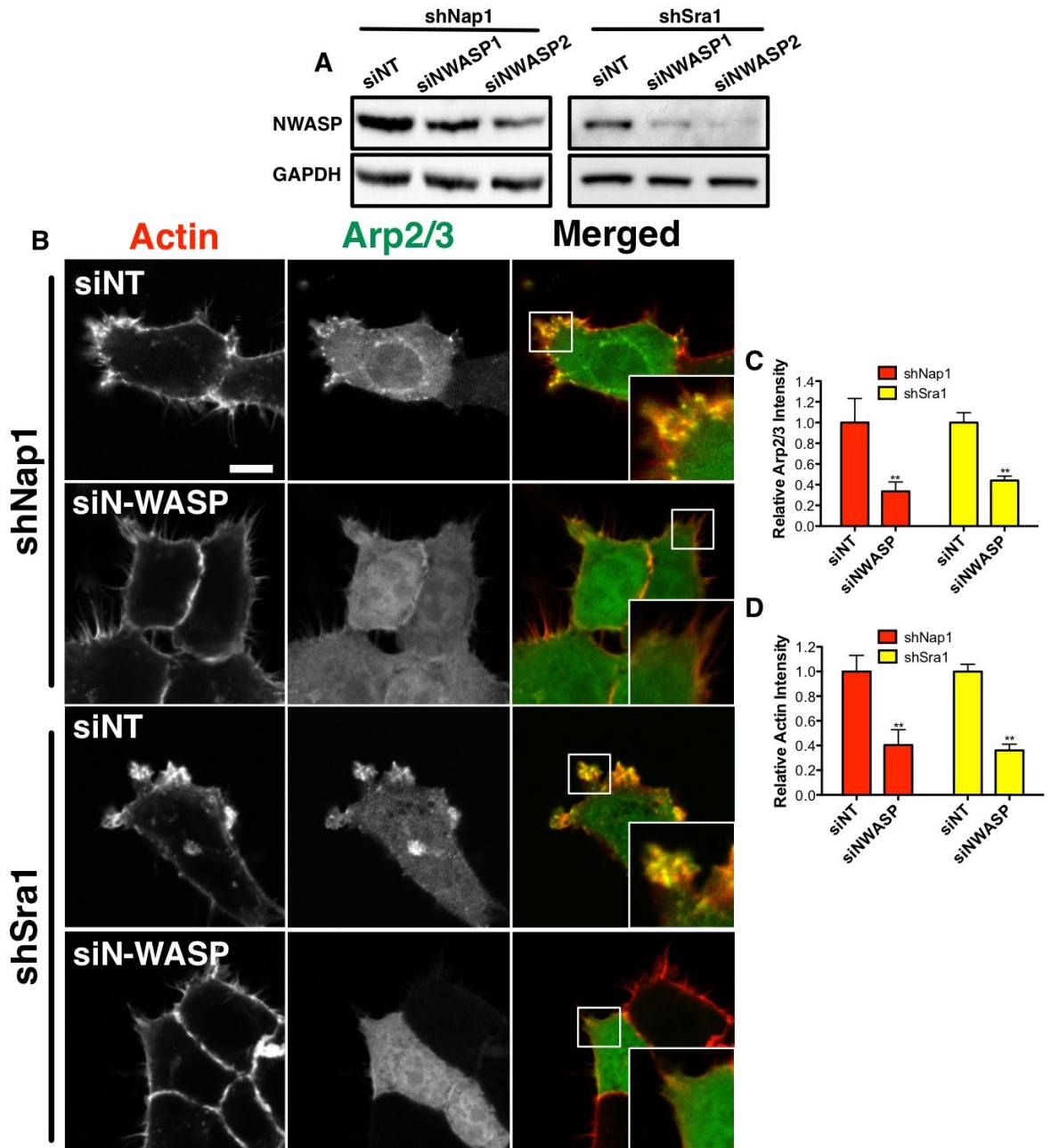


Figure 4.13 N-WASP is required for Arp2/3 complex localization

(A) Western blots showing N-WASP levels in cells treated with two separate N-WASP siRNAs with GAPDH level as control. N-WASP siRNA2 was used for major experiments due to better reduction of N-WASP. (B) p21-Arc-GFP (green) expressing Nap1 and Sra1 stable knockdown cells were treated with control siRNAs (siNT) and N-WASP siRNA (siN-WASP2). Cells were fixed and labeled with rhodamine phalloidin for actin (red) and examined by confocal microscopy during invasion into thick collagen gels. Scale bar 10 μ m. (C, D) Loss of N-WASP reduced both Arp2/3 (p21-Arc-GFP) and actin accumulation in pseudopods. (Data are shown as means \pm SD, n=5 cells, **p<0.01). All panels show A431 cells.

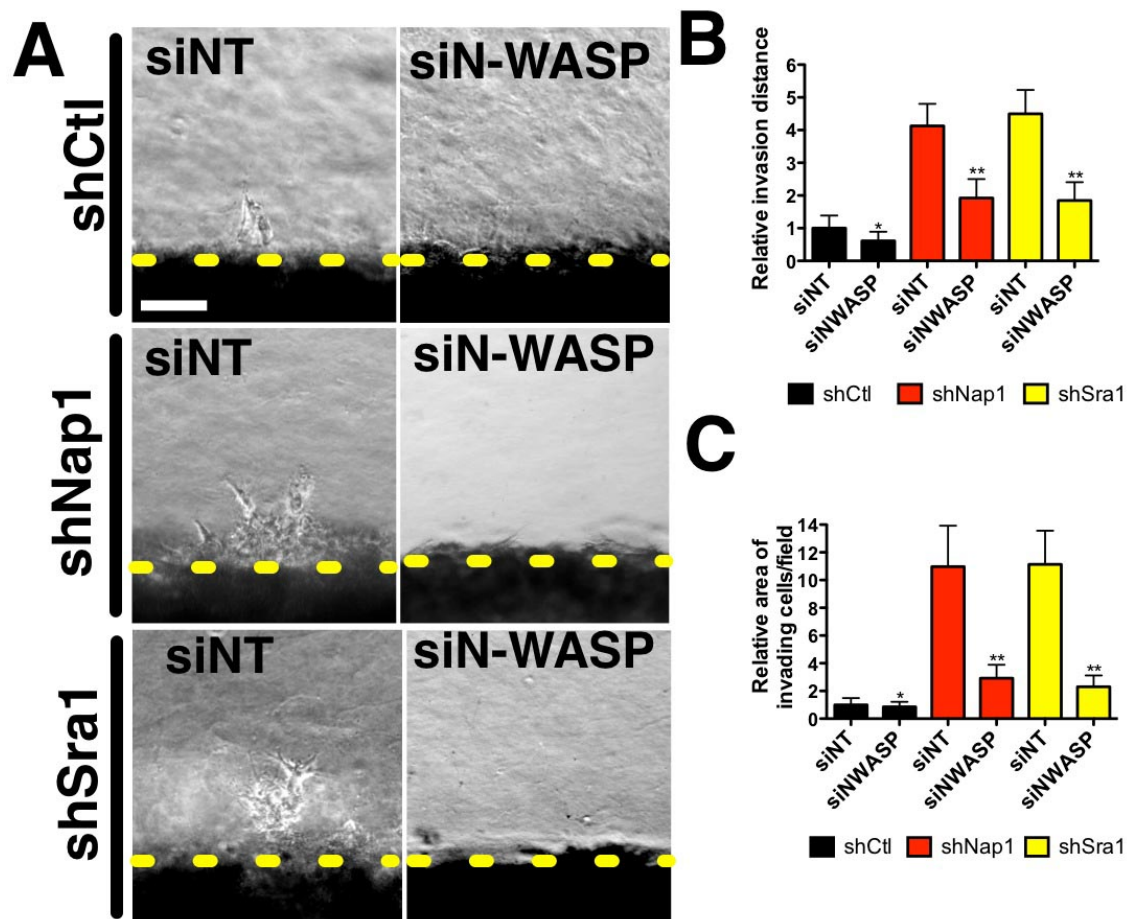


Figure 4.14 N-WASP is required for invasion

(A) Phase contrast micrographs show invasion of Nap1 and Sra1 stable knockdown cells in 3D collagen gel invasion assay after control siRNA or siN-WASP. Scale bar 100 μ m. (B) Relative invasion distance and (C) relative area of invading cells/field from collagen gel invasion assays. (Data are means \pm SEM, n=12 images from 3 independent assays, *p=not significant, **p<0.01). All panels show A431 cells.

As strong and dense actin structures are formed at the invasive front of WRC KD cells, I thought that these N-WASP generated actin protrusions might be used specifically to navigate through ECM barrier. Strikingly, two Nap1 knockdown cell lines (A & C) and the Sra1 knockdown cell line showed N-WASP enrichment at cell leading edges in the wound healing induced invasion assay (**Figure 4.15**). However, in a regular wound-healing assay, I saw only very subtle enrichment of N-WASP or Arp2/3 complex at leading edges suggesting N-WASP was specifically involved in WRC depleted cells migrating/invading against an ECM barrier (**Figure 4.16**). Notably, this phenotype was not restricted to individual cells, as the entire front of invading cells had N-WASP and Arp2/3 complex enrichment when viewed at a lower magnification (**Figure 4.16B**).

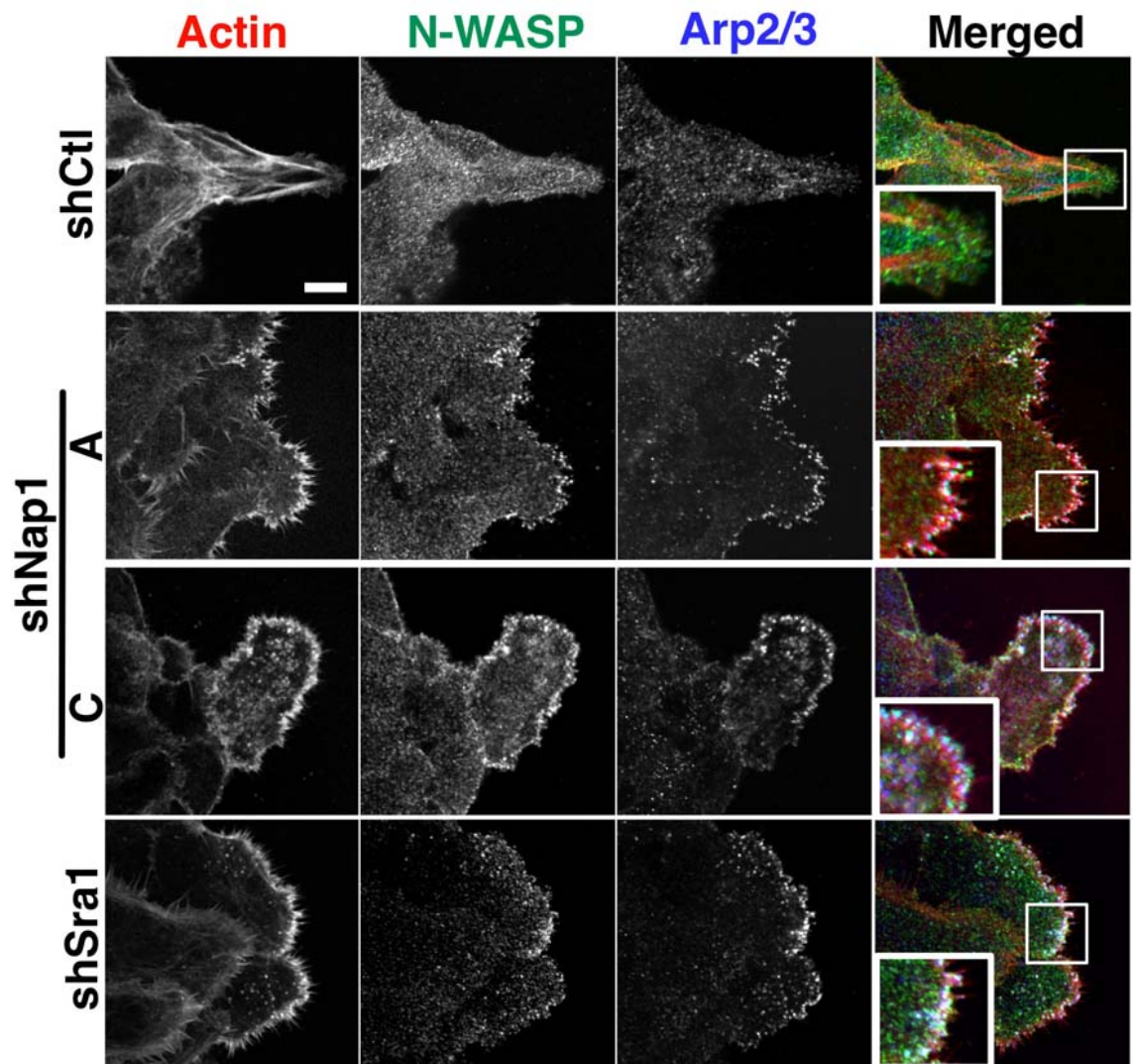


Figure 4.15 N-WASP and Arp2/3 complex co-localization in Matrigel invasion

Confocal micrographs show multiple WRC stable knockdown cell lines invading in wound healing induced Matrigel invasion assay. Cells were fixed and stained with rhodamine phalloidin for actin (red), N-WASP antibody (green) and p16-Arc antibody for Arp2/3 complex (blue). Scale bar 10 μ m. Images are representative of at least 3 independent experiments. All panels show A431 cells.

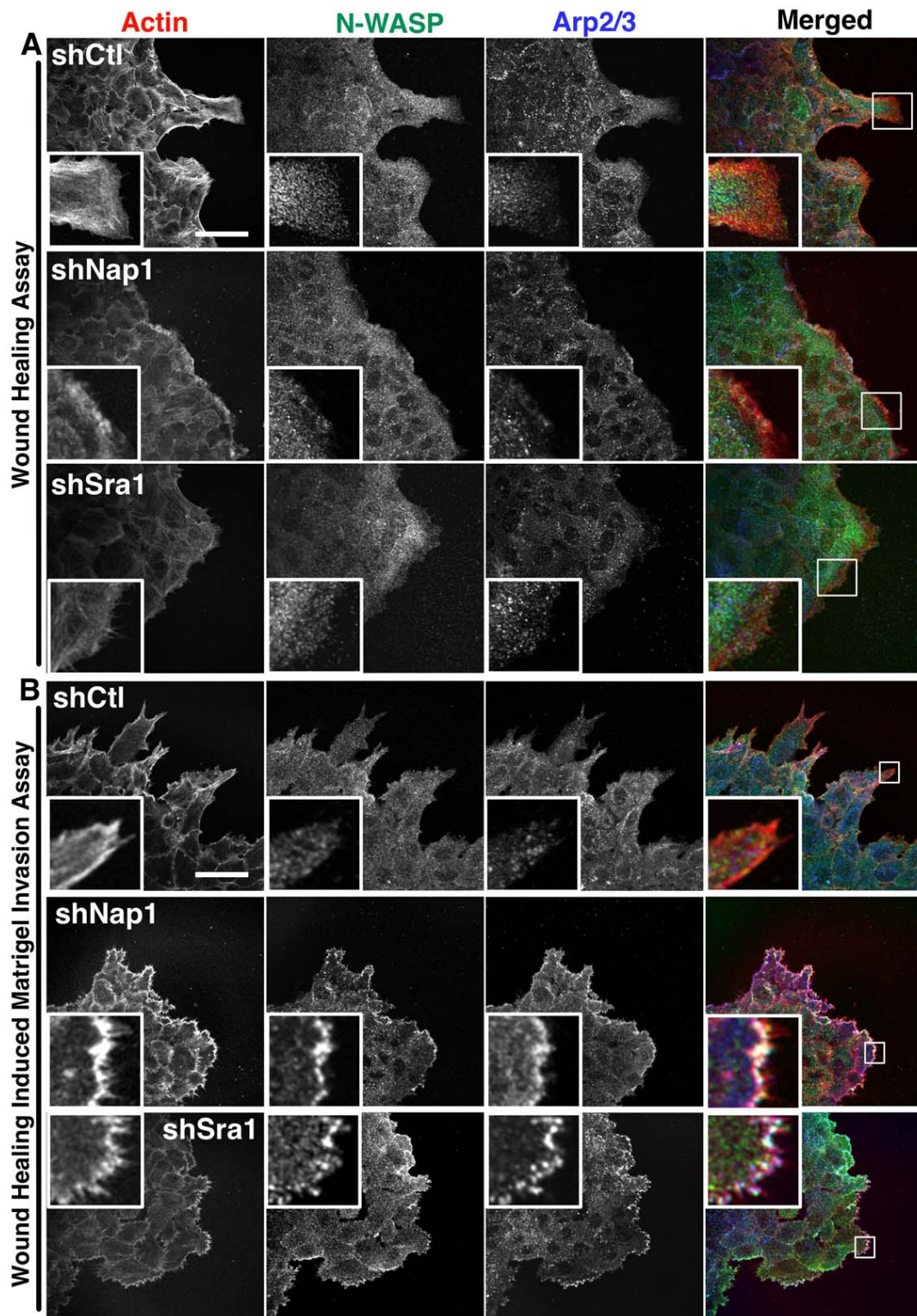


Figure 4.16 N-WASP and Arp2/3 complex localization is invasion specific

N-WASP and Arp2/3 complex is only localized to the invasive front of WRC depleted cells. All panels show A431 cells. (A) Confocal micrographs showing N-WASP and Arp2/3 complex localization in a standard wound healing assay and (B) in wound healing induced Matrigel invasion assay. shCtl, shNap1 and shSra1 cells were fixed and stained with rhodamine phalloidin for actin (red), endogenous N-WASP (green) and endogenous p16-Arc for Arp2/3 complex (blue). Images are representative of at least 3 independent experiments. Scale bar 50 μ m.

4.2.5 Loss of WRC promotes invasion in normal epithelial cells

Epithelial cancer cells are genetically unstable. To test if WRC also suppresses 3D cell motility of normal epithelial cells, WRC was transiently reduced in an immortalized normal human retinal pigment epithelial cell line, hTERT-RPE1, that is naturally invasive when in contact with collagen type-I (Van Aken et al., 2003). After knockdown of Nap1 and Sra1, hTERT-RPE1 showed heavy loss of Nap1, Sra1 and Scar2 indicating loss of WRC (**Figure 4.17A**). Indeed, these cells did not generate any lamellipodia-like protrusions after the siRNA treatment, when grown on standard tissue culture dish (**Figure 4.17B**). The result therefore confirms loss of WRC function in these treated hTERT-RPE1 cells. These cells were then tested for their ability to invade in collagen gel. Consistent with the result obtained from A431 cells, WRC depleted hTERT-RPE1 cells invaded deeper into collagen gel in the 3D collagen gel invasion assay, and more cells were invading (**Figure 4.17C,D,E**). Therefore, WRC loss leads to higher 3D cell motility in various epithelial cell lines.

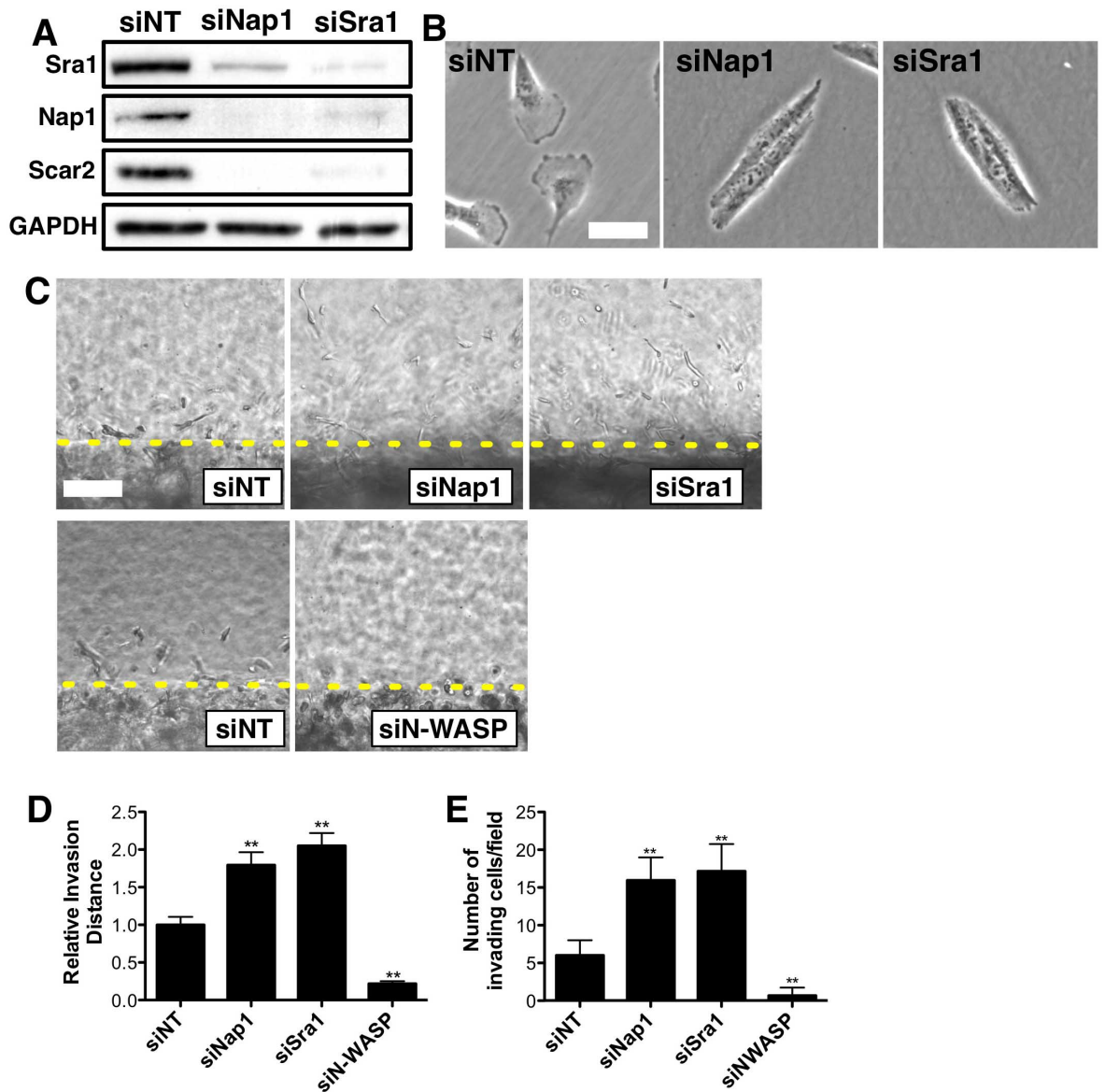


Figure 4.17 Loss of WRC promotes invasion of a normal human epithelial cell line.

All panels show hTERT-RPE1 cells. (A) WRC subunit levels in Nap1 and Sra1 depleted cells using corresponding siRNA. (B) Phase contrast micrographs show morphology of WRC KD hTERT-RPE1 cells. Scale bar 20 μ m. (C) Phase contrast micrographs show 3D collagen gel invasion assay using Nap1, Sra1, and N-WASP depleted cells. Scale bar 100 μ m. (D) Quantification of 3D collagen gel invasion assay shows the relative invasion distance and (E) the number of invading cells per field (Data are shown as means \pm SEM, n=12 images from 3 independent assays. **p<0.01).

N-WASP and Arp2/3 complex localization in WRC KD hTERT-RPE1 cells were also tested. Consistent with the observation in A431 cells, N-WASP and Arp2/3 co-localized and enriched at the tips of invasive pseudopods (**Figure 4.18A**). Interestingly, loss of WRC in hTERT-RPE1 cells increased the ability of cells to form pseudopods (**Figure 4.18B,C**), perhaps due to high N-WASP activities. Loss of N-WASP in hTERT-RPE1 cells also led to loss of pseudopods when cells were cultured in collagen gel (**Figure 4.18B,C**). Consequently, invasion into the collagen gel was also inhibited upon loss of N-WASP (**Figure 4.17C,D,E**). These data suggest N-WASP promotes formation of invasive pseudopod in hTERT-RPE1 cell too.

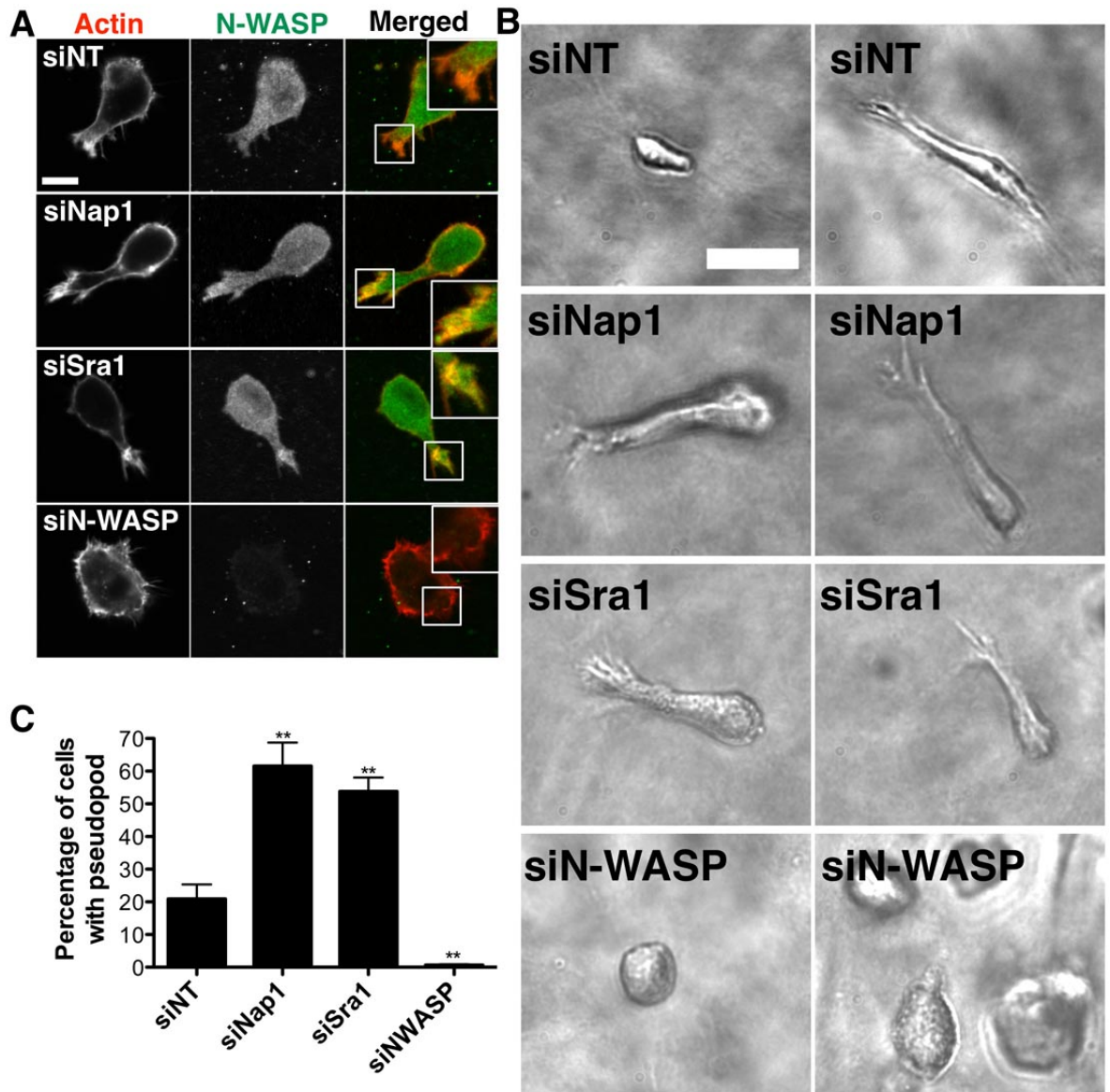


Figure 4.18 N-WASP promotes pseudopods formation in 3D

All panels show hTERT-RPE1 cells. (A) Confocal micrographs demonstrate localization of endogenous N-WASP (anti-N-WASP, green) and filamentous actin (rhodamine phalloidin, red) in control (siNT), siNap1, siSra1, and siN-WASP cells during invasion into collagen. Scale bar 10 μ m. (B,C) Phase contrast micrographs show in thick collagen gel invasion assay, depletion of Nap1 and Sra1 promoted N-WASP dependent formation of invasive pseudopods (Data are means \pm SD, n=3 independent assays. **p<0.01). Scale bar 30 μ m.

4.2.6 Rac1 and Cdc42 activation status in the absence of WRC

N-WASP is activated by Cdc42 and reportedly by Rac1 as well (Tomasevic et al., 2007). Due to the predominant N-WASP localization to the invasive front in WRC KD cells, the activation status of both small GTPases was tested in Nap1 and Sra1 stable KD cells. To measure small GTPases activation when cells were actively trying to make membrane protrusions, cells were first cultured in suspension then they were allowed to spread on collagen-coated dishes. Rac1 activation status at multiple time points of spreading cells was tested using a quantitative Rac1 G-LISA assay. Control cells cultured in serum free medium were used to mark the basal Rac1 activation level. Rac1 was properly activated in the first 10min of spreading (**Figure 4.19A**) when all cell lines had reach the maximum spreading size (**Figure 4.4**). However Rac1 activation in Nap1 and Sra1 stable KD cells was not sustained after spreading, as Rac1 activity dropped quickly to the basal level. In contrast, control cells maintained Rac1 activation over 120min, despite a small drop just after spreading (**Figure 4.19A**).

Rac1 activity showed the largest difference 60min after spreading where Rac1 activation in Nap1 and Sra1 stable KD cells had already dropped to the basal level (**Figure 4.19A**). To test if WRC KD cell lines had similar Cdc42 activation deficiency, Cdc42 and Rac1 activity was detected using a PAK1-PBD effector domain pull-down assay at the 60min time point after spreading. Consistently, Rac1 activation was reduced in WRC KD cells, however Cdc42 activation was not changed in WRC KD cells at the same time point (**Figure 4.19B**). As a result, WRC is not required for Rac1 or Cdc42 activation, and the two small GTPase may not be responsible for the enhanced N-WASP activity in WRC KD cells.

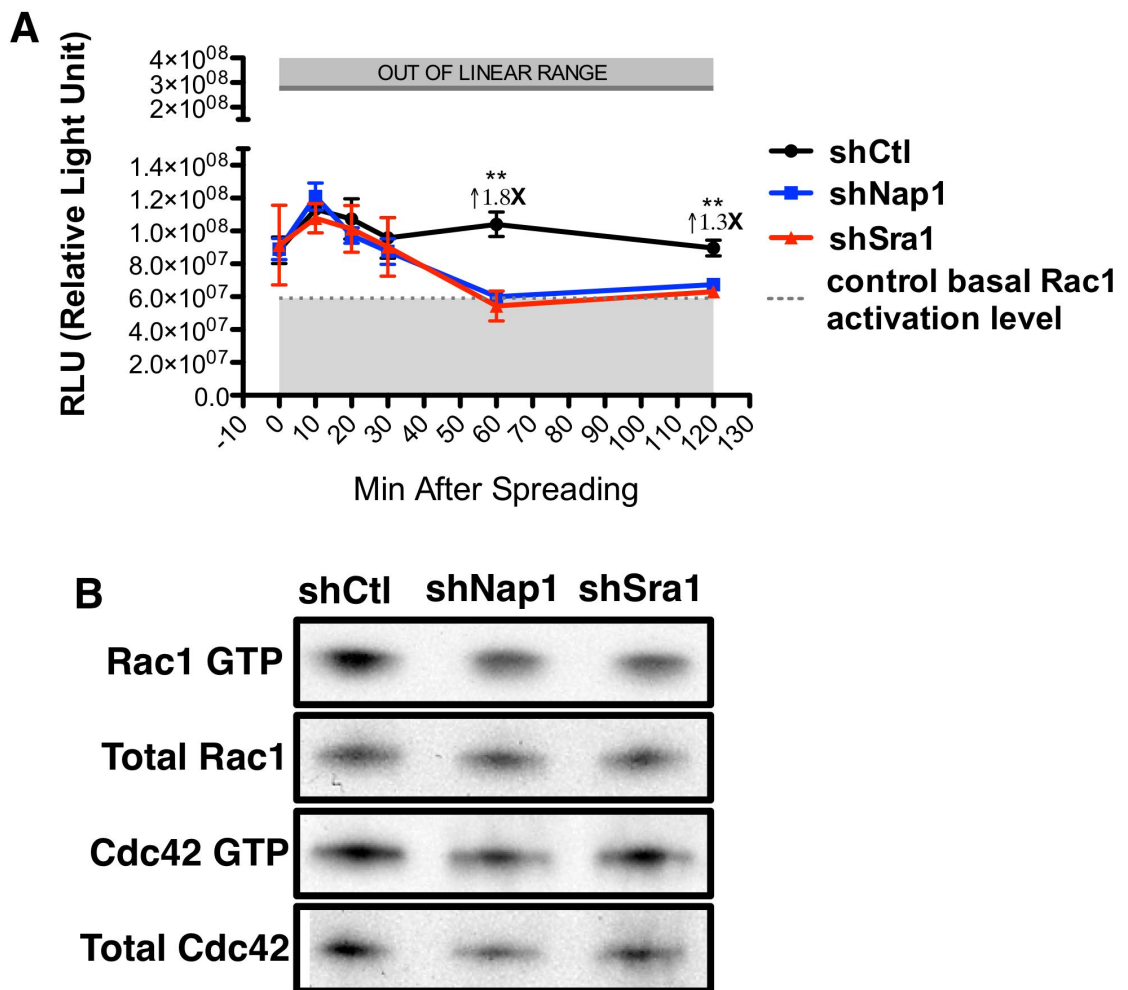


Figure 4.19 Rac1 and Cdc42 activation status in WRC KD cells

(A) Rac1 activation status in control (shCtl) and WRC KD cells during spreading on collagen at indicated time points. (Data are means±SEM at each point, n=3 independent assays. **p<0.01). (B) Western blots of PAK1-PBD effector domain pull-down assay showing Rac1 and Cdc42 activation 60min into spreading on collagen. All panels show A431 cells.

4.3 Discussion

Loss of complex subunits destabilizes WRC, as WRC cannot be properly assembled (Derivery et al., 2008). In mammalian cells due to various isoforms of a subunit, proteins of WRC contribute differently to the complex stability. Loss of Nap1 or Sra1 in A431 cells resulted in nearly complete loss of the WRC as shown by Blue NativePAGE (**Figure 4.2**). The result agrees with the crystal structure (Chen et al., 2010) where Nap1 and Sra1 are the two largest subunits of the complex. Given Sra1 and PIR121 are 88% identical, it is interesting that loss of PIR121 had very little impact on the total WRC level (**Figure 4.1&4.2**). It is unlikely that PIR121 would be dramatically different from Sra1 in terms of structure. Therefore it is possible that the 'Sra1 complex' is the dominant WRC in cells, while the 'PIR121 complex' is expressed at a much lower level. Consequently, removal of the 'PIR121 complex' will only have a minor impact on the total amount of WRC.

On the other hand, Scar1 compensated the loss of Scar2 by forming more 'Scar1 complexes'. It is interesting that in control cells, despite Scar1 expression, little 'Scar1 complex' was detected. Only when Scar2 was reduced, Scar1 formed more complexes. Perhaps loss of Scar2 protein made Scar1 protein more accessible to other complex subunits resulting in more effective formation of Scar1 complex. This burst of 'Scar1 complex' formation may also stabilize Scar1 protein making Scar1 appeared to be slightly over expressed (**Figure 4.2A&B**). Nonetheless, Scar1 did not fully compensate for the loss of Scar2, as the total WRC level was still reduced.

Loss of WRC is known to reduce lamellipodia formation (Silva et al., 2009). In Hela cells, depletion of WRC also promotes membrane blebbing (Derivery et al., 2008). Similarly, complete loss of WRC (Nap1 and Sra1) reduced lamellipodia formation and promoted membrane blebbing in A431 cells (**Figure 4.3**). These WRC KD cells had spreading defects and 2D migration defects (**Figure 4.4&4.7**), as they were unable to produce membrane protrusions. Apparently, membrane blebs were unable to help spreading and migration, although Nap1 and Sra1 stable knockdown cells were blebby when culture on dishes.

To move in a complex 3D environment, cells mostly use actin based membrane protrusions to navigate through extracellular matrix (mesenchymal), although an alternative actin independent membrane bleb based mechanism is also observed (amoeboid) (Friedl and Wolf, 2009, Sanz-Moreno et al., 2008, Pinner and Sahai, 2008). WRC is the major regulator of actin-based membrane protrusions. Although complete loss of WRC promoted formation of membrane blebs when cells were cultured on dishes, actin-based protrusions were generated when cells (A431 and hTERT-RPE1) were moving in 3D collagen gel. Loss of WRC function surprisingly promoted N-WASP dependent Arp2/3 activation, which then contributed to the invasive pseudopods formation. Thus loss of WRC in the two tested cell types did not promote amoeboid cell migration in collagen gel.

N-WASP localization is clearly enhanced when WRC is not functional. It is important to understand how N-WASP activation is enhanced in WRC KD cells. Although Cdc42 is the established activator of N-WASP, Cdc42 activation was not changed in WRC KD cells suggesting extra factors may be required for high N-WASP activity in WRC KD cells. It is also likely that Cdc42 localizes to the tips of invasive pseudopods to specifically recruit and activate N-WASP without elevating global Cdc42 activation. On the other hand, Rac1 is reported to activate N-WASP too (Tomasevic et al., 2007). However N-WASP activation by Rac1 is not well established in vivo, and in WRC KD cells Rac1 activation is not persistent. Therefore, Rac1 is unlikely to enhance N-WASP activation in WRC KD cells.

It is interesting that N-WASP did not compensate for the 2D migration defect of WRC KD cells. In the wound healing assay N-WASP did not enrich at the moving wound edge. Only when a layer of Matrigel was added, N-WASP and Arp2/3 complex accumulated at the entire wound edge and promoted invasion of WRC KD cells. Furthermore, loss of N-WASP effectively suppressed invasion. N-WASP is therefore specifically required for cells to move through ECM by making pseudopods protruding into the ECM. Indeed N-WASP is known to be required for the formation of invadopodia, which are specialized actin rich membrane protrusions extending into ECM from the ventral surface of cells cultured atop of the ECM (Desmarais et al., 2009). I therefore propose that N-WASP is the primary NPF used by cells to invade ECM barrier, while WRC mediates planar cell migration.

To conclude, disruption of WRC function promotes cell motility in 3D collagen gel. The invasive behaviour demonstrated by WRC KD cells supports a study on human tumour samples where loss of Sra1 (CYFIP1) is frequent in invasive epithelial cancers (Silva et al., 2009). This enhanced motility in collagen gel is driven by N-WASP dependent Arp2/3 complex mediated actin polymerization at the invasive front. The two major actin assembly promoting proteins WRC and N-WASP therefore play opposing roles in the invasion of epithelial cells.

Chapter 5: Focal adhesion kinase is required for invasion and cell transformation

5.1 Introduction

In addition to cell migration, formation of membrane protrusions is also important for cell-ECM adhesion, and vice versa. During cell migration expansion of membrane protrusions often precedes adhesion formation, therefore molecules involved in regulating membrane protrusions can also impact on adhesion formation (DeMali and Burridge, 2003). WRC localizes to the leading edge of a migrating cell to regulate lamellipodia formation and dynamics. Loss of WRC abolishes lamellipodia formation, so it is likely that WRC also indirectly regulates cell-ECM adhesion.

Although how protrusions and adhesions are coupled molecularly remains poorly understood, expanding lamellipodia create new adhesion sites close to the leading edge (Choi et al., 2008). Adhesions once formed also contribute to the stability of membrane protrusions (Borm et al., 2005). Additionally, adhesions at the back of the leading edge are sites of active signaling. Engagement of integrins at these sites initiates 'outside in' signal cascades (Legate et al., 2009) to many effector proteins including Rac1 small GTPase that directly regulates WRC, and hence the dynamics of lamellipodia.

Although many proteins are involved in conducting integrin initiated signalling, focal adhesion kinase (FAK) is a major player in this process. FAK is both a cytoplasmic tyrosine kinase and a large adaptor protein. However before activation, FAK is folded preventing the kinase activity and protein interactions. Autophosphorylation of FAK at Y397 opens up FAK allowing kinase activation. FAK is then phosphorylated by Src kinases that bind to pY397 creating multiple high affinity binding sites for other signalling proteins (**Figure 1.13**) (Toutant et al., 2002, Lietha et al., 2007). FAK can subsequently activate Rac1 through interaction with PI3K (Chen and Guan, 1994) or p130Cas/DOCK180 (Sakai et al., 1994, Cote and Vuori, 2007) possibly leading to indirect regulation of WRC and lamellipodia. Alternatively, FAK can indirectly activate WRC via Erk that is activated by phosphorylation at the end of FAK initiated MAP kinase cascade (Pearson et al., 2001). Activated Erk then phosphorylates Scar2 and Abi1. This Erk dependent phosphorylation is required for Arp2/3 complex and actin binding of WRC leading to WRC activation (Mendoza et al., 2011). Collectively, it is reasonable to

speculate that FAK is capable of using multiple signalling pathways to regulate WRC dependent membrane protrusions.

While FAK can possibly modulate WRC activity, it is not known if WRC also affects FAK activities. FAK is clearly important for both adhesion and membrane protrusions. Loss of FAK leads to loss of membrane protrusions and enlarged focal adhesions (Schober et al., 2007). Interestingly, in many cell types loss of WRC also leads to the same phenotype suggesting WRC also regulates focal adhesions (Silva et al., 2009, Escobar et al., 2010). It is likely that WRC also modulates adhesions and FAK activities, so the interplay of the two proteins can coordinate membrane protrusions and adhesions.

Additionally, FAK and many other adhesion molecules play important roles in cancer cell invasion, cell proliferation and survival (McLean et al., 2005). FAK promotes matrix degradation through degradative focal adhesions to facilitate invasion (Wang and McNiven, 2012). Abnormal adhesion may contribute to the invasive phenotype observed in WRC KD cells. Interestingly, FAK is reported to interact directly with N-WASP. This interaction leads to N-WASP phosphorylation at Tyr256 by FAK leading to prolonged N-WASP activation (Wu et al., 2004).

To explore the possibility that loss of WRC alters FAK activation contributing to the invasive phenotype, focal adhesions and the status of FAK activation were investigated in WRC KD cells. As a result, I discovered over activation of FAK in WRC KD cells. This high FAK activity is required for N-WASP/Arp2/3 complex mediated invasion. Unexpectedly, loss of WRC also promoted FAK mediated cell transformation.

5.2 Focal adhesion kinase promotes N-WASP dependent invasion

5.2.1 Loss of WRC alters cell-substrate adhesion

A431 WRC KD cells demonstrated enhanced adhesion strength to standard tissue culture dishes, as cells were resistant to dispase digestion, which cleaves ECM without affecting cell-cell junctions (**Figure 5.1A**). Similarly, loss of WRC in hTERT-RPE1 cells also led to enhanced adhesion when cells were cultured on glass (**Figure 5.1B**). These observations suggest cell-substrate adhesions are strengthened upon loss of WRC.

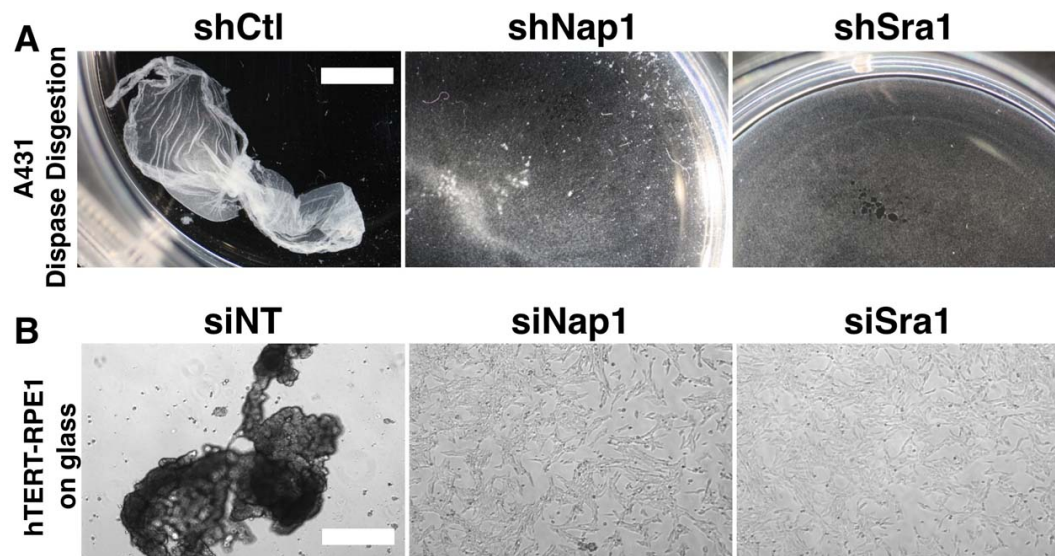


Figure 5.1 Loss of WRC enhances cell-substrate adhesion

(A) Dispase resistance in A431 WRC KD cells (6mg/ml dispase in PBS for 30min). Scale bar 0.5cm. (B) Enhanced adhesion to glass upon loss of WRC in hTERT-RPE1 cells. Scale bar 500 μ m.

In fact, when A431 WRC KD cells were plated on collagen coated glass bottom dishes, WRC KD cells formed stable focal adhesions, as most adhesions in WRC KD cells had a lifetime longer than 20min. In contrast, most adhesions in control cells had a lifetime shorter than 10min (**Figure 5.2A,B**). Additionally, WRC KD cells had larger but fewer focal adhesions (**Figure 5.2A,B**). Thus, loss of WRC affected focal adhesion dynamics, an effect that has been hinted at previously (Yamazaki et al., 2005, Silva et al., 2009, Ryu et al., 2009) but not previously measured.

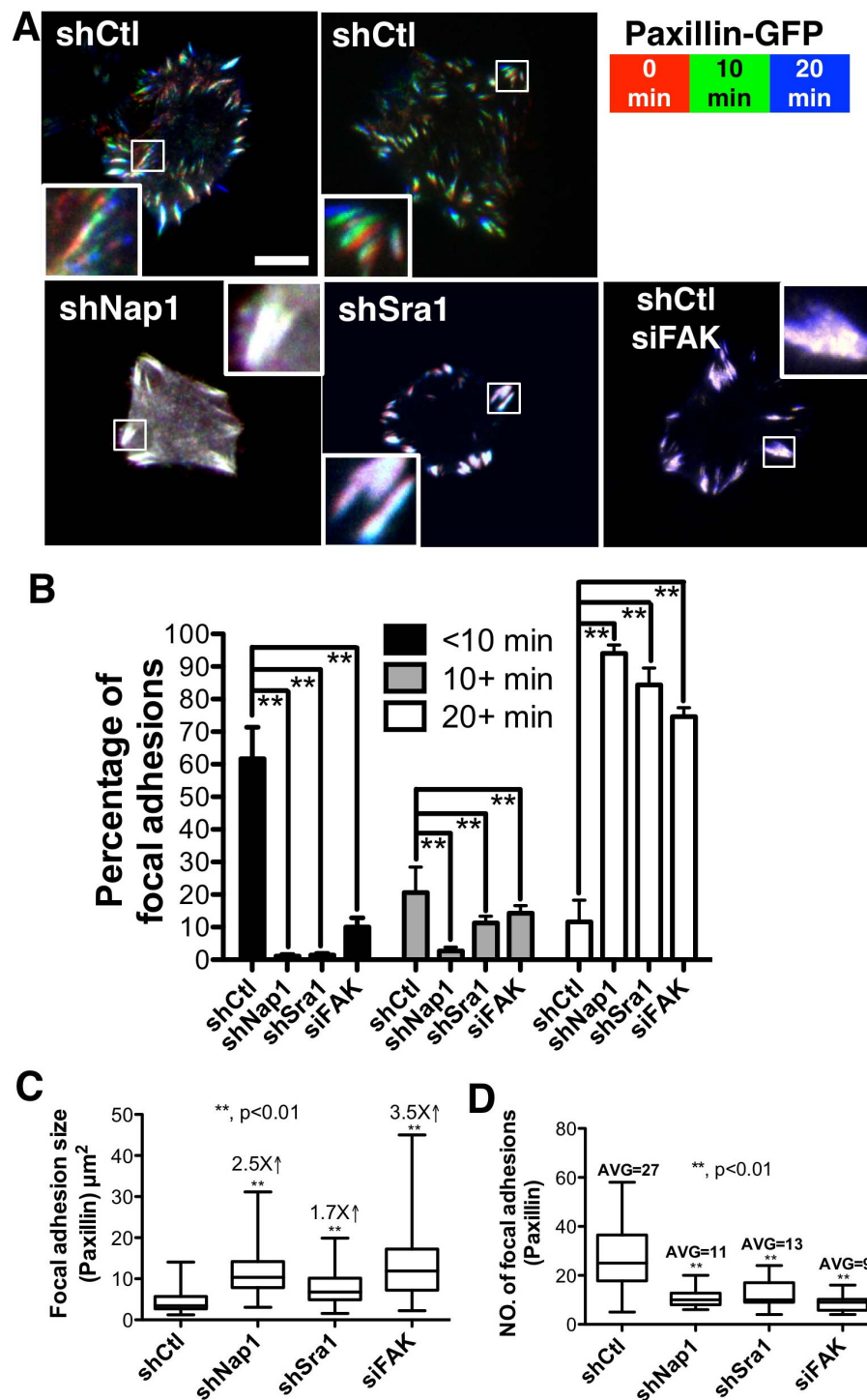


Figure 5.2 Loss of WRC alters focal adhesion dynamics

All panels show A431 cells. (A) TIRF micrographs of Paxillin-GFP expressing cells demonstrate change of focal adhesion dynamics in shCtl cells, Nap1 and Sra1 stable knockdown cells, and FAK knockdown cells (siFAK). Scale bar 10µm. (B) Quantification of independent TIRF micrographs from each cell line shows a shift of focal adhesion dynamics (Data are shown as means±SEM, n=3 cells, **p<0.01). (C) Quantification of focal adhesions imaged with TIRF microscope shows dramatic increase of focal adhesion size (Data are shown as Min-Max, n=158, **p<0.01) but reduced focal adhesion number (D) (Data are shown as Min-Max, n=20 cells, **p<0.01) as labelled by Paxillin antibody in WRC and FAK (siFAK) knockdown cells.

5.2.2 Focal adhesion kinase is over activated without WRC

As loss of WRC in A431 cells had caused significant change in adhesion dynamics, and multiple adhesion molecules could respond to this change, I surveyed the levels of candidate adhesion molecules in WRC knockdown cells. While the gross overall expression levels of $\alpha 5$ integrin, paxillin, vinculin, Erk, and phosphor-Erk (pErk), remained unchanged (not shown), total FAK expression levels were increased in A431 cells, but even more strikingly, the basal levels of FAK phosphorylation at Y397, which is often used to report FAK activity, was also increased by at least twofold, indicating that the additional FAK is active (**Figure 5.3A,B**). Importantly, the same increase in FAK expression and activation was also detected in cells cultured in 3D collagen gel suggesting the change of adhesion regulation and signalling was altered in 3D as well (**Figure 5.3C,D**).

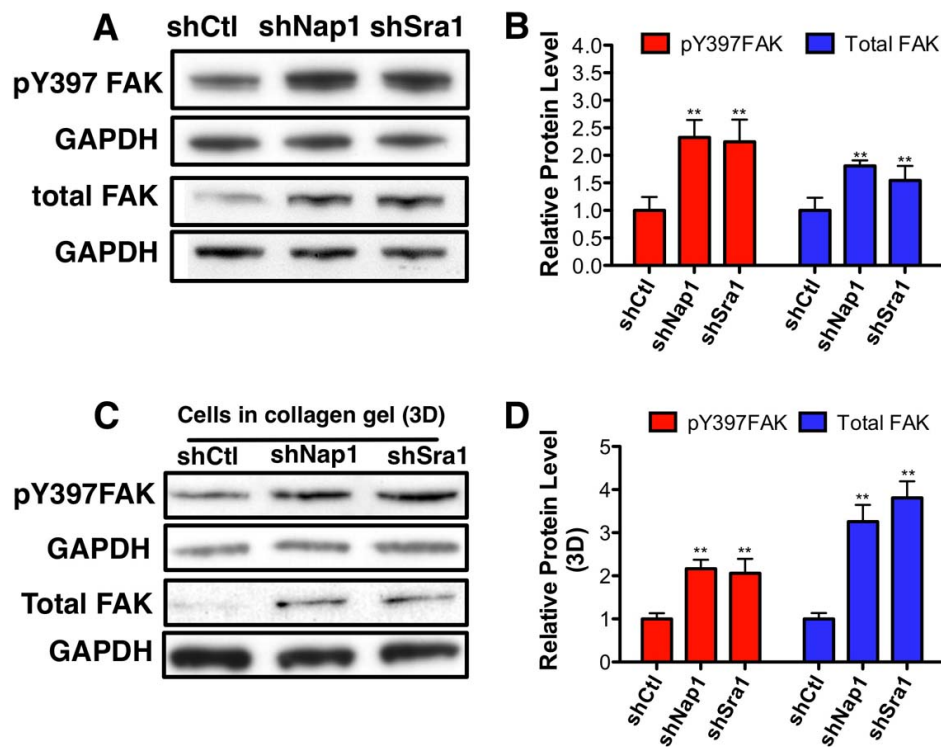


Figure 5.3 Over activation of FAK in WRC KD cells

(A) Western blot showing pY397FAK level and total FAK level in control and WRC KD cells. (B) Relative protein levels of total FAK and pY397FAK (Data are shown as means \pm SEM, n=5 experiments, **p<0.01). (C) Western blot showing pY397FAK and total FAK level in 3D collagen gel. (D) Relative protein levels of pY397FAK and total FAK in 3D collagen gel (Data are shown as means \pm SEM, n=3 experiments, **p<0.01. *p=NS). All panels show A431 cells.

Although it is thought that loss of FAK or WRC lead to similar phenotypes, the comparison was made across studies using different cellular systems from various research groups. To check if FAK and WRC indeed have a similar regulatory role on focal adhesions in the same cell type, FAK was reduced in A431 cells using RNAi. When these FAK reduced A431 cells were plated on collagen coated glass bottom dishes, stable focal adhesions were formed. FAK KD cells also had larger but fewer focal adhesions (**Figure 5.2**). Notably, loss of FAK also prevented lamellipodia formation in spreading A431 cells and in hTERT-RPE1 cells (**Figure 5.4**), despite intact WRC in these two cell types suggesting FAK might actually be required for WRC mediated lamellipodia formation. Therefore FAK could be more activated to compensate the loss of WRC.

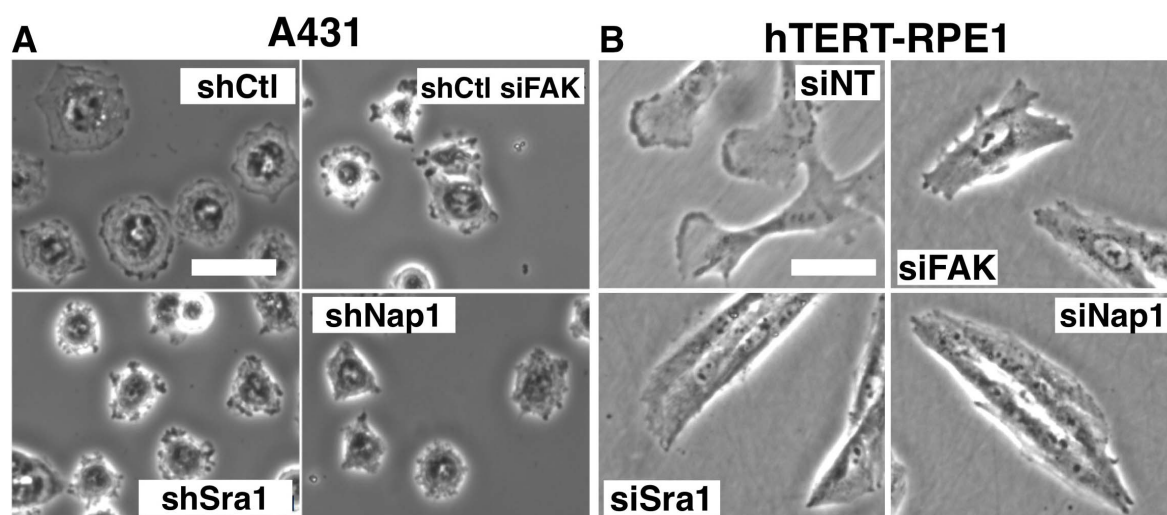


Figure 5.4 FAK is required for lamellipodia formation

Phase contrast micrographs show morphology of (A) A431 cells on collagen coated dish and (B) hTERT-RPE1 cells on plastic upon loss of FAK (siFAK). Scale bars 20µm. Stable A431 WRC KD cells (shSra1 and shNap1) and hTERT-RPE1 cells transiently reduced WRC (siSra1 and siNap1) are shown as comparisons.

5.2.3 Focal adhesion kinase promotes N-WASP dependent cell invasion

As FAK is a major driver of cancer invasion (Brunton and Frame, 2008, Frame et al., 2011), enhanced FAK signalling in WRC depleted cells might also contribute to their increased invasiveness. When Nap1 and Sra1 knockdown cells were treated with FAK siRNA, invasion in 3D collagen gels was severely impaired (**Figure 5.5**). Thus, FAK is required for the invasion of WRC KD cells.

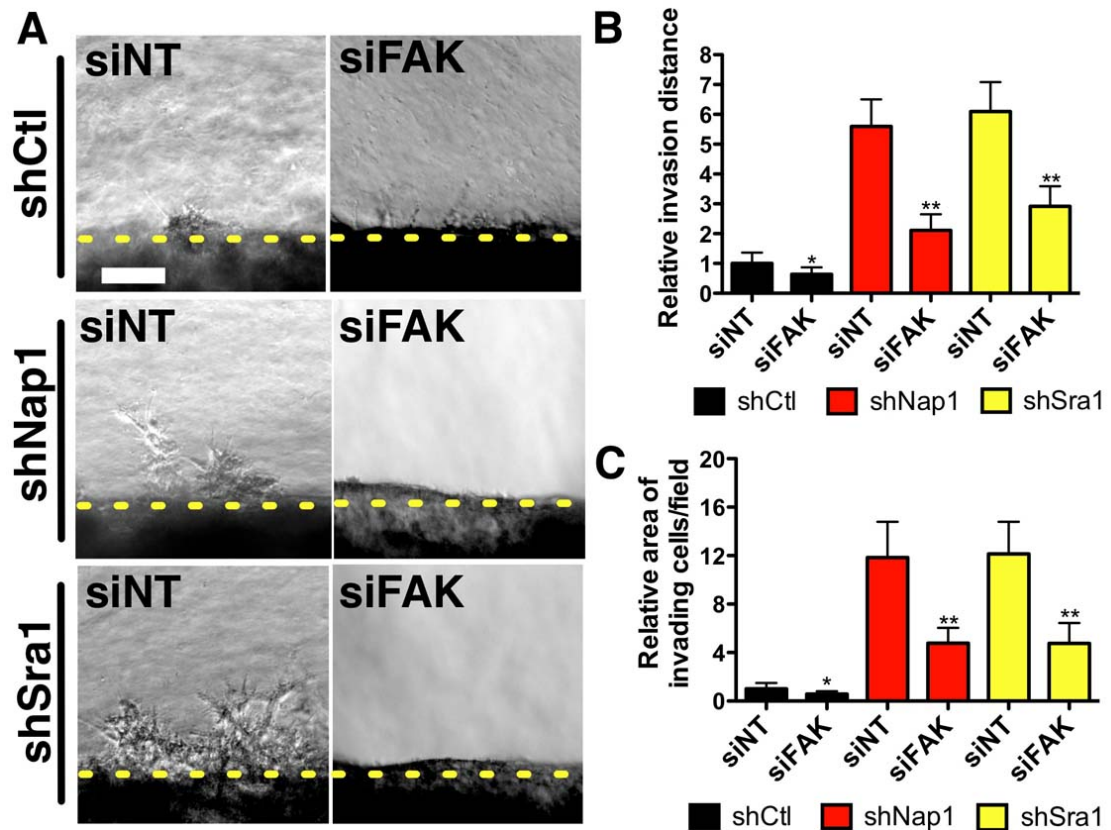


Figure 5.5 FAK is required for invasion

(A) Phase contrast micrographs show reduction of FAK (siFAK) inhibited invasion of Nap1 and Sra1 stable knockdown cells into thick collagen gels. Scale bar 100 μ m. (B) Relative invasion distance and (C) the relative area of invading cells/field. (Data are means \pm SEM, n=12 images, 3 independent assays, *p=NS, **p<0.01). All panels show A431 cells.

As N-WASP localizes to the tips of invasive pseudopods to promote invasion, the localization of active FAK (pY397FAK) was also tested. Interestingly, pY397FAK also co-localized with GFP-N-WASP to the invasive pseudopods in a thick collagen gel invasion assay (**Figure 5.6A**). While patches of pY397FAK frequently localised along the long protrusions of control cells, the relative fluorescence intensity of pY397FAK doubled in WRC depleted cells. GFP-N-WASP and actin were also co-enriched at these sites (**Figure 5.6B**).

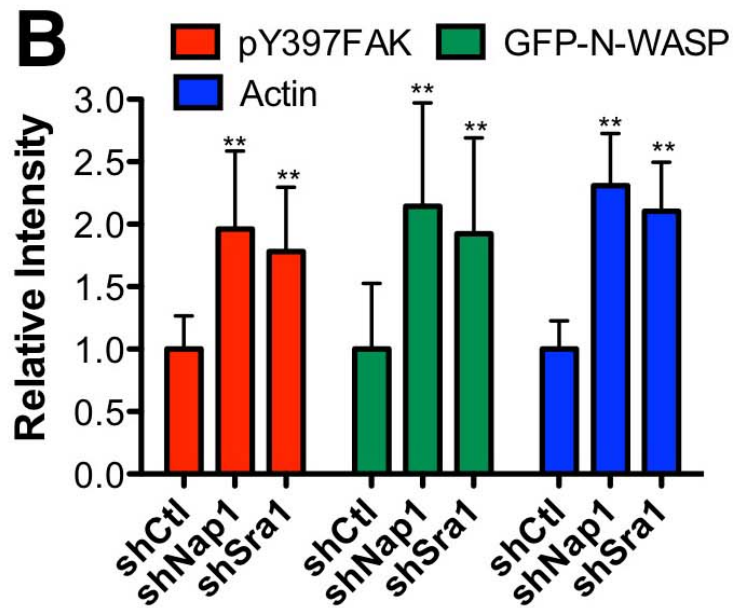
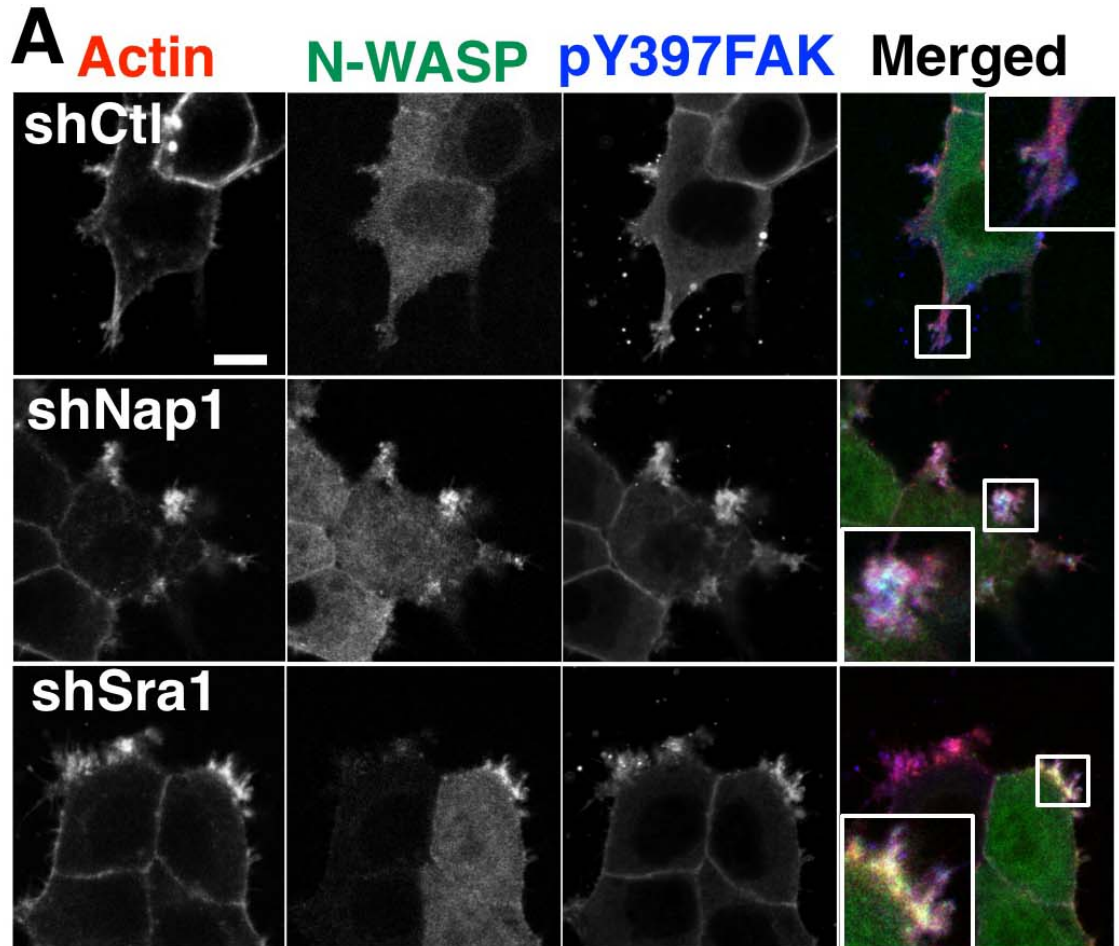


Figure 5.6 FAK co-localizes with N-WASP

(A) Confocal micrographs show GFP-N-WASP (green) expressing A431 control or Nap1 and Sra1 knockdown cells invading in thick collagen gels. Cells were fixed and labelled with rhodamine phalloidin for actin (red), and pY397FAK antibody for active FAK (blue). Scale bar 10 μ m. (B) pY397FAK was enriched at pseudopods of Sra1 and Nap1 depleted cells with GFP-N-WASP and actin. (Data are shown as means \pm SD, n=6 cells, **p<0.01).

FAK is known to interact directly with N-WASP to enhance N-WASP activation by phosphorylation at Tyr256 (Wu et al., 2004). The co-localization of pY397FAK and N-WASP at the invasive pseudopod tips implicates that FAK may interact with N-WASP at these sites to regulate N-WASP activity. Indeed, depletion of FAK in shNap1 or shSra1 cells triggered the loss of N-WASP and Arp2/3 complex and the reduction of actin at the front of cells in thick collagen gel invasion assays (**Figure 5.7A-E**). However, N-WASP phosphorylation at Tyr256 (pY256N-NWASP) was not changed in WRC KD cells cultured on dish (**Figure 5.8A**). In collagen, loss of WRC, promoted accumulation of pY256N-NWASP to the tips of invasive pseudopods (**Figure 5.8B,C**). Therefore FAK recruits and enriches active N-WASP and Arp2/3 complex to the invasive front to promote invasion.

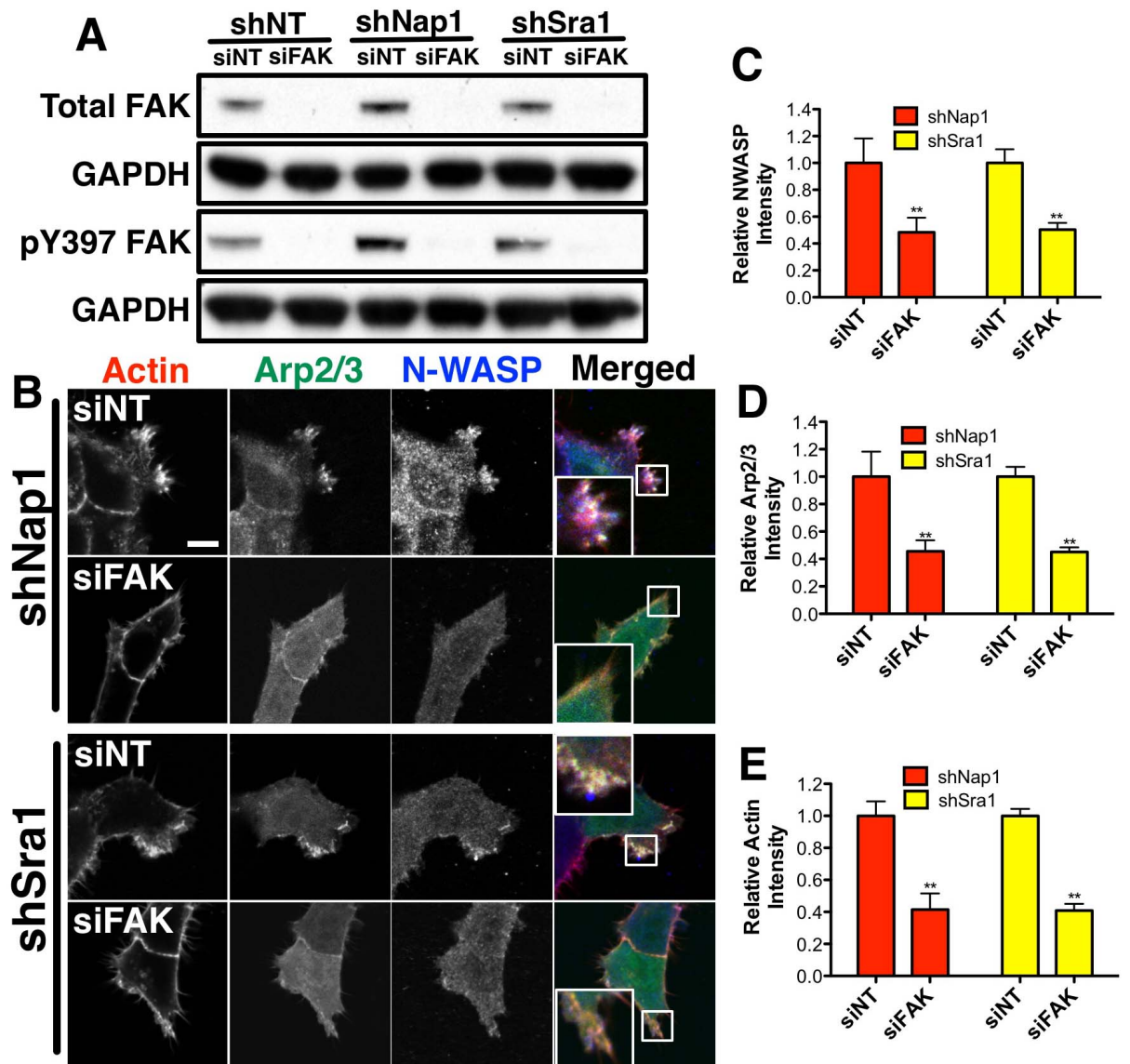


Figure 5.7 FAK is required for N-WASP and Arp2/3 complex localization

(A) Western blot showing total FAK level, pY397FAK and GAPDH control of cells treated with FAK siRNA (siFAK) or non-targeting siRNA (siNT). (B) Confocal micrographs show p21-Arc-GFP (green) expressing shNap1 and shSra1 cells. Cells were treated with FAK or NT siRNAs. Cells invading in thick collagen gels were fixed and stained with rhodamine phalloidin for actin (red) and N-WASP antibody (blue). Scale bar 10 μ m. (C,D,E) FAK depletion reduced N-WASP, Arp2/3 (p21-Arc-GFP) and actin relative fluorescence intensity relative to NT. (Data are shown as means \pm SD, n=6 cells, **p<0.01). All panels show A431 cells.

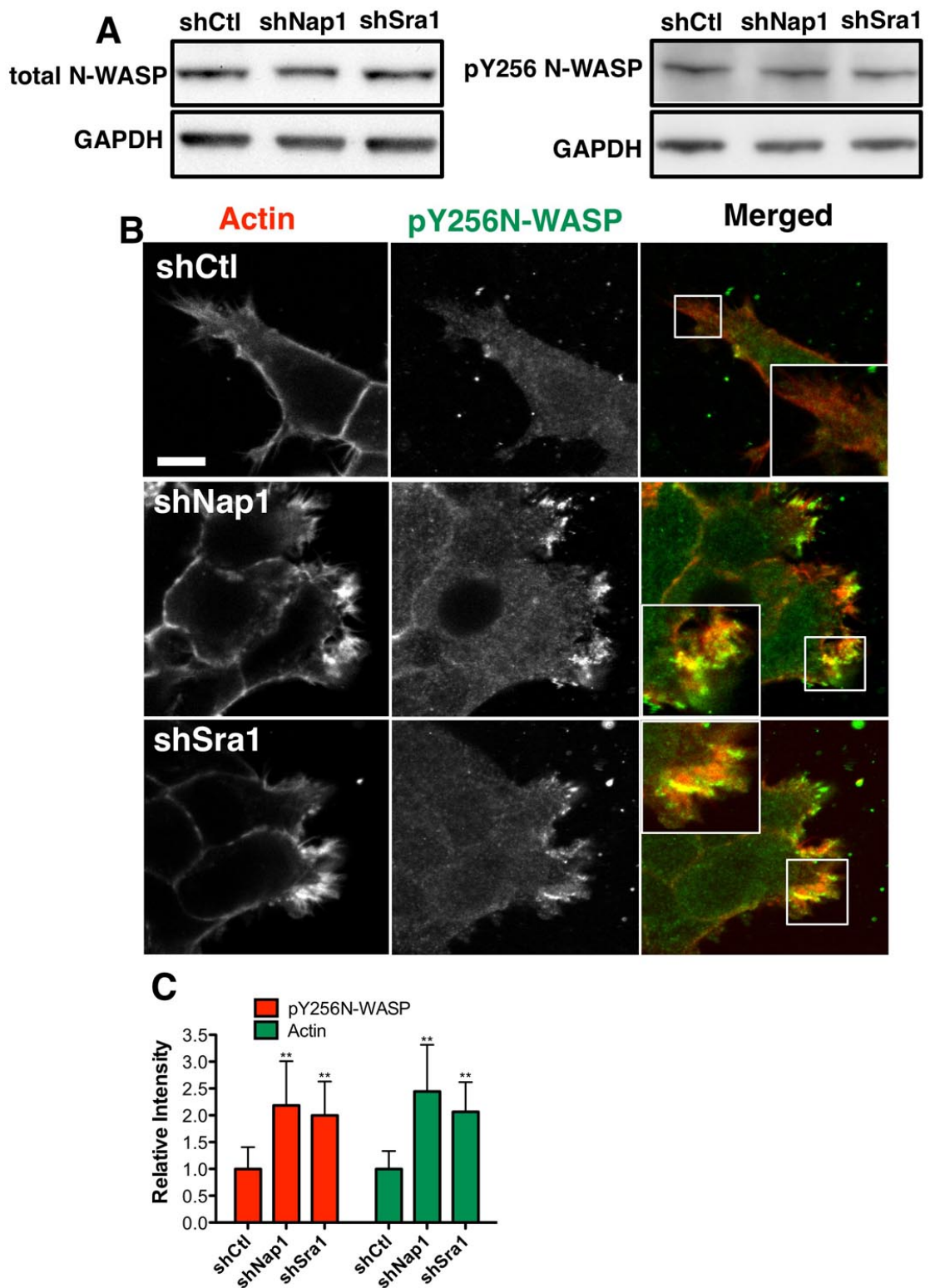


Figure 5.8 N-WASP is phosphorylated at the invasive pseudopods

(A) Western blot showing total N-WASP level, pY256N-WASP and GAPDH control. (B) Confocal micrographs show shCtl, shNap1 and shSra1 cells invading in thick collagen gels. Cells were fixed and stained with rhodamine phalloidin for actin (red) and pY256 N-WASP antibody (green). Scale bar 10 μ m. (C) pY256N-WASP was enriched at pseudopods of Sra1 and Nap1 depleted cells. (Data are shown as means \pm SD, n=6 cells, **p<0.01). All panels show A431 cells.

5.2.4 Focal adhesion kinase promotes cell transformation

In addition to invasion, FAK also contributes to cell transformation and tumorigenesis. To test cell transformation, WRC KD A431 cells were cultured in soft agarose assay, where cells survive through anchorage independent growth. Interestingly, the number of visible colonies was sharply increased in WRC depleted cells by day 14 in soft agarose assay (**Figure 5.9A,D**). Additionally, WRC depleted cells generated larger (7-8 fold) colonies than the control cells, indicating anchorage independent proliferation hence cell transformation (**Figure 5.9B,E**). However, WRC depleted cells grew at the same rate as controls in standard 2D culture conditions on plastic (**Figure 5.9G**), indicating that they are capable of adhering to a rigid 2D substrate and growing normally in an anchorage-dependent manner. FAK inhibitor (1 μ M PF-562271) treatment potently inhibited proliferation of WRC depleted and control cells in soft agarose (**Figure 5.9B,E**), as did FAK siRNA, which reduced the colony size by at least 50% (**Figure 5.9C,F**). FAK was also required for adhesion dependent growth in A431 cells, as FAK inhibitor and FAK depletion both reduced cell proliferation on tissue culture dishes (**Figure 5.9H,I**). Thus, WRC depletion enhances anchorage independent growth and this effect is FAK dependent. Consistently, when WRC was transiently removed from Hela cells, active FAK was also increased and more colonies were formed in the soft agarose assay suggesting enhanced cell transformation upon loss of WRC (**Figure 5.10**).

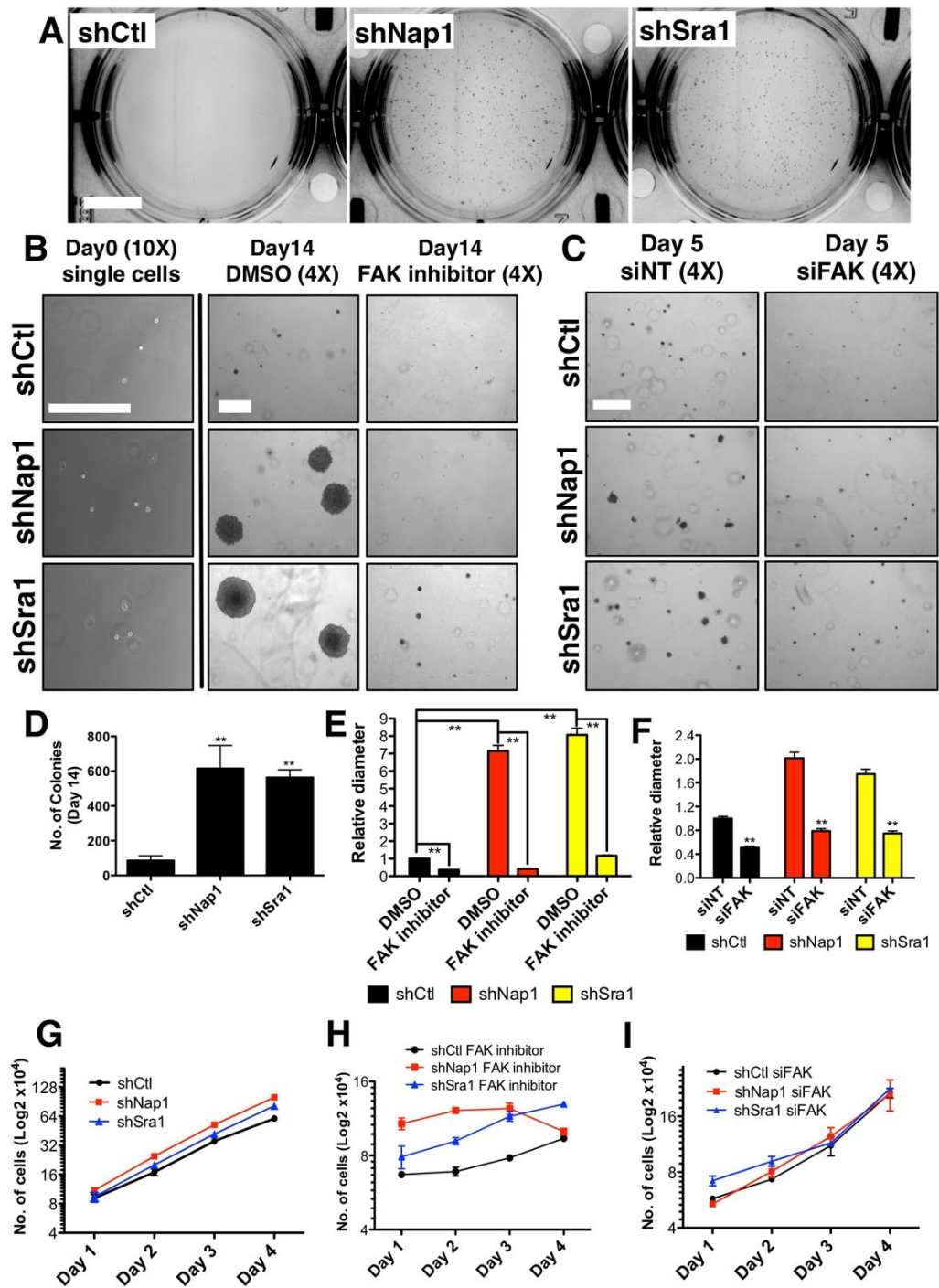


Figure 5.9 Loss of WRC promotes FAK dependent cell transformation

(A) The number of visible colonies in soft agarose was increased in Nap1 and Sra1 depleted cells by day 14. Scale bar 1cm. (B) Colonies formed by shCtl, shNap1, and shSra1 cells in soft agarose assay in the presence of FAK inhibitor or DMSO (vehicle). Scale bar 500 μ m. (C) FAK dependence of colony formation in shCtl, shNap1 and shSra1 cells treated with siNT or siFAK. Scale bar 500 μ m. (D) Colony number from (A) (Data are means \pm SD, n=3, **p<0.01). (E) Colony size from (B) (Data are means \pm SEM, n=30, **p<0.01). (F) Colony size from (C) (Data are means \pm SEM, n=30, **p<0.01). (G) Growth curves of shCtl cells (black), Nap1 stable knockdown cells (red), Sra1 stable knockdown cells (blue) cultured on dish. (H) Growth curves of cells treated with FAK inhibitor and (I) with FAK siRNAs on standard tissue culture dish. Growth curve is presented in Log2 scale. (Data are means \pm SD at each time point, n=3). (G1~3) All panels show A431 cells.

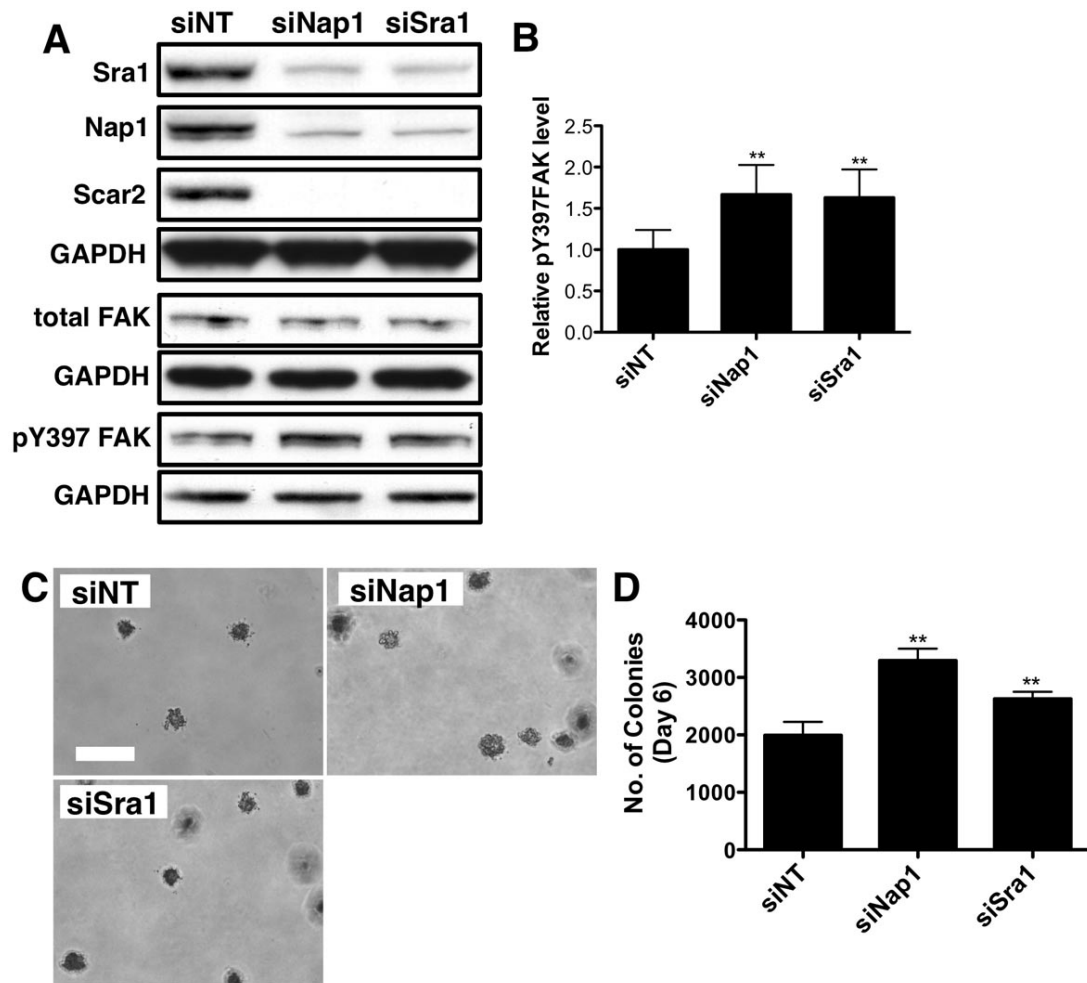


Figure 5.10 Hela cells are transformed upon loss of WRC

(A, B) Immunoblots and quantifications show increased pY397FAK level in WRC depleted Hela cells. (Data are shown as means \pm SEM, n=3 experiments, **p<0.01). (C,D) Loss of Nap1 and Sra1 in Hela cells increased the number of colonies formed in soft agarose. Scale bar 500 μ m. (Data are shown as means \pm SD, n=3 independent assays. **p<0.01). All panels show Hela cells.

Because of cell transformation upon loss of WRC, the ability of WRC depleted cells to form tumours and grow in vivo was then tested. Nude mice injected subcutaneously with stable WRC knockdown cells were sacrificed at early time points as these tumours have grown rapidly and quickly reached the maximum allowed size (1.5cm in diameter) resulting a low survival rate. In contrast, most nude mice injected with control cells did not develop large tumours, and survived over more than six weeks (**Figure 5.11A,B**). Immunohistochemical staining of tumour sections with pY397FAK antibody revealed that the pY397FAK level was substantially increased in vivo (**Figure 5.11C**). Consistently, WRC depleted cells

cultured in 3D collagen gel also had much higher pY397FAK level (**Figure 5.3C,D**). Thus, loss of WRC promotes FAK activation and tumour growth in vivo.

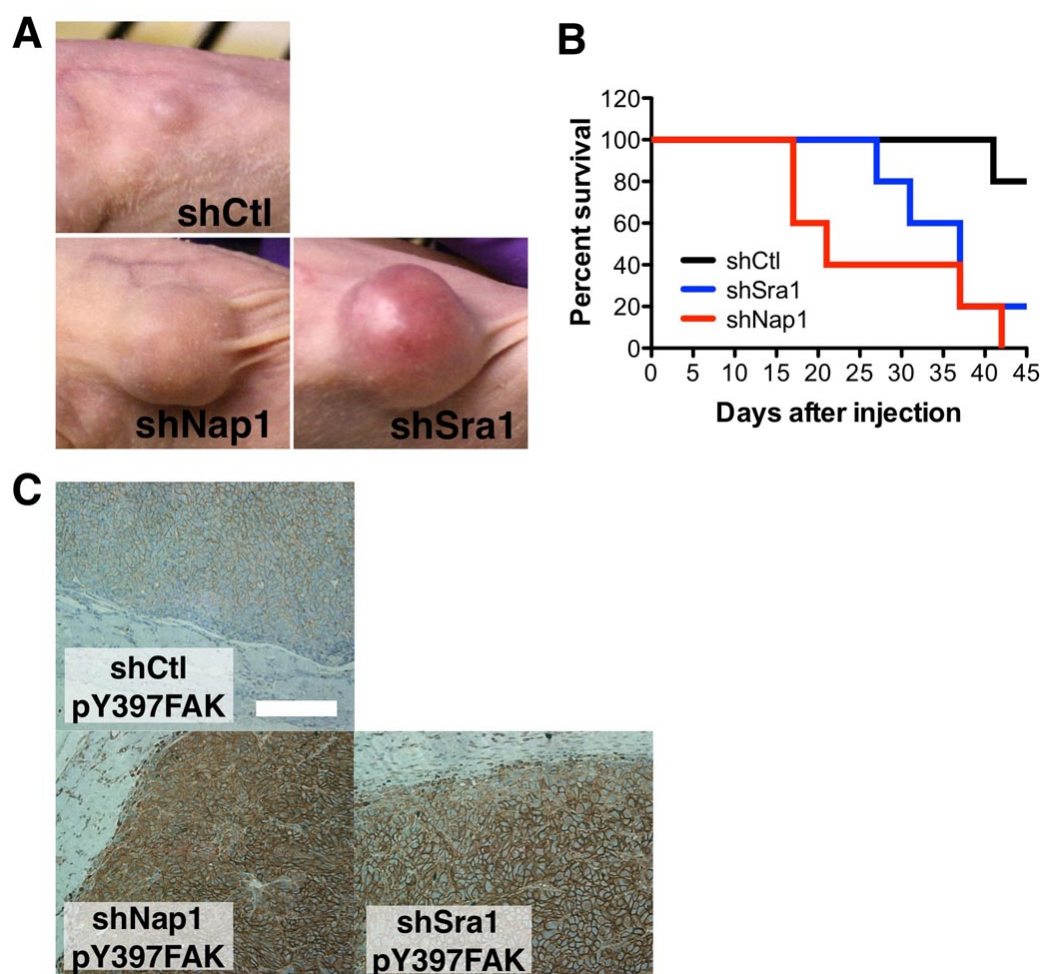


Figure 5.11 Loss of WRC promotes tumour formation in vivo

(A) Tumours formed by control (shCtl) and WRC KD cells (shNap1 and shSra1). (B) Survival curve of subcutaneous injected nude mice, which were sacrificed when tumour reaches 1.5cm in diameter. ($p < 0.01$, Logrank test for trend) (C) Immunohistochemistry of the tumour sections with pY397FAK antibody showing shCtl and WRC subunit depleted as indicated. Scale bar 200 μ m.

FAK promotes proliferation and survival, often through activation of PI3K/Akt or MAP kinase pathways (Igishi et al., 1999, Bouchard et al., 2007). As might be predicted (Ashton et al., 2010, Sonoda et al., 1999, Yamamoto et al., 2003), phospho-Akt (S473) (pAkt) level was increased by more than 5-fold in the stable WRC knockdown cells cultured in 3D collagen gel (**Figure 5.12A,B**). High Akt activation was also observed in the same cells grown on dish (**Figure 5.12C,D**). In contrast, phospho-ERK remained unchanged (**Figure 5.12E**), suggesting that the Ras/MAP kinase pathway was not hyper-activated by WRC loss. Similarly, Hela Nap1 and Sra1 knockdown cells also had high pY397FAK (**Figure 5.10A,B**) and phospho-Akt level (**Figure 5.12F,G**). These Hela WRC depleted cells were also more transformed (**Figure 5.10**). As the PI3K/Akt pathway promotes cell proliferation and survival, these results collectively indicate that loss of WRC promotes hyper-activation of FAK and the PI3k/Akt pathway, which in turn promotes increased anchorage independent growth and tumour growth in vivo.

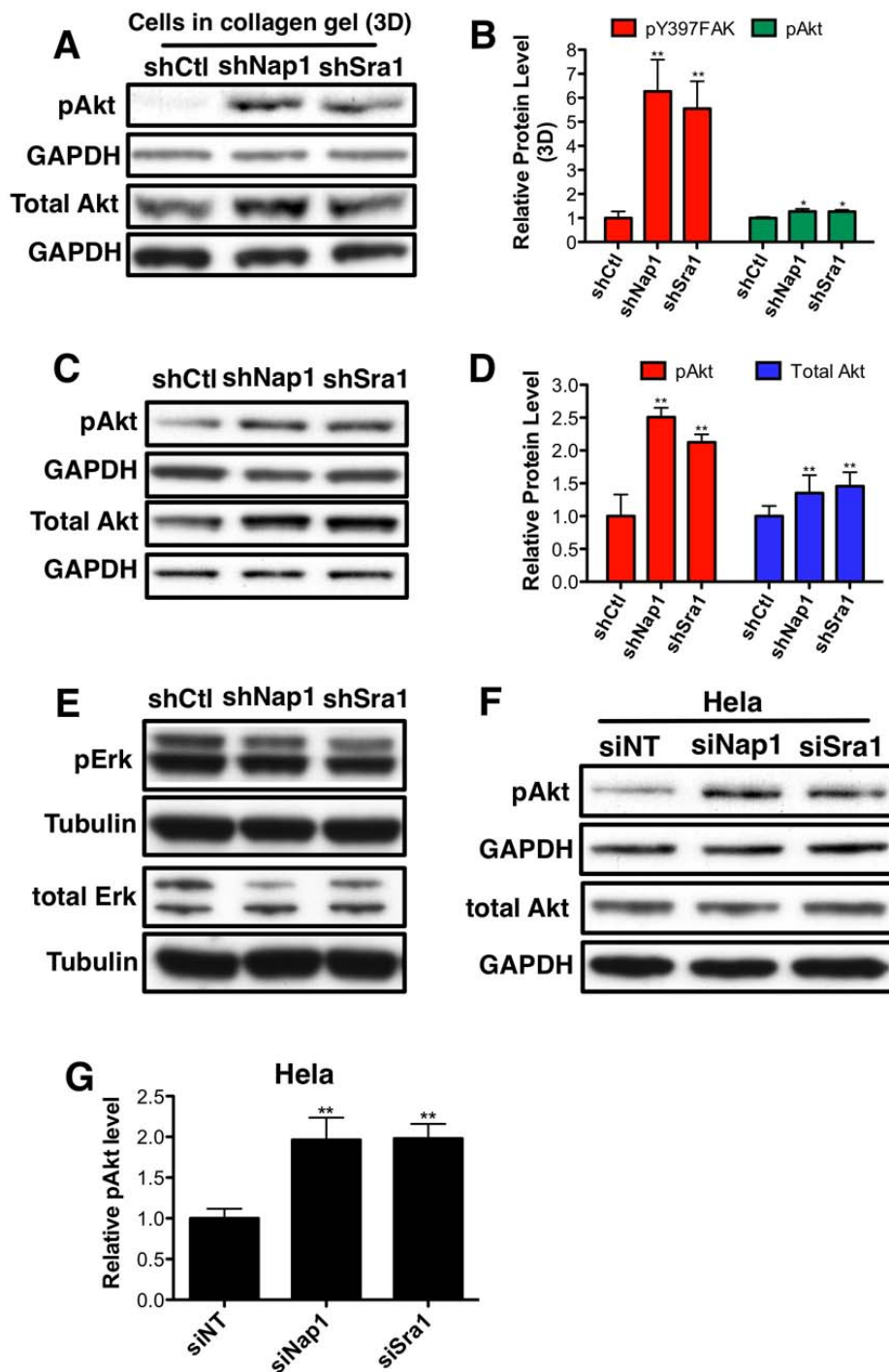


Figure 5.12 Loss of WRC promotes Akt activation

(A,B) Immunoblots and quantifications show increased pAkt level in WRC depleted A431 cells in 3D collagen gel (Data are shown as means \pm SEM, n=3 experiments, **p<0.01. *p=NS). (C,D) Immunoblots and quantifications show increased pAkt level in WRC depleted A431 cells cultured on dish. (Data are shown as means \pm SEM, n=5 experiments, **p<0.01). (E) pErk and total Erk level as indicated in A431 cells. (F,G) Immunoblots and quantifications show increased pAkt level in WRC depleted HeLa cells. (Data are shown as means \pm SEM, n=3 experiments, **p<0.01).

5.3 Loss of WRC promotes formation of degradative focal adhesions

To achieve efficient invasion, cells actively remodel the surrounding matrix using metalloproteinases that degrade ECM. Active FAK has recently been reported to be required for the formation of degradative focal adhesions to facilitate matrix degradation (Wang and McNiven, 2012). High active FAK levels in WRC depleted cells might therefore stimulate matrix degradation to promote invasion. While A431 cells were not amenable to various types of degradation assays (not shown), hTERT-RPE1 cells generated degradative invadopodia on the fluorescent gelatin degradation assay (**Figure 5.13A**). While most control hTERT-RPE1 cells formed invadopodia identified by classical centrally located puncta (Gimona et al., 2008), an invadopodia/adhesion marker, α -actinin (Schoumacher et al., 2010), and correlating gelatin degradation, most WRC depleted hTERT-RPE1 cells formed large degradative focal adhesions, as labeled by strong actin stress fibers and α -actinin (**Figure 5.13A,C**). The formation of degradative focal adhesions also led to a two-fold increase in degradation area in WRC depleted hTERT-RPE1 cells (**Figure 5.13D**).

As hTERT-RPE1 WRC KD cells also had high active FAK level (**Figure 5.13E,F**), FAK was thought to promote the formation of degradative focal adhesions. Depletion of FAK in these WRC KD cells prevented degradative focal adhesions formation (**Figure 5.13B**). As a result, the degradation area was heavily reduced too (**Figure 5.13D**). Thus loss of WRC promoted FAK dependent matrix degradation by the formation of degradative focal adhesions, which could contribute to the increased invasiveness of cells in various 3D assays.

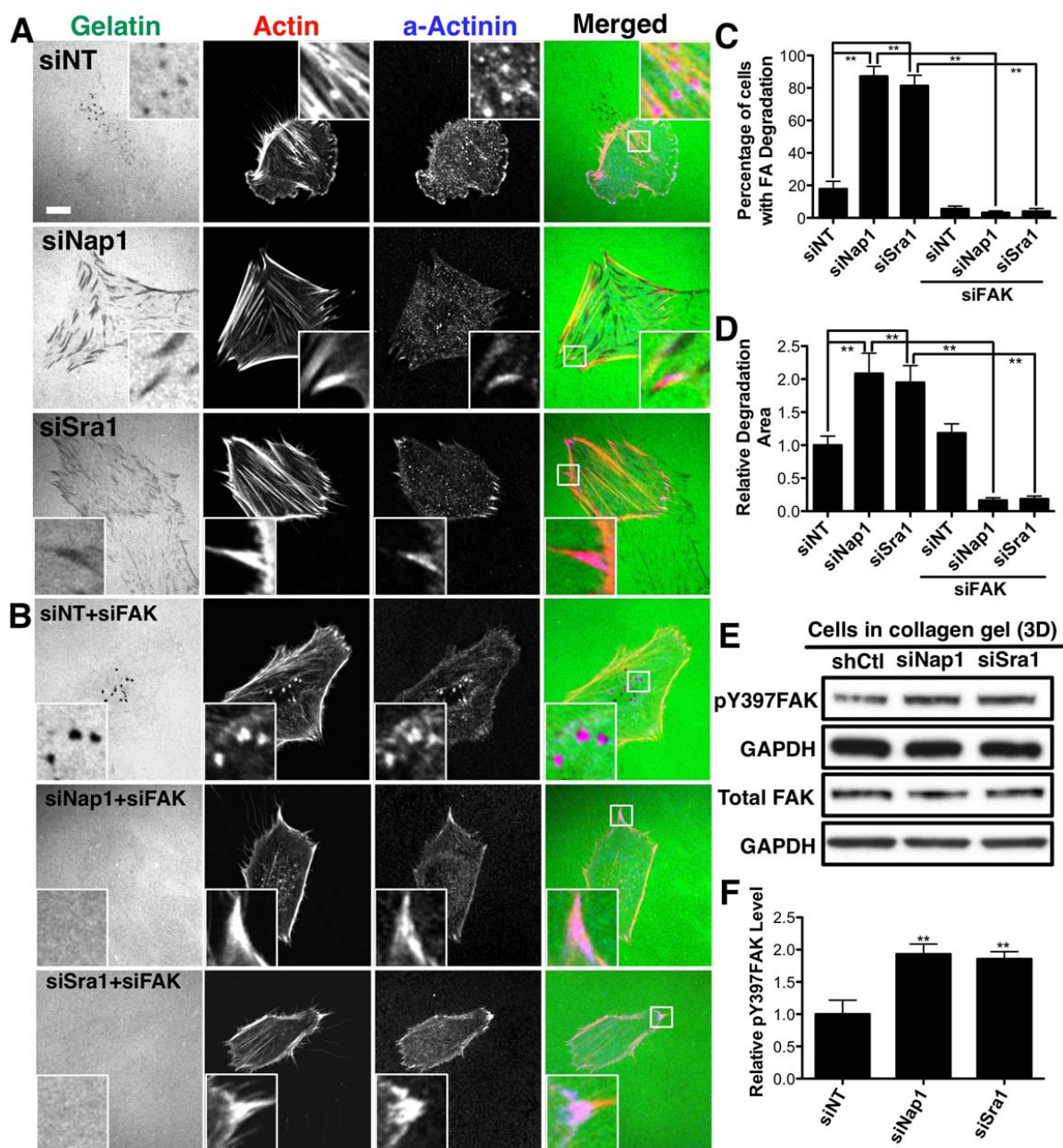


Figure 5.13 Loss of WRC promotes matrix degradation through FAK dependent degradative focal adhesions.

All panels show hTERT-RPE1 cells. (A) Cells were treated with control siRNA (siNT), Nap1 siRNA (siNap1) and Sra1 siRNA (siSra1), (B) or FAK siRNA (siFAK) in indicated cells. All samples were subjected to fluorescent gelatin degradation assay. Confocal micrographs show fluorescent gelatin (green), actin (rhodamine phalloidin, red), and α -actinin (anti- α -actinin, blue). Scale bar 10 μ m. (C) Percentage of cells with degradative focal adhesions (Data are means \pm SEM, n=3 independent assays, **p<0.01). (D) Relative area of degradation per cell (Data are means \pm SEM, n=57, **p<0.01). (E) Increased pY397FAK level in cells cultured in collagen gel. (F) Quantifications of pY397FAK level E. (Data are shown as means \pm SEM, n=3 experiments, **p<0.01).

5.4 Discussion

Cell-ECM adhesions and membrane protrusions at the cell front must be tightly coordinated to allow effective cell migration. It is therefore not surprising that loss of WRC leads to altered adhesion strength and focal adhesion dynamics. Cell-ECM adhesions are tightly linked to the actin cytoskeleton through integrin cytoplasmic tail, talin, vinculin and α -actinin (Vicente-Manzanares et al., 2009). Nascent adhesions are first formed within the lamellipodia where WRC drives extensive actin polymerisation. Formation of nascent adhesions is dependent on actin polymerisation. Then, maturation of these nascent adhesions happens when α -actinin cross-links polymerized actin within the lamellipodia (Choi et al., 2008). Loss of WRC abolishes actin polymerisation needed for lamellipodia formation and alters nascent adhesion formation. As a result, cells have to use alternative ways to form and to mature adhesions leading to global change of adhesion dynamics.

Loss of WRC leads to formation of large stable focal adhesions suggesting adhesion turnover is disrupted. Focal adhesion stability was addressed using video microscopy (20min) in this study. However FRAP based assays should also be used. By using various fluorescence probes, the dynamics of many adhesion proteins could be studied. The adhesion protein that is affected most by WRC loss could also be identified. Nonetheless, focal adhesion turnover is dependent on FAK, which recruits microtubule associated dynamin to adhesion sites to promote adhesion turnover by endocytosis. Interestingly, this is a process dependent on microtubule targeting to focal adhesions. Stable growth of microtubule towards focal adhesions is therefore required (Ezratty et al., 2005). Acetylation is an important marker for microtubule stabilization (Takemura et al., 1992). Loss of microtubule acetylation in WRC deficient cells is reported in the literature (Yokota et al., 2007), so it is possible that loss of WRC leads to unstable microtubules leading to defective focal adhesion turnover by dynamin.

WRC depleted cells and FAK depleted cells have identical defects in focal adhesion dynamics and membrane protrusion formation (**Figure 5.2&5.4**). Loss of WRC in many cell types promoted FAK activation suggesting FAK may try to compensate WRC loss by over activation. Alternatively, a large number of FAK proteins can cluster on these large focal adhesions in WRC KD cells leading to

excessive FAK auto-activation. However activated FAK is not able to promote focal adhesion turnover possibly due to defective actin and microtubule cytoskeletons. Nonetheless, further investigations are needed to understand the mechanism of FAK over activation upon loss of WRC.

WRC KD cells use N-WASP and Arp2/3 complex to move in 3D collagen gel. It is therefore interesting that active FAK also co-localized with N-WASP and Arp2/3 complex in the invasive pseudopods of WRC KD cells. As N-WASP and Arp2/3 complex localization was FAK dependent and FAK is present in pseudopods (**Figure 5.6&5.7**), it is possible that FAK recruits N-WASP hence Arp2/3 complex through the direct protein interaction to pseudopods. Consequently, cells are forming FAK containing structures related to focal adhesions at the leading edges that recruit N-WASP and Arp2/3 complex to trigger actin assembly and invasion.

To activate FAK, an activator protein is required to trigger FAK FERM domain dissociation from the kinase domain before FAK Tyr397 can be auto-phosphorylated (Lietha et al., 2007). However this activator protein has yet to be identified. FAK interacts with Arp2/3 complex in the inactive dephosphorylated form. Interestingly, Arp2/3 complex binds directly to FAK FERM domain, and this interaction is abolished when FAK is active (Serrels et al., 2007). Although this interaction is reported to mildly activate Arp2/3 (Serrels et al., 2007), it is also possible that Arp2/3 complex can be the activator protein to open up FAK by dissociating FAK FERM domain from the kinase domain allowing FAK auto-phosphorylation. Therefore co-localization of FAK and Arp2/3 complex in the invasive pseudopods may enhance FAK activation too, which then recruits N-WASP to activate Arp2/3 complex completing a positive feed back loop.

As additional effects of FAK activation, cell transformation and tumour growth are also promoted in the absence of WRC. In a normal epithelium, cells attach to the underlying basement membrane through integrins, which then initiate FAK mediated survival signals to the epithelial cells (Stupack and Cheresch, 2002). Loss of anchorage to basement membrane leads to FAK inactivation and anoikis of epithelial cells, a specific form of apoptosis (van de Water et al., 1999, Kim et al., 2003, Frisch and Francis, 1994). However high FAK activation bypasses anoikis resulting in cell transformation (Frisch et al., 1996, Ma et al., 2008). Loss of WRC

in cells promoted FAK dependent cell survival and proliferation in soft agar. It is possible that high FAK activation in WRC KD cells leads to anoikis resistance. However this speculation needs to be confirmed using specific anoikis assays, where cells are cultured in suspension and apoptosis markers are tested.

In contrast to 2D cell migration, invasion in a 3D matrix required metalloproteinases that actively remodel ECM to facilitate cell motility. FAK play a role in collagen gel remodelling (Fraley et al., 2010). Matrix remodelling usually requires metalloproteinase activities in addition to mechanical forces. FAK can form a complex with p130Cas and MT1-MMP, a major metalloproteinase, to promote matrix degradation through focal adhesions. Loss of WRC in hTERT-RPE1 cells promoted FAK dependent degradative focal adhesion formation (**Figure 5.13**). Therefore invading WRC KD cells can form FAK containing structures related to degradative focal adhesions at the tips of invasive pseudopods to enhance matrix remodelling leading to more aggressive invasion.

To conclude, loss of WRC leads to changes in focal adhesion dynamics and FAK over activation. High FAK activation subsequently promotes N-WASP mediated invasion and enhanced matrix degradation through large focal adhesions. As an additional effect of FAK activation, loss of WRC also promoted cell transformation and tumour genesis in vivo.

Chapter 6: HSPC300 is unique

6.1 Introduction

HSPC300 is the smallest and least studied subunit of WRC. Loss of HSPC300 protects Von Hippel-Lindau patients from clear cell renal cell carcinoma (ccRCC) (Cascon et al., 2007). Further investigation shows that HSPC300 is required for ccRCC cell proliferation, migration, and invasion. Hence loss of HSPC300 is protective towards clear cell renal cell carcinoma (Escobar et al., 2010). This is in direct contrast to the function of Sra1 in epithelial cancers where loss of Sra1 promotes invasive tumors (Silva et al., 2009). These unique functions suggest HSPC300 can function independently of WRC. In fact, HSPC300 is known to exist as free homotrimers (Derivery et al., 2008). Although free HSPC300 serves as templates for WRC assembly, it is unknown if this pool of free HSPC300 proteins could have other important biological functions. Through this study, free HSPC300 is suggested to cooperate with N-WASP to promote invasion independently of WRC.

6.2 HSPC300 is required for invasion independently of WRC

6.2.1 HSPC300 is required for invasion of WRC depleted cells

WRC KD cells have very little total complex expression, but a considerable amount of HSPC300 remained in these cells. Quantification of the various Western blots showed about 60% HSPC300 remains in WRC KD cells (**Figure 6.1A**). While when HSPC300 expression was reduced in A431 cells, loss of HSPC300 resulted in heavy loss of WRC, as major complex subunits were no longer expressed (**Figure 6.1B**). The observation confirms that HSPC300 is critical for complex formation, yet can exist independently of WRC (Derivery et al., 2008).

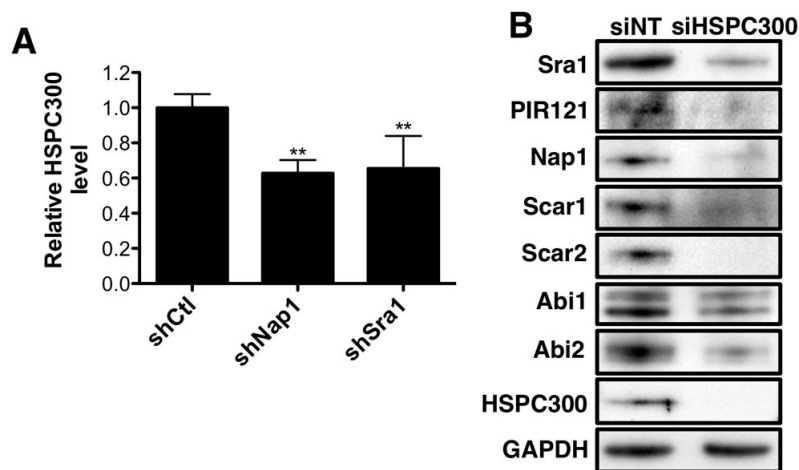


Figure 6.1 HSPC300 is stable without WRC

(A) Quantification of various western blots showing relative levels of HSPC300 remaining in WRC KD cell. (Data are shown as means \pm SEM, n=5 experiments, **p<0.01). (B) Western blots showing protein levels of individual subunits of Scar/WAVE complex in HSPC300 knockdown cells demonstrating complete loss of WRC. All panels show A431 cells.

To investigate if the remaining HSPC300 is required for invasion, HSPC300 was reduced in control and WRC KD A431 cells using siRNAs. Cells were subjected to a 3D collagen gel invasion assay. Interestingly, loss of the remaining HSPC300 in WRC KD cells potently inhibited invasion of WRC KD cells without promoting invasion of control cells (**Figure 6.2A,B,C,D**). To exclude the possibility that the invasion suppression phenotype upon loss of HSPC300 was due to removal of residue complex in WRC KD cells, double Nap1/Sra1 knockdown cells were tested

in 3D collagen gel invasion assay, where the double Nap1/Sra1 knockdown cells invaded as well as Sra1 stable knockdown cells (**Figure 6.2E**). Collectively, these data strongly suggest HSPC300 is required for invasion independently of WRC.

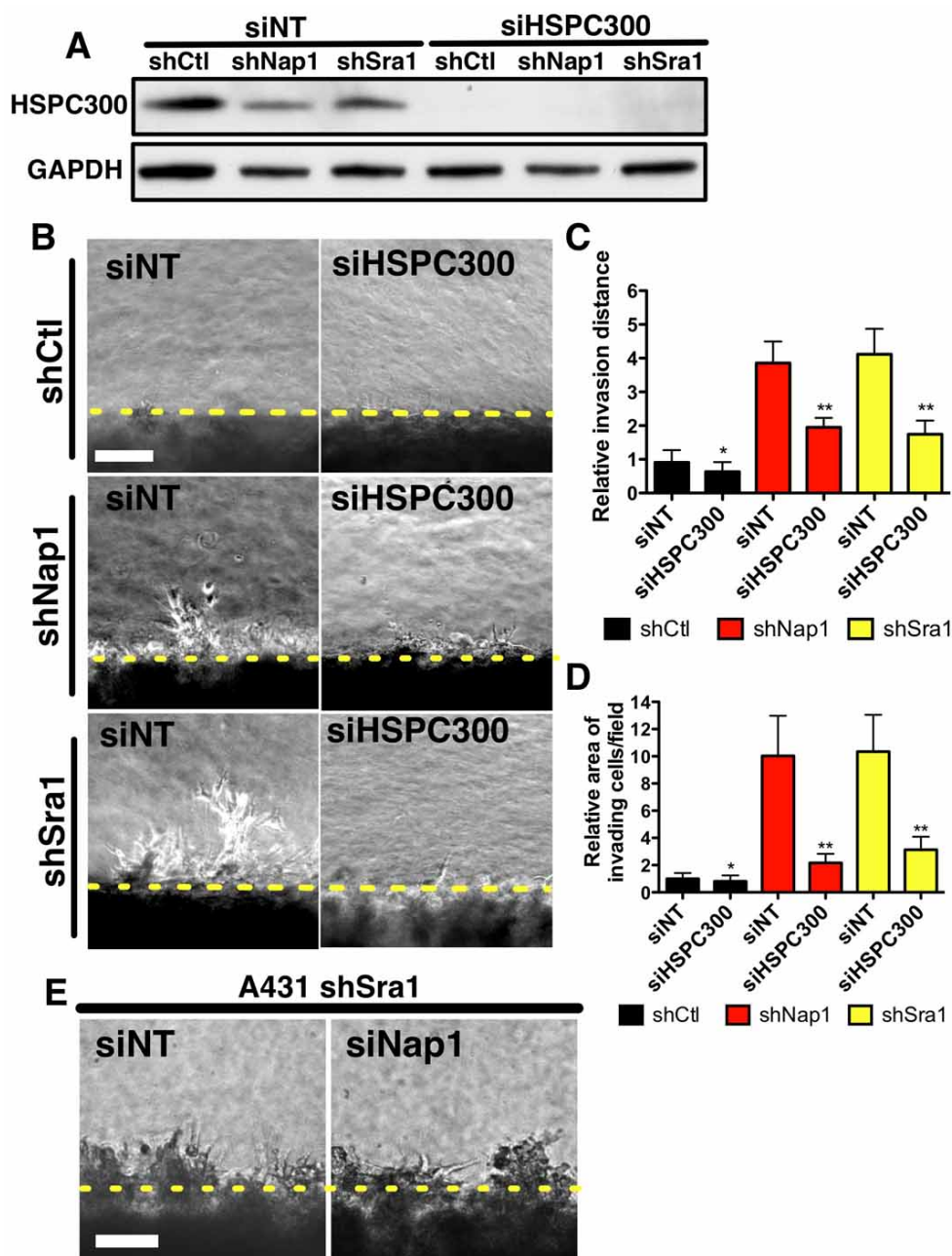


Figure 6.2 Free HSPC300 is required for invasion

(A) Western blots showing HSPC300 protein level after HSPC300 siRNA treatment. (B) Phase contrast micrographs of shCtl, shNap1 and shSra1 cells treated with HSPC300 siRNA (siHSPC300) or siNT as indicated and invaded into thick collagen gels. Scale bar 100 μ m. (C) Relative invasion distance and (D) relative area of invading cells per field from (B). (n=9 images from 3 independent experiments). (E) Phase contrast micrographs of shSra1 cells treated with Nap1 siRNA (siNap1) or siNT invading into collagen gels. Scale bar 100 μ m. All panels show A431 cells.

6.2.2 HSPC300 is required for N-WASP and Arp2/3 complex localization

WRC KD cells use N-WASP and Arp2/3 complex dependent mechanisms to invade. HSPC300 might be required in this N-WASP mediated process to promote invasion. To test this possibility, N-WASP and Arp2/3 complex localization was tested in HSPC300 reduced cells in thick collagen gel invasion assay. Unlike the loss of other WRC subunits, loss of HSPC300 in control cells did not promote N-WASP and Arp2/3 complex localization to the invasive front. In WRC KD cells, loss of the residual HSPC300 surprisingly inhibited N-WASP and Arp2/3 complex localization to the invasive pseudopods (**Figure 6.3**). Similarly, loss of HSPC300 in hTERT-RPE1 cells inhibited invasion and prohibited formation of pseudopods in collagen gel (**Figure 6.4**). A phenotype that was identical to N-WASP loss. In contrast, loss of Nap1 promoted formation of N-WASP rich pseudopods (**Figure 6.4**). Therefore HSPC300 is required for N-WASP and Arp2/3 complex mediated invasion of WRC KD cells. This is a strikingly different phenotype in cells depleted of HSPC300 than in cells depleted of Sra1 or Nap1 indicating that HSPC300 has a pro-invasive role outside of the WRC.

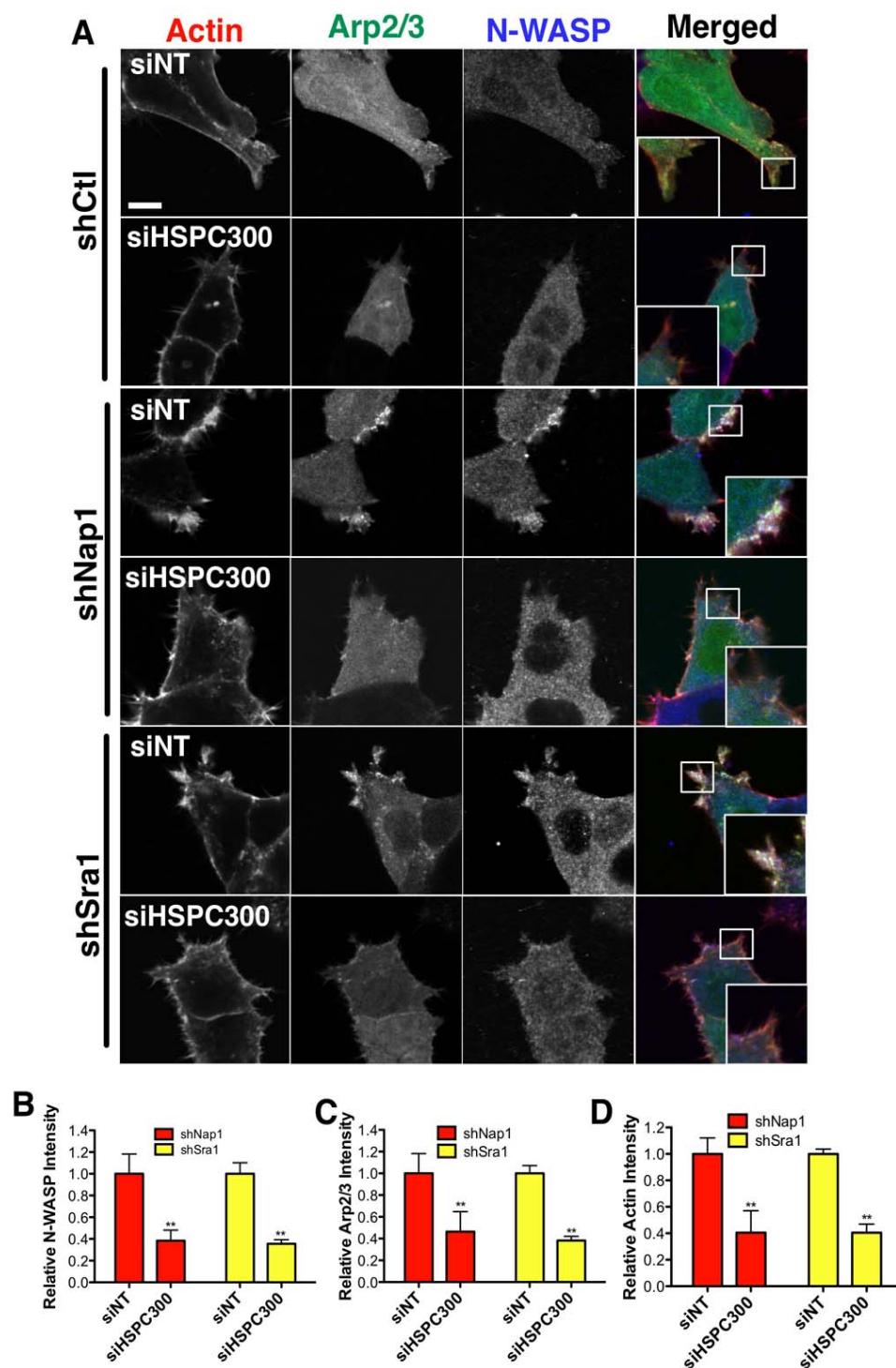


Figure 6.3 HSPC300 is required for N-WASP and Arp2/3 complex localization

(A) Confocal micrographs of WRC KD cells treated with siNT and siHSPC300 expressing p21-Arc-GFP (green). Cells invaded into collagen gels were fixed and stained with rhodamine phalloidin for actin (red), and N-WASP antibody (blue). Scale bar 10 μ m. (B,C,D) Loss of HSPC300 reduced N-WASP, Arp2/3 (p21-Arc-GFP) and actin relative fluorescence intensity. (Data are shown as means \pm SD, n=6 cells, **p<0.01). All panels show A431 cells.

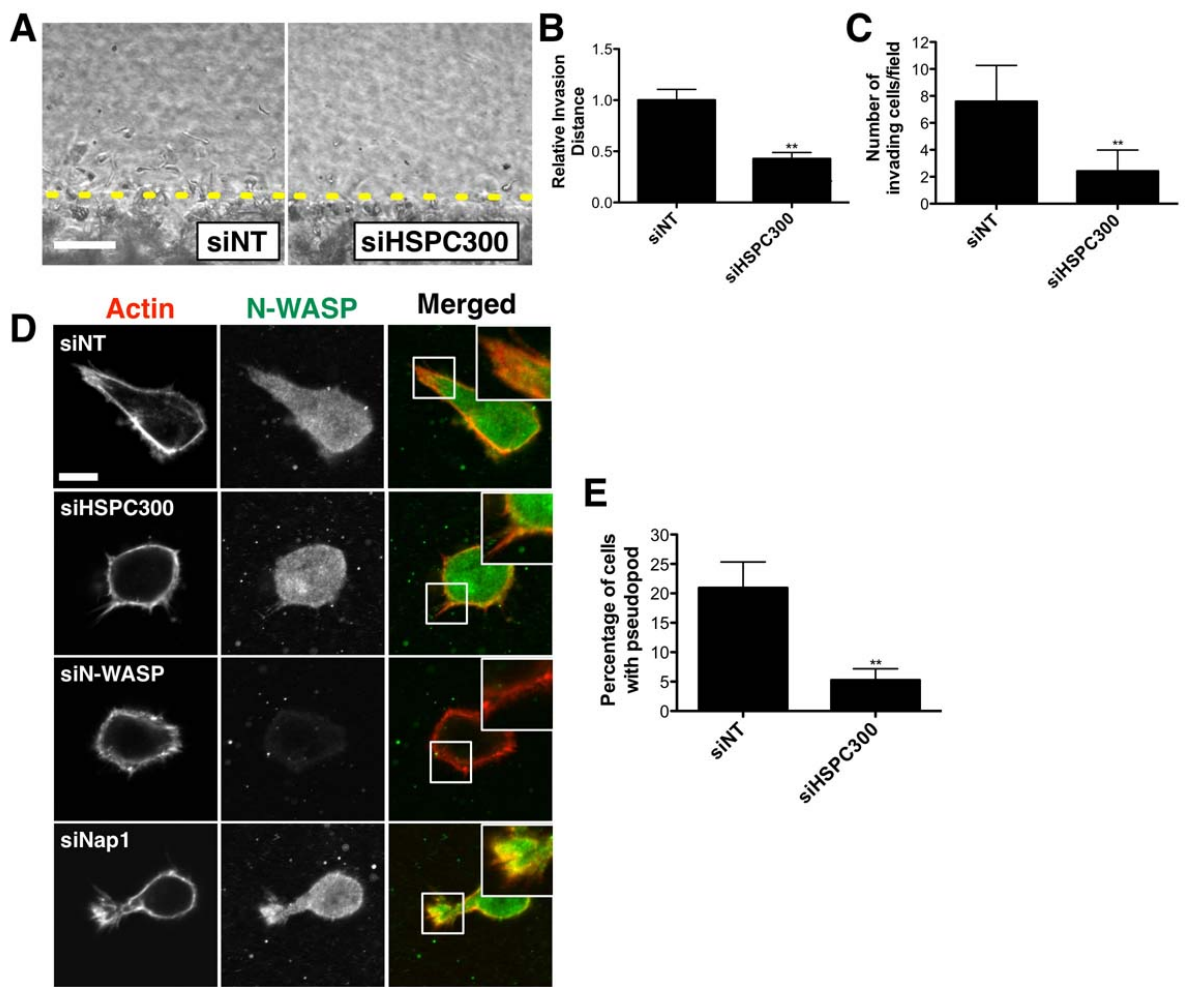


Figure 6.4 HSPC300 promotes invasion and pseudopods formation

All panels show hTERT-RPE1 cells. (A) Phase contrast micrographs of cells treated with control siRNA (siNT) and HSPC300 siRNA (siHSPC300) invading in 3D collagen gel invasion assay. Scale bar 100μm. (B) Quantification of the 3D invasion assay shows the relative invasion distance and (C) the number of invading cells per field (Data are shown as means±SEM, n=12 from 3 independent assays. **p<0.01). (D) Confocal micrographs demonstrate localization of endogenous N-WASP (anti-N-WASP, green) and filamentous actin (rhodamine phalloidin, red) in control (siNT), siHSPC300, siN-WASP and siNap1 cells during invasion into thick collagen gel. Scale bar 10μm. (E) Loss of HSPC300 reduced the number of cells with pseudopods in thick collagen gel invasion assay. (Data are means±SD, n=3 independent assays. **p<0.01).

6.2.3 HSPC300 interacts with N-WASP

HSPC300 appears to cooperate with N-WASP directly to promote invasion, as both proteins robustly co-immunoprecipitated from control, and WRC depleted cells (**Figure 6.5A**). This interaction was also confirmed in GFP-N-WASP expressing Nap1 depleted cells (**Figure 6.5B**). HSPC300 could thus promote invasion together with N-WASP at the cell front through this interaction. This link between HSPC300 and N-WASP provides a potential molecular mechanism for how loss of WRC can be pro-invasive and explains how HSPC300 can be pro-invasive (Escobar et al., 2010) separately from its involvement in WRC.

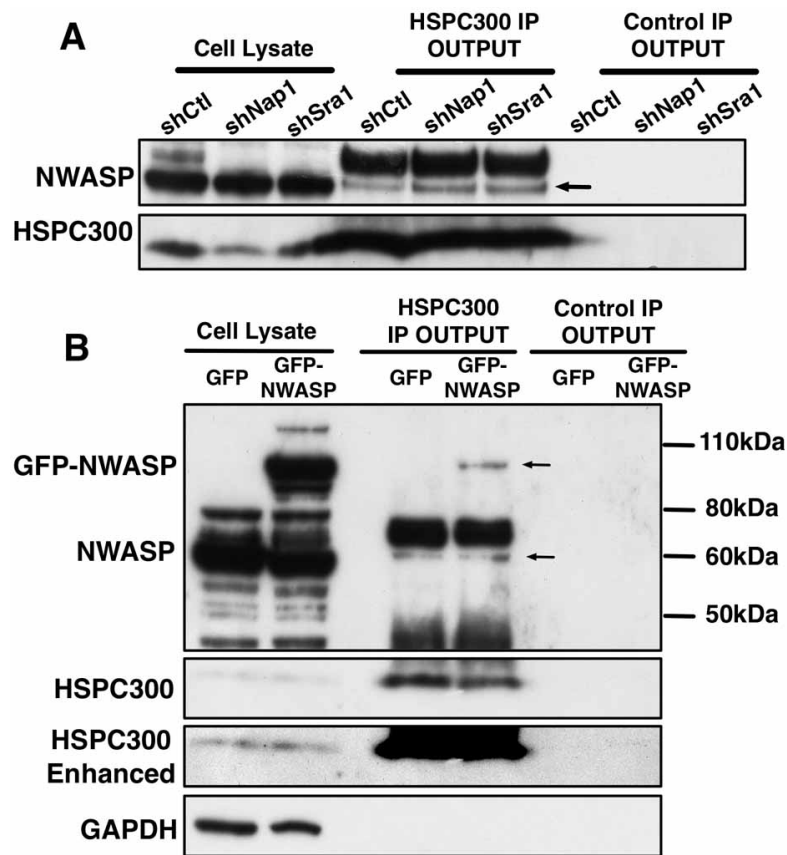


Figure 6.5 HSPC300 interacts with N-WASP

(A) Endogenous HSPC300 and N-WASP coimmunoprecipitation in A431 cells. Arrows in A,B indicate N-WASP. (B) Endogenous HSPC300 and GFP-N-WASP coimmunoprecipitation in GFP-N-WASP expressing A431 Nap1 depleted cells.

6.3 Discussion

Recent publications suggest that HSPC300 may be pro-invasive (Cai et al., 2009, Cascon et al., 2007, Escobar et al., 2010, Maranchie et al., 2004), while I clearly find that WRC suppresses invasion. It is therefore speculated that HSPC300 might have a pro-invasive activity that was independent of its role in WRC. Indeed, by using cells with nearly no WRC expression, HSPC300 was demonstrated to promote invasion independently of WRC (**Figure 6.2**). This study hence reveals a novel pro-invasive function of free HSPC300.

Free HSPC300 may cooperate with N-WASP in WRC KD cells to promote invasion. N-WASP and Arp2/3 complex localization requires HSPC300. HSPC300 interacted with N-WASP even when WRC was absent suggesting this interaction was not dependent on WRC (**Figure 6.5**). Without further analysis, it is not clear if the interaction is direct. However the possibility that Abi1 mediates the HSPC300-N-WASP interaction independently of WRC cannot be excluded. As Abi1 expression was not significantly affected by the loss of WRC, Abi1 could link HSPC300 to N-WASP through direct interactions with both proteins.

Abi1 interacts with and activates N-WASP through a C-terminal SH3 domain, but the N-WASP activating ability of Abi1-SH3 domain alone is 45-fold weaker than the full Abi1 protein suggesting Abi1 N-terminus is also required for N-WASP activation (Innocenti et al., 2005). Interestingly, HSPC300 structurally resembles the longer helix of the two helices at Abi N-terminus (Linkner et al., 2011), so free HSPC300 may activate N-WASP directly as well. HSPC300 and helices of Abi1 are buried at the center of WRC, only when WRC is disassembled HSPC300 is

released to promote invasion. Therefore WRC could be an important check on the pro-invasive function of HSPC300.

Chapter 7: NHS, a novel WRC binding protein

7.1 Introduction

Scar/WAVE homology domain (WHD) is a defining feature of all Scar proteins. Until recently the three Scar proteins were the only WHD containing proteins thought to exist in human cells. However, in *Drosophila*, a novel protein called guanylate kinase holder (GUKH) was identified to have a region with similarity to WHD of *Drosophila* Scar1 and WHD of mouse Scar1 (Mathew et al., 2002). The Human GUKH gene was later identified as Nance-Horan syndrome (NHS) gene (Katoh and Katoh, 2004). Interestingly NHS protein also contains WHD at the N-terminus (**Figure 7.1A**). In contrast to Scar proteins, the VCA domain that is required for Arp2/3 complex activation is not present in NHS so NHS may be unable to initiate actin polymerization (Brooks et al., 2010).

Mutations in NHS gene cause Nance-Horan syndrome, which is an X-linked developmental disorder characterized by bilateral congenital cataracts, dental anomalies, facial dysmorphism and mental retardation (Burdon et al., 2003). Interestingly, loss of NHS gene exon1, which encodes NHS WHD, leads to typical features of Nance-Horan syndrome suggesting the importance of NHS WHD (Brooks et al., 2004). The NHS gene is alternatively spliced resulting in a number of NHS isoforms (**Figure 7.1B**). Only NHS-1A and NHS-A proteins (NHS A proteins) contain a WHD suggesting they are responsible for the Nance-Horan syndrome caused by NHS gene exon1 deletion (Brooks et al., 2010).

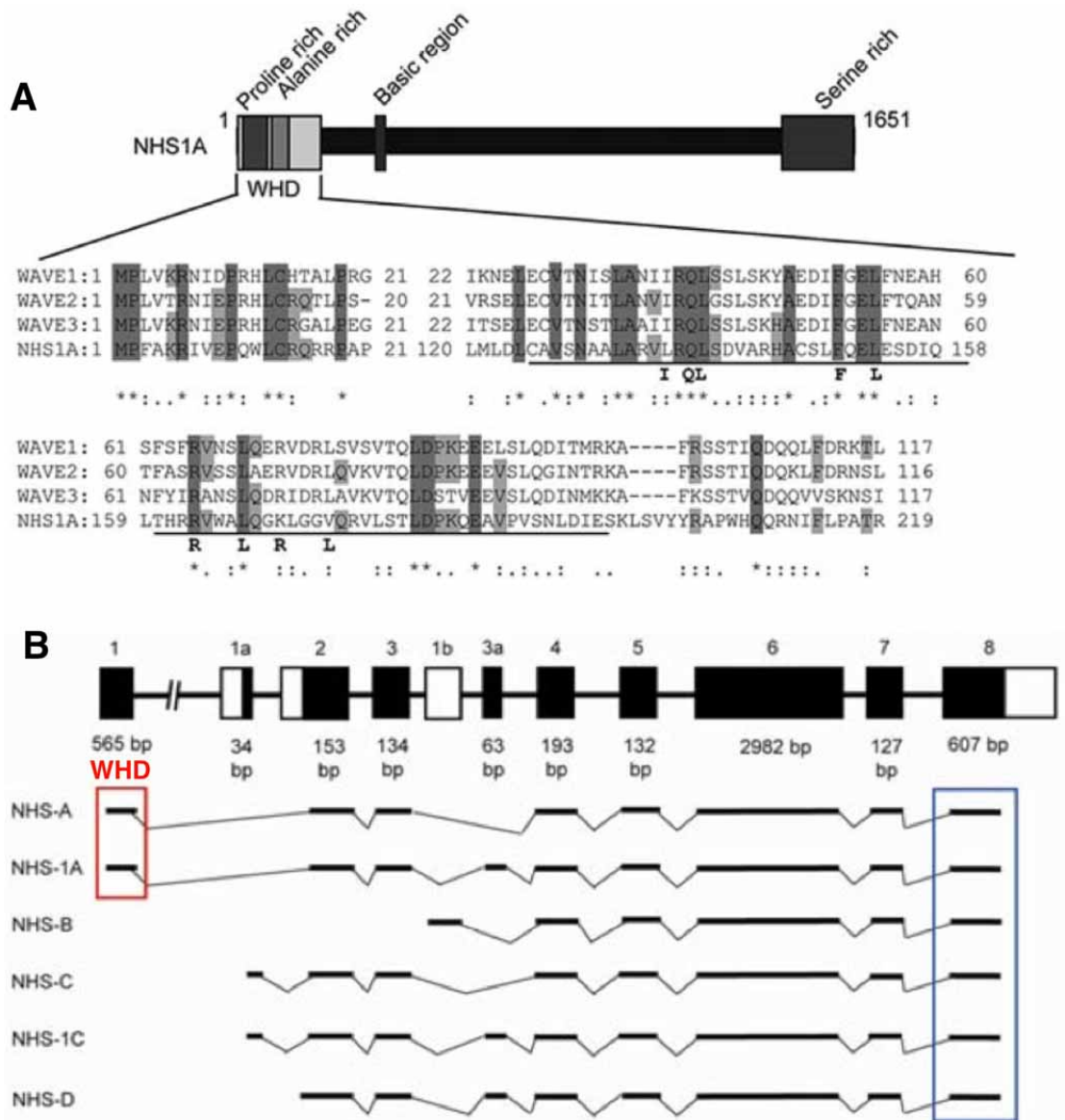


Figure 7.1 NHS contains WHD

(A) Proteins sequences of NHS and Scar (WAVE) 1,2,3 aligned showing WHD homology. (B) Isoforms of HNS protein due to alternative splicing of NHS gene. Red box highlights WHD on NHS A proteins. Figure adapted from (Brooks et al., 2010)

Little is known about the cell biology of the two NHS A proteins. Expression of GFP-NHS-A shows protein localization at cell-cell junctions. This localization is NHS WHD dependent, as deletion of NHS WHD renders the protein cytoplasmic highlighting the significance of WHD in NHS protein function (Sharma et al., 2008, Sharma et al., 2006). NHS-A was later identified to interact with the tight junction marker ZO-1, and localizes to tight junctions (Sharma et al., 2009). However the biological function of NHS at cell-cell junctions are not known.

Although the exact function of NHS A proteins is unknown, it is clear NHS WHD is important. In Scar proteins, WHD is required for direct interactions with Abi proteins (Innocenti et al., 2004) and HSPC300 (Chen et al., 2010). This interaction allows the assembly of WRC. It is likely that NHS WHD can interact with WRC subunits forming a WRC-like complex. However due to the lack of VCA on NHS-A proteins, this putative complex should be defective towards Arp2/3 and could have a dominant negative effects on WRC. This is an interesting perspective, as the mechanism of WRC activation has been explored extensively (Linkner et al., 2011, Ismail et al., 2009, Steffen et al., 2004), but very little is known about how WRC is switched off. In this chapter, NHS is demonstrated to interact with subunits of WRC directly. While the putative 'NHS complex' is hard to identify, NHS negatively regulates Rac1 activation leading to suppression of WRC activation.

7.2 NHS-1A is a putative negative regulator of WRC

7.2.1 NHS-1A interacts with WRC subunits

To identify if NHS WHD is functional, a direct protein interaction with HSPC300 was tested. As demonstrated by Brooks and colleagues using yeast two-hybrid screening, HSPC300 interacts with NHS WHD directly. This interaction was also confirmed by co-immunoprecipitation (Brooks et al., 2010). To test if this direct binding of NHS-1A allows interactions with other WRC subunits, GFP-NHS1A was immunoprecipitated from MCF7 breast cancer cells using GFP-trap and various WRC subunits were probed. As expected, the interaction with Nap1, Sra1, Scar2 and Abi1 was readily detected (**Figure 7.2A**). Therefore NHS-1A can interact with the whole WRC through a direct interaction with HSPC300.

Due to interactions with WRC subunits, NHS was proposed to form a WRC like 'NHS complex'. To test this idea, Myc-NHS-1A was over expressed in MCF7 cells and subjected to Blue NativePAGE to resolve possible complexes. However when an Sra1 antibody was used, only WRC was detected with or without NHS-1A over expression. Stable Sra1 MCF7 knockdown cells were used as a control for WRC detection on the NativePAGE (**Figure 7.2B**). In contrast, when NHS-1A containing complex was probed with a Myc antibody, a smearing blot was obtained on NativePAGE above the band for WRC (**Figure 7.2B**). As a result, NHS-1A may not form a WRC like complex, but unique complexes containing NHS-1A are possible.

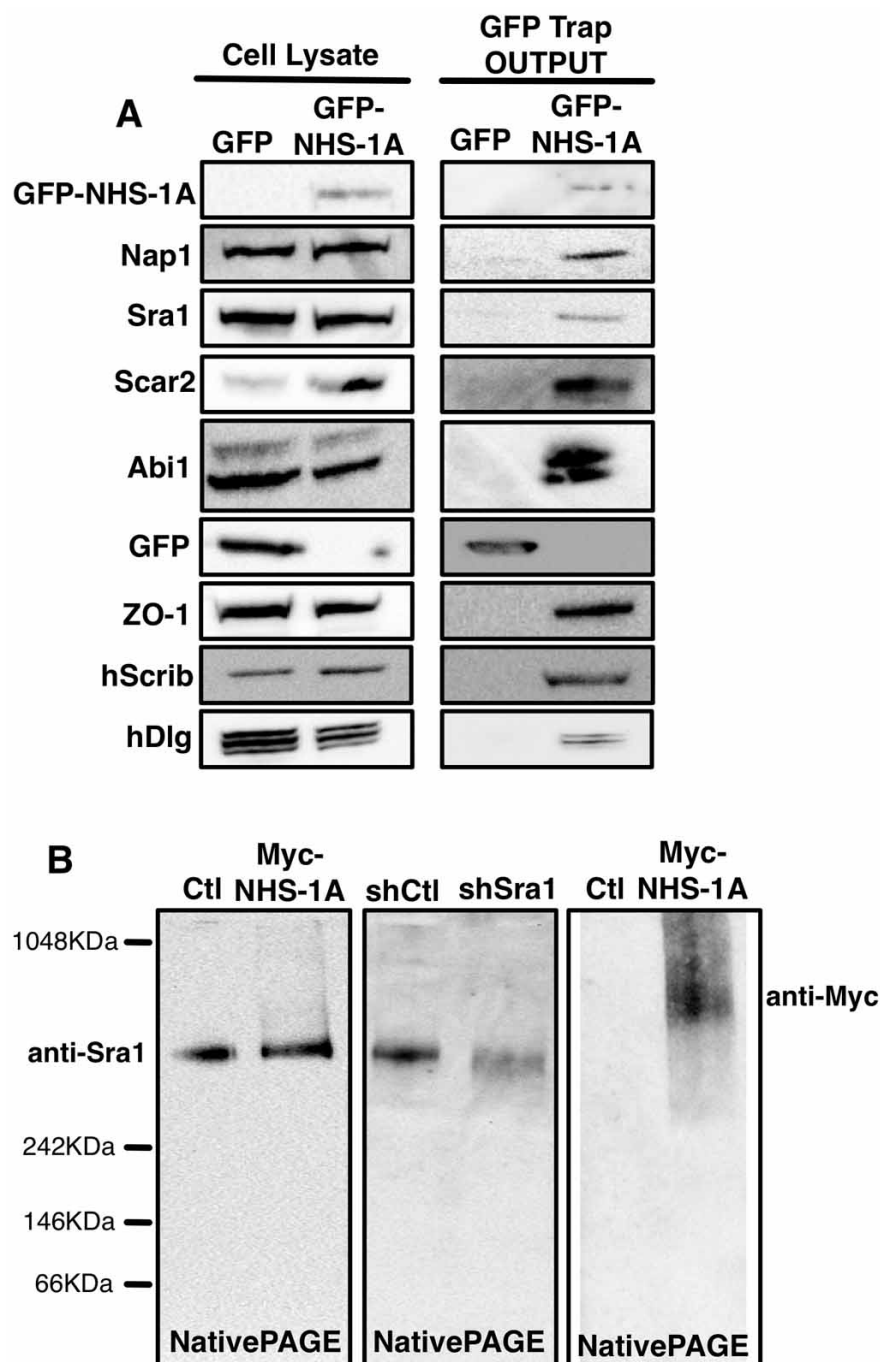


Figure 7.2 NHS interacts with multiple proteins

(A) GFP-NHS-1A is expressed in MCF7 cells and subjected to GFP trap. Proteins interactions are probed as indicated. (B) Blue NativePAGE shows intact WRC in MCF7 cells over expressing Myc-NHS-1A, and putative NHS complex as detected by an anti-Myc antibody.

7.2.2 NHS-1A localizations

Having established the link between NHS-1A and WRC, the localization of GFP-NHS-1A was studied in various cell types. The localization and dynamics of WRC was tested and established in B16F10 melanoma cells (Chapter 1), so GFP-NHS-1A was expressed in migrating B16F10 cells and imaged as the cell migrated. GFP-NHS-1A was observed to behave similarly to WRC in migrating B16F10, where GFP-NHS-1A localized to leading edge of the expanding lamellipodium (Figure 7.3).

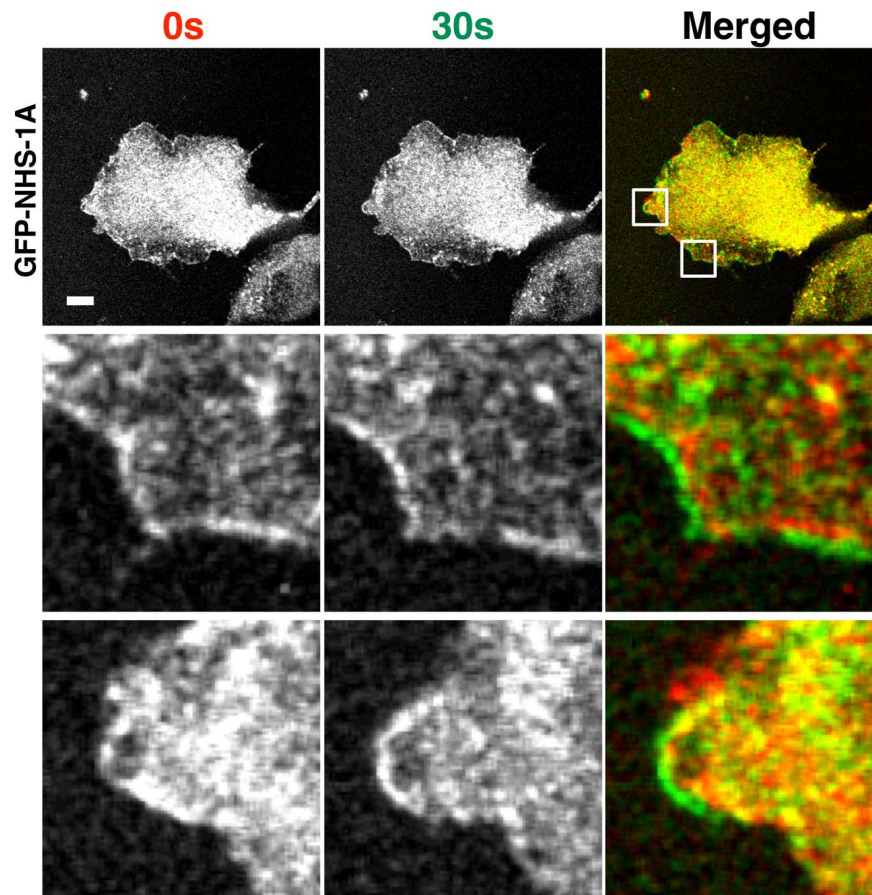


Figure 7.3 NHS-1A localization at the leading edge in a mouse melanoma cell line

GFP-NHS-1A was expressed in a migrating B16F10 mouse melanoma cell on fibronectin coated glass bottom dish. Still images at indicated time points were pseudo-coloured accordingly and merged to show GFP-NHS-1A dynamics and localization. Scale bar 10 μ m.

When GFP-NHS-1A was expressed in MCF7 human breast cancer cells, the GFP tagged protein also localized nicely to the cell edge (**Figure 7.4A**). However in MCF7 cells, GFP-NHS-1A also localized strongly to cell-cell junctions. Notably, in cells with strong GFP-NHS-1A expression, the cell edge localization was not observed but cell-cell junction localization was not affected (**Figure 7.4B**). As WRC was reported to localize at cell-cell junctions in A431 cells, co-localization of NHS-1A with WRC was investigated. NHS-1A was found to co-localize with WRC at cell-cell junctions in A431 cells (**Figure 7.5A**). Similarly, in MCF7 cells, Abi1 and NHS-1A co-localized at cell-cell junction (**Figure 7.5B**), however loss of WRC in MCF7 cells did not abolish NHS1A localization to cell-cell junction (**Figure 7.5C,D**). Collectively, these data demonstrate that NHS-1A is able to localize to cell edge and cell-cell junctions.

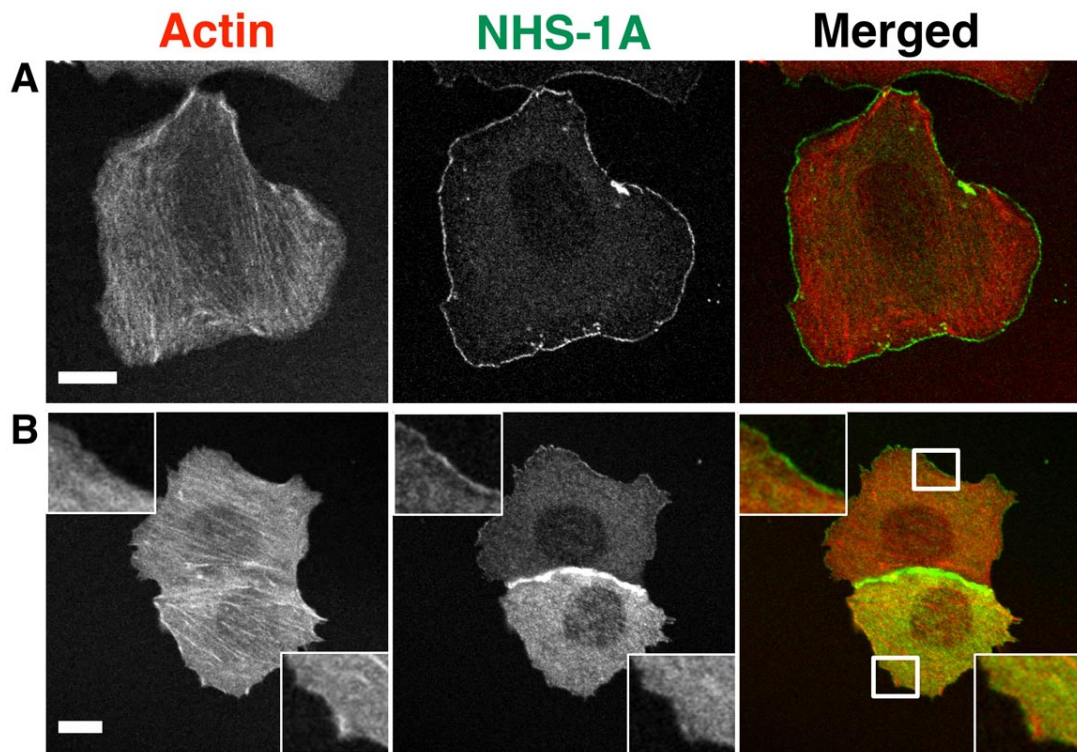


Figure 7.4 NHS-1A localization at the leading edge and cell-cell junction in a human epithelial cell line

(A) Confocal micrographs showing NHS-1A localization at the leading edge and (B) at cell-cell junctions. Live MCF7 cells co-expressing Lifeact-RFP (Actin, red) and GFP-NHS-1A (NHS-1A, green) were imaged. Scale bar 10 μ m.

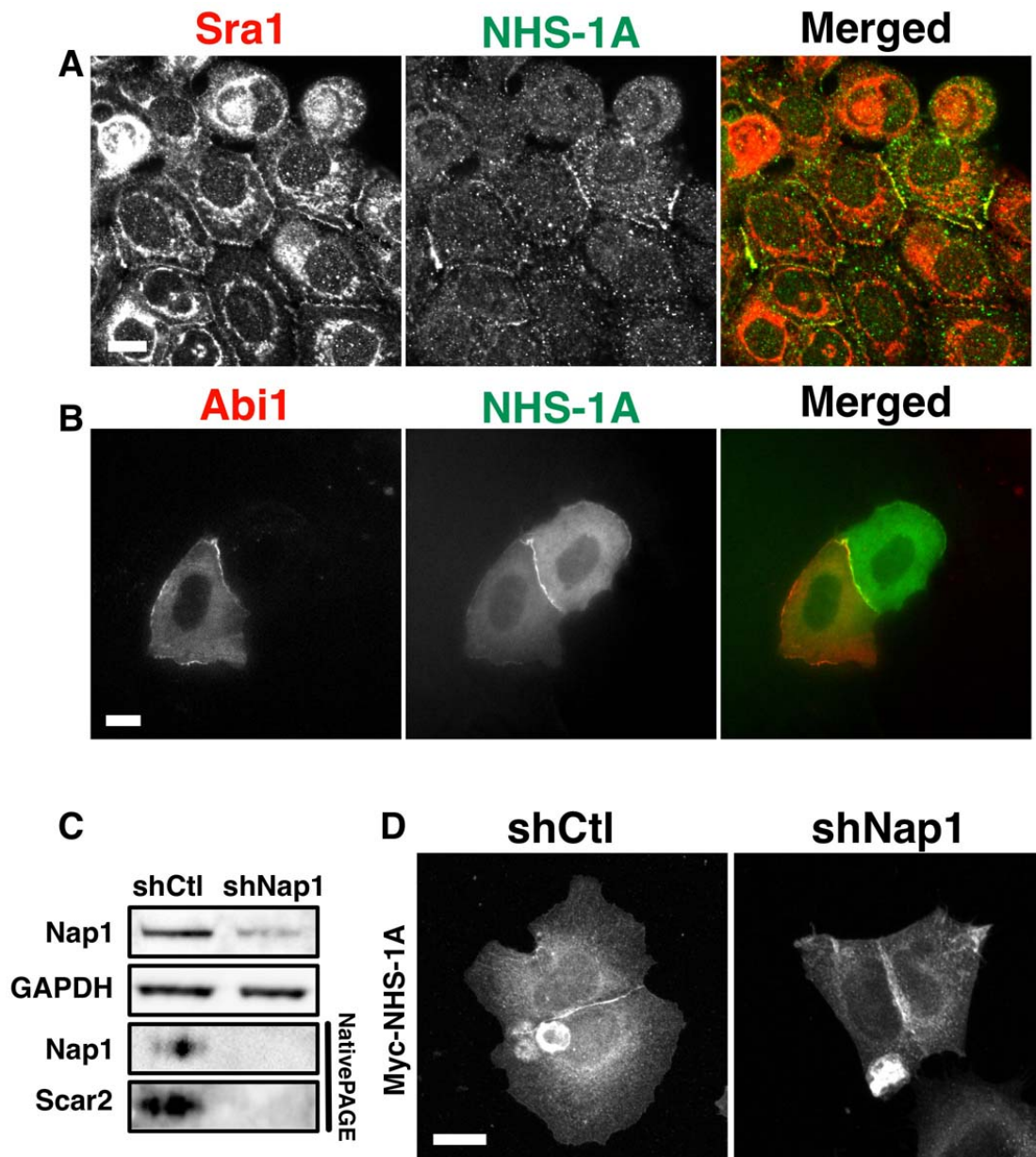


Figure 7.5 Co-localization of WRC and NHS-1A at cell-cell junctions

(A) Confocal micrographs showing WRC (Sra1) and NHS-1A localisation. A431 cells expressing Myc-NHS-1A were fixed and stained with an Sra1 antibody for Sra1 (red), and a Myc antibody for Myc-NHS-1A (green). (B) Epifluorescence micrographs (TIRF microscope) of GFP-NHS-1A (NHS-1A, green) and Abi-RFP (Abi1, red) expressing live MCF7 cell showing co-localization of WRC and NHS-1A. (C) Western blots showing sufficient reduction of WRC in MCF7 shNap1 cells. (D) Myc-MHS-1A expressing control (shCtl) and Nap1 stable knockdown MCF7 cells (shNap1) were fixed and labelled with a Myc antibody for Myc-NHS-1A and examined by confocal microscopy. Scale bar 10µm.

7.2.3 NHS-1A is not required for cell-cell junction

Because of the predominant localization of NHS1A at cell-cell junctions, the function of NHS-1A on cell-cell adhesion was explored. The *Drosophila* NHS ortholog, GUKH, interacts with Dlg and Scribble at *Drosophila* synapses. The proper synaptic localization of *Drosophila* Scribble requires GUKH (Mathew et al., 2002). Human Scribble (hScrib) however localizes to cell-cell junctions in an E-cadherin dependent fashion (Navarro et al., 2005). Together with human Dlg (hDlg), hScrib also directs basolateral membrane formation hence setting up the apical/basal polarity in the epithelium (Zhan et al., 2008, Dow et al., 2003). As NHS-1A also localizes to cell-cell junctions, the interaction with hScrib and hDlg was tested. Interestingly, by using GFP trap, NHS-1A was identified to interact with both hScrib and hDlg. Its interaction with ZO-1 was also confirmed (**Figure 7.2**).

NHS-1A was speculated to regulate apical/basal polarity due to the interaction with hScrib and hDlg. To test this idea, four stable NHS knockdown MCF7 cells lines (a-d) were generated. While there was no antibody for NHS available, mRNA level of these stable cell lines were tested using QRT-PCR (**Figure 7.6A**). Stable cell lines b & d were selected for subsequent experiments as they had sufficient reduction of NHS mRNA. As shRNAs used were not specific to NHS-1A, so all NHS isoforms were reduced. Disruption of hScrib and hDlg localization is enough to trigger loss of cell polarity leading to mammary tumorigenesis (Zhan et al., 2008, Gardiol et al., 2006, Watson et al., 2002). hScrib and hDlg localization in NHS KD cells was then studied. However loss of NHS proteins did not cause mis-localization of hScrib or hDlg, and the actin cytoskeleton at cell-cell junctions was not changed (**Figure 7.6B,C**). As a result, despite all the interactions, NHS-1A has no obvious function on hScrib or hDlg localization at cell-cell junctions.

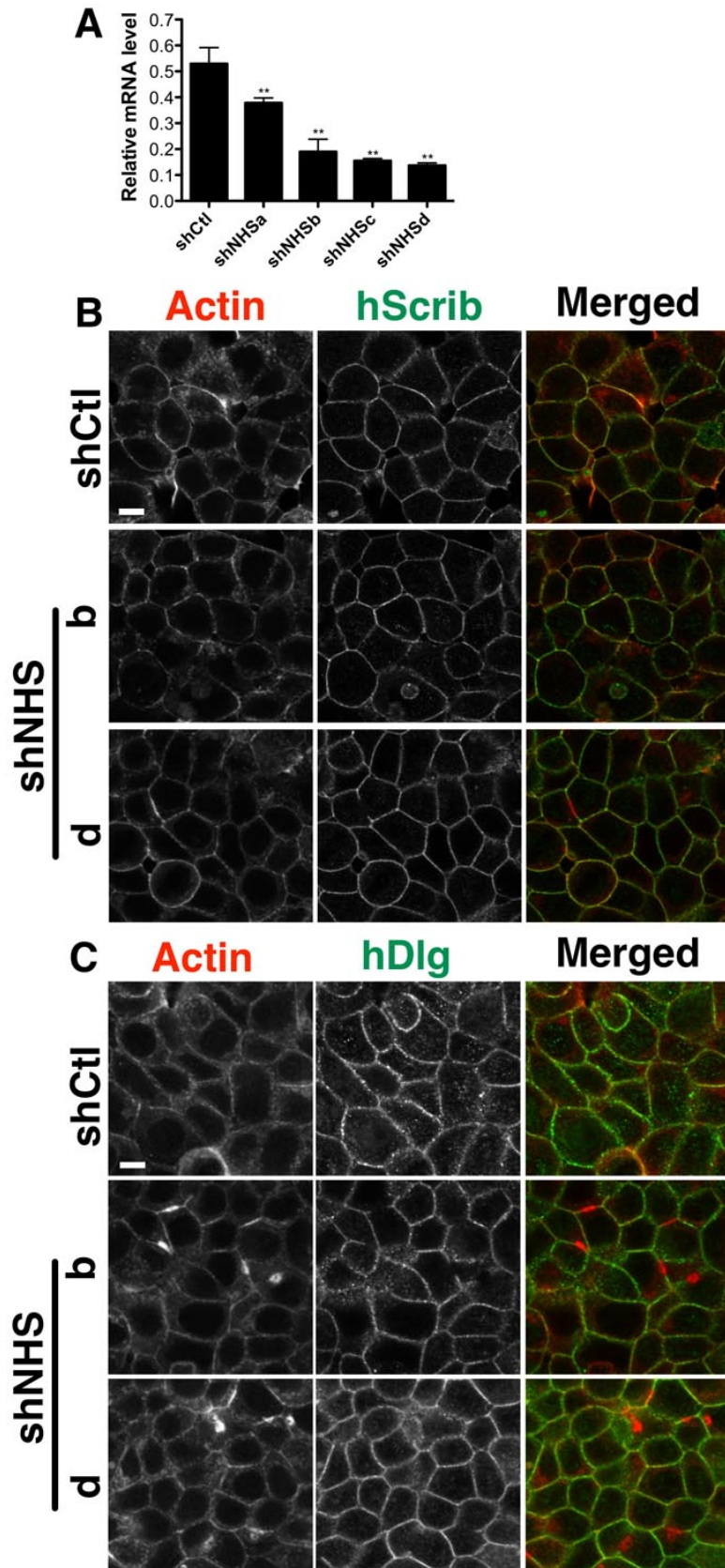


Figure 7.6 NHS is not required for cell-cell junctions

(A) Quantitative RT-PCR shows reduction of NHS mRNA level in various NHS stable known down cell lines (shNHSa-d). (B,C) shCtl and shNHS cells were fixed and stained with rhodamine phalloidin for actin (red), and endogenous hScrib (B) or hDlg (C) (green) using corresponding antibodies. Samples were examined by confocal microscopy. All panels show MCF7 cells. Scale bar 10 μ m.

7.2.4 NHS-1A is a negative regulator of Rac1

Although NHS has little function at cell-cell junctions, loss of NHS in MCF7 cells promoted cell spreading on collagen coated dishes. During spreading control cell (shCtl) generated polarized membrane protrusions, while cells without NHS had large broad lamellipodia around the cell. In fact, because of the large protrusions the cell area was increased by at least 2-fold in NHS KD cells (**Figure 7.7A,C**). As WRC is required for making membrane protrusions, this phenotype suggests WRC might be hyper active without NHS.

Rac1 is required for WRC activation. Despite the direct interaction of NHS-1A with WRC via HSPC300, NHS-1A might also regulate Rac1 activation through the interaction with hScrib, which is also involved in the regulation of Rac1 and Cdc42 activation with a guanine nucleotide exchange factor (GEF), β PIX (Audebert et al., 2004, Nola et al., 2008, Momboisse et al., 2009, Osmani et al., 2006). Indeed, stable reduction of hScrib in MCF7 cells led to spreading defects similar to loss of WRC, as minimum membrane protrusions were produced and cell were smaller (**Figure 7.7A,B,C**).

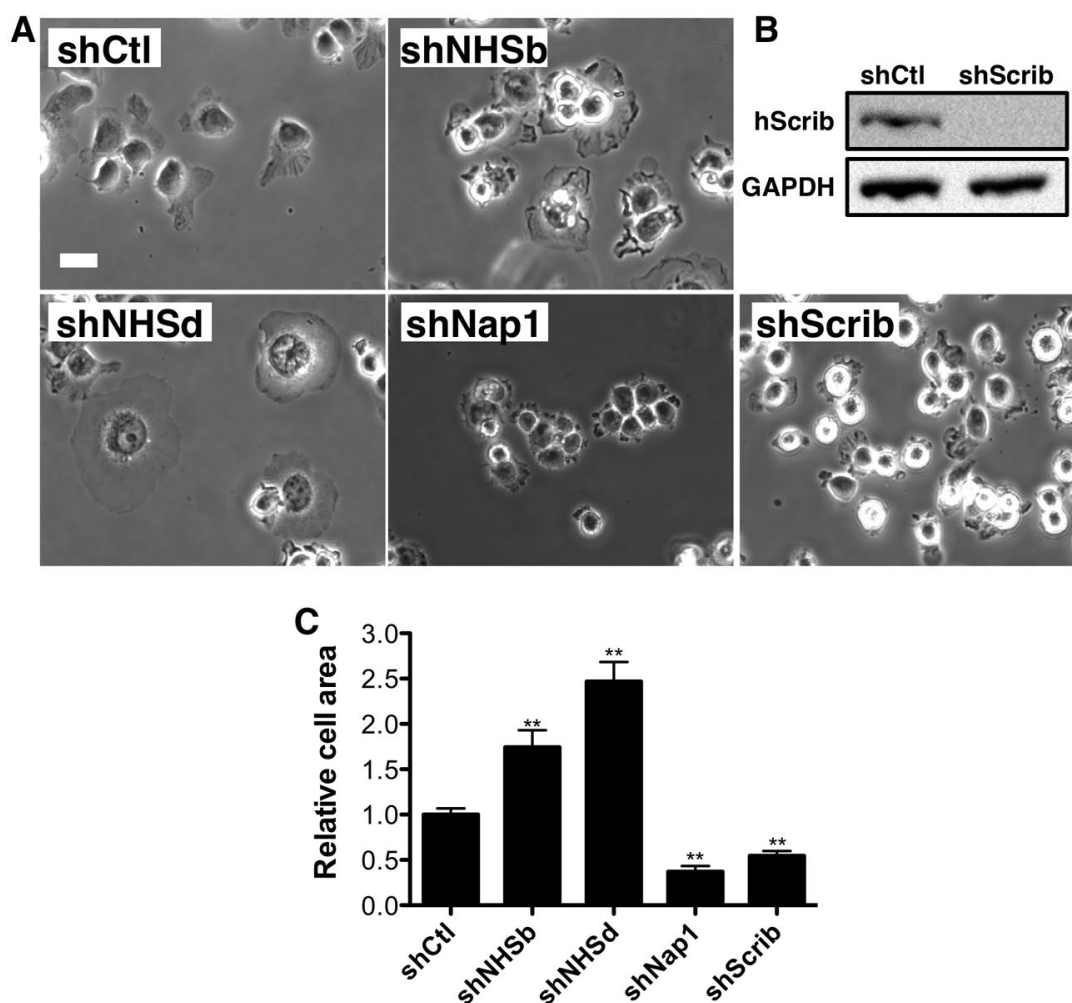


Figure 7.7 Loss of NHS promotes spreading on collagen

(A) Phase contrast micrographs of control and various stable cells lines as indicated during spreading on collagen coated glass bottom dishes. Scale bar 50 μ m. (B) Western blot showing hScrib level in control and stable hScrib KD cells (shScrib). (C) Quantification of the relative cell area in A. (Data are means \pm SEM, n=22, **p<0.01). All panels show MCF7 cells

Localization of WRC was subsequently studied in NHS stable knockdown cell lines during spreading on collagen. In control cells, WRC, as labelled by Abi1 and Scar2 staining, localized specifically to the leading edge of polarised lamellipodia. WRC however localized around NHS KD cells with little polarisation. In contrast, little localization of WRC was observed in hScrib KD cells (**Figure 7.8**). Collectively, loss of NHS may permit WRC mediated membrane extension, while loss of hScrib reduced WRC mediated membrane extension.

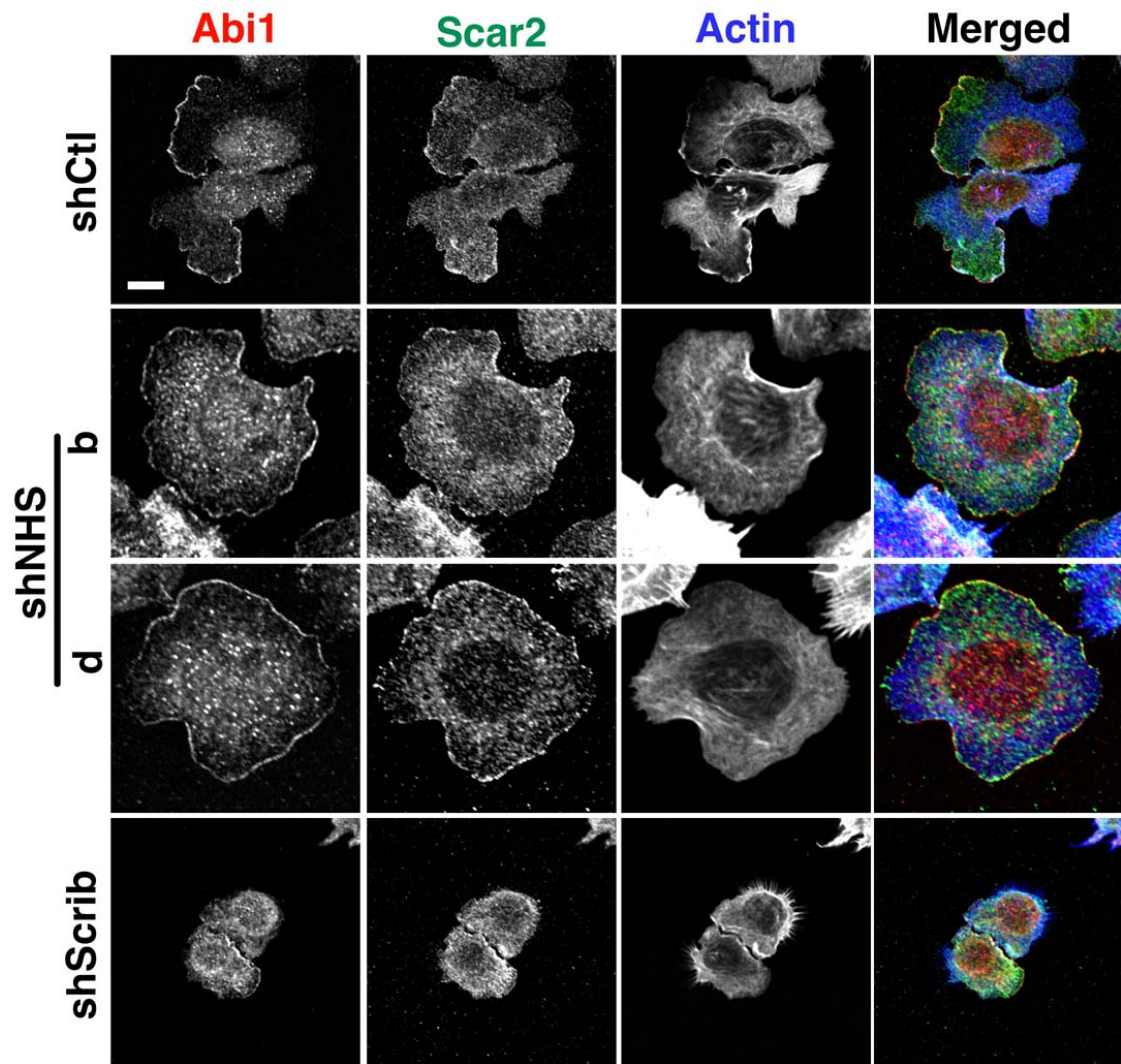


Figure 7.8 Loss of NHS promotes WRC localization during spreading

Confocal micrographs demonstrate localization of endogenous Abi1 (anti-Abi1, red) and Scar2 (anti-Scar2, green) and filamentous actin (rhodamine phalloidin, red) in control cells and indicated stable knockdown cell lines during spreading. All panels show MCF7 cells. Scale bar 10 μ m.

NHS may regulate WRC activity by modulating Rac1 activation. Indeed, loss of NHS promoted a large increase in Rac1 activation during cell spreading on collagen. In contrast, loss of WRC in MCF7 cells reduced Rac1 activation (consistent with the observation in WRC KD A431 cells) (**Figure 7.9A**). As Rac1 activation reached near maximum 20min after initiation of spreading, Rac1 activation in hScrib KD cells was also tested at the time point. As expected, loss of hScrib suppressed Rac1 activation during spreading (**Figure 7.9B**). NHS is thus concluded to negatively regulate Rac1 activation, possibly by suppressing hScrib/ β PIX function.

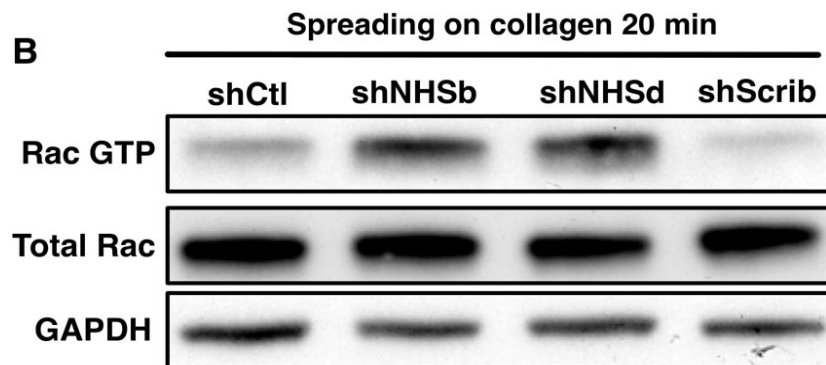
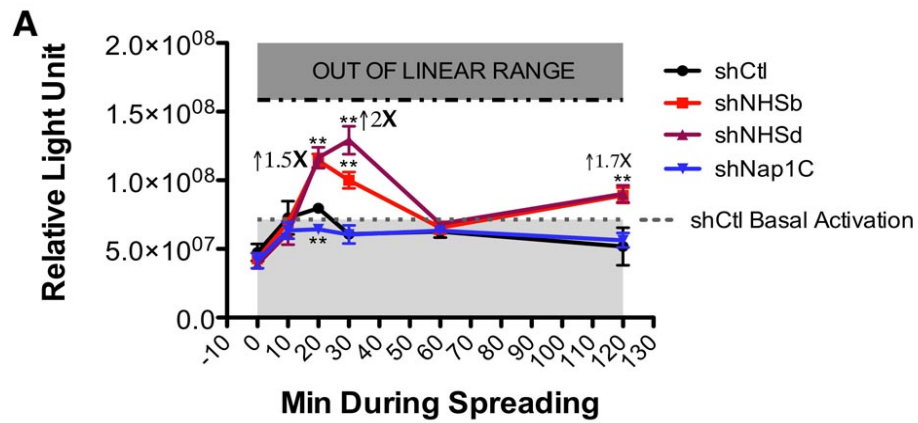


Figure 7.9 Loss of NHS promotes Rac1 activation

(A) Rac1 activation status in control (shCtl) and NHS KD cells during spreading on collagen at indicated time points. (Data are shown as means \pm SEM, n=3 experiments at each time point, **p<0.01). (B) Western blots of PAK1-PBD effector domain pull-down assay showing Rac1 activation 20min upon spreading on collagen of NHS and hScrb stable knockdown cell lines. All panels show MCF7 cells.

7.3 Discussion

NHS is the first non-Scar protein identified to have WHD expressed by human cells. During *NHS* gene identification, two paralogous genes namely *NHS-like1&2* (NHSL1&2) were so identified (Brooks et al., 2004, Brooks et al., 2010). NHSL proteins also contain WHD, so the three NHS proteins are classified as members of the new NHS protein family (Brooks et al., 2010). The presence of WHD and the lack of VCA on these proteins initiated the idea of NHS being a negative regulator of WRC by forming non-functional 'WRC' like complexes. Although a direct interaction between NHS WHD and HSPC300 was identified, and interactions with other WRC subunits were also confirmed (**Figure 7.2A**), the existence of NHS centered 'WRC' like complex remains uncertain. NHS is a large protein (~160 KD). The putative WRC like 'NHS complex' should be about 100 KD larger than WRC when resolved using a NativePAGE. When an HSPC300 antibody or an Sra1 antibody was used as a probe, the only complex identified was WRC on the NativePAGE (Chapter 3 and **Figure 7.2B**). Therefore, 'NHS complex' may not exist in vivo. Alternatively, protein expression level of NHS might be low in tested cells lines, so 'NHS complex' was too little to detect. Only WRC was revealed on NativePAGE even when NHS was over expressed, while over expressed NHS-1A perhaps forms large unstable complexes (smearing blot) without WRC components. Collectively, NHS may not negatively regulate WRC by competing for WRC subunits and forming a defective WRC like complex.

NHS-1A localized to leading edges of lamellipodia and cell-cell junctions. NHS WHD is required for NHS-1A localization to cell-cell junctions and possibly for leading edge localization as well, as loss of WHD renders NHS-1A cytoplasmic (Sharma et al., 2008). However loss of WRC did not stop NHS-1A localizing to cell-cell junctions (**Figure 7.5**), the interaction between WRC and NHS WHD therefore is not required for junction localization. Given the large size of NHS WHD (219 aa vs 116aa of Scar2 WHD), other unidentified protein-protein interactions could lead to NHS-1A junction localization.

Like GUKH the *Drosophila* ortholog, NHS also interacted with hScrib and hDlg (**Figure 7.2A**). Unlike *Drosophila* Scribble, hScrib localization to cell-cell junction was not NHS dependent, and the over all structure of cell-cell junctions remained

intact without NHS (**Figure 7.6**). NHS is thus concluded to have minimum functions on cell-cell junctions despite interactions with WRC, hScrib and hDlg.

Loss of NHS however promoted cell spreading on collagen. With reduced NHS expression, cells generated large lamellipodia with WRC decorating the edge. Further investigation revealed that NHS negatively regulated Rac1 activation during spreading. As hScrib was required for cell spreading and Rac1 activation (**Figure 7.7&7.9**), NHS could use the interaction with hScrib to control Rac1 activation. hScrib anchors β PIX to plasma membrane to promote Rac1 activation (Audebert et al., 2004). It is possible that WRC is activated as a result of hScrib/ β PIX mediated Rac1 activation, as loss of hScrib prevented membrane extension and Rac1 activation (**Figure 7.8**). Although further investigation is required, NHS may interfere with hScrib/ β PIX binding leading to disruption of β PIX membrane localization hence reduced Rac1 activation.

As a result, the functional significance of NHS-WRC interaction and NHS-hScrib interaction requires further investigation, but NHS can negatively regulate WRC through Rac1.

Chapter 8: Summary and future directions

8.1 Summary

Localization of WRC at the leading edge of lamellipodia was demonstrated using multiple fluorescent probes (**Chapter 3**). Loss of WRC resulted in defects in lamellipodia formation, and migration defects on rigid substrates highlighting the important role of WRC in 2D planar cell migration. However when cell motility was tested in multiple 3D collagen gel or Matrigel based invasion assays, WRC surprisingly suppressed cell invasion (**Chapter 4**). Further Investigations revealed that loss of WRC promoted N-WASP/Arp2/3 complex activity in 3D collagen gels leading to N-WASP mediated invasion. I therefore discovered that the two major actin assembly promoting proteins WRC and N-WASP play opposing roles in 3D epithelial cell migration.

Loss of WRC altered focal adhesion structure and dynamics leading to high FAK activation (**Chapter 5**). Interestingly, N-WASP/Arp2/3 activity and invasion was FAK dependent, and active FAK co-localized with N-WASP at the invasive cell front in 3D. As active FAK interacts directly with N-WASP and enhances N-WASP activation, FAK can promote N-WASP activity leading to enhanced cell motility in 3D without WRC. Active FAK also promoted matrix degradation via degradative focal adhesions providing an additional mechanism for the invasive phenotype displayed by cells without WRC. Unexpectedly, WRC disruption promoted FAK dependent cell transformation and tumour formation in vivo. Consequently, WRC is an important check on FAK activity in 3D. Loss of WRC promotes FAK mediated invasion and cell transformation.

Since loss of WRC promoted N-WASP dependent invasion, the interplay between the two proteins was explored. Surprisingly, free HSPC300 was required for N-WASP mediated invasion independently of WRC, and HSPC300 was able to interact with N-WASP (**Chapter 6**). During WRC formation, HSPC300 is cooperated to the center of the complex, so its interaction with N-WASP would be unfavorable. Additionally as HSPC300 homotrimers are templates for WRC assembly, in normal cells, HSPC300 would prefer WRC formation. It is therefore possible that loss of WRC releases HSPC300 to interact with N-WASP hence promoting N-WASP activity and invasion in 3D.

A putative negative regulator of WRC was also investigated in this thesis. NHS is a recently identified WHD containing protein that lacks VCA. It is proposed that NHS can negatively regulate WRC by competing for WRC subunits. However my data suggests an indirect mechanism where NHS suppresses Rac1 activation leading to reduced WRC activation (**Chapter 7**).

8.2 Future directions

N-WASP is activated by Cdc42 (Kolluri et al., 1996) or Rac1 (Tomasevic et al., 2007). Enrichment of N-WASP and Arp2/3 complex at the invasive pseudopods of cells invading in 3D collagen gel indicates specific activation of N-WASP. Although there is no global change on Cdc42 activation upon loss of WRC (**Figure 4.19B**), it is necessary to test Cdc42 activation status at the invasive pseudopods using a biosensor. In WRC depleted cells, Cdc42 could be locally activated at invasive pseudopods leading to N-WASP activation. Likewise, localized Rac1 activation also needs to be tested at the invasive pseudopods, although local Rac1 activation is most likely reduced due to the global reduction of Rac1 activation in cells without WRC (**Figure 4.19A**).

Loss of WRC promoted FAK activation in a number of cell types. FAK over expression and activation is involved in cancer (McLean et al., 2005). Expression of a WRC subunit, Sra1, is also reduced in human epithelial cancers (Silva et al., 2009). The data in this thesis support WRC as a tumour suppressor through FAK. However, to further investigate the link between WRC and FAK in cancer, it is necessary to correlate WRC expression with FAK expression/activation in real human epithelial cancers.

HSPC300 is shown to be stable without WRC, and is required for N-WASP mediated invasion. This surprising function puts HSPC300 in a similar position as FAK, which also regulates N-WASP activity in WRC deleted cells. Loss of HSPC300 in RPE1 cells cultured in collagen gel led to heavy reduction of active FAK (pY397FAK) (**Figure 8.1**). Once again this change in FAK activation is in direct contrast to WRC loss induced FAK over activation. Therefore free HSPC300 may control FAK activation when WRC is absent providing a molecular link

between FAK and WRC. Mouse embryos lacking HSPC300 are known to have apoptotic cells, and HSPC300 loss suppresses cell transformation perhaps due to low FAK activation in these cells (Escobar et al., 2010). Although the theory needs to be further tested, HSPC300 may play a role in FAK activation hence cell transformation and tumorigenesis.

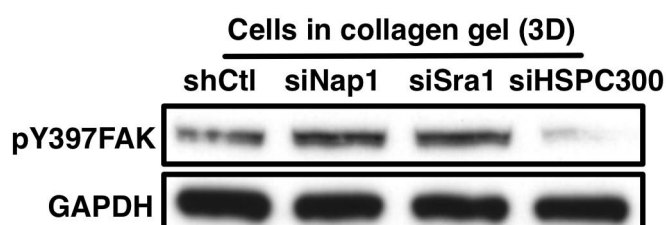


Figure 8.1 HSPC300 is required for FAK activation

Western blot showing reduced pY397FAK level upon loss of HSPC300 in RPE1 cell.

HSPC300 is required for N-WASP function in the invasive pseudopods. Co-immunoprecipitation shows that HSPC300 can interact with N-WASP (**Figure 6.4**). However it is not clear if this interaction is direct. For further investigations, it is essential to address this question using purified proteins. In addition, the potential N-WASP activating ability of HSPC300 may also be tested using purified proteins in an actin polymerization assay.

Finally, NHS negatively regulates Rac1 activation in tested cells (**Figure 7.9**), but the mechanism is not clear. Due to the interaction with hScrib, I propose NHS regulates Rac1 activation through negative regulation of hScrib/ β PIX complex. β PIX is recently reported to activate Rac1 at nascent adhesions promoting lamellipodia formation and to prevent adhesion maturation (Kuo et al., 2011). Over expression of β PIX results in reduced focal adhesion size, while loss of β PIX increases focal adhesion size (Kuo et al., 2011). Interestingly, in addition to high Rac1 activation, loss of NHS also resulted in loss of focal adhesions, a phenotype that resembles β PIX over expression (**Figure 8.2**). This preliminary data reinforces the idea of NHS being a negative regulator of β PIX. Although the interaction between NHS and hScrib can be detected using co-immunoprecipitation, the interaction needs to be verified using purified proteins. Likewise, the interaction of NHS with β PIX needs to be identified.

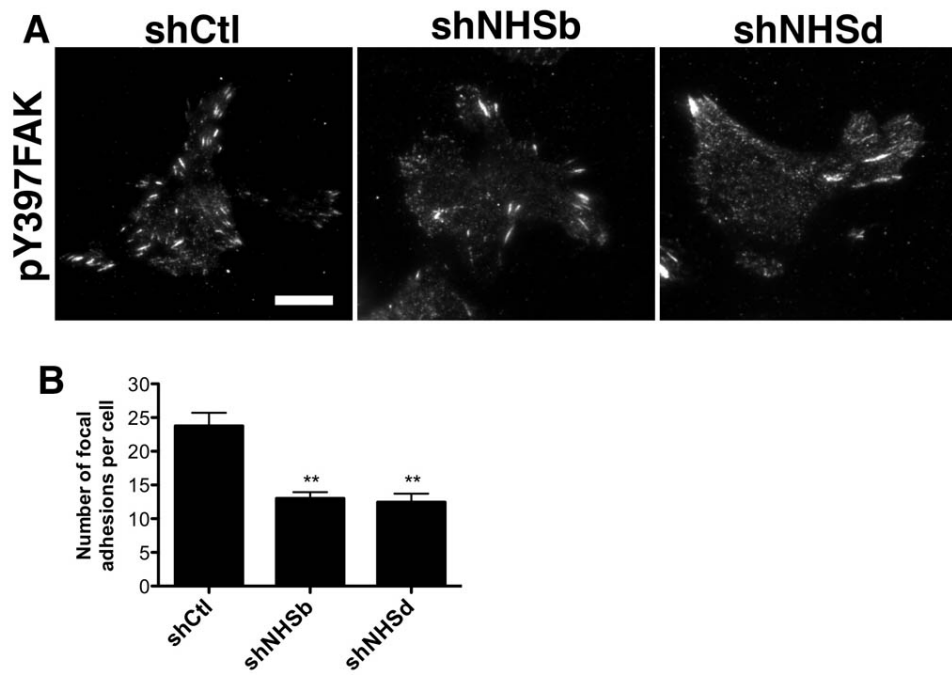


Figure 8.2 Loss of NHS reduces focal adhesions

(A) TIRF micrographs showing reduction of focal adhesion (pY397FAK) numbers in NHS depleted MCF7 cells. Scale bar 10 μ m. (B) Quantification of A. (Data are shown as means \pm SEM, n=30, **p<0.01).

8.3 Conclusions

To conclude, I addressed the aims of this thesis by revealing the novel role of WRC as an invasion suppressor in 3D. I demonstrated a FAK/N-WASP/Arp2/3 complex mediated invasion mechanism and a previously unknown function of free HSPC300 in cell invasion. I therefore conclude that loss of WRC activates FAK and releases HSPC300 leading to enhanced N-WASP activity and invasion. Through FAK, WRC also controls matrix degradation, cell transformation and tumor formation, while NHS suppresses WRC by negatively regulating Rac1 activation. Collectively WRC is concluded to exert potential tumor suppressor function/activity (**Figure 8.3**).

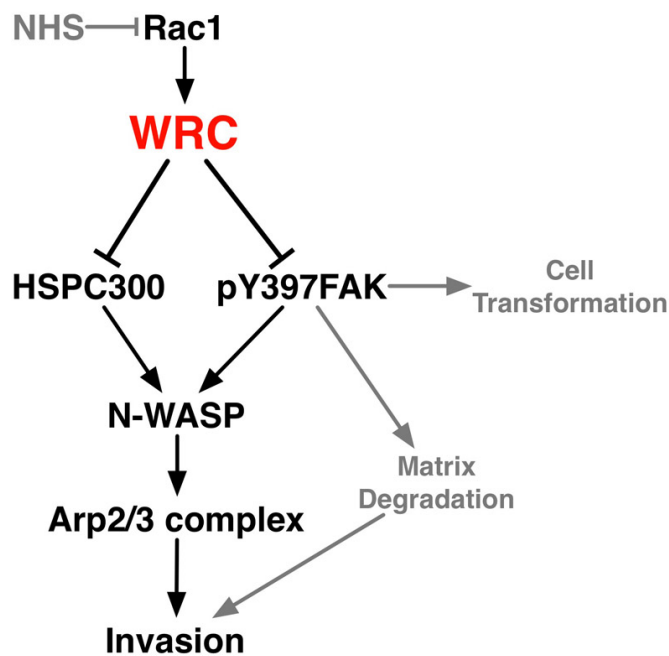


Figure 8.3 Graphic summary

Schematic diagram summarizing major findings in this thesis. While NHS negatively regulates WRC through suppression of Rac1 activation, loss of WRC promotes N-WASP dependent cell invasion by FAK over activation and releasing of free HSPC300. Active FAK also contributes to matrix degradation and cell transformation.

Chapter 9: References

- ANITEI, M., STANGE, C., PARSHINA, I., BAUST, T., SCHENCK, A., RAPOSO, G., KIRCHHAUSEN, T. & HOFACK, B. 2010. Protein complexes containing CYFIP/Sra/PIR121 coordinate Arf1 and Rac1 signalling during clathrin-AP-1-coated carrier biogenesis at the TGN. *Nat Cell Biol*, 12, 330-40.
- ARTYM, V. V., ZHANG, Y., SEILLIER-MOISEWITSCH, F., YAMADA, K. M. & MUELLER, S. C. 2006. Dynamic interactions of cortactin and membrane type 1 matrix metalloproteinase at invadopodia: defining the stages of invadopodia formation and function. *Cancer Res*, 66, 3034-43.
- ASHTON, G. H., MORTON, J. P., MYANT, K., PHESSÉ, T. J., RIDGWAY, R. A., MARSH, V., WILKINS, J. A., ATHINEOS, D., MUNCAN, V., KEMP, R., NEUFELD, K., CLEVERS, H., BRUNTON, V., WINTON, D. J., WANG, X., SEARS, R. C., CLARKE, A. R., FRAME, M. C. & SANSOM, O. J. 2010. Focal adhesion kinase is required for intestinal regeneration and tumorigenesis downstream of Wnt/c-Myc signaling. *Dev Cell*, 19, 259-69.
- AUDEBERT, S., NAVARRO, C., NOURRY, C., CHASSEROT-GOLAZ, S., LECINE, P., BELLAICHE, Y., DUPONT, J. L., PREMONT, R. T., SEMPÈRE, C., STRUB, J. M., VAN DORSSELAER, A., VITALE, N. & BORG, J. P. 2004. Mammalian Scribble forms a tight complex with the betaPIX exchange factor. *Curr Biol*, 14, 987-95.
- BALABAN, N. Q., SCHWARZ, U. S., RIVELINE, D., GOICHBURG, P., TZUR, G., SABANAY, I., MAHALU, D., SAFRAN, S., BERSHADSKY, A., ADDADI, L. & GEIGER, B. 2001. Force and focal adhesion assembly: a close relationship studied using elastic micropatterned substrates. *Nat Cell Biol*, 3, 466-72.
- BANIN, S., TRUONG, O., KATZ, D. R., WATERFIELD, M. D., BRICKELL, P. M. & GOUT, I. 1996. Wiskott-Aldrich syndrome protein (WASP) is a binding partner for c-Src family protein-tyrosine kinases. *Curr Biol*, 6, 981-8.
- BANNO, A. & GINSBERG, M. H. 2008. Integrin activation. *Biochem Soc Trans*, 36, 229-34.
- BASS, M. D., ROACH, K. A., MORGAN, M. R., MOSTAFAVI-POUR, Z., SCHOEN, T., MURAMATSU, T., MAYER, U., BALLESTREM, C., SPATZ, J. P. & HUMPHRIES, M. J. 2007. Syndecan-4-dependent Rac1 regulation determines directional migration in response to the extracellular matrix. *J Cell Biol*, 177, 527-38.
- BEGLOVA, N., BLACKLOW, S. C., TAKAGI, J. & SPRINGER, T. A. 2002. Cysteine-rich module structure reveals a fulcrum for integrin rearrangement upon activation. *Nat Struct Biol*, 9, 282-7.
- BENESCH, S., POLO, S., LAI, F. P., ANDERSON, K. I., STRADAL, T. E., WEHLAND, J. & ROTTNER, K. 2005. N-WASP deficiency impairs EGF internalization and actin assembly at clathrin-coated pits. *J Cell Sci*, 118, 3103-15.
- BENINGO, K. A., DEMBO, M., KAVERINA, I., SMALL, J. V. & WANG, Y. L. 2001. Nascent focal adhesions are responsible for the generation of strong propulsive forces in migrating fibroblasts. *J Cell Biol*, 153, 881-8.
- BERGERT, M., CHANDRADOSS, S. D., DESAI, R. A. & PALUCH, E. 2012. Cell mechanics control rapid transitions between blebs and lamellipodia during migration. *Proc Natl Acad Sci U S A*, 109, 14434-9.
- BLASER, H., REICHMAN-FRIED, M., CASTANON, I., DUMSTREI, K., MARLOW, F. L., KAWAKAMI, K., SOLNICA-KREZEL, L., HEISENBERG, C. P. & RAZ, E. 2006. Migration of zebrafish primordial germ cells: a role for myosin contraction and cytoplasmic flow. *Dev Cell*, 11, 613-27.
- BOCZKOWSKA, M., REBOWSKI, G., PETOUKHOV, M. V., HAYES, D. B., SVERGUN, D. I. & DOMINGUEZ, R. 2008. X-ray scattering study of activated Arp2/3 complex with bound actin-WCA. *Structure*, 16, 695-704.

- BORM, B., REQUARDT, R. P., HERZOG, V. & KIRFEL, G. 2005. Membrane ruffles in cell migration: indicators of inefficient lamellipodia adhesion and compartments of actin filament reorganization. *Exp Cell Res*, 302, 83-95.
- BOUCHARD, V., DEMERS, M. J., THIBODEAU, S., LAQUERRE, V., FUJITA, N., TSURUO, T., BEAULIEU, J. F., GAUTHIER, R., VEZINA, A., VILLENEUVE, L. & VACHON, P. H. 2007. Fak/Src signaling in human intestinal epithelial cell survival and anoikis: differentiation state-specific uncoupling with the PI3-K/Akt-1 and MEK/Erk pathways. *J Cell Physiol*, 212, 717-28.
- BOULAY, P. L., COTTON, M., MELANCON, P. & CLAING, A. 2008. ADP-ribosylation factor 1 controls the activation of the phosphatidylinositol 3-kinase pathway to regulate epidermal growth factor-dependent growth and migration of breast cancer cells. *J Biol Chem*, 283, 36425-34.
- BRONNER-FRASER, M. 1994. Neural crest cell formation and migration in the developing embryo. *FASEB J*, 8, 699-706.
- BROOKS, S. P., COCCIA, M., TANG, H. R., KANUGA, N., MACHESKY, L. M., BAILLY, M., CHEETHAM, M. E. & HARDCASTLE, A. J. 2010. The Nance-Horan syndrome protein encodes a functional WAVE homology domain (WHD) and is important for co-ordinating actin remodelling and maintaining cell morphology. *Hum Mol Genet*, 19, 2421-32.
- BROOKS, S. P., EBENEZER, N. D., POOPALASUNDARAM, S., LEHMANN, O. J., MOORE, A. T. & HARDCASTLE, A. J. 2004. Identification of the gene for Nance-Horan syndrome (NHS). *J Med Genet*, 41, 768-71.
- BRUNTON, V. G. & FRAME, M. C. 2008. Src and focal adhesion kinase as therapeutic targets in cancer. *Curr Opin Pharmacol*, 8, 427-32.
- BUCCIONE, R., ORTH, J. D. & MCNIVEN, M. A. 2004. Foot and mouth: podosomes, invadopodia and circular dorsal ruffles. *Nat Rev Mol Cell Biol*, 5, 647-57.
- BUGYI, B. & CARLIER, M. F. 2010. Control of actin filament treadmilling in cell motility. *Annu Rev Biophys*, 39, 449-70.
- BURDON, K. P., MCKAY, J. D., SALE, M. M., RUSSELL-EGGITT, I. M., MACKEY, D. A., WIRTH, M. G., ELDER, J. E., NICOLL, A., CLARKE, M. P., FITZGERALD, L. M., STANKOVICH, J. M., SHAW, M. A., SHARMA, S., GAJOVIC, S., GRUSS, P., ROSS, S., THOMAS, P., VOSS, A. K., THOMAS, T., GECZ, J. & CRAIG, J. E. 2003. Mutations in a novel gene, NHS, cause the pleiotropic effects of Nance-Horan syndrome, including severe congenital cataract, dental anomalies, and mental retardation. *Am J Hum Genet*, 73, 1120-30.
- CAI, X., XIAO, T., JAMES, S. Y., DA, J., LIN, D., LIU, Y., ZHENG, Y., ZOU, S., DI, X., GUO, S., HAN, N., LU, Y. J., CHENG, S., GAO, Y. & ZHANG, K. 2009. Metastatic potential of lung squamous cell carcinoma associated with HSPC300 through its interaction with WAVE2. *Lung Cancer*, 65, 299-305.
- CALALB, M. B., ZHANG, X., POLTE, T. R. & HANKS, S. K. 1996. Focal adhesion kinase tyrosine-861 is a major site of phosphorylation by Src. *Biochem Biophys Res Commun*, 228, 662-8.
- CAMPELLONE, K. G. & WELCH, M. D. 2010. A nucleator arms race: cellular control of actin assembly. *Nat Rev Mol Cell Biol*, 11, 237-51.
- CANTLEY, L. C. 2002. The phosphoinositide 3-kinase pathway. *Science*, 296, 1655-7.
- CARMAN, C. V. & SPRINGER, T. A. 2003. Integrin avidity regulation: are changes in affinity and conformation underemphasized? *Curr Opin Cell Biol*, 15, 547-56.
- CASCON, A., ESCOBAR, B., MONTERO-CONDE, C., RODRIGUEZ-ANTONA, C., RUIZ-LLORENTE, S., OSORIO, A., MERCADILLO, F., LETON, R., CAMPOS, J. M., GARCIA-SAGREDO, J. M., BENITEZ, J., MALUMBRES, M. & ROBLEDO, M. 2007. Loss of the actin regulator HSPC300 results in clear cell renal cell carcinoma protection in Von Hippel-Lindau patients. *Hum Mutat*, 28, 613-21.

- CASWELL, P. T., SPENCE, H. J., PARSONS, M., WHITE, D. P., CLARK, K., CHENG, K. W., MILLS, G. B., HUMPHRIES, M. J., MESSENT, A. J., ANDERSON, K. I., MCCAFFREY, M. W., OZANNE, B. W. & NORMAN, J. C. 2007. Rab25 associates with alpha5beta1 integrin to promote invasive migration in 3D microenvironments. *Dev Cell*, 13, 496-510.
- CHARRAS, G. T., YARROW, J. C., HORTON, M. A., MAHADEVAN, L. & MITCHISON, T. J. 2005. Non-equilibration of hydrostatic pressure in blebbing cells. *Nature*, 435, 365-9.
- CHEN, H. C. & GUAN, J. L. 1994. Association of focal adhesion kinase with its potential substrate phosphatidylinositol 3-kinase. *Proc Natl Acad Sci U S A*, 91, 10148-52.
- CHEN, Z., BOREK, D., PADRICK, S. B., GOMEZ, T. S., METLAGEL, Z., ISMAIL, A. M., UMETANI, J., BILLADEAU, D. D., OTWINOWSKI, Z. & ROSEN, M. K. 2010. Structure and control of the actin regulatory WAVE complex. *Nature*, 468, 533-8.
- CHOI, C. K., VICENTE-MANZANARES, M., ZARENO, J., WHITMORE, L. A., MOGILNER, A. & HORWITZ, A. R. 2008. Actin and alpha-actinin orchestrate the assembly and maturation of nascent adhesions in a myosin II motor-independent manner. *Nat Cell Biol*, 10, 1039-50.
- CORY, G. O., GARG, R., CRAMER, R. & RIDLEY, A. J. 2002. Phosphorylation of tyrosine 291 enhances the ability of WASp to stimulate actin polymerization and filopodium formation. Wiskott-Aldrich Syndrome protein. *J Biol Chem*, 277, 45115-21.
- COTE, J. F. & VUORI, K. 2007. GEF what? Dock180 and related proteins help Rac to polarize cells in new ways. *Trends Cell Biol*, 17, 383-93.
- CUEVAS, B. D., LU, Y., MAO, M., ZHANG, J., LAPUSHIN, R., SIMINOVITCH, K. & MILLS, G. B. 2001. Tyrosine phosphorylation of p85 relieves its inhibitory activity on phosphatidylinositol 3-kinase. *J Biol Chem*, 276, 27455-61.
- CUKIERMAN, E., PANKOV, R., STEVENS, D. R. & YAMADA, K. M. 2001. Taking cell-matrix adhesions to the third dimension. *Science*, 294, 1708-12.
- CUNNINGHAM, C. C. 1995. Actin polymerization and intracellular solvent flow in cell surface blebbing. *J Cell Biol*, 129, 1589-99.
- CUNNINGHAM, C. C., GORLIN, J. B., KWIATKOWSKI, D. J., HARTWIG, J. H., JANMEY, P. A., BYERS, H. R. & STOSSEL, T. P. 1992. Actin-binding protein requirement for cortical stability and efficient locomotion. *Science*, 255, 325-7.
- CUNNINGHAM-EDMONDSON, A. C. & HANKS, S. K. 2009. p130Cas substrate domain signaling promotes migration, invasion, and survival of estrogen receptor-negative breast cancer cells. *Breast Cancer (London)*, 2009, 39-52.
- DAHL, J. P., WANG-DUNLOP, J., GONZALES, C., GOAD, M. E., MARK, R. J. & KWAK, S. P. 2003. Characterization of the WAVE1 knock-out mouse: implications for CNS development. *J Neurosci*, 23, 3343-52.
- DAI, Z. & PENDERGAST, A. M. 1995. Abi-2, a novel SH3-containing protein interacts with the c-Abl tyrosine kinase and modulates c-Abl transforming activity. *Genes Dev*, 9, 2569-82.
- DAVIDSON, A. J. & INSALL, R. H. 2011. Actin-based motility: WAVE regulatory complex structure reopens old SCARs. *Curr Biol*, 21, R66-8.
- DEMALI, K. A., BARLOW, C. A. & BURRIDGE, K. 2002. Recruitment of the Arp2/3 complex to vinculin: coupling membrane protrusion to matrix adhesion. *J Cell Biol*, 159, 881-91.
- DEMALI, K. A. & BURRIDGE, K. 2003. Coupling membrane protrusion and cell adhesion. *J Cell Sci*, 116, 2389-97.

- DERIVERY, E., FINK, J., MARTIN, D., HOUDUSSE, A., PIEL, M., STRADAL, T. E., LOUVARD, D. & GAUTREAU, A. 2008. Free Brick1 is a trimeric precursor in the assembly of a functional wave complex. *PLoS One*, 3, e2462.
- DERRY, J. M., OCHS, H. D. & FRANCKE, U. 1994. Isolation of a novel gene mutated in Wiskott-Aldrich syndrome. *Cell*, 79, following 922.
- DESMARAIS, V., YAMAGUCHI, H., OSER, M., SOON, L., MOUNEIMNE, G., SARMIENTO, C., EDDY, R. & CONDEELIS, J. 2009. N-WASP and cortactin are involved in invadopodium-dependent chemotaxis to EGF in breast tumor cells. *Cell Motil Cytoskeleton*, 66, 303-16.
- DION, V., SHIMADA, K. & GASSER, S. M. 2010. Actin-related proteins in the nucleus: life beyond chromatin remodelers. *Curr Opin Cell Biol*, 22, 383-91.
- DJAKOVIC, S., DYACHOK, J., BURKE, M., FRANK, M. J. & SMITH, L. G. 2006. BRICK1/HSPC300 functions with SCAR and the ARP2/3 complex to regulate epidermal cell shape in Arabidopsis. *Development*, 133, 1091-100.
- DODDING, M. P. & WAY, M. 2009. Nck- and N-WASP-dependent actin-based motility is conserved in divergent vertebrate poxviruses. *Cell Host Microbe*, 6, 536-50.
- DOEHN, U., HAUGE, C., FRANK, S. R., JENSEN, C. J., DUDA, K., NIELSEN, J. V., COHEN, M. S., JOHANSEN, J. V., WINTHER, B. R., LUND, L. R., WINTHER, O., TAUNTON, J., HANSEN, S. H. & FRODIN, M. 2009. RSK is a principal effector of the RAS-ERK pathway for eliciting a coordinate promotile/invasive gene program and phenotype in epithelial cells. *Mol Cell*, 35, 511-22.
- DOW, L. E., BRUMBY, A. M., MURATORE, R., COOMBE, M. L., SEDELIES, K. A., TRAPANI, J. A., RUSSELL, S. M., RICHARDSON, H. E. & HUMBERT, P. O. 2003. hScrib is a functional homologue of the Drosophila tumour suppressor Scribble. *Oncogene*, 22, 9225-30.
- DUBAND, J. L. 2010. Diversity in the molecular and cellular strategies of epithelium-to-mesenchyme transitions: Insights from the neural crest. *Cell Adh Migr*, 4, 458-82.
- DUBIELECKA, P. M., LADWEIN, K. I., XIONG, X., MIGEOTTE, I., CHORZALSKA, A., ANDERSON, K. V., SAWICKI, J. A., ROTTNER, K., STRADAL, T. E. & KOTULA, L. 2011. Essential role for Abi1 in embryonic survival and WAVE2 complex integrity. *Proc Natl Acad Sci U S A*, 108, 7022-7.
- EDEN, S., ROHATGI, R., PODTELEJNIKOV, A. V., MANN, M. & KIRSCHNER, M. W. 2002. Mechanism of regulation of WAVE1-induced actin nucleation by Rac1 and Nck. *Nature*, 418, 790-3.
- EHRBAR, M., SALA, A., LIENEMANN, P., RANGA, A., MOSIEWICZ, K., BITTERMANN, A., RIZZI, S. C., WEBER, F. E. & LUTOLF, M. P. 2011. Elucidating the role of matrix stiffness in 3D cell migration and remodeling. *Biophys J*, 100, 284-93.
- ENOMOTO, A., MURAKAMI, H., ASAI, N., MORONE, N., WATANABE, T., KAWAI, K., MURAKUMO, Y., USUKURA, J., KAIBUCHI, K. & TAKAHASHI, M. 2005. Akt/PKB regulates actin organization and cell motility via Girdin/APE. *Dev Cell*, 9, 389-402.
- ESCOBAR, B., DE CARCER, G., FERNANDEZ-MIRANDA, G., CASCON, A., BRAVO-CORDERO, J. J., MONTOYA, M. C., ROBLEDO, M., CANAMERO, M. & MALUMBRES, M. 2010. Brick1 is an essential regulator of actin cytoskeleton required for embryonic development and cell transformation. *Cancer Res*, 70, 9349-59.
- EZRATTY, E. J., PARTRIDGE, M. A. & GUNDERSEN, G. G. 2005. Microtubule-induced focal adhesion disassembly is mediated by dynamin and focal adhesion kinase. *Nat Cell Biol*, 7, 581-90.
- FACKLER, O. T. & GROSSE, R. 2008. Cell motility through plasma membrane blebbing. *J Cell Biol*, 181, 879-84.

- FRALEY, S. I., FENG, Y., KRISHNAMURTHY, R., KIM, D. H., CELEDON, A., LONGMORE, G. D. & WIRTZ, D. 2010. A distinctive role for focal adhesion proteins in three-dimensional cell motility. *Nat Cell Biol*, 12, 598-604.
- FRAME, M. C., PATEL, H., SERRELS, B., LIETHA, D. & ECK, M. J. 2011. The FERM domain: organizing the structure and function of FAK. *Nat Rev Mol Cell Biol*, 11, 802-14.
- FRANKE, T. F., HORNIK, C. P., SEGEV, L., SHOSTAK, G. A. & SUGIMOTO, C. 2003. PI3K/Akt and apoptosis: size matters. *Oncogene*, 22, 8983-98.
- FRIEDL, P. & GILMOUR, D. 2009. Collective cell migration in morphogenesis, regeneration and cancer. *Nat Rev Mol Cell Biol*, 10, 445-57.
- FRIEDL, P. & WOLF, K. 2003. Tumour-cell invasion and migration: diversity and escape mechanisms. *Nat Rev Cancer*, 3, 362-74.
- FRIEDL, P. & WOLF, K. 2009. Proteolytic interstitial cell migration: a five-step process. *Cancer Metastasis Rev*, 28, 129-35.
- FRISCH, S. M. & FRANCIS, H. 1994. Disruption of epithelial cell-matrix interactions induces apoptosis. *J Cell Biol*, 124, 619-26.
- FRISCH, S. M., VUORI, K., RUOSLAHTI, E. & CHAN-HUI, P. Y. 1996. Control of adhesion-dependent cell survival by focal adhesion kinase. *J Cell Biol*, 134, 793-9.
- FUKUNAGA, R. & HUNTER, T. 1997. MNK1, a new MAP kinase-activated protein kinase, isolated by a novel expression screening method for identifying protein kinase substrates. *EMBO J*, 16, 1921-33.
- GARDIOL, D., ZACCHI, A., PETRERA, F., STANTA, G. & BANKS, L. 2006. Human discs large and scrib are localized at the same regions in colon mucosa and changes in their expression patterns are correlated with loss of tissue architecture during malignant progression. *Int J Cancer*, 119, 1285-90.
- GAWDEN-BONE, C., ZHOU, Z., KING, E., PRESCOTT, A., WATTS, C. & LUCOCQ, J. 2010. Dendritic cell podosomes are protrusive and invade the extracellular matrix using metalloproteinase MMP-14. *J Cell Sci*, 123, 1427-37.
- GERISCH, G., BRETSCHNEIDER, T., MULLER-TAUBENBERGER, A., SIMMETH, E., ECKE, M., DIEZ, S. & ANDERSON, K. 2004. Mobile actin clusters and traveling waves in cells recovering from actin depolymerization. *Biophys J*, 87, 3493-503.
- GIMONA, M., BUCCIONE, R., COURTNEIDGE, S. A. & LINDER, S. 2008. Assembly and biological role of podosomes and invadopodia. *Curr Opin Cell Biol*, 20, 235-41.
- GINSBERG, M. H., PARTRIDGE, A. & SHATTIL, S. J. 2005. Integrin regulation. *Curr Opin Cell Biol*, 17, 509-16.
- GOHL, C., BANOVIC, D., GREVELHORSTER, A. & BOGDAN, S. 2010. WAVE forms hetero- and homo-oligomeric complexes at integrin junctions in *Drosophila* visualized by bimolecular fluorescence complementation. *J Biol Chem*, 285, 40171-9.
- GUAN, J. L. & SHALLOWAY, D. 1992. Regulation of focal adhesion-associated protein tyrosine kinase by both cellular adhesion and oncogenic transformation. *Nature*, 358, 690-2.
- HAUGE, C. & FRODIN, M. 2006. RSK and MSK in MAP kinase signalling. *J Cell Sci*, 119, 3021-3.
- HEMSATH, L., DVORSKY, R., FIEGEN, D., CARLIER, M. F. & AHMADIAN, M. R. 2005. An electrostatic steering mechanism of Cdc42 recognition by Wiskott-Aldrich syndrome proteins. *Mol Cell*, 20, 313-24.
- HIGGS, H. N. & POLLARD, T. D. 2000. Activation by Cdc42 and PIP(2) of Wiskott-Aldrich syndrome protein (WASp) stimulates actin nucleation by Arp2/3 complex. *J Cell Biol*, 150, 1311-20.
- HOLMES, K. C., POPP, D., GEBHARD, W. & KABSCH, W. 1990. Atomic model of the actin filament. *Nature*, 347, 44-9.

- HOTARY, K., LI, X. Y., ALLEN, E., STEVENS, S. L. & WEISS, S. J. 2006. A cancer cell metalloprotease triad regulates the basement membrane transmigration program. *Genes Dev*, 20, 2673-86.
- HOWE, L. R., LEEVERS, S. J., GOMEZ, N., NAKIELNY, S., COHEN, P. & MARSHALL, C. J. 1992. Activation of the MAP kinase pathway by the protein kinase raf. *Cell*, 71, 335-42.
- IBARRA, N., BLAGG, S. L., VAZQUEZ, F. & INSALL, R. H. 2006. Nap1 regulates Dictyostelium cell motility and adhesion through SCAR-dependent and -independent pathways. *Curr Biol*, 16, 717-22.
- IGISHI, T., FUKUHARA, S., PATEL, V., KATZ, B. Z., YAMADA, K. M. & GUTKIND, J. S. 1999. Divergent signaling pathways link focal adhesion kinase to mitogen-activated protein kinase cascades. Evidence for a role of paxillin in c-Jun NH(2)-terminal kinase activation. *J Biol Chem*, 274, 30738-46.
- INNOCENTI, M., GERBOTH, S., ROTTNER, K., LAI, F. P., HERTZOG, M., STRADAL, T. E., FRITTOLI, E., DIDRY, D., POLO, S., DISANZA, A., BENESCH, S., DI FIORE, P. P., CARLIER, M. F. & SCITA, G. 2005. Abi1 regulates the activity of N-WASP and WAVE in distinct actin-based processes. *Nat Cell Biol*, 7, 969-76.
- INNOCENTI, M., ZUCCONI, A., DISANZA, A., FRITTOLI, E., ARECES, L. B., STEFFEN, A., STRADAL, T. E., DI FIORE, P. P., CARLIER, M. F. & SCITA, G. 2004. Abi1 is essential for the formation and activation of a WAVE2 signalling complex. *Nat Cell Biol*, 6, 319-27.
- ISMAIL, A. M., PADRICK, S. B., CHEN, B., UMETANI, J. & ROSEN, M. K. 2009. The WAVE regulatory complex is inhibited. *Nat Struct Mol Biol*, 16, 561-3.
- KATOH, M. & KATOH, M. 2004. Identification and characterization of human GUKH2 gene in silico. *Int J Oncol*, 24, 1033-8.
- KAVERINA, I., KRYLYSHKINA, O. & SMALL, J. V. 1999. Microtubule targeting of substrate contacts promotes their relaxation and dissociation. *J Cell Biol*, 146, 1033-44.
- KAVERINA, I., ROTTNER, K. & SMALL, J. V. 1998. Targeting, capture, and stabilization of microtubules at early focal adhesions. *J Cell Biol*, 142, 181-90.
- KAVERINA, I., STRADAL, T. E. & GIMONA, M. 2003. Podosome formation in cultured A7r5 vascular smooth muscle cells requires Arp2/3-dependent de-novo actin polymerization at discrete microdomains. *J Cell Sci*, 116, 4915-24.
- KIM, A. S., KAKALIS, L. T., ABDUL-MANAN, N., LIU, G. A. & ROSEN, M. K. 2000. Autoinhibition and activation mechanisms of the Wiskott-Aldrich syndrome protein. *Nature*, 404, 151-8.
- KIM, B., VAN GOLEN, C. M. & FELDMAN, E. L. 2003. Degradation and dephosphorylation of focal adhesion kinase during okadaic acid-induced apoptosis in human neuroblastoma cells. *Neoplasia*, 5, 405-16.
- KIM, D., KIM, S., KOH, H., YOON, S. O., CHUNG, A. S., CHO, K. S. & CHUNG, J. 2001. Akt/PKB promotes cancer cell invasion via increased motility and metalloproteinase production. *FASEB J*, 15, 1953-62.
- KITAMURA, T., KITAMURA, Y., YONEZAWA, K., TOTTY, N. F., GOUT, I., HARA, K., WATERFIELD, M. D., SAKAUE, M., OGAWA, W. & KASUGA, M. 1996. Molecular cloning of p125Nap1, a protein that associates with an SH3 domain of Nck. *Biochem Biophys Res Commun*, 219, 509-14.
- KITAMURA, Y., KITAMURA, T., SAKAUE, H., MAEDA, T., UENO, H., NISHIO, S., OHNO, S., OSADA, S., SAKAUE, M., OGAWA, W. & KASUGA, M. 1997. Interaction of Nck-associated protein 1 with activated GTP-binding protein Rac. *Biochem J*, 322 (Pt 3), 873-8.

- KLIPPEL, A., ESCOBEDO, J. A., HIRANO, M. & WILLIAMS, L. T. 1994. The interaction of small domains between the subunits of phosphatidylinositol 3-kinase determines enzyme activity. *Mol Cell Biol*, 14, 2675-85.
- KOBAYASHI, K., KURODA, S., FUKATA, M., NAKAMURA, T., NAGASE, T., NOMURA, N., MATSUURA, Y., YOSHIDA-KUBOMURA, N., IWAMATSU, A. & KAIBUCHI, K. 1998. p140Sra-1 (specifically Rac1-associated protein) is a novel specific target for Rac1 small GTPase. *J Biol Chem*, 273, 291-5.
- KOCH, T. M., MUNSTER, S., BONAKDAR, N., BUTLER, J. P. & FABRY, B. 2012. 3D Traction forces in cancer cell invasion. *PLoS One*, 7, e33476.
- KOLLURI, R., TOLIAS, K. F., CARPENTER, C. L., ROSEN, F. S. & KIRCHHAUSEN, T. 1996. Direct interaction of the Wiskott-Aldrich syndrome protein with the GTPase Cdc42. *Proc Natl Acad Sci U S A*, 93, 5615-8.
- KORN, E. D., CARLIER, M. F. & PANTALONI, D. 1987. Actin polymerization and ATP hydrolysis. *Science*, 238, 638-44.
- KOROBOVA, F. & SVITKINA, T. 2008. Arp2/3 complex is important for filopodia formation, growth cone motility, and neuritogenesis in neuronal cells. *Mol Biol Cell*, 19, 1561-74.
- KORONAKIS, V., HUME, P. J., HUMPHREYS, D., LIU, T., HORNING, O., JENSEN, O. N. & MCGHIE, E. J. 2011. WAVE regulatory complex activation by cooperating GTPases Arf and Rac1. *Proc Natl Acad Sci U S A*, 108, 14449-54.
- KUBOW, K. E. & HORWITZ, A. R. 2011. Reducing background fluorescence reveals adhesions in 3D matrices. *Nat Cell Biol*, 13, 3-5; author reply 5-7.
- KUNDA, P., CRAIG, G., DOMINGUEZ, V. & BAUM, B. 2003. Abi, Sra1, and Kette control the stability and localization of SCAR/WAVE to regulate the formation of actin-based protrusions. *Curr Biol*, 13, 1867-75.
- KUO, J. C., HAN, X., HSIAO, C. T., YATES, J. R., 3RD & WATERMAN, C. M. 2011. Analysis of the myosin-II-responsive focal adhesion proteome reveals a role for beta-Pix in negative regulation of focal adhesion maturation. *Nat Cell Biol*, 13, 383-93.
- LAI, F. P., SZCZODRAK, M., BLOCK, J., FAIX, J., BREITSPRECHER, D., MANNHERZ, H. G., STRADAL, T. E., DUNN, G. A., SMALL, J. V. & ROTTNER, K. 2008. Arp2/3 complex interactions and actin network turnover in lamellipodia. *EMBO J*, 27, 982-92.
- LE, J., MALLERY, E. L., ZHANG, C., BRANKLE, S. & SZYMANSKI, D. B. 2006. Arabidopsis BRICK1/HSPC300 is an essential WAVE-complex subunit that selectively stabilizes the Arp2/3 activator SCAR2. *Curr Biol*, 16, 895-901.
- LEBENSOHN, A. M. & KIRSCHNER, M. W. 2009. Activation of the WAVE complex by coincident signals controls actin assembly. *Mol Cell*, 36, 512-24.
- LEFEVER, T., PEDERSEN, E., BASSE, A., PAUS, R., QUONDAMATTEO, F., STANLEY, A. C., LANGBEIN, L., WU, X., WEHLAND, J., LOMMEL, S. & BRAKEBUSCH, C. 2010. N-WASP is a novel regulator of hair-follicle cycling that controls antiproliferative TGF{beta} pathways. *J Cell Sci*, 123, 128-40.
- LEGANT, W. R., MILLER, J. S., BLAKELY, B. L., COHEN, D. M., GENIN, G. M. & CHEN, C. S. 2010. Measurement of mechanical tractions exerted by cells in three-dimensional matrices. *Nat Methods*, 7, 969-71.
- LEGATE, K. R., WICKSTROM, S. A. & FASSLER, R. 2009. Genetic and cell biological analysis of integrin outside-in signaling. *Genes Dev*, 23, 397-418.
- LI, A., DAWSON, J. C., FORERO-VARGAS, M., SPENCE, H. J., YU, X., KONIG, I., ANDERSON, K. & MACHESKY, L. M. 2010. The actin-bundling protein fascin stabilizes actin in invadopodia and potentiates protrusive invasion. *Curr Biol*, 20, 339-45.

- LI, A., MA, Y., YU, X., MORT, R. L., LINDSAY, C. R., STEVENSON, D., STRATHDEE, D., INSALL, R. H., CHERNOFF, J., SNAPPER, S. B., JACKSON, I. J., LARUE, L., SANSOM, O. J. & MACHESKY, L. M. 2011. Rac1 drives melanoblast organization during mouse development by orchestrating pseudopod-driven motility and cell-cycle progression. *Dev Cell*, 21, 722-34.
- LI, P., BANJADE, S., CHENG, H. C., KIM, S., CHEN, B., GUO, L., LLAGUNO, M., HOLLINGSWORTH, J. V., KING, D. S., BANANI, S. F., RUSSO, P. S., JIANG, Q. X., NIXON, B. T. & ROSEN, M. K. 2012. Phase transitions in the assembly of multivalent signalling proteins. *Nature*, 483, 336-40.
- LIETHA, D., CAI, X., CECCARELLI, D. F., LI, Y., SCHALLER, M. D. & ECK, M. J. 2007. Structural basis for the autoinhibition of focal adhesion kinase. *Cell*, 129, 1177-87.
- LIM, Y., HAN, I., JEON, J., PARK, H., BAHK, Y. Y. & OH, E. S. 2004. Phosphorylation of focal adhesion kinase at tyrosine 861 is crucial for Ras transformation of fibroblasts. *J Biol Chem*, 279, 29060-5.
- LINDER, S., NELSON, D., WEISS, M. & AEPFELBACHER, M. 1999. Wiskott-Aldrich syndrome protein regulates podosomes in primary human macrophages. *Proc Natl Acad Sci U S A*, 96, 9648-53.
- LINKNER, J., WITTE, G., STRADAL, T., CURTH, U. & FAIX, J. 2011. High-resolution X-ray structure of the trimeric Scar/WAVE-complex precursor Brk1. *PLoS One*, 6, e21327.
- LIU, S., CALDERWOOD, D. A. & GINSBERG, M. H. 2000. Integrin cytoplasmic domain-binding proteins. *J Cell Sci*, 113 (Pt 20), 3563-71.
- MA, Z., LIU, Z., MYERS, D. P. & TERADA, L. S. 2008. Mechanotransduction and anoikis: death and the homeless cell. *Cell Cycle*, 7, 2462-5.
- MACHESKY, L. M., ATKINSON, S. J., AMPE, C., VANDEKERCKHOVE, J. & POLLARD, T. D. 1994. Purification of a cortical complex containing two unconventional actins from *Acanthamoeba* by affinity chromatography on profilin-agarose. *J Cell Biol*, 127, 107-15.
- MACHESKY, L. M. & INSALL, R. H. 1998. Scar1 and the related Wiskott-Aldrich syndrome protein, WASP, regulate the actin cytoskeleton through the Arp2/3 complex. *Curr Biol*, 8, 1347-56.
- MACHESKY, L. M., MULLINS, R. D., HIGGS, H. N., KAISER, D. A., BLANCHOIN, L., MAY, R. C., HALL, M. E. & POLLARD, T. D. 1999. Scar, a WASp-related protein, activates nucleation of actin filaments by the Arp2/3 complex. *Proc Natl Acad Sci U S A*, 96, 3739-44.
- MAEDA, K., NAKATA, T., NODA, Y., SATO-YOSHITAKE, R. & HIROKAWA, N. 1992. Interaction of dynamin with microtubules: its structure and GTPase activity investigated by using highly purified dynamin. *Mol Biol Cell*, 3, 1181-94.
- MARANCHIE, J. K., AFONSO, A., ALBERT, P. S., KALYANDRUG, S., PHILLIPS, J. L., ZHOU, S., PETERSON, J., GHADIMI, B. M., HURLEY, K., RISS, J., VASSELLI, J. R., RIED, T., ZBAR, B., CHOYKE, P., WALTHER, M. M., KLAUSNER, R. D. & LINEHAN, W. M. 2004. Solid renal tumor severity in von Hippel Lindau disease is related to germline deletion length and location. *Hum Mutat*, 23, 40-6.
- MATHEW, D., GRAMATES, L. S., PACKARD, M., THOMAS, U., BILDER, D., PERRIMON, N., GORCZYCA, M. & BUDNIK, V. 2002. Recruitment of scribble to the synaptic scaffolding complex requires GUK-holder, a novel DLG binding protein. *Curr Biol*, 12, 531-9.
- MCLEAN, G. W., CARRAGHER, N. O., AVIZIENYTE, E., EVANS, J., BRUNTON, V. G. & FRAME, M. C. 2005. The role of focal-adhesion kinase in cancer - a new therapeutic opportunity. *Nat Rev Cancer*, 5, 505-15.

- MENDOZA, M. C., ER, E. E., ZHANG, W., BALLIF, B. A., ELLIOTT, H. L., DANUSER, G. & BLENIS, J. 2011. ERK-MAPK drives lamellipodia protrusion by activating the WAVE2 regulatory complex. *Mol Cell*, 41, 661-71.
- MIKI, H., MIURA, K. & TAKENAWA, T. 1996. N-WASP, a novel actin-depolymerizing protein, regulates the cortical cytoskeletal rearrangement in a PIP2-dependent manner downstream of tyrosine kinases. *EMBO J*, 15, 5326-35.
- MIKI, H., SASAKI, T., TAKAI, Y. & TAKENAWA, T. 1998. Induction of filopodium formation by a WASP-related actin-depolymerizing protein N-WASP. *Nature*, 391, 93-6.
- MILLIUS, A., WATANABE, N. & WEINER, O. D. 2012. Diffusion, capture and recycling of SCAR/WAVE and Arp2/3 complexes observed in cells by single-molecule imaging. *J Cell Sci*, 125, 1165-76.
- MILLS, J. C., STONE, N. L., ERHARDT, J. & PITTMAN, R. N. 1998. Apoptotic membrane blebbing is regulated by myosin light chain phosphorylation. *J Cell Biol*, 140, 627-36.
- MITRA, S. K., HANSON, D. A. & SCHLAEPFER, D. D. 2005. Focal adhesion kinase: in command and control of cell motility. *Nat Rev Mol Cell Biol*, 6, 56-68.
- MOGILNER, A. & OSTER, G. 1996. Cell motility driven by actin polymerization. *Biophys J*, 71, 3030-45.
- MOMBOISSE, F., LONCHAMP, E., CALCO, V., CERIDONO, M., VITALE, N., BADER, M. F. & GASMAN, S. 2009. betaPIX-activated Rac1 stimulates the activation of phospholipase D, which is associated with exocytosis in neuroendocrine cells. *J Cell Sci*, 122, 798-806.
- MULLINS, R. D., HEUSER, J. A. & POLLARD, T. D. 1998. The interaction of Arp2/3 complex with actin: nucleation, high affinity pointed end capping, and formation of branching networks of filaments. *Proc Natl Acad Sci U S A*, 95, 6181-6.
- MURPHY, D. A. & COURTNEIDGE, S. A. 2011. The 'ins' and 'outs' of podosomes and invadopodia: characteristics, formation and function. *Nat Rev Mol Cell Biol*, 12, 413-26.
- NAPOLI, I., MERCALDO, V., BOYL, P. P., ELEUTERI, B., ZALFA, F., DE RUBEIS, S., DI MARINO, D., MOHR, E., MASSIMI, M., FALCONI, M., WITKE, W., COSTA-MATTIOLI, M., SONENBERG, N., ACHSEL, T. & BAGNI, C. 2008. The fragile X syndrome protein represses activity-dependent translation through CYFIP1, a new 4E-BP. *Cell*, 134, 1042-54.
- NAVARRO, C., NOLA, S., AUDEBERT, S., SANTONI, M. J., ARSANTO, J. P., GINESTIER, C., MARCHETTO, S., JACQUEMIER, J., ISNARDON, D., LE BIVIC, A., BIRNBAUM, D. & BORG, J. P. 2005. Junctional recruitment of mammalian Scribble relies on E-cadherin engagement. *Oncogene*, 24, 4330-9.
- NEMETHOVA, M., AUINGER, S. & SMALL, J. V. 2008. Building the actin cytoskeleton: filopodia contribute to the construction of contractile bundles in the lamella. *J Cell Biol*, 180, 1233-44.
- NOBES, C. D. & HALL, A. 1995. Rho, rac, and cdc42 GTPases regulate the assembly of multimolecular focal complexes associated with actin stress fibers, lamellipodia, and filopodia. *Cell*, 81, 53-62.
- NOLA, S., SEBBAGH, M., MARCHETTO, S., OSMANI, N., NOURRY, C., AUDEBERT, S., NAVARRO, C., RACHEL, R., MONTCOUQUIOL, M., SANS, N., ETIENNE-MANNEVILLE, S., BORG, J. P. & SANTONI, M. J. 2008. Scrib regulates PAK activity during the cell migration process. *Hum Mol Genet*, 17, 3552-65.
- NOZUMI, M., NAKAGAWA, H., MIKI, H., TAKENAWA, T. & MIYAMOTO, S. 2003. Differential localization of WAVE isoforms in filopodia and lamellipodia of the neuronal growth cone. *J Cell Sci*, 116, 239-46.

- NUSBLAT, L. M., DOVAS, A. & COX, D. 2011. The non-redundant role of N-WASP in podosome-mediated matrix degradation in macrophages. *Eur J Cell Biol*, 90, 205-12.
- O'TOOLE, T. E., KATAGIRI, Y., FAULL, R. J., PETER, K., TAMURA, R., QUARANTA, V., LOFTUS, J. C., SHATTIL, S. J. & GINSBERG, M. H. 1994. Integrin cytoplasmic domains mediate inside-out signal transduction. *J Cell Biol*, 124, 1047-59.
- OBAR, R. A., SHPETNER, H. S. & VALLEE, R. B. 1991. Dynamin: a microtubule-associated GTP-binding protein. *J Cell Sci Suppl*, 14, 143-5.
- OLIVER, T., DEMBO, M. & JACOBSON, K. 1995. Traction forces in locomoting cells. *Cell Motil Cytoskeleton*, 31, 225-40.
- OSMANI, N., VITALE, N., BORG, J. P. & ETIENNE-MANNEVILLE, S. 2006. Scrib controls Cdc42 localization and activity to promote cell polarization during astrocyte migration. *Curr Biol*, 16, 2395-405.
- PADRICK, S. B. & ROSEN, M. K. 2010. Physical mechanisms of signal integration by WASP family proteins. *Annu Rev Biochem*, 79, 707-35.
- PARSONS, J. T., HORWITZ, A. R. & SCHWARTZ, M. A. 2010. Cell adhesion: integrating cytoskeletal dynamics and cellular tension. *Nat Rev Mol Cell Biol*, 11, 633-43.
- PARSONS, J. T., MARTIN, K. H., SLACK, J. K., TAYLOR, J. M. & WEED, S. A. 2000. Focal adhesion kinase: a regulator of focal adhesion dynamics and cell movement. *Oncogene*, 19, 5606-13.
- PEARSON, G., ROBINSON, F., BEERS GIBSON, T., XU, B. E., KARANDIKAR, M., BERMAN, K. & COBB, M. H. 2001. Mitogen-activated protein (MAP) kinase pathways: regulation and physiological functions. *Endocr Rev*, 22, 153-83.
- PESKIN, C. S., ODELL, G. M. & OSTER, G. F. 1993. Cellular motions and thermal fluctuations: the Brownian ratchet. *Biophys J*, 65, 316-24.
- PETIT, V. & THIERY, J. P. 2000. Focal adhesions: structure and dynamics. *Biol Cell*, 92, 477-94.
- PIJNENBORG, R., BLAND, J. M., ROBERTSON, W. B. & BROSENS, I. 1983. Uteroplacental arterial changes related to interstitial trophoblast migration in early human pregnancy. *Placenta*, 4, 397-413.
- PIJNENBORG, R., VERCRUYSE, L. & BROSENS, I. 2011. Deep placentation. *Best Pract Res Clin Obstet Gynaecol*, 25, 273-85.
- PINNER, S. & SAHAI, E. 2008. PDK1 regulates cancer cell motility by antagonising inhibition of ROCK1 by RhoE. *Nat Cell Biol*, 10, 127-37.
- POLLARD, T. D. 1984. Polymerization of ADP-actin. *J Cell Biol*, 99, 769-77.
- POLLARD, T. D. & BORISY, G. G. 2003. Cellular motility driven by assembly and disassembly of actin filaments. *Cell*, 112, 453-65.
- POLLITT, A. Y. & INSALL, R. H. 2009. Loss of Dictyostelium HSPC300 causes a scar-like phenotype and loss of SCAR protein. *BMC Cell Biol*, 10, 13.
- PRASS, M., JACOBSON, K., MOGILNER, A. & RADMACHER, M. 2006. Direct measurement of the lamellipodial protrusive force in a migrating cell. *J Cell Biol*, 174, 767-72.
- QUINTAVALLE, M., ELIA, L., CONDORELLI, G. & COURTNEIDGE, S. A. 2010. MicroRNA control of podosome formation in vascular smooth muscle cells in vivo and in vitro. *J Cell Biol*, 189, 13-22.
- QURASHI, A., SAHIN, H. B., CARRERA, P., GAUTREAU, A., SCHENCK, A. & GIANGRANDE, A. 2007. HSPC300 and its role in neuronal connectivity. *Neural Dev*, 2, 18.
- RAKEMAN, A. S. & ANDERSON, K. V. 2006. Axis specification and morphogenesis in the mouse embryo require Nap1, a regulator of WAVE-mediated actin branching. *Development*, 133, 3075-83.

- RING, C., GINSBERG, M. H., HALING, J. & PENDERGAST, A. M. 2011. Abl-interactor-1 (Abi1) has a role in cardiovascular and placental development and is a binding partner of the alpha4 integrin. *Proc Natl Acad Sci U S A*, 108, 149-54.
- RIVERO-LEZCANO, O. M., MARCILLA, A., SAMESHIMA, J. H. & ROBBINS, K. C. 1995. Wiskott-Aldrich syndrome protein physically associates with Nck through Src homology 3 domains. *Mol Cell Biol*, 15, 5725-31.
- ROBINSON, R. C., TURBEDSKY, K., KAISER, D. A., MARCHAND, J. B., HIGGS, H. N., CHOE, S. & POLLARD, T. D. 2001. Crystal structure of Arp2/3 complex. *Science*, 294, 1679-84.
- RODAL, A. A., SOKOLOVA, O., ROBINS, D. B., DAUGHERTY, K. M., HIPPENMEYER, S., RIEZMAN, H., GRIGORIEFF, N. & GOODE, B. L. 2005. Conformational changes in the Arp2/3 complex leading to actin nucleation. *Nat Struct Mol Biol*, 12, 26-31.
- ROHATGI, R., MA, L., MIKI, H., LOPEZ, M., KIRCHHAUSEN, T., TAKENAWA, T. & KIRSCHNER, M. W. 1999. The interaction between N-WASP and the Arp2/3 complex links Cdc42-dependent signals to actin assembly. *Cell*, 97, 221-31.
- ROHATGI, R., NOLLAU, P., HO, H. Y., KIRSCHNER, M. W. & MAYER, B. J. 2001. Nck and phosphatidylinositol 4,5-bisphosphate synergistically activate actin polymerization through the N-WASP-Arp2/3 pathway. *J Biol Chem*, 276, 26448-52.
- ROTTNER, K., HALL, A. & SMALL, J. V. 1999. Interplay between Rac and Rho in the control of substrate contact dynamics. *Curr Biol*, 9, 640-8.
- ROUILLER, I., XU, X. P., AMANN, K. J., EGILE, C., NICKELL, S., NICASTRO, D., LI, R., POLLARD, T. D., VOLKMANN, N. & HANEIN, D. 2008. The structural basis of actin filament branching by the Arp2/3 complex. *J Cell Biol*, 180, 887-95.
- RYU, J. R., ECHARRI, A., LI, R. & PENDERGAST, A. M. 2009. Regulation of cell-cell adhesion by Abi/Diaphanous complexes. *Mol Cell Biol*, 29, 1735-48.
- SABRI, S., FOUADI, A., BOUKOUR, S., FRANC, B., CHARRIER, S., JANDROT-PERRUS, M., FARNDAL, R. W., JALIL, A., BLUNDELL, M. P., CRAMER, E. M., LOUACHE, F., DEBILI, N., THRASHER, A. J. & VAINCHENKER, W. 2006. Deficiency in the Wiskott-Aldrich protein induces premature proplatelet formation and platelet production in the bone marrow compartment. *Blood*, 108, 134-40.
- SAKAI, R., IWAMATSU, A., HIRANO, N., OGAWA, S., TANAKA, T., MANO, H., YAZAKI, Y. & HIRAI, H. 1994. A novel signaling molecule, p130, forms stable complexes in vivo with v-Crk and v-Src in a tyrosine phosphorylation-dependent manner. *EMBO J*, 13, 3748-56.
- SANZ-MORENO, V., GADEA, G., AHN, J., PATERSON, H., MARRA, P., PINNER, S., SAHAI, E. & MARSHALL, C. J. 2008. Rac activation and inactivation control plasticity of tumor cell movement. *Cell*, 135, 510-23.
- SCHAGGER, H., CRAMER, W. A. & VON JAGOW, G. 1994. Analysis of molecular masses and oligomeric states of protein complexes by blue native electrophoresis and isolation of membrane protein complexes by two-dimensional native electrophoresis. *Anal Biochem*, 217, 220-30.
- SCHALLER, M. D., BORGMAN, C. A., COBB, B. S., VINES, R. R., REYNOLDS, A. B. & PARSONS, J. T. 1992. pp125FAK a structurally distinctive protein-tyrosine kinase associated with focal adhesions. *Proc Natl Acad Sci U S A*, 89, 5192-6.
- SCHENCK, A., BARDONI, B., MORO, A., BAGNI, C. & MANDEL, J. L. 2001. A highly conserved protein family interacting with the fragile X mental retardation protein (FMRP) and displaying selective interactions with FMRP-related proteins FXR1P and FXR2P. *Proc Natl Acad Sci U S A*, 98, 8844-9.
- SCHLAEPFER, D. D., HANKS, S. K., HUNTER, T. & VAN DER GEER, P. 1994. Integrin-mediated signal transduction linked to Ras pathway by GRB2 binding to focal adhesion kinase. *Nature*, 372, 786-91.

- SCHLAEPFER, D. D., HAUCK, C. R. & SIEG, D. J. 1999. Signaling through focal adhesion kinase. *Prog Biophys Mol Biol*, 71, 435-78.
- SCHLAEPFER, D. D. & HUNTER, T. 1996. Evidence for in vivo phosphorylation of the Grb2 SH2-domain binding site on focal adhesion kinase by Src-family protein-tyrosine kinases. *Mol Cell Biol*, 16, 5623-33.
- SCHOBBER, M., RAGHAVAN, S., NIKOLOVA, M., POLAK, L., PASOLLI, H. A., BEGGS, H. E., REICHARDT, L. F. & FUCHS, E. 2007. Focal adhesion kinase modulates tension signaling to control actin and focal adhesion dynamics. *J Cell Biol*, 176, 667-80.
- SCHOUMACHER, M., GOLDMAN, R. D., LOUVARD, D. & VIGNJEVIC, D. M. 2010. Actin, microtubules, and vimentin intermediate filaments cooperate for elongation of invadopodia. *J Cell Biol*, 189, 541-56.
- SCHWARTZ, M. A. & ASSOIAN, R. K. 2001. Integrins and cell proliferation: regulation of cyclin-dependent kinases via cytoplasmic signaling pathways. *J Cell Sci*, 114, 2553-60.
- SEARS, R., LEONE, G., DEGREGORI, J. & NEVINS, J. R. 1999. Ras enhances Myc protein stability. *Mol Cell*, 3, 169-79.
- SEARS, R., NUCKOLLS, F., HAURA, E., TAYA, Y., TAMAI, K. & NEVINS, J. R. 2000. Multiple Ras-dependent phosphorylation pathways regulate Myc protein stability. *Genes Dev*, 14, 2501-14.
- SERRELS, B., SERRELS, A., BRUNTON, V. G., HOLT, M., MCLEAN, G. W., GRAY, C. H., JONES, G. E. & FRAME, M. C. 2007. Focal adhesion kinase controls actin assembly via a FERM-mediated interaction with the Arp2/3 complex. *Nat Cell Biol*, 9, 1046-56.
- SHARMA, A. & MAYER, B. J. 2008. Phosphorylation of p130Cas initiates Rac activation and membrane ruffling. *BMC Cell Biol*, 9, 50.
- SHARMA, S., ANG, S. L., SHAW, M., MACKEY, D. A., GECZ, J., MCAVOY, J. W. & CRAIG, J. E. 2006. Nance-Horan syndrome protein, NHS, associates with epithelial cell junctions. *Hum Mol Genet*, 15, 1972-83.
- SHARMA, S., BURDON, K. P., DAVE, A., JAMIESON, R. V., YARON, Y., BILLSON, F., VAN MALDERGEM, L., LORENZ, B., GECZ, J. & CRAIG, J. E. 2008. Novel causative mutations in patients with Nance-Horan syndrome and altered localization of the mutant NHS-A protein isoform. *Mol Vis*, 14, 1856-64.
- SHARMA, S., KOH, K. S., COLLIN, C., DAVE, A., MCMELLON, A., SUGIYAMA, Y., MCAVOY, J. W., VOSS, A. K., GECZ, J. & CRAIG, J. E. 2009. NHS-A isoform of the NHS gene is a novel interactor of ZO-1. *Exp Cell Res*, 315, 2358-72.
- SHARMA, T. & ETTENSOHN, C. A. 2011. Regulative deployment of the skeletogenic gene regulatory network during sea urchin development. *Development*, 138, 2581-90.
- SHI, Y., ALIN, K. & GOFF, S. P. 1995. Abl-interactor-1, a novel SH3 protein binding to the carboxy-terminal portion of the Abl protein, suppresses v-abl transforming activity. *Genes Dev*, 9, 2583-97.
- SIEG, D. J., HAUCK, C. R., ILIC, D., KLINGBEIL, C. K., SCHAEFER, E., DAMSKY, C. H. & SCHLAEPFER, D. D. 2000. FAK integrates growth-factor and integrin signals to promote cell migration. *Nat Cell Biol*, 2, 249-56.
- SILVA, J. M., EZHKOVA, E., SILVA, J., HEART, S., CASTILLO, M., CAMPOS, Y., CASTRO, V., BONILLA, F., CORDON-CARDO, C., MUTHUSWAMY, S. K., POWERS, S., FUCHS, E. & HANNON, G. J. 2009. Cyfip1 is a putative invasion suppressor in epithelial cancers. *Cell*, 137, 1047-61.
- SMALL, J. V., ISENBERG, G. & CELIS, J. E. 1978. Polarity of actin at the leading edge of cultured cells. *Nature*, 272, 638-9.
- SONODA, Y., WATANABE, S., MATSUMOTO, Y., AIZU-YOKOTA, E. & KASAHARA, T. 1999. FAK is the upstream signal protein of the phosphatidylinositol 3-kinase-

- Akt survival pathway in hydrogen peroxide-induced apoptosis of a human glioblastoma cell line. *J Biol Chem*, 274, 10566-70.
- SOSSEY-ALAOUI, K., SU, G., MALAJ, E., ROE, B. & COWELL, J. K. 2002. WAVE3, an actin-polymerization gene, is truncated and inactivated as a result of a constitutional t(1;13)(q21;q12) chromosome translocation in a patient with ganglioneuroblastoma. *Oncogene*, 21, 5967-74.
- STEFFEN, A., FAIX, J., RESCH, G. P., LINKNER, J., WEHLAND, J., SMALL, J. V., ROTTNER, K. & STRADAL, T. E. 2006. Filopodia formation in the absence of functional WAVE- and Arp2/3-complexes. *Mol Biol Cell*, 17, 2581-91.
- STEFFEN, A., ROTTNER, K., EHINGER, J., INNOCENTI, M., SCITA, G., WEHLAND, J. & STRADAL, T. E. 2004. Sra-1 and Nap1 link Rac to actin assembly driving lamellipodia formation. *EMBO J*, 23, 749-59.
- STOVOLD, C. F., MILLARD, T. H. & MACHESKY, L. M. 2005. Inclusion of Scar/WAVE3 in a similar complex to Scar/WAVE1 and 2. *BMC Cell Biol*, 6, 11.
- STUPACK, D. G. & CHERESH, D. A. 2002. Get a ligand, get a life: integrins, signaling and cell survival. *J Cell Sci*, 115, 3729-38.
- SUETSUGU, S., HATTORI, M., MIKI, H., TEZUKA, T., YAMAMOTO, T., MIKOSHIBA, K. & TAKENAWA, T. 2002. Sustained activation of N-WASP through phosphorylation is essential for neurite extension. *Dev Cell*, 3, 645-58.
- SUETSUGU, S., MIKI, H. & TAKENAWA, T. 1999. Identification of two human WAVE/SCAR homologues as general actin regulatory molecules which associate with the Arp2/3 complex. *Biochem Biophys Res Commun*, 260, 296-302.
- SUETSUGU, S., YAMAZAKI, D., KURISU, S. & TAKENAWA, T. 2003. Differential roles of WAVE1 and WAVE2 in dorsal and peripheral ruffle formation for fibroblast cell migration. *Dev Cell*, 5, 595-609.
- SURANENI, P., RUBINSTEIN, B., UNRUH, J. R., DURIN, M., HANEIN, D. & LI, R. 2012. The Arp2/3 complex is required for lamellipodia extension and directional fibroblast cell migration. *J Cell Biol*, 197, 239-51.
- SUZUKI, T., MIKI, H., TAKENAWA, T. & SASAKAWA, C. 1998. Neural Wiskott-Aldrich syndrome protein is implicated in the actin-based motility of *Shigella flexneri*. *EMBO J*, 17, 2767-76.
- SVITKINA, T. M. & BORISY, G. G. 1999. Arp2/3 complex and actin depolymerizing factor/cofilin in dendritic organization and treadmilling of actin filament array in lamellipodia. *J Cell Biol*, 145, 1009-26.
- SVITKINA, T. M., BULANOVA, E. A., CHAGA, O. Y., VIGNJEVIC, D. M., KOJIMA, S., VASILIEV, J. M. & BORISY, G. G. 2003. Mechanism of filopodia initiation by reorganization of a dendritic network. *J Cell Biol*, 160, 409-21.
- TADOKORO, S., SHATTIL, S. J., ETO, K., TAI, V., LIDDINGTON, R. C., DE PEREDA, J. M., GINSBERG, M. H. & CALDERWOOD, D. A. 2003. Talin binding to integrin beta tails: a final common step in integrin activation. *Science*, 302, 103-6.
- TAKAGI, J., ERICKSON, H. P. & SPRINGER, T. A. 2001. C-terminal opening mimics 'inside-out' activation of integrin alpha5beta1. *Nat Struct Biol*, 8, 412-6.
- TAKAGI, J., PETRE, B. M., WALZ, T. & SPRINGER, T. A. 2002. Global conformational rearrangements in integrin extracellular domains in outside-in and inside-out signaling. *Cell*, 110, 599-11.
- TAKEMURA, R., OKABE, S., UMEYAMA, T., KANAI, Y., COWAN, N. J. & HIROKAWA, N. 1992. Increased microtubule stability and alpha tubulin acetylation in cells transfected with microtubule-associated proteins MAP1B, MAP2 or tau. *J Cell Sci*, 103 (Pt 4), 953-64.

- TIMPSON, P., MCGHEE, E. J., ERAMI, Z., NOBIS, M., QUINN, J. A., EDWARD, M. & ANDERSON, K. I. 2011. Organotypic collagen I assay: a malleable platform to assess cell behaviour in a 3-dimensional context. *J Vis Exp*, e3089.
- TOMASEK, J. J., GABBIANI, G., HINZ, B., CHAPONNIER, C. & BROWN, R. A. 2002. Myofibroblasts and mechano-regulation of connective tissue remodelling. *Nat Rev Mol Cell Biol*, 3, 349-63.
- TOMASEVIC, N., JIA, Z., RUSSELL, A., FUJII, T., HARTMAN, J. J., CLANCY, S., WANG, M., BERAUD, C., WOOD, K. W. & SAKOWICZ, R. 2007. Differential regulation of WASP and N-WASP by Cdc42, Rac1, Nck, and PI(4,5)P2. *Biochemistry*, 46, 3494-502.
- TORRES, E. & ROSEN, M. K. 2003. Contingent phosphorylation/dephosphorylation provides a mechanism of molecular memory in WASP. *Mol Cell*, 11, 1215-27.
- TOUTANT, M., COSTA, A., STUDLER, J. M., KADARE, G., CARNAUD, M. & GIRAULT, J. A. 2002. Alternative splicing controls the mechanisms of FAK autophosphorylation. *Mol Cell Biol*, 22, 7731-43.
- VAN AKEN, E. H., DE WEVER, O., VAN HOORDE, L., BRUYNEEL, E., DE LAEY, J. J. & MAREEL, M. M. 2003. Invasion of retinal pigment epithelial cells: N-cadherin, hepatocyte growth factor, and focal adhesion kinase. *Invest Ophthalmol Vis Sci*, 44, 463-72.
- VAN DE WATER, B., NAGELKERKE, J. F. & STEVENS, J. L. 1999. Dephosphorylation of focal adhesion kinase (FAK) and loss of focal contacts precede caspase-mediated cleavage of FAK during apoptosis in renal epithelial cells. *J Biol Chem*, 274, 13328-37.
- VICENTE-MANZANARES, M., CHOI, C. K. & HORWITZ, A. R. 2009. Integrins in cell migration--the actin connection. *J Cell Sci*, 122, 199-206.
- VIGNJEVIC, D., YARAR, D., WELCH, M. D., PELOQUIN, J., SVITKINA, T. & BORISY, G. G. 2003. Formation of filopodia-like bundles in vitro from a dendritic network. *J Cell Biol*, 160, 951-62.
- VINZENZ, M., NEMETHOVA, M., SCHUR, F., MUELLER, J., NARITA, A., URBAN, E., WINKLER, C., SCHMEISER, C., KOESTLER, S. A., ROTTNER, K., RESCH, G. P., MAEDA, Y. & SMALL, J. V. 2012. Actin branching in the initiation and maintenance of lamellipodia. *J Cell Sci*, 125, 2775-85.
- WALSH, D. & MOHR, I. 2004. Phosphorylation of eIF4E by Mnk-1 enhances HSV-1 translation and replication in quiescent cells. *Genes Dev*, 18, 660-72.
- WANG, Y. & MCNIVEN, M. A. 2012. Invasive matrix degradation at focal adhesions occurs via protease recruitment by a FAK-p130Cas complex. *J Cell Biol*, 196, 375-85.
- WATSON, R. A., ROLLASON, T. P., REYNOLDS, G. M., MURRAY, P. G., BANKS, L. & ROBERTS, S. 2002. Changes in expression of the human homologue of the Drosophila discs large tumour suppressor protein in high-grade premalignant cervical neoplasias. *Carcinogenesis*, 23, 1791-6.
- WEBB, D. J., DONAIS, K., WHITMORE, L. A., THOMAS, S. M., TURNER, C. E., PARSONS, J. T. & HORWITZ, A. F. 2004. FAK-Src signalling through paxillin, ERK and MLCK regulates adhesion disassembly. *Nat Cell Biol*, 6, 154-61.
- WEINER, O. D., MARGANSKI, W. A., WU, L. F., ALTSCHULER, S. J. & KIRSCHNER, M. W. 2007. An actin-based wave generator organizes cell motility. *PLoS Biol*, 5, e221.
- WOLF, K. & FRIEDL, P. 2009. Mapping proteolytic cancer cell-extracellular matrix interfaces. *Clin Exp Metastasis*, 26, 289-98.
- WOZNIAK, M. A., MODZELEWSKA, K., KWONG, L. & KEELY, P. J. 2004. Focal adhesion regulation of cell behavior. *Biochim Biophys Acta*, 1692, 103-19.

- WU, C., ASOKAN, S. B., BERGINSKI, M. E., HAYNES, E. M., SHARPLESS, N. E., GRIFFITH, J. D., GOMEZ, S. M. & BEAR, J. E. 2012. Arp2/3 is critical for lamellipodia and response to extracellular matrix cues but is dispensable for chemotaxis. *Cell*, 148, 973-87.
- WU, X., SUETSUGU, S., COOPER, L. A., TAKENAWA, T. & GUAN, J. L. 2004. Focal adhesion kinase regulation of N-WASP subcellular localization and function. *J Biol Chem*, 279, 9565-76.
- XIA, H., NHO, R. S., KAHM, J., KLEIDON, J. & HENKE, C. A. 2004. Focal adhesion kinase is upstream of phosphatidylinositol 3-kinase/Akt in regulating fibroblast survival in response to contraction of type I collagen matrices via a beta 1 integrin viability signaling pathway. *J Biol Chem*, 279, 33024-34.
- YAMAGUCHI, H., LORENZ, M., KEMPIAK, S., SARMIENTO, C., CONIGLIO, S., SYMONS, M., SEGALL, J., EDDY, R., MIKI, H., TAKENAWA, T. & CONDEELIS, J. 2005. Molecular mechanisms of invadopodium formation: the role of the N-WASP-Arp2/3 complex pathway and cofilin. *J Cell Biol*, 168, 441-52.
- YAMAMOTO, D., SONODA, Y., HASEGAWA, M., FUNAKOSHI-TAGO, M., AIZU-YOKOTA, E. & KASAHARA, T. 2003. FAK overexpression upregulates cyclin D3 and enhances cell proliferation via the PKC and PI3-kinase-Akt pathways. *Cell Signal*, 15, 575-83.
- YAMAZAKI, D., FUJIWARA, T., SUETSUGU, S. & TAKENAWA, T. 2005. A novel function of WAVE in lamellipodia: WAVE1 is required for stabilization of lamellipodial protrusions during cell spreading. *Genes Cells*, 10, 381-92.
- YOKOTA, Y., RING, C., CHEUNG, R., PEVNY, L. & ANTON, E. S. 2007. Nap1-regulated neuronal cytoskeletal dynamics is essential for the final differentiation of neurons in cerebral cortex. *Neuron*, 54, 429-45.
- YU, J., ZHANG, Y., MCILROY, J., RORDORF-NIKOLIC, T., ORR, G. A. & BACKER, J. M. 1998. Regulation of the p85/p110 phosphatidylinositol 3'-kinase: stabilization and inhibition of the p110alpha catalytic subunit by the p85 regulatory subunit. *Mol Cell Biol*, 18, 1379-87.
- YU, W., SUN, X., CLOUGH, N., COBOS, E., TAO, Y. & DAI, Z. 2008. Abi1 gene silencing by short hairpin RNA impairs Bcr-Abl-induced cell adhesion and migration in vitro and leukemogenesis in vivo. *Carcinogenesis*, 29, 1717-24.
- YU, X. & MACHESKY, L. M. 2012. Cells assemble invadopodia-like structures and invade into matrigel in a matrix metalloprotease dependent manner in the circular invasion assay. *PLoS One*, 7, e30605.
- ZAIDEL-BAR, R., ITZKOVITZ, S., MA'AYAN, A., IYENGAR, R. & GEIGER, B. 2007. Functional atlas of the integrin adhesome. *Nat Cell Biol*, 9, 858-67.
- ZAMBONIN-ZALLONE, A., TETI, A., CARANO, A. & MARCHISIO, P. C. 1988. The distribution of podosomes in osteoclasts cultured on bone laminae: effect of retinol. *J Bone Miner Res*, 3, 517-23.
- ZHAN, L., ROSENBERG, A., BERGAMI, K. C., YU, M., XUAN, Z., JAFFE, A. B., ALLRED, C. & MUTHUSWAMY, S. K. 2008. Deregulation of scribble promotes mammary tumorigenesis and reveals a role for cell polarity in carcinoma. *Cell*, 135, 865-78.